Investigations into the effects of cholesterol inhibitors on cancer cells *in vitro*

David John Garnett

Doctorate of Philosophy

March 2014

ACKNOWLEDGEMENTS

I am indebted to my supervisor Prof. Trevor Greenhough who has been supportive and kind throughout. His original leap of faith in this project was remarkably generous.

I also wish to acknowledge the help of Mike Collins at Leksing Ltd for providing several new analogues to the Proadifen molecule.

The statistical treatments applied to the mRNA data could not have been completed without the help of Dr Varrie Ogilvie of Fios Genomics Ltd. I would also like to thank John Clews, Chemistry Department, for the many NMR spectra and Karen Walker of the EM Unit for the electron microscopy, both at Keele University.

Finally, I owe a debt of thanks to Jenny Moran for always making me feel welcome at the Institute of Science Technology and Medicine, Keele.

In memory of

David Thomas Youngman

1944 - 2010

ABSTRACT

Cholesterol-rich membrane microdomains have a significant role in cancer progression, particularly in metastasis, and there is evidence that cholesterol inhibitors, most notably statins, can change the behaviour of cancer cells *in vitro* and *in vivo*. Cholesterol-rich rafts act as loci for signal receptor-ligand binding, providing a stable scaffold for protein interaction. The purpose of this research was to test the hypothesis that the abundance of these inclusions can be controlled with cholesterol inhibitors and to investigate the effects of these treatments on cancer cells using simple *in vitro* assays. Flask shaped cholesterol-rich scaffolds in the membrane called caveolae, characterised by the presence of the protein Caveolin-1, are generally associated with proliferation suppression during oncogenesis but with tumour promotion during metastasis. This dual role may be coordinated by the cholesterol content of the raft environment and so be vulnerable to cholesterol inhibitors such as the statins.

A variety of techniques were used to assess the proteome, mRNA expression, cholesterol and Cav-1 levels in cells treated with a variety of cholesterol synthesis inhibitors in an attempt to understand the processes that affect metastatic behaviours *in vitro*. A number of novel derivatives of one particular inhibitor of cholesterol Δ24 reductase (Proadifen) were

included in these *in vitro* assays. The structure of the molecule was iteratively changed to determine the important features of the molecule that give rise to Δ-24 enzyme inhibition.

It was found that inhibition of cholesterol synthesis asymmetrically reduces the prevalence of rafts and caveolae and is associated with multiple effects on cancer cell behaviour and, perhaps most significantly, with changes to gene expression. Targeted blockade of the mevalonate pathway using Δ-24 and Δ-7 reductase inhibitors could prevent the successful transduction of extrinsic signals that coordinate some cancer cell behaviour. The toxicity profiles of the inhibitors used in this project are poor, but further analogues may be developed in the future that could have clinical relevance.

LIST OF ABBREVIATIONS

AFM	Atomic force microscopy
ATP	Adenosine triphosphate
Cox	Cyclooxygenase
DHA	Docosahexienoic acid
DHCR	Dehydrocholesterol reductase
DISC	Death inducing signalling complex
DRM	Detergent resistant microdomain
EGF[R]	Epidermal growth factor [receptor]
FBS	Foetal bovine serum
GCS	Glucosylceramide synthase
GM3	monosialodihexosylganglioside
GPI	Glycophosphatidylinositol
HMG-CoA	3-hydroxy-3-methylglutaryl-coenzyme A
HMGCS1	Gene coding for 3-hydroxy-3-methylglutaryl-coenzyme A synthase
IGF	Insulin-like growth factor
IL	Interleukin
IR	Insulin receptor
MDR	Multi-drug resistance
MM	Multiple myeloma
MMP	Matrix metalloproteinase
MVS	Mevalonate synthase
MβCD	Methyl-β-cyclodextrin
PBS	Phosphate buffered saline
PDGF[R]	Platelet derived growth factor [receptor]
PUFA	Polyunsaturated fatty acid
RTF	Receptor tyrosine kinase
S1P	Sphingosine-1-phosphate
SEM	Scanning electron microscopy
SQS	Squalene synthase
TEM	Transmission electron microscopy
TNF	Tumour necrosis factor

CONTENTS

TABLE OF FIGURES

INDEX OF TABLES

1 INTRODUCTION

Cancer is the name given to the uncontrolled replication of cells, commonly characterised by invasion of these cells into neighbouring tissue and their spread through the body in the blood or lymphatic system. Common causes of cancer can be divided into environmental and genetic types. The most common environmental cause is the consumption of tobacco products which can produce malignant tumours of the lung (Kuper et al., 2002). Other environmental agents that can trigger cancer include radiation and exposure to asbestos particles. Genetic or hereditary cancers – or a predisposition towards their occurrence – include retinoblastoma and some Downs syndrome related cancers that typically afflict young children. However, hereditary causes of cancer are responsible for a relatively small percentage (3-10%) of cancer related deaths. Some cancers, such as cervical cancer, are caused by a virus. Still others have an unknown aetiology. Cancer, in all its forms, kills an estimated 13% of the global population(Jemal et al., 2011).

When a cancerous tumour occurs in an organ it is often discovered upon biopsy or X-ray to be a discreet entity occupying a defined area or portion of the organ. Complete removal of this 'primary' tumour by surgery or by radiation for example, can often be accomplished. Indeed, the entire organ may be removed for an additional margin of safety. However, this does not necessarily remove the risk of morbidity or mortality since some cells from the tumour may have migrated to distal areas of the body in a

process known as metastasis. These cells may have successfully adapted to their new host organ and be developing into a 'secondary' or 'daughter' cancer growth. The idea that the migrating cell may find the most suitable targets for invasion by cognition of extra-cellular signals is called the seed-and-soil theory first posited by Fuchs (Fuchs, 1882), and then later popularised by Paget (Paget, 1889). It has been estimated that only 10-15% of cancer related deaths are attributable to the primary growth (Sleeman and Steeg, 2010) which means that the process of metastasis currently accounts for some 10-12% of all human deaths.

The processes by which a healthy cell becomes a malignant cell and then later a metastatic cell are complex and many different cellular processes are implicated. For example, the immune system is involved since the cell must evade the normal immune surveillance. Mutations leading to genetic transformation may be triggered by oxidative stress and this is exacerbated by inflammatory response, so the immune system has multiple involvements. Likewise, the normal restraints on growth such as contact inhibition must first be removed so the cell can multiply freely; as the mutant cells reach their natural boundary within an organ they are able to switch off production of the adhesive molecules -that normally tether them to their proper locations - and migrate to new territories. This is a process that is made more complicated due to the fact that it must be a reversible step so that when the cell arrives at a suitable site for invasion, cell adhesion must be switched back on again for the cell to attach itself to the new substrate. Increased motility is another characteristic of cancer cells. It was first noted in 1863 by Virchow (Virchow, 1863) that amoeboid movements of cells were visible in

isolates from newly excised tumours. What was originally described by Willis (Willis, 1952) as the 'possible elaboration of toxic or lytic substances' from the cancer cell are now understood to be the cells production of attachment factors - such as integrins - and enzymes such as matrix metalloproteinases that degrade and prepare the path for the invading cell. Each step in this long and involved process appears to be one of deliberate design but is, in fact, simply a probabilistic function that can be mathematically defined. For a cell to successfully negotiate the hurdles of apoptosis, de-attachment, migration, and invasion a number of consecutive mutations must arise and the chances of these occurring in the correct sequence in a particular cell are slim. However, the numbers of cells produced by the first genetic aberrations – typically, activation of an oncogene and de-activation of a proliferation suppressor gene, dramatically shift the odds in the cancer cells favour. For example, a breast tumour with a diameter of 2cm is likely to shed over 10 million cells per day (Greaves, 2000) into surrounding tissue and blood and by their nature these cells are highly prolific. It thus becomes a statistical event, rather than a design event, as to whether the cancer cell will eventually become fully metastatic. It is widely agreed that, depending on cell type, a minimum of 5-6 genes must be switched for the cell to achieve successful metastasis. Each of these genes codes for a protein that becomes part of the cellular machinery of the cell and each in turn acts upon a pathway or multiple pathways that control the new phenotype. Some of the most crucial pathways involved in the metastasis of cancer are signalling systems that enable the cell to coordinate its behaviour and to monitor its environment. These signalling proteins use the cell membrane as a platform, often traversing the plasma membrane bilayer or arranged on the external face of the

membrane. These mediate signal transduction from the outside of the cell into the cytoplasm and ultimately the DNA and effectively report the status of the cell microenvironment and, through paracrine signalling, the status of the cell and its neighbours. Membrane bound signal receptors are most commonly found in distinct areas of the membrane called rafts, which are more rigid than segments composed entirely of phospholipids. These areas are particularly rich in cholesterol and ceramide. Raft mediated signalling will clearly be affected if the level of cholesterol is reduced and the area available for signalling is diminished.

1.1 The Plasma membrane and the formation of rafts

The plasma membrane is not simply a cell structure that separates the living cytoplasm, nucleus and organelles from the outside environment. It is the locus of activity for primary cell functions as diverse as endocytosis and signal transduction. A plasma membrane typically consists of perhaps 1500 lipid species and more than a hundred different proteins (Gennis, 1989) – all in rapid flux, making signalling dynamics in this system particularly hard to fathom. The ability of the membrane to reinforce itself prior to G1 phase separation or to interdigitate and then fuse with similar bilayers is crucial for various cell processes. The plasma membrane has the ability to segregate the fluid mosaic of phospholipids into local temporal domains that have significant functionalities (Jacobson et al., 2007), (Dykstra et al., 2003), (Simons and Toomre, 2000). Many of the more subtle activities of the plasma membrane – and increasingly apparent, of organelle membranes – are due to membrane inclusions that perform specific roles in respect of signal transduction. These domains are most often referred to as membrane rafts (Simons and Ikonen, 1997) and typically comprise high levels of sphingosine, ceramide, protein and cholesterol and low levels of phospholipids. It is generally believed that the structural integrity afforded by this combination of sphingolipid, sterol and other minor components affords these membrane regions particular rigidity, allowing anchorage, orientation and conformation of signal proteins (Brown and London, 2000). The role of these proteins in cell-cell and cell-environment signalling is increasingly understood. Lipid rafts are implicated in signalling cascades as diverse as mutagenesis-derived apoptosis (Gajate et al., 2009), endocrine and autocrine loops and

numerous lipid-protein related signalling such as angiogenesis and immune signalling (Patra, 2008).

For many years the existence, size and prevalence of such lipid inclusions was controversial (Munro, 2003), (Hancock, 2006), (Edidin, 2003) but it is now clear from immunogold electron microscopy, atomic force microscopy and other techniques that stable microdomains of different sizes do indeed exist and can be visualized and separated from the rest of the membrane with relative ease. Ultracentrifuge techniques have permitted the isolation of these lipid regions due to their innately different buoyancy in sucrose-density gradients. It has also become clear that rafts range in size from 10-200nm in scale, are temporal in nature, and have distinct compositions that correspond to their individual signal associations. In MDA-MB-231 cells (cells used in this study), Flotillin-1 is found primarily in microdomains and this has been verified by atomic force microscopy coupled with labelled antibody imaging (Orsini et al., 2012).

Many of the cell membrane functions would not be possible if the larger surface area were as rigid as the raft microdomain. Most of the plasma membrane requires the fluid mosaic structure as described by Singer and Nicholson (Singer and Nicolson, 1972). Cell division, for example would not be possible if the membrane was too rigid and likewise cell fusion-like processes such as endocytosis and invagination depend on sufficient fluidity of the phospholipid matrix. Phospholipid interdigitation is a process that is driven thermodynamically and does not rely on cell ATP. Thus the plasma membrane is an ocean of phospholipids, glycolipids and transmembrane proteins that has diffusion

properties and other mobility related activities, while containing localized areas that provide stability not available in the rest of the bilayer (van Deurs et al., 2003). It is also known that rafts of 26±13nm diffuse as single entities for minutes at a time and when GPI-anchored proteins are present these proteins have significantly reduced diffusion compared to non-raft transmembrane proteins (Pralle et al., 2000). Protein conformation for signalling requires stable spatial orientation in respect of co-signalling molecules and rafts provide this stable environment. In particular, rafts are the location for many different types of signalling in cancers including sarcomas, myelomas, breast, lung and prostate cancer. This signalling controls proliferation, apoptotic dysregulation and metastasis and so lipid rafts may thus be a suitable target for chemotherapeutic intervention. Directing drugs against rafts *per se* may however have negative consequences since many of the processes mediated by raft proteins are entirely benign.

Increased membrane fluidity generally correlates with increased metastasis: for example, tumour cell adhesion in mice inoculated with MT3 breast cancer cells is correlated to fluidity. Here, electron paramagnetic resonance was used to assess the fluidity of spin labelled cells in different growth phases. It was found that fluidity strongly correlated with the phase of proliferation with confluent cells having the most fluid plasma membranes (Zeisig et al., 2007). Lymphocytes isolated from normal mice exhibit far greater cell capping than leukemic cells yet the membrane fluidity is greater in leukemic cells (Dunlap et al., 1979). The same is true in human cells (Ben-Bassat et al.,

1977) and points to the Bretcher flow model of capping as an explanation (Bretscher, 1976).

Studies in model membranes reveal that a membrane can comprise liquid-ordered (I_0) phase of lipids together with a liquid disordered (I_d) phase. I_0 phase lipids show a high degree of lateral mobility but are otherwise tightly packed lipid-sterol domains (Veatch and Keller, 2005). Disordered I_d domains are less tightly packed and a third phase – the gel phase- occurs where lipids are too tightly packed for any mobility (Heberle et al., 2005). In practice, these different phases may be extracted through increasing degrees of detergent solubilisation, most often with non-ionic surfactants such as Triton-X. These phases are captured using a sucrose (or similar) density gradient on centrifugation. The more tightly packed the domain, the less entry is afforded the detergent and it is these detergent resistant microdomains that have been regarded as the same entities as rafts for many years. The question remains: are DRMs actually isolated raft domains or just parts of the membrane that share characteristics that both model membrane experiments and empirical studies ascribe to rafts? One possibility remains that the detergent itself changes the liquid ordering of the domains – actually inducing the phase separation they are used to isolate (Brown, 2006).

Two studies shed light on this possibility: Ahmed *et al* studied model membranes that were made from a range of I_o and I_d domains – verified by fluorescence quenching studies – and then solubilised by detergents (Ahmed et al., 1997). These provide evidence that Triton X100 selectively solubilised the I_d phase domains and this work has

since been reproduced using microscopy based assays. A second study by Heerklotz (Heerklotz, 2002) using calorimetry suggests that detergents can induce at least some phase separation in uniform model membranes. The DRMs isolated from cells do contain a subset of proteins not found in the Id domains and this is in accordance with the original idea of raft development. Indeed, some proteins (caveolins, flotillins, some tyrosine kinases) are routinely used as raft markers in biochemical studies of the membrane. Further removal of cholesterol by sterol sequestering agents (such as Methyl-β-cyclodextrin (Zidovetzki and Levitan, 2007)) in living cells reduce the amount of these proteins associated with the extracted DRM. Ahmed suggests that since phase behaviour is temperature dependant then chilling cells should increase the development of rafts – and most membrane detergent extractions are performed on ice – further distorting the results (Heerklotz, 2002).

However, the most compelling evidence for the existence and prevalence of rafts *in vivo* is their recently discovered role in infection by both bacteria and viruses that presumably evolved to recognise and attach to these regions. A study by Arellano-Roynoso *et al* suggests that *Brucella* bacteria produce the cyclic cholesterol sequestering compound β-12 glucan to prevent phagosyme-lysozyme fusion (Arellano-Reynoso et al., 2005). Another study by Ravid *et al* proposed that para-influenza virus (HPIV1) utilises caveolae to assemble its virion envelope and facilitate budding out of the infected cell (Ravid et al., 2010). Palmitoylation of proteins to make them targeted to rafts is a process that can activate a signal protein or prolong its action. Palmitoylation of viral glycoproteins has been linked to their ability to attach onto rafts

as part of virion-cell docking but in several studies this is not always essential for infection (Li et al., 2002), (Campbell et al., 2004) . McDonald and Pike (Macdonald and Pike, 2005) have examined the role of surfactants play in the promotion of artefact in the extraction of membrane rafts. They report a detergent free method of raft isolation using Optiprep™ [instead of sucrose solutions] combined with lysis by shearing in isotonic buffer containing Ca^{2+} and Mg^{2+}. The resultant rafts were enriched with cholesterol and key protein markers permitting separation of the caveolin rich domains without an immunoaffinity purification step.

1.2 TYPES OF MEMBRANE RAFTS

Studies of membrane proteomics have revealed that at least three (Patra, 2008) distinct types of raft exist: one that is associated with the tyrosine kinase family of proteins and is rich in cholesterol and gangliosides (Type I); the second type is rich in ceramide and is associated with the death inducing signalling complex (DISC) and Fas apoptosis signalling proteins. These Type II inclusions tend to form when the cell is subjected to chemical or radiation stress; as an example of this process γ-irradiation induces acid sphingomyelinase (aSMase) activation which hydrolyses sphingomyelin into sphingosine and ceramide. The build-up of ceramide in the membrane can then displace cholesterol from rafts. The death inducing signals are recruited and the apoptotic cascade initiated. Likewise, cholesterol rich domains are associated with various onco-receptors such as CD44, EGFR and Ras that drive proliferation. The balance of these two raft types in any given membrane would therefore appear to reflect the more fundamental genetic health of the cell. Caveolae are a third class of raft inclusions and are 50-100nm flask

shaped structures characterized by the presence of the oligomeric loop protein caveolin-1 (Cav-1). Caveolins are responsible for recruitment of receptors to cholesterol-rich sub-domains and control of the actin cytoskeleton – perhaps regulating overall membrane fluidity, reinforcing the plasma membrane against shear forces during mitosis and regulating fusion dependant processes. Caveolae, like all rafts, are loci for signal transduction taking place between the external environment and the cytoplasm.

The process by which Type II rafts are enriched with ceramide through displacement of cholesterol implies an overall shift of sterol into surrounding non-raft areas of membrane. It has been further suggested that this cholesterol subsequently leaves the membrane entirely to form circulating lipoproteins. In addition to this steady-state desorption, cancer cells are able to 'dump' cholesterol in concentrated fragments of membrane, shed from the cell as part of its anti-recognition processes. So the move towards ceramide rafts could signify a global reduction in membrane cholesterol. Membranes with lower than normal levels of cholesterol are more fluid both empirically (Vanderkooi et al., 1974) and in model systems (Cooper, 1978) and this fluidity could be a factor in the fusion of tumour cells with osteoclasts, especially macrophages (Pawelek and Chakraborty, 2008). In the case of myeloma, nuclei fused with these bone marrow derived cells resulted in hybrid cells that are both viable and invasive. Likewise, similar results were reported with melanoma and carcinoma cells.

The fusion process to produce such cells is fluidity-dependant since opposing cells must interdigitate their outer membranes in a key step towards coalescence. This interdigitation is thermodynamically favoured when the phospholipid matrix is more dynamic. If this is true then logically an inverse correlation should exist between rates of metastasis and drug refraction: treatments that promote raft mediated apoptosis through depletion of cholesterol have been proposed (Podar and Anderson, 2006) but conceivably could increase all ceramide-raft mediated signalling.

1.3 Raft components and their roles in cancer

1.3.1 Ceramides and sphingosines

Classically, ceramide has a structural role in the assembly of galactosyl-sphingolipid cell adhesion molecules (Lee et al., 2010), however, ceramide, released from the membrane by enzymes, is also known to be involved in a range of signalling activities (Colombaioni and Garcia-Gil, 2004) including the mediation of caspase -9 and -3 activation (Park et al., 2004). Tumour necrosis factor (TNF), interferon and interleukin signalling across the membrane is mediated by ceramide, leading to apoptotic responses (Zhu et al., 2006) and further, there is evidence to suggest that ceramide itself can regulate the immune response (Dasgupta et al., 2007).

Ceramides are sphinogolipids that have a wide range of signalling activities (Futerman and Hannun, 2004) as well as structural roles in membrane microdomains. One of its transmembrane signalling pathways is the TNF and interferon-stimulated caspase-mediated apoptosis (Zhu et al., 2006). Other roles of ceramide are in cell migration,

senescence and cell growth arrest (Merrill et al., 1997). They can also modulate cell adhesion molecules such as CD29 (β1-integrin) and up-regulation of such adhesion factors is seen in cancer cells (Han M, 2008). Ceramides (but not sphingolipids) suppress cell-cell adhesion and cell-fibronectin adhesion by down-regulating CD98, CD147 (a matrix metalloprotein inducer) and CD49d; and ceramides also inhibited the phosphorylation of the structural protein CD29 (Lee et al., 2010). Gamma irradiation has been shown to induce ceramide driven apoptosis (Alphonse et al., 2002) through the activation of SMase catalyzed synthesis of ceramide from sphingomyelin and its release from rafts (Haimovitz-Friedman et al., 1994). It may be significant that multi drug resistant (MDR) cells have elevated cholesterol, sphingomyelin and in particular glucosylceramide. Inhibition of the glucosylation of ceramide naturally leads to increased levels of ceramide so findings that tumour promotion is indexed to the inhibition of glucosylation are unsurprising (Lavie et al., 1999).

To initiate apoptosis some research has shown that ceramide must be converted to the ganglioside GD3 (Malisan and Testi, 2002).

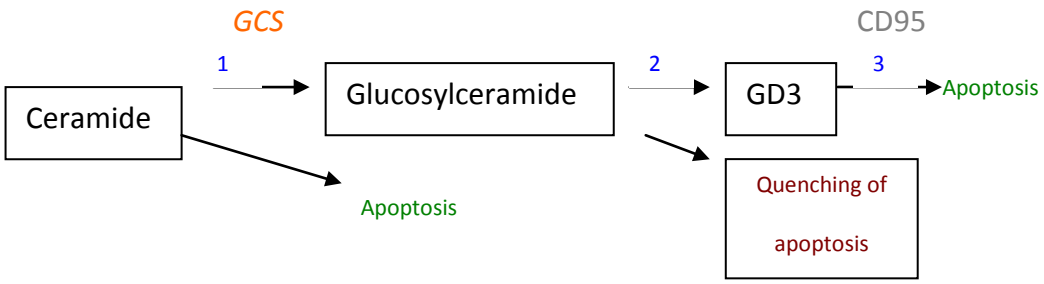

FIGURE 1: CERAMIDE CAN CAUSE OR INHIBIT APOPTOSIS

Other work looking specifically at chemosensitization suggests that glucosylation of ceramide effectively quenches the apoptotic response (di Bartolomeo and Spinedi, 2001). Ceramide is overexpressed by cells exposed to insults like radiation and chemotherapy and clearly has a central role in apoptotic and mitogenic pathways. The addition of water-soluble ceramides to cells *in vitro* causes apoptosis. Reduction of intracellular ceramide increases MDR (Modrak et al., 2006). Ceramides can be generated *de novo* or from hydrolysis of sphingomyelin by SMases. It is this latter route that elevates ceramide in cells exposed to environmental stress. The effects of this increase in ceramide concentration are likely to be similar to that of exogenously added ceramide: growth inhibition (Pushkareva et al., 1995), cell cycle arrest (Jayadev et al., 1995), induction of differentiation (Kim et al., 1991), tumour inhibition (Weinberg, 1990), apoptosis (Obeid et al., 1993) and necrosis (Mengubas et al., 1999).

Modrak *et al* compare the biological effects of a number of ceramides and note that the C4-C5 double bond is essential for activity, since dihydroceramide does not achieve apoptosis (Modrak et al., 2006). There is a question about the acyl group: de-acylated ceramide (sphingosine) is also pro-apoptotic but chain length seems to be very important - with palmitoylsphingosine (C16) being the most potent in its class.

1.3.1.1 CANCER PROTEINS AND RAFTS.

This is a list of cancer related proteins known to locate in or around rafts and caveolae (Foster et al., 2003).

Raft proteins	**Raft Associated Proteins**
CD55	Caveolin
Flotillin-1	MEK binding partner
Alkaline phosphatase	14.3.3-gamma
Vinculin	HSP90β
Insulin receptor	Actin
Rac	Ezrin
Ras	MMP-2, -9
PI3K	EGFR
	Fas (CD95)
	Integrin

TABLE 1: PROTEINS BY KNOWN LOCATION IN MEMBRANE

1.3.2 CAVEOLIN-1

Caveolin is so called because it lines the surface of the flask or cave shaped caveolae rafts (Rothberg et al., 1992) and was found to be identical to a 21 KDa vesicular integral protein previously known as VIP21. Cav-1 is the most abundant of three caveolins (with Cav-2 and Cav-3) that differ in distribution according to tissue types (Williams and Lisanti, 2004). It is anchored in the membrane by three palmitoylated points and the entire molecule acts as a scaffold for protein receptors. Caveolins actually create caveolae in certain tissues after transfection (Sowa et al., 2001), presumably by virtue of the folding conformation of the homo-oligers. They can, however, be present in caveolae-free membranes or as free cytoplasmic protein, presumably as monomers.

Caveolins are associated with cholesterol homeostasis and cell adhesion, pinocytosis and migration and they are found in various organelle membranes including the Golgi apparatus, ER and mitochondria. In the plasma membrane they occur in a heterogeneous distribution across tissue types – ubiquitous in endothelial and fibroblast cells but not found in blood, myeloid or lymphatic cell types. Cav-3 is unique to muscle cells.

Sonnino *et al (Sonnino and Prinetti, 2009)* proposed that glycosphingolipids may partition between rafts and caveolae and this would explain some inconsistencies regarding the distribution and putative role in signalling of GD3 (and other)

gangliosides. Caveolin-1 and (glyco)sphingolipid levels appear to be reciprocally regulated. Malfunctioning glycosphingolipids affect cell adhesion, invasiveness and modulate integrin and growth factor receptor mediated processes, especially cell motility and adhesion. This is a process via Src family kinases and adapter tetraspannin molecules (Prinetti et al., 2008).

The tetraspanins are sometimes referred to as the master regulators of membrane organization and are ubiquitous in nature (Hemler, 2005). The palmitoylated tetraspannin protein CD82 is a metastasis suppressor and when disabled is highly correlated to metastatic events *in vitro* and *in vivo* in a wide variety of malignancies (Tonoli and Barrett, 2005). CD82 normally regulates integrin mediated cell migration and cancer lines re-expressing CD82 show inhibited migration and invasion (Miranti, 2009). One mechanism for this may be the internalization of the surface integrins or possibly the inhibition of pre-β1 integrin processing. CD82 also inhibits EGFR signalling by the EGF ligand in caveolae but in normal cells are more commonly associated with ganglioside rich domains rather than rafts. It has been proposed that upon transformation the tetraspannins become palmitoylated and move into raft domains and this is supported by experimental evidence wherein the palmitoylation was blocked and this prevents their association with rafts (Yang et al., 2002).

Cav-1 binds to GM3 (at least in MDCK cells (Chigorno et al., 2000)) yet GM3 over-expression causes Cav-1 and insulin receptors (IR) to re-locate to outside raft or

caveolae microdomains. GM1 also displaces platelet-derived growth factor receptor (PDGFR) from caveolae suggesting that there is competition for binding sites of GM1 and GM3 with Cav-1 and the receptors. When displaced into non-raft / caveolae areas of membrane, IR and PDGFR are de-coupled from downstream signalling cascades (Inokuchi, 2007), so it is possible that a drug induced reduction of Cav-1 could nullify the pro-oncogenic activity of these signals.

Caveolin-1 is, however, highly expressed in multiple myeloma cells and is also over-expressed in multidrug resistant breast adenocarcinomas (Williams and Lisanti, 2005). It has been proposed that prevalence of Cav-1 might serve as a prognostic indicator in these diseases and also in prostate cancers (Yang et al., 1999). Invasiveness of human breast cancer cells is positively correlated to Cav-1 abundance as is post-operative recurrence of lung cancer (Yoo et al., 2003). Up-regulation of Cav-1 may be a result of growth factor mediated serine-phosphorylation which renders the protein free to disassociate from the membrane leaflet and become secreted, possibly as part of an autocrine loop (Schlegel et al., 2001). Cav-1 is up-regulated in multiple myeloma (MM) and is implicated in interleukin-6 and vascular endothelial growth factor (VEGF) induced signalling, increasing survivability of MM cells and conferring steroid resistance. The gp130 signal transducing chain of the IL-6 receptor and Cav-1 are known to be found together in rafts. IL-6 induces Src-family kinase dependant tyrosine phosphorylation of Cav-1 in a process that can be inhibited by caveolae disruption and which is a factor in cell migration. In MM VEGF signalling is known to have a pivotal role in terms of growth and angiogenesis. Related outcomes in MM of VEGF signalling *in vivo* are immunodeficiency and bone destruction. There is increasing interest in Cav-1 as a

possible therapeutic target, most notably in multiple myeloma (Podar and Anderson, 2006).

Cav-1 binds cholesterol to form oligomers and cholesterol regulates *CAV* mRNA levels (Bist et al., 1997), (Fielding et al., 1997). Podar and Anderson have proposed reducing the level of membrane cholesterol to below the 40 mol% [the % cholesterol as a fraction of total molar weight of lipid] necessary for the formation of caveolae, by the use of statins to restrict proliferative signalling in MM cells. In contrast to cholesterol, overexpression of caveolin-1 increases membrane fluidity possibly (like ceramide) by displacing sterol from the bilayer (Cai et al., 2004).

Similarly, Tahir *et al* found that prostate cancer cells secrete Cav-1 and that the protein has anti-apoptotic and pro-angiogenic activity both *in vivo* and *in vitro* (Tahir et al., 2008*J*. They hypothesize that over-expression of Cav-1 by these cancer lines is a determinant of metastasis and suggest that Cav-1 as a paracrine factor may be a "paradigm applicable to other tumours that secrete Cav-1".

So it appears that a dual role for Cav-1 exists in cancer cells at least *in vitro* (Cohen et al., 2004). Tumour suppressing activity related to Cav-1 scaffolding domain and direct inhibition of G-proteins has been shown (Li et al., 1995), and the Cav-1 gene is repressed by DNA methylation at the onset of transformation. Later however, just prior to metastasis it is de-suppressed. It is logical to suppose that either directly through the

functions of caveolae or perhaps discreetly through autocrine signalling Cav-1 plays a role in metastasis and the proliferation of neoplasias.

1.3.3 CHOLESTEROL

Cholesterol has multiple roles in cancers. It can be used as a apoptotic marker during chemotherapy of mice given colon cancer xenografts (Kennealey P., 2005); inhibits viability of prostate cancer cells (Oh et al., 2010) and is reported to accelerate the development of mammary tumours in mice and act as a driver for metastasis (Llaverias et al., 2011). Exogenous cholesterol typically induces apoptosis in all cells, not only cancer cells, and much of the data relating cholesterol to cancer comes from the use of statins that are used to lower cholesterol levels *in vivo* with some positive outcomes for cancer patients before and after diagnosis (although this very much depends upon the type of cancer) (Moyad and Merrick, 2005), (Osmak, 2012). This implies a contradictory role for the sterol: induction of apoptosis and promotion of tumour development. This can be explained if the cholesterol is either free sterol or localised in microdomains that may produce a more global effect via cell signalling and gene expression. For example, cyclooxygenase-2 is associated with metastasis and resistance to apoptosis and cholesterol appears to regulate Cox-2 activity (Zhu W., 2009). This effect is biphasic and this too could be explained if low levels of cholesterol are unable to form rafts (and induce apoptosis) while higher doses initiate raft formation and so trigger metastasis.

Polyunsaturated fatty acids (PUFA), especially docosahexaenoic acid (DHA), have a propensity to displace cholesterol by means of its lower solubility and adverse packing arrangement (Wassall and Stillwell, 2009) wherein the hydroxyl moiety of the sterol is

displaced from the aqueous-facing layer to the middle (Harroun et al., 2006) and even inverted into the cytoplasm-facing layer of the membrane (Harroun et al., 2008). The aversion that cholesterol has for the DHA fatty chains has been proposed as a driver for the formation of cholesterol rich domains and highly disordered PUFA rich regions (Wassall and Stillwell, 2009). There is also some evidence that DHA can displace acylated proteins from lipid rafts and alter caveolae lipid and protein composition (Ma et al., 2004a). The steric incompatibility of DHA with sphingolipid and cholesterol can change the size and distribution of rafts and this appears to impact raft signalling (Chapkin et al., 2008), (Ma et al., 2004b), (Seo et al., 2006).

The amount and type of sterol in any given part of the membrane can also affect the functionality of the membrane bound signalling proteins by changing the lateral pressure profile – the local forces acting on the protein and so changing its conformation (Samuli Ollila et al., 2007).

An intermediate of sterol biosynthesis, lathosterol, can also cause the formation of rafts with dipalmitoylphosphatidylcholine (Wang et al., 2004) while lanosterol and desmosterol appear to lower lipid ordering to largely the same extent as cholesterol (Martinez et al., 2004). It is interesting that mice with an enzyme blockade preventing the final conversion of desmosterol into cholesterol, rendering them completely cholesterol-free animals, produced only a ‘mild phenotype’ and were viable (Wechsler et al., 2003). That said, there is evidence that altered cholesterol metabolism and in particular lipid-raft dysfunction may play a critical role in brain and CNS disorders

(Korade and Kenworthy, 2008). It is also known that cholesterol inhibition disrupts the formation of rafts and caveolae in 3T3-L1 cells and then affects insulin receptor activation (Sanchez-Wandelmer et al., 2009). In these cells cholesterol precursors do not maintain the insulin signalling cascade.

Bruno Segui *et al* in a review of sphingolipid involvement as cancer therapeutics points out that there are "several ways [for a cancer cell] to die and many ways to resist cell death" (Segui et al., 2006) Apoptosis, necrosis, paratosis, caspase-dependant and –independent cell death some of the possibilities each with different characteristics and biochemical signatures. Sphingolipids have been reported to be involved in at least apoptosis, necrosis, autophagic cell death and mitotic catastrophe.

It is clear that some lipids inhibit cancer cell growth while others facilitate growth. The gangliosides in particular are associated with apoptotic cascades and with multidrug resistance. Gangliosides are highly expressed by cancer cells and of these the most highly metastatic express the highest levels of sialic acid residue containing sphingolipids. Reduction of these sphingolipids using antisense vectors against ganglioside GD3 synthase or glucosylceramide synthase inhibit tumour growth and metastasis (Zeng et al., 1999), (Deng W., 2002). This correlation is true for at least neuroblastoma, renal carcinoma, breast carcinoma and melanomas. Their role in tumour development is multifold: increasing cell adhesion, functioning as ligands in transduction, and possibly binding with sialic moieties on blood cells (for example) via

sialic acid-binding immunoglobin-like lectins (Siglecs) that may assist a tumour to metastasize.

Sphingosine-1-phosphate (S1P) has protumourogenic and angiogenic properties and favours cell survival and tumour growth (Taha et al., 2006), (Hait et al., 2006). Cuvillier *et al* propose that S1P prevents ceramide-induced cytochrome C release and caspase-induced apoptosis (Cuvillier et al., 2001). It also stimulates VEGF and consequently sphingosine kinase-1 (English et al., 2002). It has long been a target for drug chemists and its' inhibition is the mode of action of some of the most valuable anti-neoplastic pharmaceuticals available to clinicians. This list includes Tamoxifen and Verapamil.

Example of a GCS inhibitor

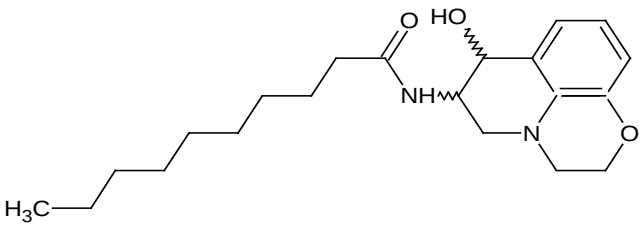

FIGURE 2: PDMP ENHANCES DOXORUBICIN-ELEVATED CERAMIDE.

Sphingolipids are able to initiate caspase activated apoptosis (Ogretmen and Hannun, 2004), caspase independent cell death (Kim et al., 2005) and possibly TNF-induced caspase independent death (Thon et al., 2005) – this latter function involves SMase.

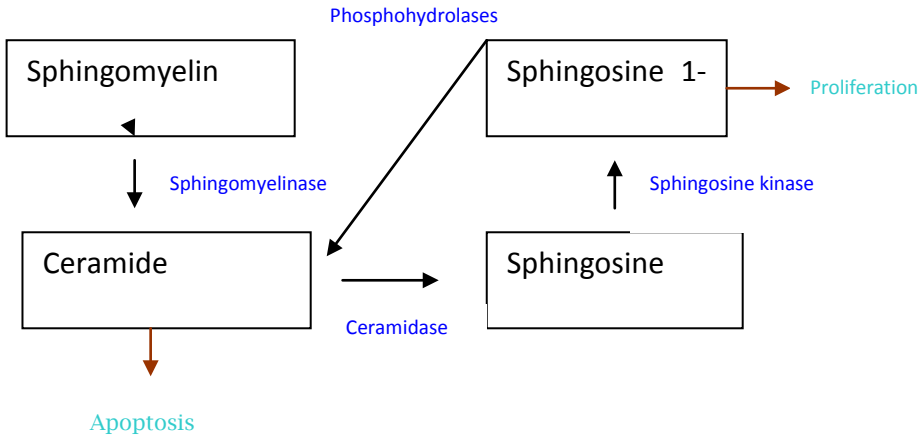

FIGURE 3: SPHINGOLIPIDS, CERAMIDE AND APOPTOSIS

Glycosphingolipid derivatives are also potential chemotherapeutics; structural analogues of glucosylceramide that are GCS inhibitors are able to reverse MDR and it is significant that clinical drugs that reverse MDR inhibit GCS (Lavie et al., 1997).

Glycosphingolipids, in particular gangliosides (sialic acid residue containing sphingolipids), appear to influence cell migration and adhesion (Bremer et al., 1984). GM3 inhibits EGF induced cell growth in A431 carcinoma line (Bremer et al., 1986) through inhibition of the receptor autophosphorylation. Sialidase gene transfection into these cells increases autophosphorylation. Meuillet *et al* describe the use of a ceramide analogue D-*threo*-1-phenyl-2-decannoylamino-3-morpholino-1-propanol (PDMP) which inhibits ceramide glucosyltransferase and this results in GM3 depletion and restores EGFR autophosphorylation to normal (Meuillet et al., 2000). By using this ceramide analogue and exogenous GM3 the authors were able to assess the impact of GM3 on receptor activation. Reduction of GM3 increases EFGR function in A431 and the reverse is also true. This suggests that gangliosides have a direct impact on EGFR. However, PDMP also increases ceramide levels in A431 cells and is known to modify membrane fluidity (Barbour et al., 1992) and moreover, Meuillet suggests that modulation of ganglioside levels could disrupt the membrane inclusions – specifically caveolae – where the EGFR is most prevalent. Likewise, it has been proposed that caveolae-based SMase is responsible for ceramide-induced apoptosis following irradiation (Veldman et al., 2001). Intracellular ceramide levels rapidly increase as part of the signalling cascade initiated by TNF, IL-1α and vitamin D3 (Mathias et al., 1998). This is mediated by ceramide-dependant protein kinase and type IIA phosphatase (Joseph et al., 1993).

1.4 DRUG INTERVENTIONS IN RAFT SIGNALING NOT RELATED TO CHOLESTEROL SIGNALING

The anti-tumour drug Edelfosine is an ether lysophospholipid analogue that induces the translocation of caspases-8 -9 -10 to rafts containing the Fas-associated death domain in leukemic cells. It also inhibits activation of ERK1/2, p38 MAPK and Akt/protein kinase B so inducing apoptosis (Na and Surh, 2008). Edelfosine has been found to promote the recruitment to rafts of Fas and CD95 death receptors and DISC in multiple myeloma cells. This apoptosis is inhibited by the depletion of cholesterol from the membrane (Gajate et al., 2009). It has been suggested that Edelfosine promotes the clustering of rafts into supra-molecular moieties that concentrate and act as scaffolds for apoptotic signalling (Gajate and Mollinedo, 2005).

Intervention in the composition of rafts and caveolae has produced interesting results. *n*-3 fatty acids were found to deplete rafts of cholesterol and sphingomyelin and increase ceramide levels. A decrease in cell proliferation and an increase in apoptosis was observed. This was associated with a decrease in raft bound epithelial growth factor receptor (EGFR). Likewise EGFR-related apoptosis is seen when cholesterol is sequestered by 2-hydroxypropyl-β-cyclodextrin. The drug Cisplatin has been shown to induce raft recruitment of the death receptor CD95 [Fas-ligand] in colon cancer cells and this is inhibited by the aSMase inhibitor Imipramine and the cholesterol sequestering drug Nystatin. Cisplatin activates aSMase and therefore ceramide production. This action correlates with a reduction of membrane viscosity and onset of CD95 mediated

apoptosis (Lacour et al., 2004). Cisplatin is used clinically to reduce tumour size, especially in lung carcinoma. Brusselmans *et al* propose squalene synthase SQS as a potential target for anti-cancer drugs (Brusselmans et al., 2007*)* and used anti-sense SQS oligonucteotides to significantly reduce *de novo* synthesis of cholesterol with an associated decrease in raft cholesterol levels. The sequences were: GAGGUUUGGAGCAGGUAUGdTdT and CAUACCUGCUCCAAACCUCdTdT. An attempt was made to use this second sequence in this study but was unsuccessful and is not reported. Lange and Ramos (Lange and Ramos, 1983) had earlier shown that membrane cholesterol is not in rapid flux with intra-cellular cholesterol and this could be the reason that membranes depleted of cholesterol by statins, siRNA or by cholesterol sequestering drugs such as Methyl-β-cyclodextrin (MBCD) are unable to quickly restore their homeostasis but may do so after drug treatment ceases. Filipin and MBCD have been shown to induce cancer cell death *in vitro* and *in vivo* (Zhuang et al., 2005). Griffoni *et al* succeeded in using anti-sense oligonucleotides to achieve a 70% reduction in Cav-1 mRNA (Griffoni et al., 2000). The application of these small interference mRNA were able to reduce the caveolae in HUVEC cells to undetectable levels using electron and confocal microscopy. Further, they reported that the use of siRNA sequences dramatically reduced capillary vessel formation in the chorio-allantoic chicken assay. They conclude that down-regulation of Cav-1 impairs angiogenesis. They deduced that the most active oligonucteotide (from the seven they tested) in supressing Cav-1 production was 5'ATGTCCCTCCGAGTCTA3' which is directed against nucleotides 20-36 of the mRNA open reading frame.

1.5 STATINS

Statins are structural analogues of HMG-CoA and they compete for binding with HMG-CoA reductase. They were originally discovered as fungal metabolites.

Statins (especially Simvastatin, Lovostatin, Atorvastatin, Fluvastatin, Rosuvastatin, Cerivastatin and Pravastatin) have been studied to see if their pro-apoptotic and anti-metastatic behaviour has therapeutic value in prostate and other cancers (Graaf et al., 2004). Elevated levels of circulating cholesterol promote tumour growth and reduce apoptosis in cancer cells (Hager et al., 2006). *In vitro* experiments point to a suppression by statins of growth in breast cancer (Kotamraju et al., 2007), colorectal (Agarwal et al., 1999), prostate (Sivaprasad et al., 2006), leukaemia (Xia et al., 2001) and lung (Khanzada U., 2005) and other cancer cells.

Further, the routine taking of statin based anti-hypocholesteraemia drugs is negatively correlated with both cancer related morbidity and mortality (Demierre et al., 2005).

The role of statins in metastasis on a molecular level has been recently reviewed by Papadopoulos *et al* (Papadopoulos et al., 2011). The idea that membrane rafts could be disrupted by statins and so used to impact raft-dependant signalling events has been suggested by others, notably Simons and Toomre as early as 2000 (Simons and Toomre, 2000).

Statins, through their truncation of the mevalonate pathway, disable the synthesis of isoprenoids. Without isoprenylation many important proteins such as Rho and Ras are unable to locate and anchor to the membrane where they must function. This is

another possible explanation of the anti-oncogenic activity of statins (Wang et al., 2008). The isoprenoid intermediate products resulting from targeted manipulation of the mevalonate pathway using statins, 6-fluoromevalonate, bisphosphonates, zaragozic acid and others has been reported (Henneman et al., 2011).

Statins are reported to have a biphasic impact on angiogenesis with low does increasing angiogenic markers and high doses reducing angiogenic activity (Weis et al., 2002). They have been shown to inhibit the *in vitro* invasion of human breast cancer cells (Denoyelle et al., 2001), human pancreatic cells (Kusama et al., 2001), brain glioma cells (Gliemroth et al., 2003) and melanoma cells (Collisson et al., 2003). This effect was reversible in breast and pancreatic cells (Farina et al., 2002) by supplementation of geranylgeranyl pyrophosphate indicating that inhibition of isoprenylation is of key importance in these cell types.

One possible mechanism that has been proposed is that insulin growth factor receptor (IGF-1R), known to have a role in the proliferation of prostate cancer cells (Pollak et al., 1998) is depleted by the exposure of cells to statins. Statins have also been studied for their anti-metastatic functionality in prostate cancer via their down regulation of insulin-like growth factor 1 (IGF-1) receptor (Sekine et al., 2008). Here, IGF regulates the growth of prostate cancer cells and inhibition of IGF-1R (by anti-sense) suppresses tumour growth and reduces metastasis (Reinmuth et al., 2002). Cholesterol depletion by statins to effect an IGF blockade was proposed by Sekine *et al* (Sekine et al., 2008) as a possible treatment for prostate cancer.

De novo production of cholesterol is undertaken by the mevalonate/isoprenoid pathway. Squalene synthase (SQS) is the enzyme that triggers the switch to the sterol biosynthetic branch of the pathway and as such is a determinant of cell membrane concentration.

Pathway assembled from multiple references (Swinney et al., 1994), (Walker et al., 1993), (Korosec et al., 2008).

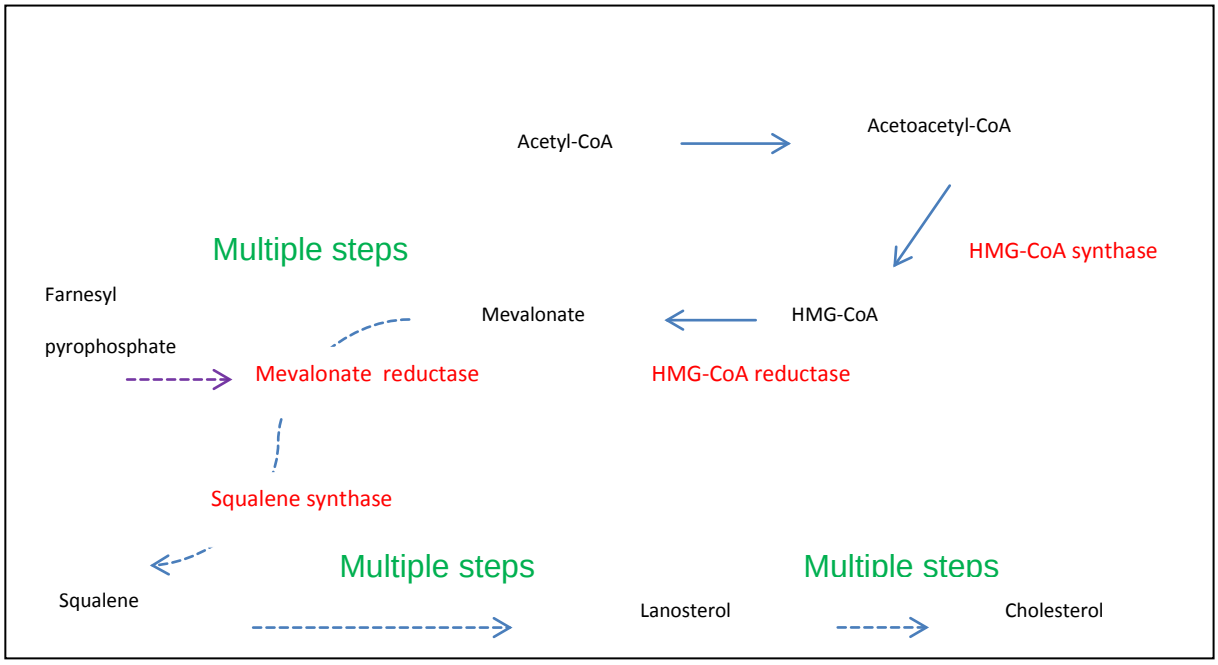

FIGURE 4: SIMPLIFIED CHOLESTEROL SYNTHESIS PATHWAY

to become acetoacetyl-CoA. HMG-CoA synthase converts acetoacetyl-CoA into HMG-CoA which is the feedstock for the mevalonate pathway. It is this molecule that statins mimic and thereby bind competitively with HMG-CoA reductase, the rate limiting enzyme in the formation of mevalonate. There is evidence that this pathway can be directly activated by up-regulation of gene expression of all the subsequent enzymes by

a family of transcription factors called sterol regulatory element binding proteins (Weber et al., 2004).

Mevalonic acid is metabolised to geranyl pyrophosphate and farnesyl pyrophosphate that can then be used for iso-prenylation of proteins – including activation of the Ras/Rho pathway – and the synthesis of ubiquitin. These secondary effects are blocked by statins and it has been assumed that these (as opposed to the lowering of cholesterol *per se*) have been uniquely responsible for the anti-cancer effects observed (Sebti, 2005), (Andela et al., 2003). Other cholesterol inhibitors, notably Proadifen (diethylaminoethyl diphenylpropyl acetate) (Holmes and Bentz, 1960), have a profound membrane fluidizing effect (Swenson E.S., 1992) *in vitro* compared to the statins and this property may augment their ability to disrupt raft or caveolae domains.

1.6 Rafts and gene expression

1.6.1 Oncogenes

Dysregulation of transcription factors involved in signal transduction is a likely consequence of cholesterol raft de-population since the expression of many genes is responsive to external stimuli – such as hormones – mediated across the bilayer. This is a consequence of the eukaryotic cells' devolution of control to external chemical semiotics that inform the nucleus of the environmental status. The response of the nucleus, in terms of gene expression, can be dysregulated by interference with the signal transduction through truncation of the signal pathway at the membrane. One possible effect of such dysregulation could be intracellular accumulation of

transcriptional regulators. In multiple myeloma for example, the proteasome inhibitor drug Bortezomib causes a build-up of NF-κb inhibitor IκB which (indirectly) activates apoptotic pathways. Similar effects are conceivable if autocrine/ paracrine loops are interrupted by reduced signalling at the membrane-raft transduction sites (specifically receptor tyrosine kinases (RTK) and G-coupled proteins that are known to occupy these sites).

Most oncogenes contribute to cell transformation because their products are regulatory growth factors or transcription factors. These include growth stimulating genes such as *PDGF*. Roughly 30% of oncogenes code for protein kinases which are recruited to the inner layer of the cell membrane where they mediate signal protein phosphorylation. This is a characteristic shared with several autocrine/paracrine growth factors. The metastatic phenotype is independent of the tumourigenic –phenotype and this characteristic has been reviewed by Liotta (Liotta, 1988). One of the most studied oncogene families is *Ras* or Ras^{H} gene. Transfection of this gene into non-metastatic cancer cells leads to an increase in the intrinsic aggressiveness of these cells by means of a cascade of gene expression leading to full metastatic conversion (Egan et al., 1987). *Ras*, for example, does not cause *Ras*-transfected cells to proliferate faster (*in vitro* or *in vivo*) but there is a difference in the invasiveness of the transfected cells. It enables the cells to grow in serum depleted media – i.e. it allows the cells to produce autocrine growth factors, and this is a crucial metastatic step. This behaviour of *Ras* is associated with a significant up-regulation of p21 protein and the expression of this protein correlates well to the transfected cell's metastatic potential (DeFeo et al., 1981). High

expression of p21 leads to very high *in vivo* metastasis – intravenous injection of 5 x 10^4 normal cells appropriately transfected with oncogene and enhancers can produce over 200 metastases in the lungs of mice (Nicolson, 1987). Lymphoma cells (such as the BJAB line used in these experiments) show no requirement for collagenases or laminin receptors for their invasiveness but these proteins are up-regulated after transfection with *ras* and lymphoma cells are then able to attach to and invade collagen-containing tissue. It is clear that the activation of oncogenes is a critical step in the evolution of a tumour cell into an invasive metastatic cancer.

RTK are a group of ligand binding proteins that normally act as receptors for growth factors and hormones such as EGFR, VEGFR and PDGFR. Kinase inactivation blocks production of all down-stream signalling molecules including *c-myc* and *c-fos*. PDGF receptor activation would normally be followed by phosphorylation of *src* family proteins and increase of *src* kinase activity. *src* proto-oncogene is associated with numerous types of cancer.

1.6.2 TUMOUR SUPPRESSOR GENES

Interestingly, when *p53* was first discovered in 1979 it was thought to be an oncogene but is actually a tumour suppressor gene. This type of gene is associated with negative control of proliferation. Inactivation of *p53* (and others) is linked to tumour development in many cancers e.g. small cell lung cancer. Thus tumour cell proliferation is governed by the competing forces of oncogenes and growth suppressors. An accumulation of genetic changes both in oncogenic and suppressor genes are early but necessary steps towards metastatic cancer.

Lipid metabolism interventions (by gene knock-down) and effects on cancer cells

Effect of Intervention	**Cell Type**	**Consequence**
Decrease of glycosyl ceramide	Murine melanoma; MCF-7 breast cancer	Reduction of tumourogenicity (Deng W., 2002) and restoration of drug induced apoptosis (Liu et al., 2004)
Increase in GD3 expression	Human leukaemia	Increase in apoptosis (De Maria et al., 1997)
Increase in GM3	Murine carcinoma	Increase in apoptosis (Watanabe et al., 2002)
Increase in ganglioside sialidase	Murine melanoma	Reduction of metastasis (Tokuyama S., 1997)
Reduction of sphingomyelin	Murine lymphoma	Resistance to anti-FAS induced apoptosis (Miyaji et al., 2005)
Increase of C-18 ceramide	Human squamous cell carcinoma	Induction of apoptosis (Koybasi et al., 2004)
Decreased S1P	Murine NIH3T3 fibroblasts; human HEK293 kidney; human PC-3 and LNCaP prostate cancer	Increase in apoptosis (Mandala et al., 2000), (Le Stunff et al., 2002), (Pchejetski et al., 2005)
Increase in S1P	Human Jurkat leukaemia; human PC-3 and LNCaP prostate cancer	Inhibition of ceramide induced apoptosis (Olivera et al., 1999), (Pchejetski et al., 2005)

TABLE 2: EFFECTS IN CANCER OF GENETIC CHANGES TO LIPIDS

2 MATERIALS AND METHODS

2.1 CELL LINES

All experiments were conducted using either one or two cell lines. The main line studied was MDA-MB-231. This line is a human breast adenocarcinoma that grows in monolayer. It was taken from a Caucasian woman of 51 years by pleural effusion (Cailleau et al., 1974). To compare the effect of Proadifen on a non-adherent line, the Burkett's lymphoma BJAB cell line was also used in one analysis of the proteome by microarray. In the final series of assays a third cell line, a grade 3 human lung carcinoma called CaLu-1 was included. All cells were obtained from Cell Lines Service, Eppenheim, Germany.

2.2 TEST AGENTS

Most of the test compounds were sourced from chemical suppliers (see Table 4 Page 53). Those that were synthesized by the author and those analogues prepared in contracted laboratories were tested for structure and purity by NMR. The primary test agent was *N,N*-diethylaminoethyl 2, 2-diphenylethanoate hydrochloride (Proadifen) known to inhibit the final stages of cholesterol biosynthesis, leading to a build-up of the precursor lanosterol. It is known to be surface-active in artificial membranes (Anders and Mannering, 1966) and has been studied in the context of cholesterol regulation and therapeutic enhancement (Fernandez et al., 1978), (Brodie et al., 1958), (Galeotti et al., 1983), (Ravis and Feldman, 1979), (Fouts and Brodie, 1956). It was observed that this compound prolonged the hypnotic action of hexobarbital in rats and mice without altering the toxicity (Cook et al., 1954). It was later found that this effect occurred in combination with secobarbital, pentobarbital, butethal, ortal, phenobarbital and chloral hydrate (Anders and Mannering,

1966). By contrast, no synergistic effect was discernible with barbital and thiopental, thioethamyl and methylparafygol. Thus, this enhancement effect is difficult to predict - it does inhibit the de-methylation of neperidine but not of N-methylaniline or N-ethyl aniline.

TABLE 3: PRIMARY TEST AGENTS USED IN THIS STUDY

Commercially available drug	Experimental use in this study	Biological activity
Nocodazole	Phagokinetic track experiment	Used as a positive control as it prevents the formation of microtubules. This part of the cytoskeleton is essential for the cells motility.
Proadifen	All experiments	Possible Δ24 reductase inhibitor. Membrane fluidizer and drug potentiator
Fluphenazine	All experiments	A piperidine phenothiazine used in medicine since the 1970s as an anti-psychotic in the treatment of schizophrenia. Currently in clinical trials against some blood cancers. Believed to alter DNA turnover and may affect hormone expression.
Pravastatin	Cav-1 assay, RNA assay and cholesterol assay	A typical cholesterol lowering statin and is approved for use in humans. Like all statins it is an inhibitor of 3-hydroxy-3-methyl-glutaryl-CoA reductase and so acts as a blockade of the isoprenoid pathway by preventing the synthesis of mevalonate and, in turn, squalene.
Simvastatin	Cav-1 assay and anti-Tub-1 assay	Typical HMG-CoA inhibiting treatment for hypercholesteremia. Very similar to Pravastatin.
AY9944	Cav-1 assay , proteomic assay and cholesterol assay	An amphiphilic diamine that blocks cholesterol synthesis by inhibiting 7-dehydrocholesterol reductase and Δ7, Δ8 isomerase. It is a teratogen. Used to help locate the blockade point of Proadifen
BIB515	Cav-1 assay and cholesterol assay	A specific inhibitor of 2,3-Oxidosqualene cyclase preventing the conversion of [3S]-oxidosqualene to lanosterol. Used to help locate the blockade point of Proadifen
Triparenol	Cav-1 assay	Δ24-dehydrocholesterol reductase. Used to help locate the blockade point of Proadifen
Ro-48-8071	Cholesterol assay	Inhibitor of oxidosqualene cyclase – causes a reduction in cholesterol similar in range to Simvastatin
BIBX1382	Cholesterol assay	Specific epidermal growth factor inhibitor considered as anti-tumour agent
Ergoesterol	Cholesterol and Cav-1 assay	Simulates a Δ-24 reductase inhibitor by competitive inhibition.
Methyl β-cyclodextrin	Proteome assay, Cav-1 assay, cholesterol assay and RNA assay	Cyclic oligomer of glucose able to entrap cholesterol in its hydrophobic core and specifically sequester the sterol from the membrane (Rodal et al., 1999).
Clotrimazole	Anti-Cav-1 assay and cholesterol assay	Anti-fungal imidazole compound that induces apoptosis in breast cancer cells, disrupts glycolysis and interferes with Ca^{+} ion transport across the plasma membrane
D-erythro-MAPP	Galactin-8 assay	Inhibits ceramidase and elevates endogenour ceramide leading to apoptosis (Bielawska et al., 1996)
BM15766	Cholesterol assays	Piperazine derivative that, like AY9944, inhibits Δ7 reductase leading to an accumulation of 7-dehydrocholesterol and 8-dehydrocholesterol (Lindenthal et al., 2002).

Table 4: Solvents and stock concentrations of test agents

Agent	Stock concentration	Solvent	Notes	Source
Methyl-β-cyclodextrin	0.05% w/v	100% Hanks Balanced Salts (Hanks)	Cholesterol sequestrator	Sigma Chemicals Ltd
Cholesterol	0.1M	20% Dimethylsulfoxide (DMSO); 40:40 (v/v Hanks: ethanol)		Sigma Chemicals Ltd
AY9944	0.007M	100% Dimethyl sulfoxide	(trans-N,N-bis[2-Chlorophenylmethyl]-1,4-cyclohexanedimethanamine HCl	Tocris Bioscience Ltd
Fluphenazine	0.01M	10% Ethanol in Hanks		Sigma Chemicals Ltd
Clotrimazole	0.02M	50:50 v/v Ethanol: Hanks		Sigma Chemicals Ltd
Proadifen	0.015M	100% Hanks	2-(N,N-diethylamino)ethyl 2,2-diphenylethanoate	Dynthesized by DG
Pravastatin	0.01M	100% Hanks		Sigma Chemicals Ltd
Ergosterol	0.1M	Chloroform:DMSO:Dulbeco's saline 50:30:20 v/v/v		Sigma Chemicals Ltd
VL15	0.05M	Dichloromethane:DMSO: Phosphate buffered saline 20:30:50 v/v/v	2-(N-ethylamino)ethyl 2,2-diphenylpentanoate	Synthesised by DG
VL20	0.01M	Ethanol:DMSO:Dulbeco's saline 20:10:70 v/v/v	2-(Diethylamino)ethyl 2-phenylethanoate	Synthesised by DG
2,2-Diphenyloctanoic acid amide	0.01M	100% DMSO		Synthesised by Leksing Ltd
2,2-Diphenylheptanoic acid amide	0.01M	100% DMSO		Synthesised by Leksing Ltd
2,2-Diphenylhexanoic acid amide	0.01M	100% DMSO		Synthesised by Leksing Ltd
2,2-Diphenylpentanamide	0.01M	100% DMSO		Synthesised by Leksing Ltd
2,2-Diphenylpentanoic acid morpholino ethyl ester	0.1M	Dulbeco's buffered saline		Synthesised by Leksing Ltd
2,2-Diphenylpentanoic acid	0.1M	Hanks		Synthesised by Leksing Ltd
3-(Diethylamino)propyl 2,2-diphenylpentanoate	0.1M	Hanks		Synthesised by Leksing Ltd

2-(Piperidin-1-yl)ethyl 2,2-diphenylpentanoate	0.01M	Hanks		Synthesised by Leksing Ltd
BIBB515		DMSO	1-(4-Chlorobenzoyl)-4-[[4-(4,5-dihydro-2-oxazolyl)phenyl]methylene]-piperidine	Cayman Chemicals
BIBX1382		DMSO	N-(3-Chloro-4-fluorophenyl)-N-(methyl-4-piperidyl)-pyrimido[5,4-d]pyrimidine-2,8-diamine .2HCl	Tocris Bioscience Ltd
Ro48-8071		Methyl acetate/Dulbeccos 0.25mg/ml	(4-Bromophenyl)[2-fluoro-4-[[6-(methyl-2-propenylamino)hexyl] oxy]phenyl]-methanone	Cayman Chemicals

2.2.1 PROADIFEN ANALOGUES TESTED, SYNTHESIZED *DE NOVO*

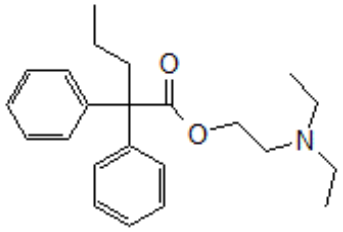

2-(diethylamino)ethyl
2,2-diphenylpentanoate
Proadifen
Molecular Weight: 338.46

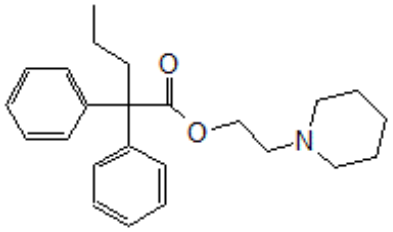

2-(piperidin-1-yl)ethyl
2,2-diphenylpentanoate
Molecular Weight: 365.51

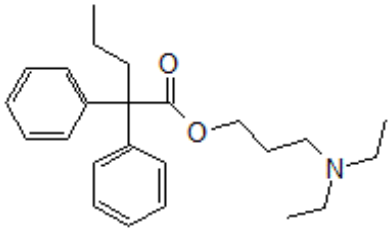

3-(diethylamino)propyl
2,2-diphenylpentanoate
Molecular Weight: 367.52

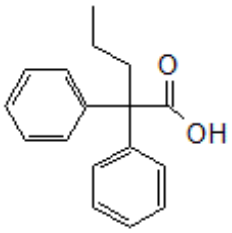

2,2-diphenylpentanoic acid
Molecular Weight: 254.32

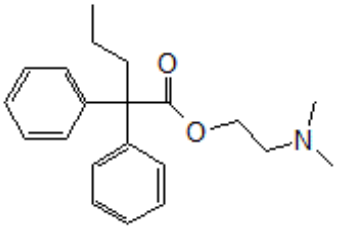

2-(dimethylamino)ethyl
2,2-diphenylpentanoate
Molecular Weight: 325.44

FIGURE 5: PROADIFEN AND ITS ANALOGUES

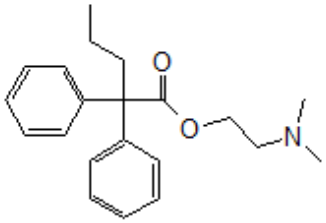

2-(dimethylamino)ethyl
2,2-diphenylpentanoate

Molecular Weight: 325.44

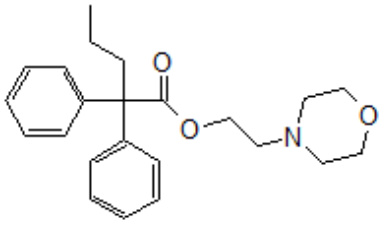

2-morpholinoethyl 2,2-diphenylpentanoate

Molecular Weight: 367.48

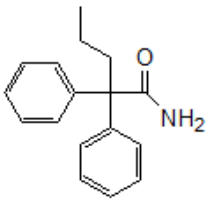

2,2-diphenylpentanamide
Molecular Weight: 253.34

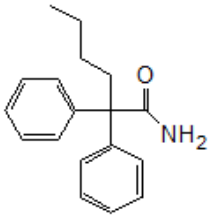

2,2-diphenylhexanamide
Molecular Weight: 267.37

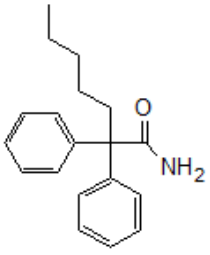

2,2-diphenylheptanamide
Molecular Weight: 281.39

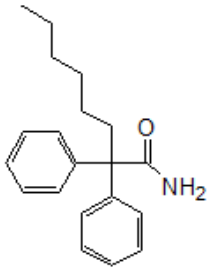

2,2-diphenyloctanamide
Molecular Weight: 295.42

FIGURE 6: ADDITIONAL PROADIFEN ANALOGUES

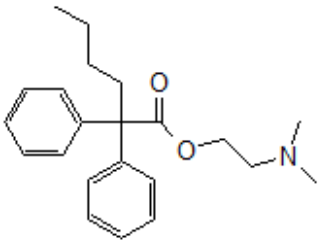

2-(dimethylamino)ethyl
2,2-diphenylhexanoate
Molecular Weight: 339.47

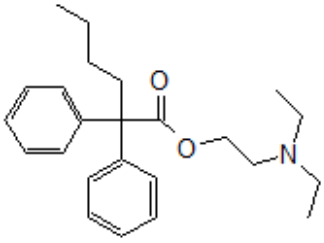

2-(diethylamino)ethyl
2,2-diphenylhexanoate
Molecular Weight: 367.52

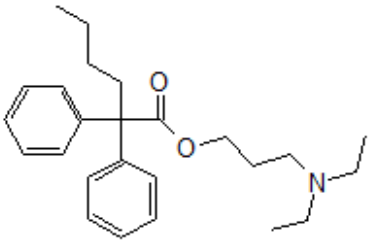

3-(diethylamino)propyl
2,2-diphenylhexanoate
Molecular Weight: 381.55

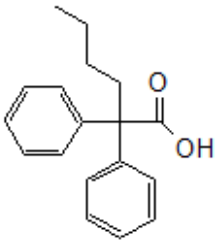

2,2-diphenylhexanoic acid
Molecular Weight: 268.35

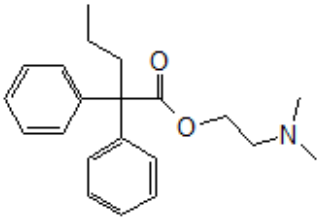

2-(dimethylamino)ethyl
2,2-diphenylpentanoate

Molecular Weight: 325.44

FIGURE 7: ITERATIVE DERIVATIVES BASED ON C5 AND C6

2.2.2 DOSES

The dose is the final concentration in the treatment media. In the case of the statins these were chosen to be equivalent to the plasma statin concentration in patients receiving the maximum standard dose of statin. For example, in the case of Simvastatin this dose is normally no more than 80mg/day (BNF, 2012). In the case of Proadifen the original work from the 1950's indicated the maximum tolerated dose *in vivo* (rats) and this was used in most experiments (Fouts and Brodie, 1956). In one proteomic assay, a dose of 10x this level of Proadifen was used without significant toxicity to see if there additional response. Proadifen analogues were treated as though they were Proadifen in the absence of any clinical or animal data. No significant toxicity was observed but in the proteolysis assay the data were scaled by a cell viability test to exclude toxic effects. All other compounds were used according to their maximum solubility in media or PBS, or according to manufacturer's application notes.

2.3 ASSAYS

For many years, the mainstay of experimental work on anti-cancer drugs was a simple growth assay performed on cell monolayers (Eccles, 2001). Such a proliferation based assay can reveal some effects of research drugs but is best suited to cytotoxic drugs such as the alkylating agents. They are very useful in high throughput screens, but they do not help elucidate the more subtle and the more complex effects of the test agents, and teach little about the metastatic potential of the cells under treatment. Clearly the ideal assay to study multiple attributes of a treatment is *in vivo* and typically involve intravenous introduction of metastatic lung (or breast) cells into mice or rats and then

specialised imaging techniques (or dissections) to monitor tumour spread and growth. The conditions in an *in vitro* assay can never fully model the environmental and metabolic effects of a whole animal but some *in vitro* assays have been designed to elucidate the effects of drugs on particular metastatic phenomena such as motility, protease secretion, cell adhesion, de-adherence, angiogenesis etc.

Typically these involve a highly invasive cancer lines. For example, in a study of organo-metallic half-sandwich RuII compounds, the chosen cell lines were MDA-MB-231 and MCF-7 which proved highly useful (Bergamo et al., 2010). Here, HBL-100 non-tumourogenic human epithelial cells were used as the control line. This is the reason why MDA-MB-231 was used as the main cell type in these experiments. The human lung carcinoma CaLu-1 also used in this study is likewise known to be a highly invasive cancer. In theory, however, any aggressive cancer cell should be amenable to these test protocols.

2.3.1 PHAGOKINETIC TRACK ASSAY

In these experiments motility of MDA-MB-231 cells was determined by measuring the size of a phagokinetic track in a carpet of gold colloid over time. It is a variation of the method described by Niinaka *et al* (Niinaka et al., 2001). Briefly, the gold colloid is prepared by boiling 11ml water, 6ml 36.5mM Na_2CO_3 and 1.8ml 14.5mM $AuCl_4H$. To this hot mixture 1.8ml of 0.1% formaldehyde is added. Within a few seconds there is a colour change from clear to dark purple and the colloid is ready for immediate use.

Extra-large coverslips were dipped into sterile 1% BSA solution and then dipped again into 100% ethanol. These are then air-dried. These slides were placed individually in the centre of a 90mm Petri dish and the colloid is pored over the slide coverslip until one side is completely immersed. These are left for 24 hours at r.t. and then removed using forceps and air-dried again at 37^{o}C. When dry they are individually placed in the centre of a fresh Petri dish and the cell suspension (+/- treatments prepared as described earlier) is pipetted directly onto the coverslip at 1ml per slip. The dishes are covered and incubated for 24 hours before being examined with a brightfield microscope by removing the coverslip and inverting it onto a clean microscope slide. Individual tracks can best be seen at x400 but a field of view at x100 is most suitable for image analysis.

2.3.2 LIGHT MICROSCOPY

These images are representative samples of photomicrographs taken of treated and untreated MDA-MB-231 cells after 24 hours, post passage.

2.3.3 ELECTRON MICROSCOPY

Cells were grown in 12 well plates each containing a piece of pre-sterilised (with 75% alcohol) acetate approximately 2mm x 3mm. Cells were cultured in the normal way and after trypsinisation, centrifugation and re-suspension they were pipetted gently onto the surface of the acetate. The wells were covered with fresh media containing 10% FBS and either of PBS, Proadifen, AY9944 or MβCD and placed in an incubator at 37.5^{o}C for 24 hours. The acetate strips were removed with forceps and washed in PBS and then for 1 hour steeped in 1% glutaraldehyde and sodium cacodylate. These were then

successively treated at the Keele Electron Microscopy Unit, with ruthenium tetroxide, thiocarbohydrazide, osmium tetroxide, thicarbohydrazide and osmium teroxide (RTOTO method (Kutz et al., 1985)) prior to scanning in an Hitachi S4500 machine, or for TEM, a JEOL1230 at between +1 and +30kV. The treatment doses of these cultures were as follows: Proadifen 16μM; MβCD 0.00083%; AY9944 8μM.

2.3.4 PROTEOMIC ANALYSIS METHODS

These experiments were conducted on MDA-MB-231, an adherent breast cancer line known to be highly metastatic and BJAB Burkett's B-lymphoma cells, a transformed cell line that grows in suspension.

The purpose of the experiment was to determine what effect a large dose of the test agent would have on signal proteins and other cancer related proteins in these two cell lines. 656 proteins were analysed from whole cell lysates including a range of cancer markers, proteins associated with metastatic potential, angiogenesis and apoptosis markers. A large number of other proteins were also included in the assay. Some signalling proteins are known to be located in cholesterol rich rafts and these are listed in Table 1 while others have an unknown location in the membrane. Many of the 656 proteins are cytoplasmic and are therefore outside the scope of this study. However, many of these are likely to be directly or indirectly responsive to membrane-bound signals.

Antibody arrays provide high-throughput screening platforms for accurate protein expression profiling and their application lends itself to tissue samples and cell lysates.

2.3.4.1 PRINCIPLE

Antibodies are covalently immobilized on glass slides in duplicates. Multiple positive markers (Cy3 fluorophore) and negative controls (BSA) are included on the array and provide internal references. Cells from treated and control groups are lysed and the protein content extracted and measured. The proteins are then biotinylated and conjugated with the antibodies on the array. The slides are washed and then detected with Cy3-steptavidin in a classic 'probe sandwich' using a microarray laser scanner at 480nm.

2.3.4.2 PROCEDURE

MD-MBA231 cells were cultured in Dulbeco's MEM + 10% FBS with stabilized antibiotic-antimycotic. Final concentration contained 100,000 units penicillin G, 100mg streptomycin sulphate and 0.25mg amphotericin B per litre of media. All cells were subject to a 4 day passage regimen. BJAB cells were cultured in MEM + 10% FBS + stabilized antibiotic-antimycotic in Nunc 175cm^2 flasks in 5% CO_2 at 37^{o}C.

2.3.4.3 TREATMENTS

Treatment comprised *N,N*-diethylaminoethyldiphenylethanoate hydrochloride made up in Hank's Balanced Salt solution to give a final concentration in the media of 10µM and 100µM. AY9944 and Pravastatin were also tested in this assay with MDA-MB-231 cells

but not BJAB. Control flasks contained only the same volume of Hanks solution. Test solutions were made up freshly and brought to 37^{o}C immediately prior to treatment.

All chemicals and media were purchased from Sigma Chemicals, UK except where specified. The antibody array slides and associated reagents were purchased from Full Moon Biosystems Inc, USA.

Treatment and control solutions each were added directly to three culture flasks at 80% of confluence for 24 hrs prior to harvesting. Cells from each triplicate were pooled after the trypsinisation step. The tests were performed in accordance with the manufacturers' protocols (Bioscience). Briefly, 1 x 10^{6} MDA-MB-231 cells were harvested from the flasks using Trypsin (Bovine pancreas)-EDTA solution made up to 25g Trypsin in 1 litre of DMEM. BJAB cells were centrifuged without further treatment. Cell pallets were then washed in 5ml phosphate buffered saline (PBS) three times with aspiration and re-centrifugation steps at room temperature. The cells were then washed a final time in PBS at 4^{o}C in 1.3ml Eppendorf tubes. To each tube was added 1 tube of Full Moon Biosystems lysis beads and 250µl Extraction Buffer. This was vortexed for a total of 6 minutes in 1 minute stages over an hour while between vortexing the samples were kept on wet ice. The cells were then re-centrifuged at 15000 rpm at 4^{o}C for 15 minutes. The clear supernatant was then discarded.

The protein concentration was assayed using a BCA protein assay kit at this stage. 1mg of biotin reagent was dissolved in 100µl *N,N*-Dimethylformamide. The protein solution was reduced using a vacuum-orbital evaporator until the protein concentration per

100µl is 400µg protein. 25µl of this solution is mixed with 25µl of labelling buffer and 1.5µl of the biotin-DMF solution. This is incubated with shaking at room temperature for 2 hours.

Each tube of protein is added to 6ml of the coupling reagent and vortexed. This is poured gently over the array slide in a Petri dish until the slide is submerged. This was rocked at room temperature for 1 hour. The slide was then washed with the wash solution twice and rinsed with Chromasolv™ grade water. The slide was immediately submerged in 30ml of Cy3-streptavidin solution and incubated with rocking for 10 minutes. It was then extensively washed in the wash solution three times and finally in Chromasolv™ grade water. After drying with N_2 the slide was read in the array scanner.

2.3.4.4 STATISTICAL TREATMENT

Each assay was run once with three technical replicates. The graphs of the mean results are plotted for the marker set of proteins with error bars showing ± the standard error which is derived from the coefficient of variation.

2.3.5 CELL-MATRIX ADHERENCE METHODS

This assay was found to be amenable to the cells and to the treatments and was used to monitor the effects of Proadifen on the re-adherence of newly passaged cells onto the culture flask surface over time. The assay was augmented with a simple kit to detect cell death and necrosis to examine if those cells that remained attached to the plate were indeed living or showing signs of injury or death.

Cells were maintained and treated as previously described. The water soluble nuclear stain aniline blue was used to permit the use of the plate reader to measure cell density at 500nm. The plate reader was a Biochrom Expert Plus with computer interface. In each of the cell re-attachment / attachment tests all liquid (containing any free floating cells) from the well was gently removed using a pipette prior to scanning.

Necrosis and apoptosis were detected using an Enzo Life Science detection kit. Apoptosis is detected using an Annexin V-Cy3 conjugate that binds to phosphatidylserine on the outside of the cell wall. Necrosis is detected by loss of integrity of the plasma membrane and generates a far red emission signal localized to the nucleus. This is done using a membrane impermeable DNA intercalating dye 7-AAD. Thus, the treated 96 well plates are scanned at two wavelengths: E*x*/E*m* 550/570 for the Annexin probe and E*x*/E*m* 546/647 for the 7-AAD. Although these signals are sufficiently distant to be multiplexed, in these experiments separate scans were performed in less than one minute.

2.3.6 RNA EXPRESSION PROFILING METHODS

The purpose of including this kind of analysis in this study was to try to reveal more about the mechanism by which a cholesterol inhibitor actually reduces or enhances the level of any given protein. The protein antibody array data provides only the quantity of protein available to the antibody but this increase or decrease in protein can arise from either increased or decreased feed-stock up-stream in the canonical pathway but it may be due to an up-regulation of part or all of the pathway components and substrates. Using the same treatments, cells and conditions described in Proteomic Analysis (Page 66) an expression profile of some 47,000 genes (or gene elements) was obtained to determine if instruction signals to the DNA were the origin of the protein shifts observed.

2.3.6.1 PROTOCOL FOR THE RNA EXPRESSION PROFILE ASSAY

Determination of mRNA expression of proteins can now be accomplished using Illumina bead-chip assays and this was performed by Gen-Probe Inc, San Diego, USA.

2.3.6.2 METHODOLOGY OF CELL TREATMENT FOR MRNA ASSAY

Cells were treated in 3 x 174ml culture flasks (Nunc) containing 40ml of Dulbeco's DMEM with 10% (v/v) FBS per treatment. Negative control flasks contained only the FBS supplemented media. Primary treatments were Pravastatin, Proadifen and MβCD. Opportunistically, two additional treatments were added: lysophosphatidylcholine (LPC) known to fluidize cell membranes and the phenothiazine Fluphenazine which is a candidate anti-cancer treatment. Treatments were 24 hours and treatment start time was 24 hours after sub-culture. Incubation was at 5.0% CO_2. Cells from each treatment were harvested with trypsin 10% w/v and immediately spun down to a cell pellet. The cells were then re-suspended in PBS containing 0.1% of Sigma Protease inhibitor cocktail and then re-centrifuged. The resultant cell pellet was then stored in LN_2 prior to RNA extraction.

2.3.6.3 RNA PURIFICATION USING THE QIAGEN RNEASY MAXI KIT

7.5ml of Buffer RLT was added to each pellet and then the suspension was homogenised using a needle and syringe. Each sample was transferred to an RNeasy column and placed in a 50ml centrifuge tube. This was spun for 5 minutes at 3000-5000 x g. The flow through was discarded. 15ml of Buffer RW1 was added to the column and it was further centrifuged for 5 minutes. The flow through was discarded. This operation was repeated with Buffer RPE for 2 minutes and then again for 10 minutes. The column was then placed in a fresh collection tube and the RNA eluted into 150µl of RNA free water by further centrifugation under the same conditions.

2.3.6.4 PREPARATION OF POLY-A CONTAINING MRNA USING THE MRNA-SEQ SAMPLE PREP KIT (QIAGEN)

This protocol uses poly-T oligo-attached magnetic beads. Briefly, the beads are prepared in buffer as per the manufacturer's instructions. The RNA samples are heated for 5 minutes at 65^{o}C and then placed on ice. The beads in Bead Binding Buffer are added to 50µl of total RNA and the supernatant removed after 5 minutes. 50µl of 10mM Tris-HCl is added and then the tubes are heated to 80^{o}C for 2 minutes. Then the tubes are placed on the magnet leaving the supernatant containing the mRNA. The samples are further heated and washed to elute mRNA from the beads yielding 10-20µl mRNA.

16µl mRNA is then added to the fragmentation buffer (4µl) and the tubes are incubated in a PCR thermal cycler at 94^{o}C for 5 minutes. 2µl of stop buffer is added and the samples are placed on wet ice. 3M NaOAC (pH5.2) 2µl, glycogen (2µl) and 200 proof ethanol (60µl) is then added to the tubes and these are then centrifuged at 14,000rpm for 25 minutes at 4^{o}C. The pellet of RNA is then washed with 70% ethanol and then air dried for 10 minutes.

2.3.6.5 RNA QUANTIFICATION

RNA quantification was performed by absorbance (OD A260nm) on the NanoDrop™ 1000 (Thermo Fisher). 2 x 1µL aliquots were analysed and the mean concentration calculated using a conversion factor of 44.6. The A260/A230nm and A260/A280nm purity ratios were also determined.

2.3.6.6 RNA NORMALIZATION

RNA was normalised to 50ng/µL in a 20µL final volume using RNase-free water. Samples were formatted into a low volume 96-well plate and passed to Gen-Probe Ltd for genotyping.

TABLE 5: RNA CONCENTRATIONS AND DNA YIELDS

Source Sample /ID	Final Stock RNA conc. (ng/µL)	A260/A280 Ratio	A260/A230 Ratio	Total Estimated Yield of Stock DNA (µg)
Proadifen A1	413.8	2.110	2.636	413.8
Proadifen A2	570.6	2.123	2.808	570.6
Proadifen A3	653.8	2.133	1.365	653.8
Proadifen A4	448.3	2.103	3.619	448.3
Pravastatin B1	525.7	2.140	1.874	525.7
PravastatinB2	761.0	2.129	0.961	761.0
PravastatinB3	652.8	2.132	2.998	652.8
PravastatinB4	840.2	2.129	2.833	840.2
Control C1	897.2	2.124	2.600	897.2
Control C2	670.4	2.150	1.639	670.4
Control C3	951.4	2.121	2.654	951.4
Control C4	1,063.4	2.122	2.544	1063.4
MβCD D1	557.3	2.154	2.026	557.3
MβCD D2	762.7	2.139	1.770	762.7
MβCD D3	707.0	2.119	2.941	707.0
MβCD D4	698.7	2.135	1.641	698.7
LPC E1	615.6	2.123	3.011	615.6
LPC E2	N/A	N/A	N/A	N/A
LPC E3	685.1	2.106	2.734	685.1
LPC E4	362.0	2.115	1.963	362.0
Fluphenazine F1	597.7	2.129	2.846	597.7
Fluphenazine F2	583.8	2.123	3.226	583.8
Fluphenazine F3	932.2	2.127	1.845	932.2
Fluphenazine F4	626.7	2.139	2.877	626.7

First Strand cDNA is prepared using reverse transcriptase and random primers. LPC E2 was not done due to cell death/ contamination. E2 space was re-allocated randomly to an extra replicate of A4.

11.1µl mRNA is added to 1µl random primers. This is then incubated in a PCR thermal cycler at 65^{o}C for 5 minutes and placed on ice. A mixture of First Strand Buffer, 100mM DTT, 25mM dNTP Mix and RNaseOUT is added to the sample and heated to 25^{o}C for 2 minutes. 1µ Superscript II is then added the incubated in the cycler :

25^{o}C for 10 minutes

42^{o}C for 50 minutes

70^{o}C for 15 minutes

Hold at 4^{o}C

The next step is to remove the mRNA and synthesize double stranded cDNA using QIAquick PCR Kit (Qiagen). Briefly, 62.8µl of water is added to the sample along with GEX Second strand Buffer and 25mM dNTP Mix. This is incubated at 0-4^{o}C for 5 minutes and then RNaseH and DNA Pol 1 are added and then the sample is incubated at 16^{o}C for 2.5 hours.

End repair is accomplished using T4 DNA polymerase and Klenow DNA polymerase. In a 1.5ml Eppendorf tube 50µl of eluted DNA, 27.4µl water, 10µl 10x End Repair Buffer, 1.6µl of 25mM dNTP Mix, 5µl T4 DNA Polymerase, 1µl Klenow DNA polymerase and 5µl T4 PNK are added. This mixture is then incubated at 20^{o}C for 30 minutes. Adapters are then ligated to the DNA so they can be hybridised to the flow cell, using a MinElute PCR Kit (Qiagen). Here, 23µl of eluted DNA is mixed with 25µl 2x Rapid T4 DNA ligase Buffer, 1µl PE Adapter Oligo Mix and 1µl of T4 DNA ligase. This is incubated at room temperature for 15 minutes. In preparation for the Illumina Assay the ligated cDNA is separated on an agarose gel to assess the size of the template needed for PCR

enrichment. Briefly, this is done by mixing 10µl cDNA sample with 6X DNA Loading Dye and running the gel lane against 2µl 0f 100bp DNA at 120v for 60 minutes.

The purified cDNA templates can then be enriched using two primers that anneal to the ends of the adapters. This was performed using a Qiagen Qiaquick PCR Purification Kit. The PCR mix is made from 10µl 5X Phusion™ Buffer, 1µl PCR Primer PE 1.0, , 1µl PCR Primer PE 2.0, 0.5µl 25mM dNTP Mix, 0.5µl Phusion™ DNA polymerase and 7µl water. This is added to 30µl of the ligated DNA and is amplified with the manufacturer's temperature cycle protocol. The samples are then ready for the Illumina HumanHT12_V4_0_R2_15002873_B human expression microarray. MDA-MB-2312 and CaLu-1 were treated with five different drugs: Proadifen, Pravastatin, MBCD, LPC or Fluphenazine. Six groups, (including an untreated control group), were each comprised of 4 biological replicates, except for LPC which had 3 replicates.

The raw array data were assessed for quality, and outliers removed. The remaining arrays were normalised and array features annotated. A series of 15 group-wise comparisons was undertaken to identify differences (fold changes). Each fold change has associated significance statistics, but as the number of significance tests being done is equal to the number of array features, significance values are controlled for false discovery, yielding a more rigorous adjusted P value. Having chosen a threshold for significance (adjusted $p<0.01$), significant loci in each comparison were assessed for functional enrichment of KEGG pathways, and GO terms, based on their annotation information.

A total of 24 Illumina HumanHT12_V4_0_R2_15002873_B arrays were QC analysed using the open-source r-stat arrayQualityMetrics Bioconductor™ package to identify sub-standard and/or outlier arrays. No arrays were identified as outliers.

Normalisation of the 47319 features across all arrays was achieved using robust spline normalisation after data were subjected to a variance stabilizing transformation. Raw data were transformed using a variance stabilizing transformation (VST) method prior to normalisation across all arrays using the robust spline normalisation (RSN) method. Expression measures (summarised intensities) are in log base 2.

The statistical significance threshold chosen for functional enrichment analyses was adjusted $p<0.01$. Functional enrichment analyses were undertaken for each comparison that had loci significant at this threshold. Up- and down-regulated loci were assessed separately.

For each comparison, the number of array features significant at various statistical thresholds were tallied. These are summarised in the table below. As mentioned previously, for statistical robustness, only those with an adjusted p value < 0.05 should be considered. The "non-redundant markerset" row details the number of array features significant in one or more of the comparisons at the given probability threshold.

2.3.7 ADDITIONAL ANTIBODY ASSAYS

Assay for Caveolin-1, Tubulin-1 and Glactin-8.

These markers were further analysed in discreet experiments that permitted multiple treatments and doses. Note: These assays now include some of the newly synthesised Proadifen analogues.

2.3.8 TREATMENT OF CELLS FOR INDIVIDUAL ANTIBODY ASSAYS

MD-MBA231 cells were cultured in Dulbeco's MEM + 10% FBS with stabilized antibiotic-antimycotic in Sterilin 75cm2 flasks. Final concentration contained 100,000 units penicillin G, 100mg streptomycin sulphate and 0.25mg amphotericin B per litre of media. All cells were subject to a 4 day passage regimen. Approximately 2 x 10^6 cells were evenly aliquoted into Corning 96 well plates providing approximately 2 x 10^4 cells per well. Replicates were carried out in entire columns of eight wells except where specified.

Treatment comprised the agent made up in Hank's Balanced Salt solution to give a final concentration in the media of 100µM. The positive control was methyl β-cyclodextrin and the negative control contained only the same volume of Hanks solution. Cholesterol test solutions were made up in Hank's balanced salt solutions with vortexing. All test solutions were made up freshly and brought to 37^{o}C in a water bath immediately prior to treatment. All chemicals and media were purchased from Sigma Chemicals, UK except where specified.

2.3.8.1 PREPARATION OF ANTIBODIES

Fluorescein isothiocyanate (FITC) has an absorption maximum at 495nm and an emission maximum at 525nm. It is commonly used as a fluorescent antibody labelling reagent in fluorescent immunobiology and fluorescent immunohistology. This labelling is possible due to the formation of a stable thiourea bond with free amino groups on the protein. FITC-anti-Tubulin antibody was prepared using the Sigma Fluorotag kit and monoclonal anti-α-Tubulin (mouse IgG1 isotype derived from the hybridoma AA13 produced by the fusion of mouse myeloma cells and splenocytes taken from mice immunised with rat brain tubulin). It has cross reactivity to human tubulin, according to the manufacturer's instructions. Briefly, 250µl of 0.1M carbonate-bicarbonate buffer solution (pH9.0) was added to 200µg of antibody. 1.0mg of FITC was reconstituted in 2.0ml of the same buffer. 50µl of the FITC solution was added drop-wise to the antibody solution and protected from light. The reaction vessel was kept at room temperature for 2 hours with occasional shaking. Following the conjugation the solution was pipetted onto the surface of a Sephadex G-25M 10ml column pre-hydrated with 10mM phosphate buffer 27mM KCl plus 138mM NaCl pH7.4. This phosphate buffer solution was used to elute the column and the first yellow band is collected (approximately 2.5ml in total). The antibody was stored in amber at 4^{o}C or used immediately.

The second antibody used in the experiment was anti-Caveolin-1 that was purchased already linked to the cyanine dye Cy3 that has an absorption maximum at 550nm and an emission maximum at 570nm. 1.25ml of phosphate buffer solution was added to

1mg of lyophilised protein and the light-protected tube vortexed for 1 minute. It was used without further preparation.

2.3.9 A FLUORESCENCE MICROPLATE BASED ASSAY FOR METASTASIS INDICATORS

A number of methods that measure proteolysis caused by cancer cells have been developed. Many of these use quenched fluorescent (DQ) protein substrates wherein the fluorescent conjugate becomes more fluorescent when cleaved from the protein. For example, FITC-collagen and FITC-gelatin can be used to measure protease activity when included in the media since small, highly fluorescent areas underneath individual live cells, can be imaged . Indeed, super-saturated fluorescent conjugates are available from a number of biochemical suppliers for this purpose. In an adaptation of the method described by Sugiyama *et al,* a FITC-quenched gelatin soft gel was prepared as follows.

0.49g gelatin (bovine, type II, powdered) was dissolved in 10ml distilled water. 20mg fluorescein isothiocyanate was added and the tube vortexed briefly then kept at room temperature in the dark. After 1 hour 10ml acetone was added which produced a flocculation that was dispersed with a magnetic stirrer. The mixture was left in the dark for a further 24hrs after which time it was washed thoroughly with cold acetone and 50mM Tris-HCl buffer. Finally 450mg was washed with 1.0% sodium hydrogen carbonate and dried under vacuum. It was then re-dissolved in warm (30^{o}C DMEM) media containing 10% FBS and 250mg gelatin. At this point the liquid can be stored at 4^{o}C for up to 6 hours prior to use. When required the liquid is heated to 45^{o}C and then

50µl is aliquoted into each of the 96 wells on the microplate using a sterile microfilter. Plates should be used as soon as they have reached 37^{o}C. The gelatin containing media is a soft gel at 37^{o}C.

Approximately 50,000 cells in fresh complete media containing the test compounds was overlaid gently onto the gel surface. Each column of eight on the plate comprised a single treatment with the bottom (G & H) two rows having an additional dosage of cytochalisin B. This compound is a powerful anti-motility factor but does not kill the cells or prevent expression of proteases. It was hoped that the cytochalisin treatment would act as a positive control enabling the discrimination between motility effects and proteolysis effects within a single fluorescence plate based assay.

2.3.10 CHOLESTEROL ASSAYS

Cells exposed to different treatments and combinations of enzyme inhibitors were harvested. The crude cell pellet was lysed with water and mechanical disruption. These samples were then centrifuged to separate the entire cell membrane fraction and then both the supernatant (containing the solubilized cytoplasm) and the separated lipid fraction were then analysed for cholesterol and cholesterol esters using a highly sensitive fluorometric assay. The assay is based on an enzyme coupled reaction that detects hydrolysed esters and free cholesterol using cholesterol oxidase to produce hydrogen peroxide which is then detected using 10-acetyl-3,7-dihydrophenoxazine producing a highly fluorescent product, resorufin (Amundson and Zhou, 1999).

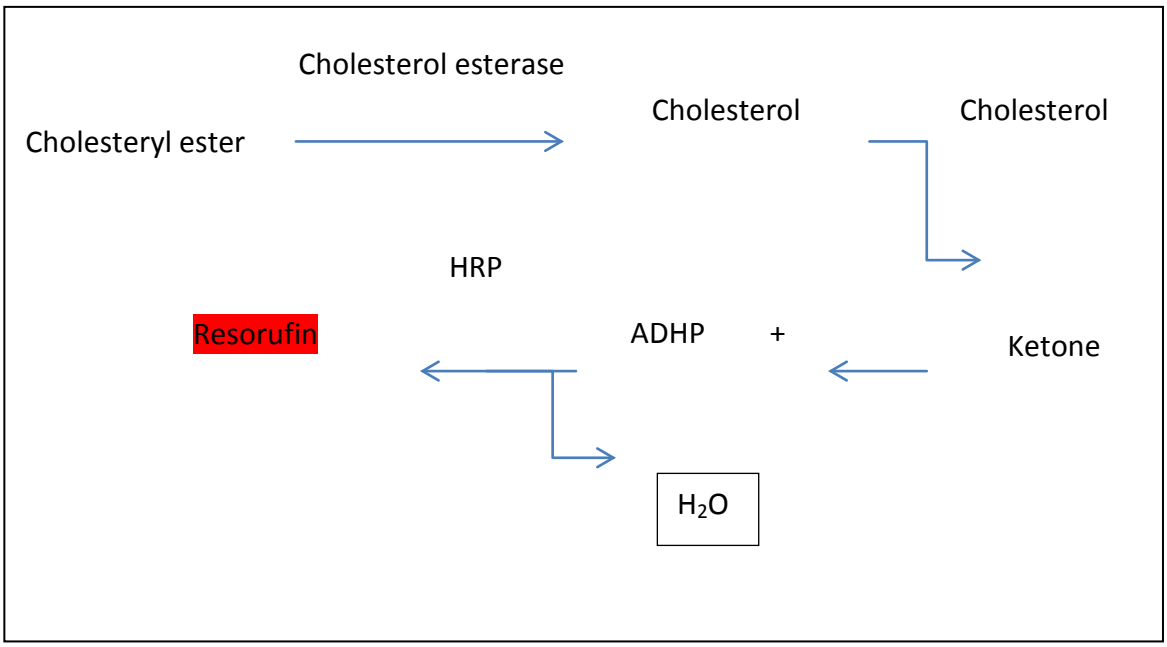

FIGURE 8: DIAGRAM OF CHOLESTEROL ASSAY REACTIONS

2.3.10.1 CELL TREATMENTS

Cells were grown in 175ml culture flasks in the normal way. Treatments were introduced when the cells were seen to be at 70% confluence by sterile injection of a stock solution so that the final concentrations were as reported. Cells were left to grow at 37^{o}C, 5% CO_2 for a further 48hrs before harvesting with trypsin. Each tube was centrifuged at 2500rpm for 3 minutes and the supernatant discarded. The tubes were then immediately re-suspended in 500µl distilled water containing 1mg/ml of Sigma protease inhibitor cocktail. The tubes were mixed vigorously in a Vortex mixer for 30 seconds and then disrupted further by repeated aspirating using a small bore hypodermic needle. At this stage, the tubes were re-centrifuged to create a small pellet and the supernatant removed for later analysis. The material at the bottom of the tubes

was re-suspended in 500µl of distilled water containing 1.0% (v/v) Triton-X and sonicated for 30 seconds at maximum amplitude with the temperature outside the tube of 0-4^{o}C. All samples were stored at -20^{o}C except immediately prior to analyses.

All reagent solutions were prepared in a phosphate buffer, pH7.4 containing 50mM NaCl and 5mM cholic acid. Cholesterol standard solutions were prepared by serial dilutions in ethanol. 50mg of powdered ADHP was prepared with 100µl dimethyl sulfoxide and 100µl of HPLC grade water. Both the oxidase and the esterase enzymes were prepared with 250µl of HPLC grade water. 50µl of the cholesterol detection cocktail was added to each of 96 wells containing 50µl each of the cell extracts (both supernatant and solubilized membrane fractions).

3 RESULTS AND DISCUSSION

3.1.1 SYNTHESIS ROUTES TO PROADIFEN AND ITS CLOSE ANALOGUES

For those molecules made by the author [see Table 4] the following describes the general approach and outcomes.

STRUCTURE OF PROADIFEN

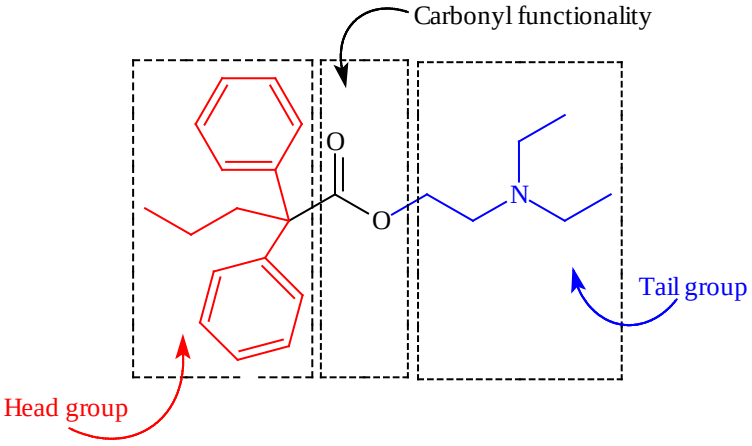

The synthesis of 2-(ethylamino)ethyl 2,2-diphenylvalerate ('VL15') and 2-(diethylamino)ethyl 2,2-diphenylvalerate (Proadifen) were readily achieved from the common starting material diphenylacetic acid (**1**). Treatment of **1** with two equivalents of butyl lithium led to the formation of the di-anionic species (**2**) which readily reacts with allyl bromide to give the alkylated product (**3**) after completion (Scheme 1).

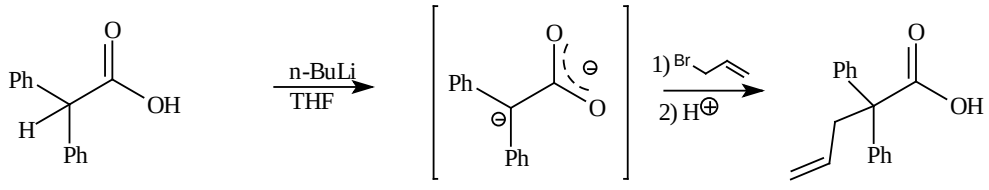

1 **2** **3**

SCHEME 1: ALKYLATION OF DIPHENYLACETIC ACID

Esterification was accomplished by the reaction of **3** with thionyl chloride to give the acid chloride **4**, followed by stirring the crude acid chloride with the appropriate aminoalcohol for 12 hours (Scheme 2). The final procedure requires hydrogenation over a palladium catalyst to reduce the double bond **5** and in the case of the mono-ethyl derivative, to remove the benzyl protecting group.

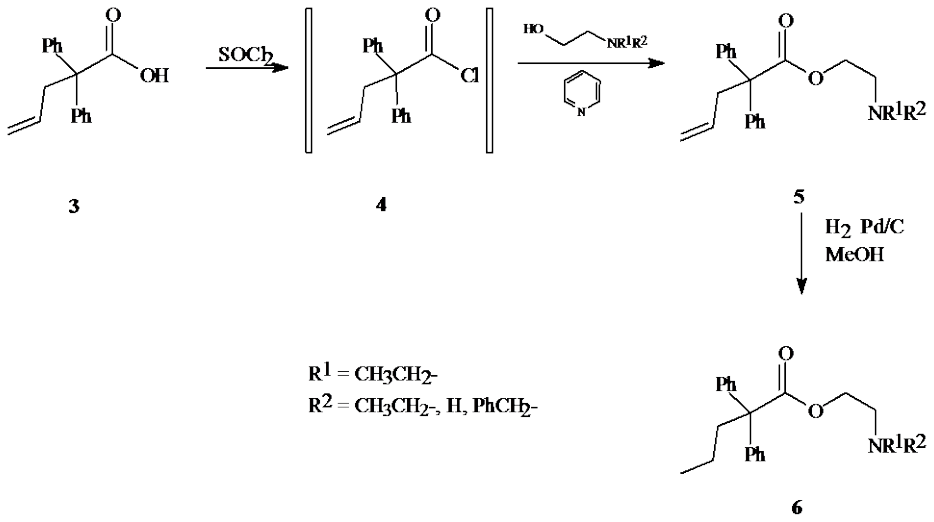

SCHEME 2: ESTERIFICATION OF ALKYL DIPHENYLACETIC ACID

3.1.1.1 PREPARATION OF 2,2-DIPHENYLPENT-4-ENOIC ACID

A solution of n-butyl lithium in hexane (2.5M, 83ml) was added dropwise to a solution of diphenylacetic acid (20g, 94mmol) in tetrahydrofuran (200ml) cooled to -78°C by a dry ice-acetone bath. The resultant solution was stirred for 1 hour before 3-bromopropene (16.3ml, 188mmol) was added drop-wise. The solution was stirred at -78°C for 1 hour and was then warmed to room temperature and stirred for 12 hours. Water (100ml), followed by dilute hydrochloric acid (2M, 100ml) was added to the

reaction mixture and the aqueous phase was extracted with diethyl ether (3×100ml). The combined ethereal extracts were dried with magnesium sulphate and the solvent removed *in vacuo* to give an off-white solid. Re-crystallisation of the solid from ethanol gave 2,2-diphenylpent-4-enoic acid as colourless crystals (19.0g, 80%).

3.1.1.2 Preparation of N-benzyl-N-ethylethanolamine

A mixture of 2-(ethylamino)ethanol (20ml, 0.21mol), benzylbromide (24.4ml, 0.21mol), potassium carbonate (29.0g, 0.21mol) and dichloromethane (150ml) was heated to reflux for 15 hours. Water (100ml) was added to the cooled reaction mixture followed by extraction with ether (3×100 ml). The organic extracts were dried with magnesium sulphate and the solvent removed under reduced pressure to give the amine as a light brown oil. Purification by distillation gave the compound as a colourless liquid (28.6g, 76%).

3.1.1.3 Preparation of 2-(ethylamino)ethyl 2,2-diphenylvalerate

2,2-Diphenylpent-4-enoic acid (9.50g, 37.7mmol) was refluxed with thionyl chloride (20ml) for 8 hours after which the excess thionyl chloride was distilled off to give the crude acid chloride. To this was added N-benzyl-N-ethylethanolamine (6.75g, 37.7mmol) dissolved in pyridine (10ml) and DMF (10ml) and the mixture stirred at room temperature for 24 hours. Water (100 ml) was added and the crude product was extracted with ether (3×50ml). The organic extracts were dried ($MgSO_4$) and the solvent removed under vacuum. The resultant product is dissolved in methanol (100ml),

10% palladium on carbon added and the mixture hydrogenated at 1 atmosphere of hydrogen for 15 hours. The solution was filtered and the solvent removed under reduced pressure to give 2-(ethylamino)ethyl 2,2-diphenylvalerate (7.92g, 65%).

3.1.1.4 Preparation of 2-(diethylamino)ethyl 2,2-diphenylvalerate

2,2-Diphenylpent-4-enoic acid (9.50g, 37.7mmol) was refluxed with thionyl chloride (20ml) for 8 hours after which the excess thionyl chloride was distilled off to give the crude acid chloride. To this was added 2-(diethylamino)ethanol (4.42g, 37.7mmol) dissolved in pyridine (10ml) and DMF (10ml) and the mixture stirred at room temperature for 24 hours. Water (100ml) was added and the crude product was extracted with ether (3×50ml). The organic extracts were washed with water (3×50ml), dried with $MgSO_4$ and the solvent removed under vacuum.

The resultant product is dissolved in methanol (100ml), 10% palladium on carbon added and the mixture hydrogenated at 1 atmosphere of hydrogen for 15 hours. The solution was filtered and the solvent removed under reduced pressure to give 2-(diethylamino)ethyl 2,2-diphenylvalerate (9.10 g, 68%).

3.1.1.5 PREPARATION OF 2-(N,N-DIETHYLAMINO)ETHYL 2,2-DIPHENYLETHANOATE

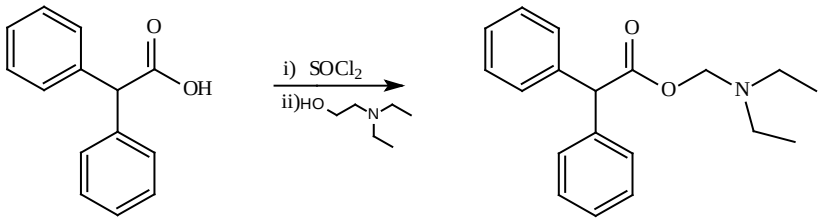

SCHEME 3: PREPARATION OF 2-(N,N-DIETHYLAMINO)ETHYL 2,2-DIPHENYLETHANOATE

A mixture of 2,2-diphenylacetic acid (5.00g, 23.6mmol) and thionyl chloride (10ml) was heated to reflux for 1 hour before the excess thionyl chloride was removed by distillation. A solution of 2-diethylaminoethanol (5.53g, 47.2mmol) in dichloromethane (10ml) and triethylamine (2ml) was added cautiously and the resultant mixture was stirred at room temperature for 2 hours. The reaction mixture was diluted with dichloromethane (50ml) and washed with saturated sodium bicarbonate solution (3×20ml) and water (1×20ml). The organic layer was dried (Na_2CO_3) and the solvent removed under reduced pressure to give the amine as a light brown liquid (6.30g, 86%). The hydrochloride salt of the above amine was readily prepared by passing dry HCl gas through an ethereal solution of the compound. The resultant solid was collected by filtration and washed well with ether to give an off-white solid.

3.1.1.6 PREPARATION OF 2-(N,N-DIETHYLAMINO)ETHYL 2,2-DIPHENYLETHANOATE

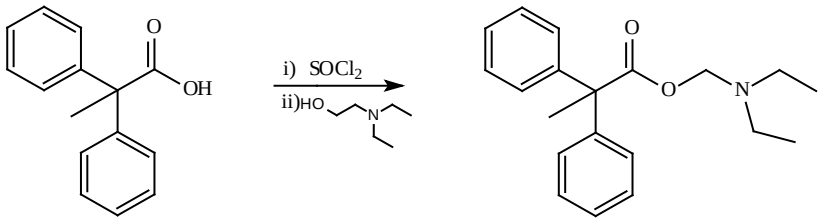

SCHEME 4: PREPARATION OF 2-(N,N-DIETHYLAMINO)ETHYL 2,2-DIPHENYLETHANOATE

A mixture of 2,2-diphenylpropionic acid (5.00g, 22.1mmol) and thionyl chloride (10ml) was heated to reflux for 1 hour before the excess thionyl chloride was removed by distillation. A solution of 2-diethylaminoethanol (5.17g, 44.2mmol) in dichloromethane (10ml) and triethylamine (2ml) was added cautiously and the resultant mixture was stirred at room temperature for 2 hours. The reaction mixture was diluted with dichloromethane (50ml) and washed with saturated sodium bicarbonate solution (3×20ml) and water (1×20ml). The organic layer was dried (Na_2CO_3) and the solvent removed under reduced pressure to give the amine as a light brown liquid (5.85g, 86%).

The hydrochloride salts of the above were prepared by passing dry HCl gas through an ethereal solution of the compound. The resultant solids were collected by filtration and washed well with diethyl ether to give an off white solid.

NMR spectra of the key novel analogues are provided in Appendix 5.

3.2 Live Cell Assay Results

- Migration assay – The ability of cells to migrate is measured in Transwell™ cell culture chambers. An 8μm pore size filter is coated on one side with fibronectin. Cells are exposed to the test compounds and then seeded in serum starved media onto the untreated side of the filter. Cells are left to migrate for 24hrs and cells on the lower surface are counted after crystal violet staining.

- Invasion assay – again performed in Transwell™ chambers, this test employs Matrigel™ solution instead of the fibronectin. Cells are treated as described above and left for 96hrs before counting takes place.

- Re-adhesion assay – Following exposure to the test drug, they are re-suspended in serum starved media and seeded in plates or wells coated in Matrigel™. They are left to adhere for 60 minutes. The media is removed and the cells washed. Adherent cells are then counted.

- Resistance to detachment assay – Petri dishes or similar vials coated with poly-L-Lysine, fibronectin and collagen are seeded with the cells. The medium is exchanged after 2 days for a serum free medium. The cells are exposed to the agent under investigation and incubated for a further 1 hour. The plates are then washed twice with a 0.008%

trypsin solution and agitated for 30 minutes. The trypsin solution is removed and the plates washed again and stained with sulforhodamine. The resistance to detachment is the mean absorbance of the treated plates divided by the control plates.

In this study it was found that the above methodologies were unsuitable for use with these test agents. Treatment with the cholesterol synthesis inhibitors causes some of the cells to spontaneously detach from the substrate surface and float freely in the media. They then have the ability to re-attach in the cleared zones measured in the above assays. Several attempts were made to use these cleared zone assays but no reliable data could be extracted. One assay that performed according to the literature was the phagokinetic track assay but this, while an elegant technique, is difficult to convert into unequivocal data. It did however reveal a difference between the effects of Simvastatin and Proadifen which then led on to further experimental work.

3.2.1 Results of phagokinetic Assay

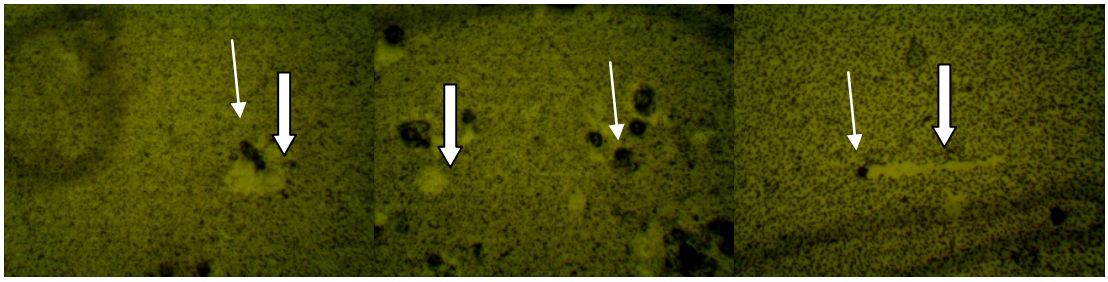

PLATE 1 EXAMPLE NEGATIVE CONTROLS

PLATES 1-4 SHOW BRIGHTFIELD MICROSCOPY AT X400 MAGNIFICATION OF MDA-MB-231 CELLS MOVING ACROSS A LAYER OF GOLD COLLOID. BLOCK ARROWS INDICATE THE TRACK OF DISPLACED PARTICLES AND THE FINE ARROWS INDICATE THE CELL.

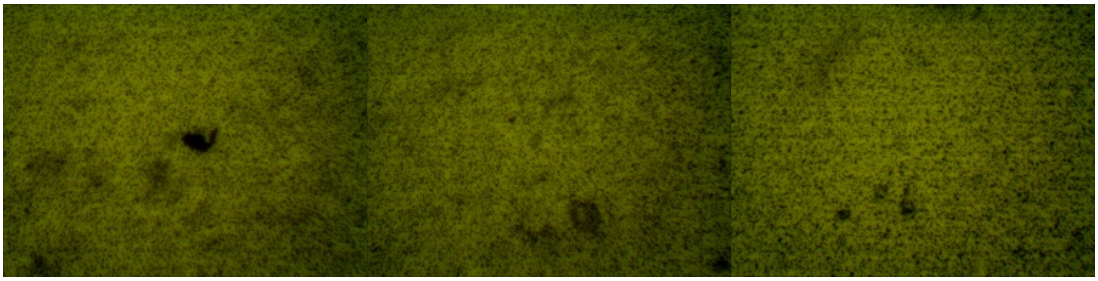

PLATE 2 FLUPHENAZINE (10µM)

IN THESE REPRESENTATIVE SLIDES CELLS ARE VISIBLE BUT THERE ARE NO TRACKS TO INDICATE MOVEMENT.

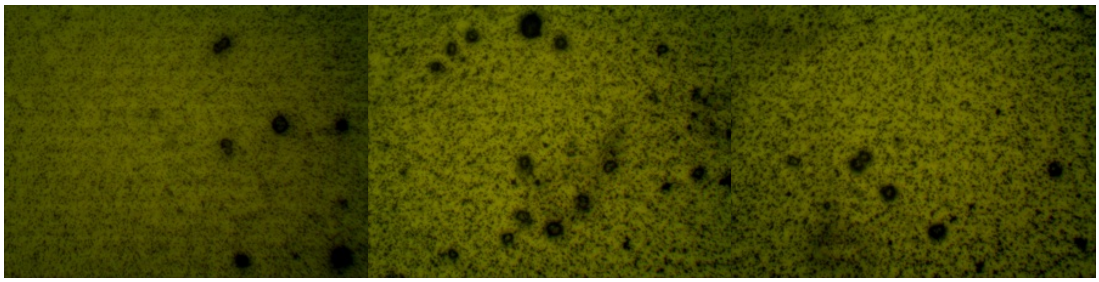

PLATE 3 PROADIFEN (10µM) E

IN THESE REPRESENTATIVE SLIDES CELLS ARE CLEARLY VISIBLE BUT NO TRACKS ARE PRESENT.

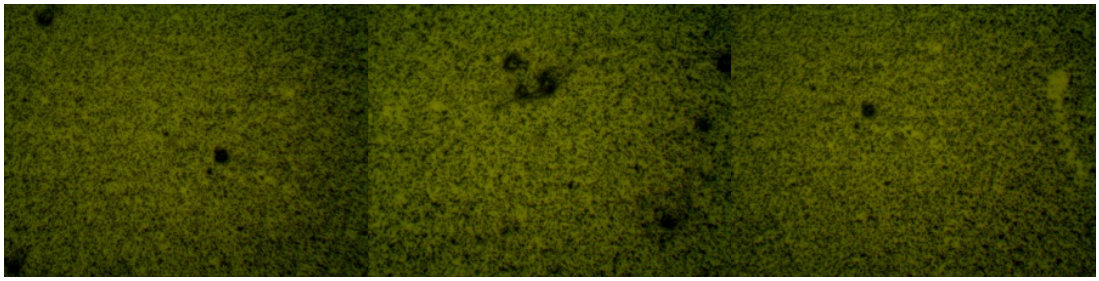

PLATE 4 SIMVASTATIN (8µM)

THE FINAL SLIDE SHOWS WHAT MAY BE A TRACK BUT THE CELL IS NOT VISIBLE SUE TO LOSS OF ADHERENCE TO THE SURFACE. THIS WAS THE ONLY TRACK SEEN THROUGHOUT THE EXPERIMENT WITH SIMVASTATIN.

THIS ASSAY DOES NOT LEND ITSELF TO EASY STATISTICAL ANALYSIS EVEN IF THE IMAGES ARE DIGITISED. IT IS ILLUSTRATIVE, HOWEVER, OF THE ABILITY OF MDA-MB-231 TO MOVE OVER A RELATIVELY SHORT TIME. DISTANCES OF UP TO 1MM IN 24 HOURS WERE RECORDED.

3.2.2 LIGHT MICROGRAPHS

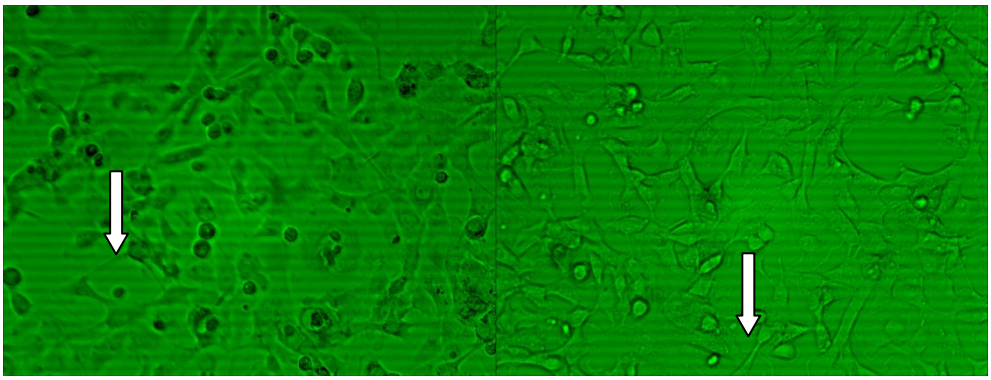

PLATE 5 CONTROL **PLATE 6 BIBB515**

PLATES 5 SHOWS A BRIGHTFIELD MICROGRAPH OF MDA-MB-231 CELLS GROWING IN DULBECCOS MEDIUM EAGLE MEDIUM (WITH NORMAL GROWTH SUPPLEMENTS) AT A MAGNIFICATION OF X400 24 HOURS AFTER SUB-CULTURE. PLATES 6-16 SHOW THE CELLS IN IDENTICAL CONDITIONS AFTER 24 HOURS WHERE THE MEDIUM CONTAINS PUTATIVE CHOLESTEROL INHIBITORS. BLOCK ARROWS INDICATE NORMAL INVADAPODIA WHILE FINE ARROWS INDICATE A MORE ROUNDED CELL MORPHOLOGY. NOTE THE CELL DENSITY IN THE TREATED CULTURES IS LIKELY TO BE A RESULT OF REDUCED PROLIFERATION OR DRUG TOXICITY. PLATE 6 SHOWS HEALTHY UNAFFECTED CELLS.

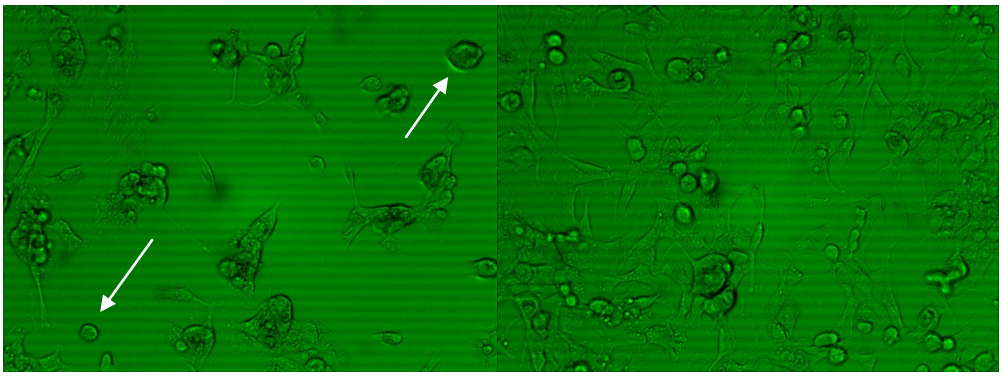

PLATE 7 BIBX1382 **PLATE 8 BM15766**

PLATES 7 & 8 SHOW CELLS DISPLAYING AN INTERMEDIATE RESPONSE WITH SOME CELLS APPEARING HEALTHY AND OTHERS CHANGING SHAPE.

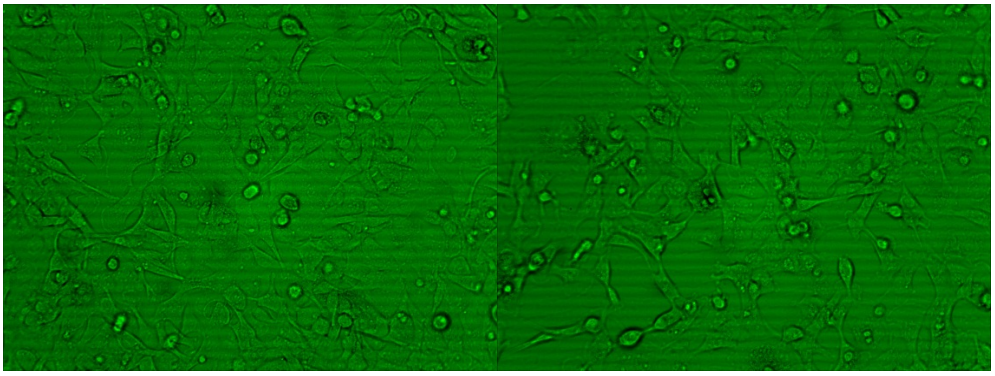

PLATE 9 CLOTRIMAZOLE **PLATE 10 AY9944 (8µM)**

CLOTRIMAZOLE HAS NO VISIBLE EFFECTS ON THESE CELLS WHILE AY9944 TREATED CELLS APPEAR TO BE HEALTHY.

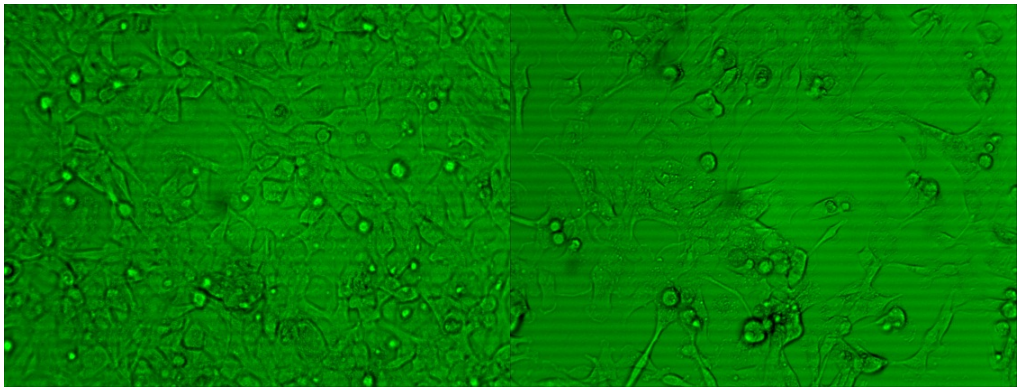

PLATE 11 FUPHENAZINE **PLATE 12 LPC**

FLUPHENAZINE TREATED CELLS PROLIFERATED RAPIDLY EXCEEDING THE DENSITY OF THE CONTROL GROUPS. THE REASON FOR THIS IS UNKNOWN. LYSPHOSPHATIDYLCHOLINE, ALTHOUGH BELOW THE CONCENTRATIONS KNOWN TO CAUSE CELL MEMBRANE DAMAGE (OR LYSIS) WERE NOT VIGEROUS BUT SHOWED A NORMAL MORPHOLOGY.

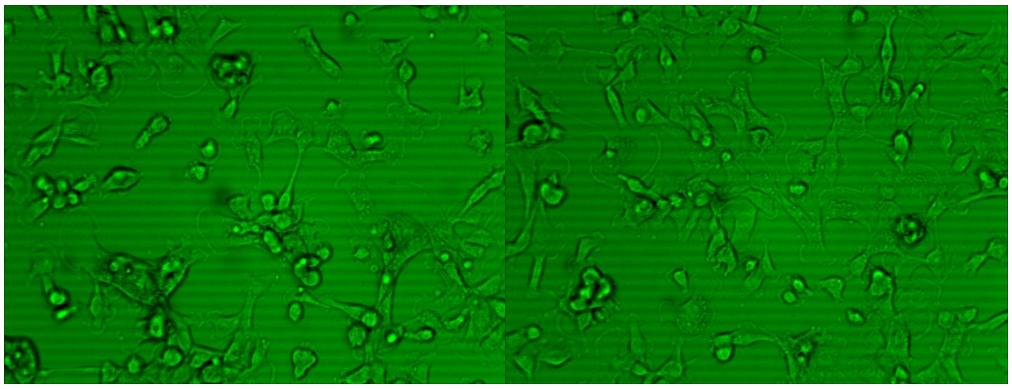

PLATE 13 MBCD **PLATE 14 PRAVASTATIN**

TREATMENT WITH MBCD CAUSED MANY CELLS TO EXHIBIT THE ROUNDED MORPHOLOGY BUT PROTRUSIONS ARE STILL VISIBLE ON SOME CELLS. PRAVASTATIN ALSO CAUSED A MIXED RESPONSE.

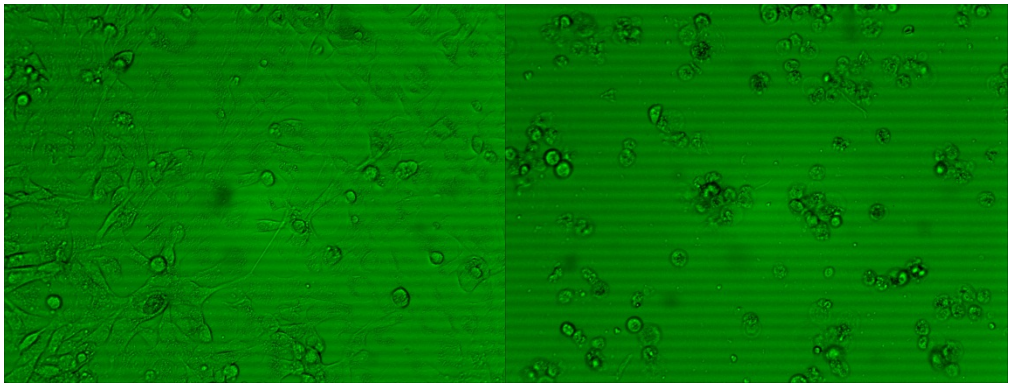

PLATE 15 PROADIFEN **PLATE 16 RO4871**

CELLS TREATED WITH PROADIFEN WERE VIABLE BUT MANY ROUNDED CELLS WITH AN ABSENCE OF INVADAPODIA ARE VISIBLE. RO4871 ABOLISHED ALL VISIBLE CELLULAR PROTRUSIONS.

Optical microscopy of treated cultures revealed some variations in morphology dependent on treatment. All slides were taken at the same stage of the experiment. BIBX1382 produced lacklustre growth and rounded, poorly formed cell structures. BM15766, AY9944 and clotrimazole produced healthy looking cells, if less prolific cultures than the negative control. Fluphenazine treatment produced vigorous proliferation with healthy cells. No signs of cell lysis were observed in the LPC treatment. Proadifen seems to produce rounded cells with fewer cilia, flagella and invadapodia and the cultures share similarities to the Pravastatin treated cells. Actually, the statin produced a mixture of normal looking cells and cells which were more rounded and had fewer protrusions.

3.2.3 SCANNING ELECTRON MICROGRAPHS

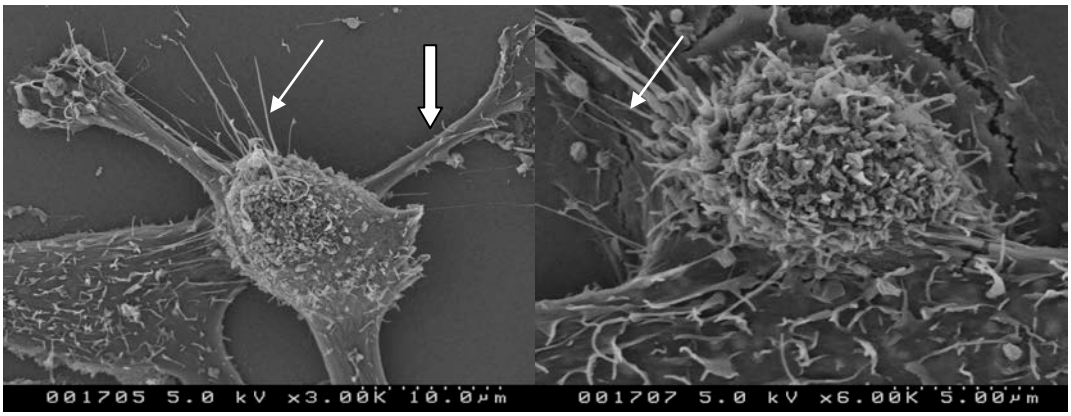

PLATES 17, 18 CONTROL (UNTREATED) MDA-MB-231 CELLS

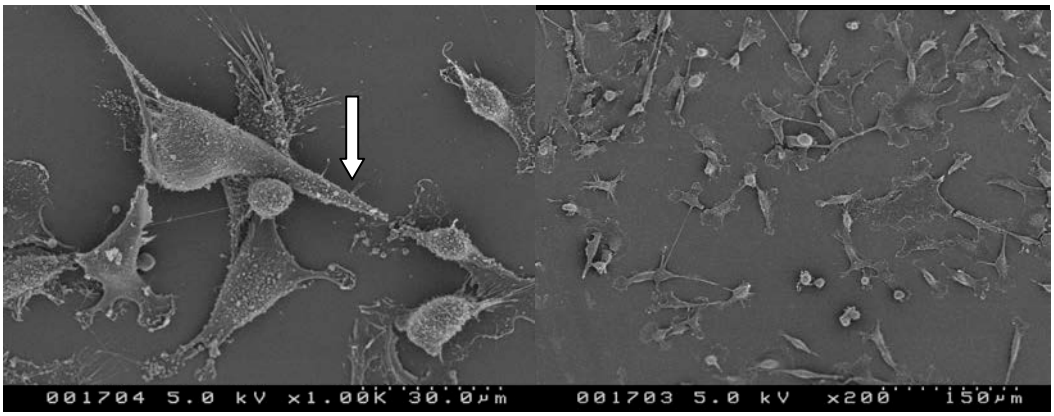

PLATES 19, 20 CONTROL (UNTREATED) MDA-MB-231 CELLS

THESE ELECTRON MICROGRAPHS SHOW MDA-MB-231 CELLS WITH AND WITHOUT TREATMENT WITH CHOLESTEROL INHIBITORS AT VARIOUS MAGNIFICATIONS. VOLTAGE AND SCALE ARE PRINTED ON EACH SLIDE. HEALTHY MDA-MB-231 CELLS DISPLAY MULTIPLE LARGE AND SMALL PROTRUSIONS THAT READILY VISIBLE UNDER THE ELECTRON MICROSCOPE. THESE RANGE FROM INVADAPODIA (BLOCK ARROWS) TO VERY SMALL CILIA (FINE ARROWS) VISIBLE CLEARLY ONLY UNDER HIGH (≥ X3000) MAGNIFICATION.

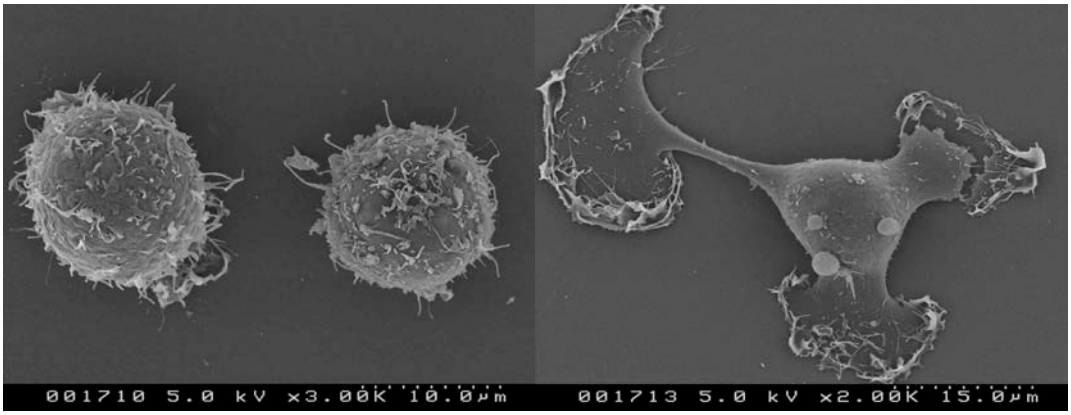

PLATES 21, 22 MDA-MB-231 CELLS TREATED WITH 0.8µM PRAVASTATIN FOR 24 HOURS.

PRAVASTATIN REDUCES BOTH THE LARGER PROTRUSIONS AND SMALLER CILIA AND FLAGELLA STRUCTURES. SOME CELLS APPEAR ROUNDED WHILE OTHERS APPEAR FLATTENED.

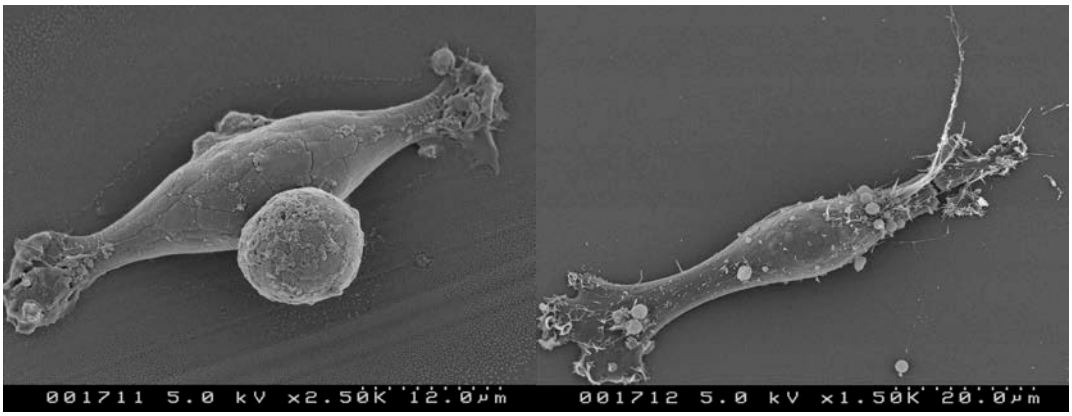

PLATES 23, 24 MDA-MB-231 CELLS TREATED WITH PROADIFEN AT 16 MM FOR 24 HOURS.

PROADIFEN APPEARS TO LEAVE THE OVERALL CELL STRUCTURE INTACT WHILE ALL TRACES OF CILIA ARE ABOLISHED.

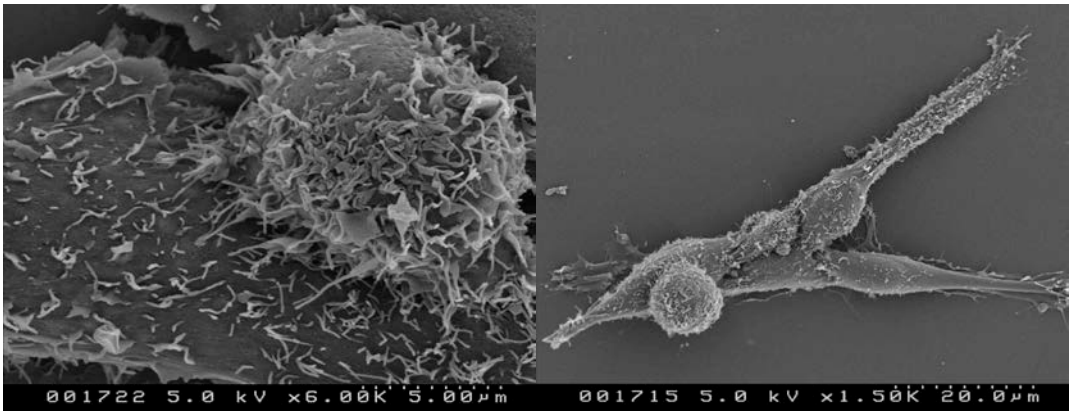

PLATES 25, 26 MDA-MB-231 CELLS TREATED WITH METHYL B-CYCLO DEXTRIN 0.00083% W/V FOR 24 HOURS

MBCD APPEARS TO LEAVE CELLS UNAFFECTED IN TERMS OF CELL MORPHOLOGY

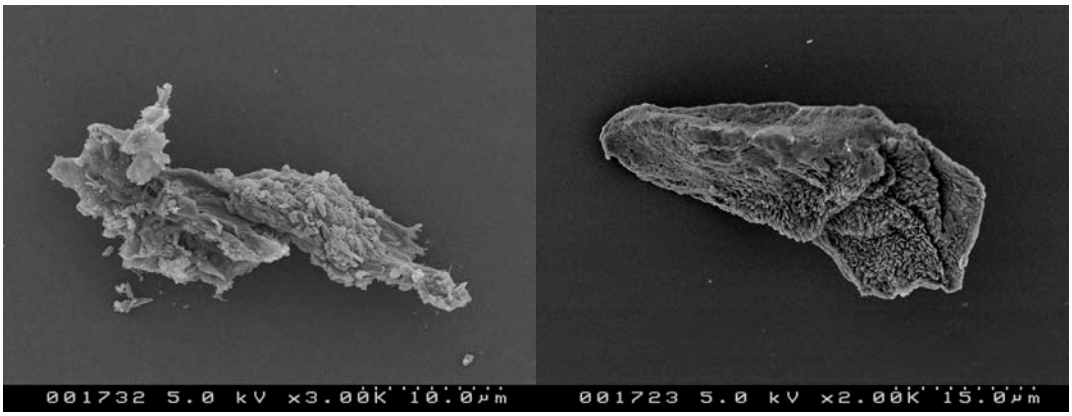

PLATES 27, 28 MDA-MB-231 CELLS TREATED WITH AY9944 9.0µM FOR 24 HOURS (THESE CELLS ARE DEAD)

EXPOSURE TO AY9944 FOR 24 HOURS LEFT ONLY CELL DEBRIS WITH A DISTINCTIVE CRENULATED SURFACE.

SEM IMAGES CONFIRM THAT PROADIFEN INDUCES MORPHOLOGICAL CHANGES CHARACTERISED BY A ROUNDING OF THE CELL (ALMOST AS THOUGH IT WERE SWOLLEN BY A HYPERTONIC MEDIA: THE MEDIA WAS, HOWEVER, CHECKED FOR OSMOTIC BALANCE) AND POORLY DEFINED – IF NOT ABSENT – CILIA AND OTHER MICROTUBULE BASED STRUCTURES. CILIA AND INVADAPODIA NOTICEABLE IN PLATE 17 AND 18, ARE ABSENT IN PLATE 23 AND ARE SCARCE IN PLATE 24.

MBCD HAS LITTLE IMPACT ON CELL MORPHOLOGY. AY9944 PRODUCED SOME DAMAGED, DEAD CELLS WITH A CRENULATED SURFACE AND SIGNS OF LYSES (PLATES 27 AND 28). MOST CELLS WERE NOT AS BADLY AFFECTED (SEE ALSO PLATE 10) SO THIS COULD BE AN ARTEFACT OF THE FIXATION PROCESS OR UNFORTUNATE SAMPLING.

3.2.4 TRANSMISSION ELECTRON MICROGRAPHS

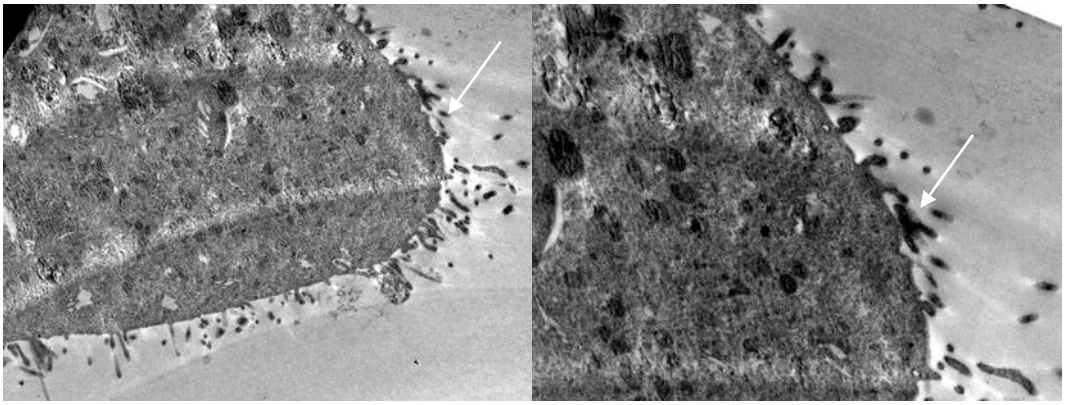

PLATES 29, 30 CONTROL (UNTREATED) MDA-MB-231 CELLS

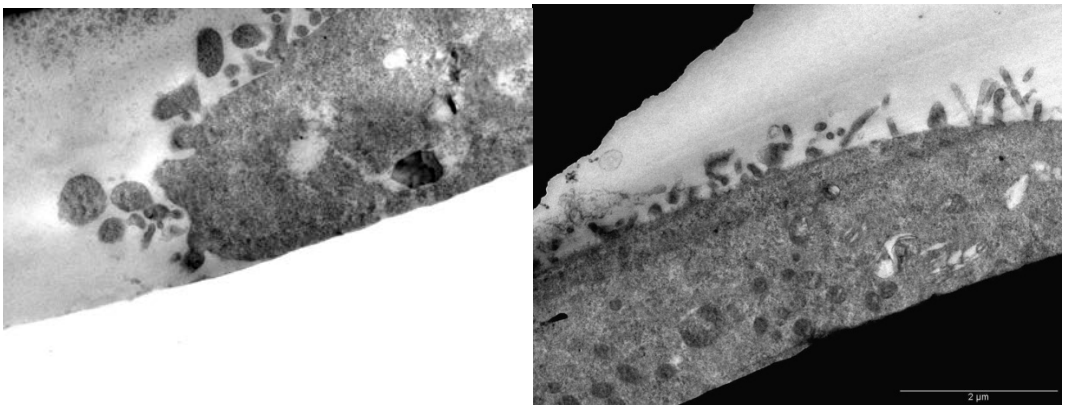

PLATES 31, 32 CONTROL (UNTREATED) MDA-MB-231 CELLS

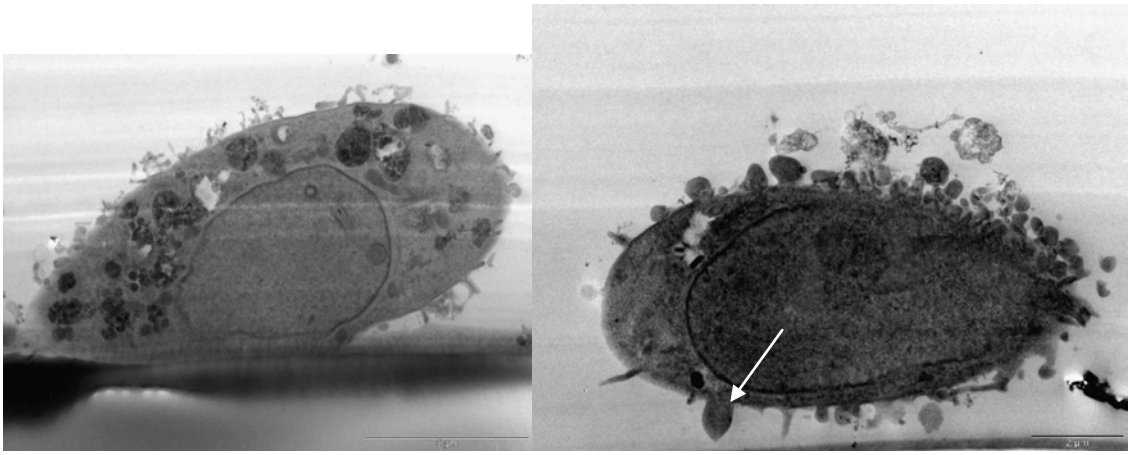

PLATES 33, 34 MDA-MB-231 CELLS TREATED WITH METHYL B-CYCLO DEXTRIN 0.00083% W/V FOR 24 HOURS

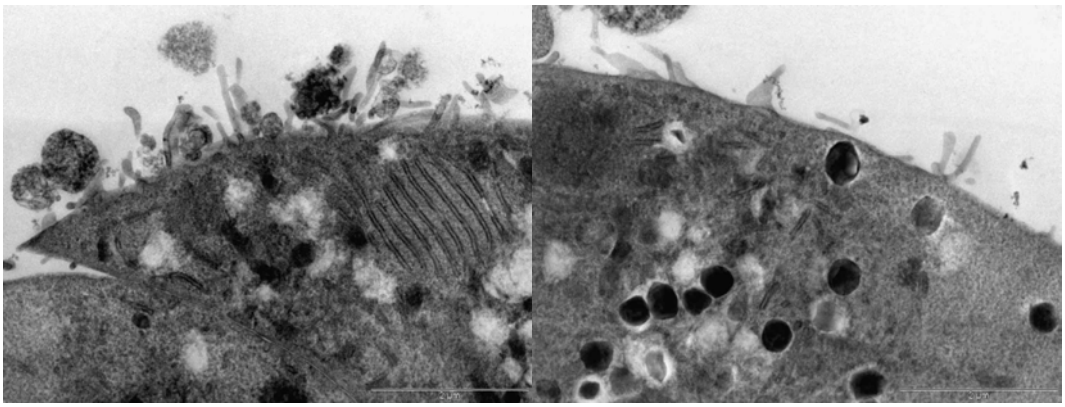

PLATES 35, 36 MDA-MB-231 CELLS TREATED WITH METHYL B-CYCLO DEXTRIN 0.00083% W/V FOR 24 HOURS

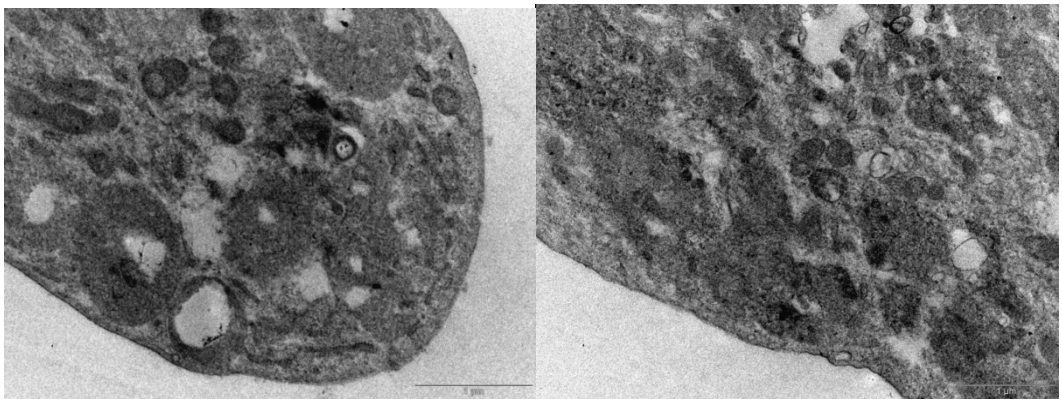

PLATES 37, 38 MDA-MB-231 CELLS TREATED WITH PROADIFEN HCL. AT 16MM FOR 24 HOURS.

TEM IMAGES OF SECTIONS THROUGH THE CELLS CONFIRM THAT MBCD DOES NOT AFFECT CELL MORPHOLOGY (PLATES 33 AND 34) WHILE PROADIFEN TREATMENT COMPLETELY – AT LEAST IN THE SELECTED SAMPLE (PLATES 37 AND 38) – INHIBITS THE FORMATION OF ALL TYPES OF CILIA (FINE ARROWS). THESE FINDINGS ARE ENTIRELY CONSISTENT WITH THE RESULTS OF THE DE-ATTACHMENT ASSAYS SINCE THE ADHESIVE PROTEINS ARE LOCALISED IN THE PRIMARY IMMOTILE CILIA. CILIA ARE ALSO KNOWN TO BE SITES FOR SOME SIGNAL TRANSDUCTION.

3.2.5 RESULTS OF VIABILITY, ADHERENCE AND RE-ATTACHMENT ASSAYS

THE FIGURES 9-10 SHOW MEAN OF TRIPLICATE VALUES FROM MORE THAN ONE EXPERIMENT. ABSORBANCE (Y-AXIS) INCREASES WITH DECREASING ADHERENCE OR VIABILITY. ERROR BARS DENOTE ± STANDARD ERRORS AND * DENOTES STATISTICAL SIGNIFICANCE AT P<0.05 (ANNOVA TWO TAILED TEST FOR DIFFERENCE FROM THE CONTROL).

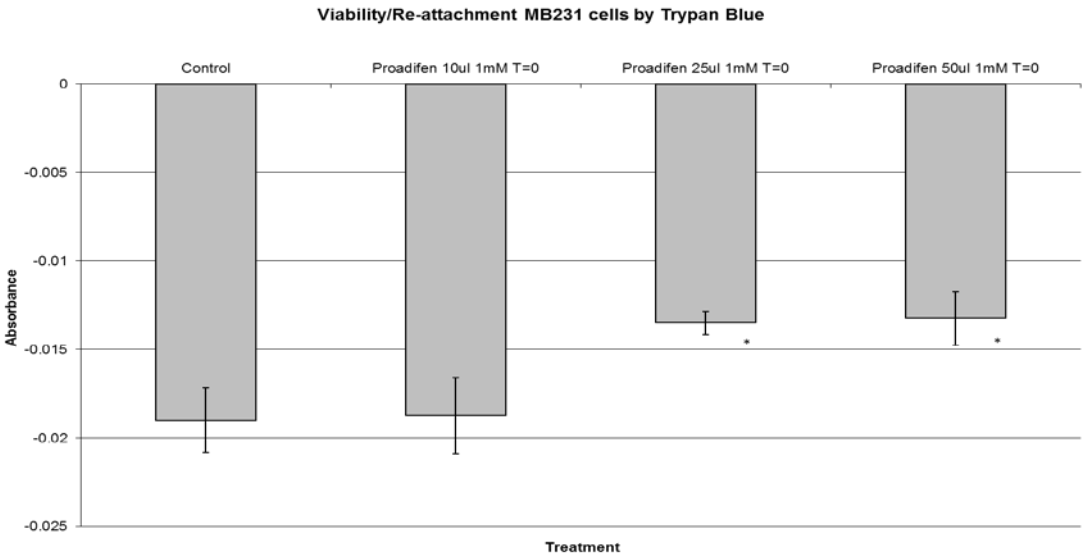

FIGURE 9: VIABILITY AND RE-ADHERRANCE MDA-MB-231 CELLS TREATED WITH PROADIFEN TIME 0 HOUR

ABSORBANCE IS THE MEASURE OF CELL SURVIVAL OR ADHERENCE. PROGRESSIVELY INCREASING DOSES CAUSED SOME IMMEDIATE CHANGE TO ADHERENCE BUT THE DIFFERENCE IS SMALL.

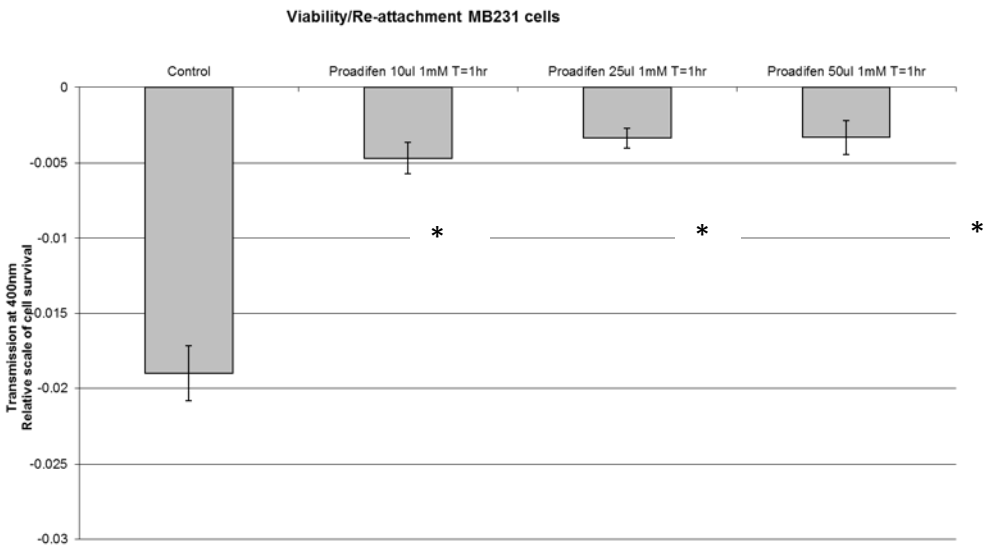

FIGURE 10: VIABILITY AND RE-ATTACHMENT OF MDA-MB-231 CELLS FOLLOWING TREATMENT WITH PROADIFEN 1HOUR

AFTER 1 HOUR THE TREATED CELLS HAVE DETACHED FROM THE PLATE REGARDLESS OF DOSE. THIS EFFECT IS SIGNIFICANT AT $P<0.05$.

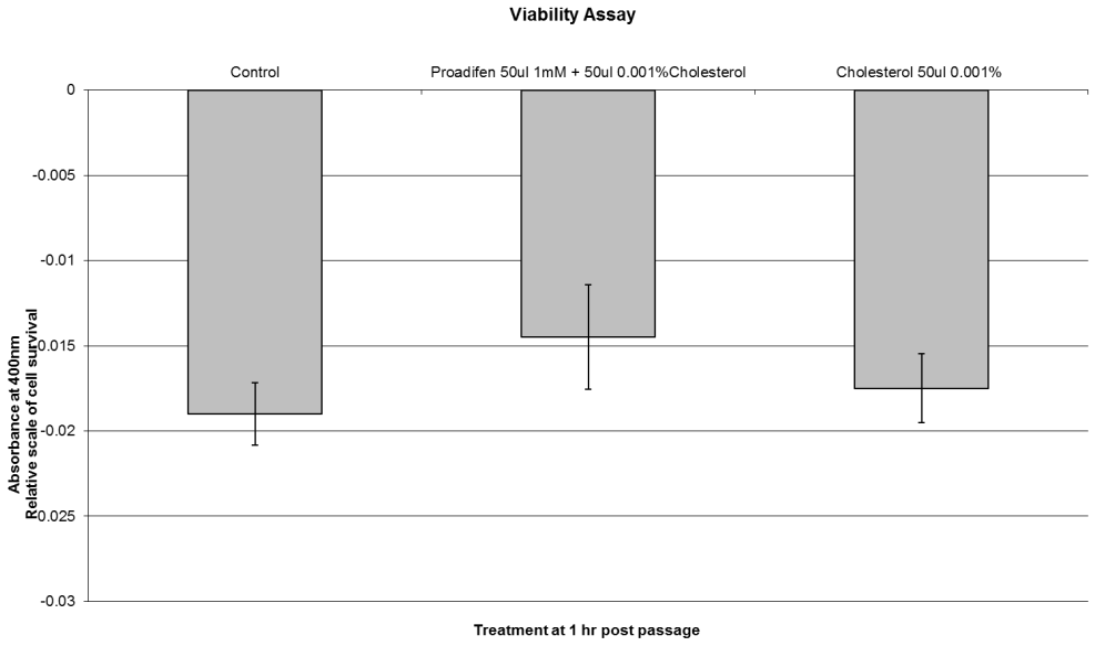

FIGURE 11: VIABILITY ASSAY MDA-MB-231 CELLS TREATED WITH PROADIFEN AND CHOLESTEROL

CO-TREATMENT OF CELLS WITH PROADIFEN AND CHOLESTEROL SUGGEST LITTLE ADDITIVE OR SYNERGISTIC EFFECTS ON OVERALL VIABILITY OR ATTACHMENT.

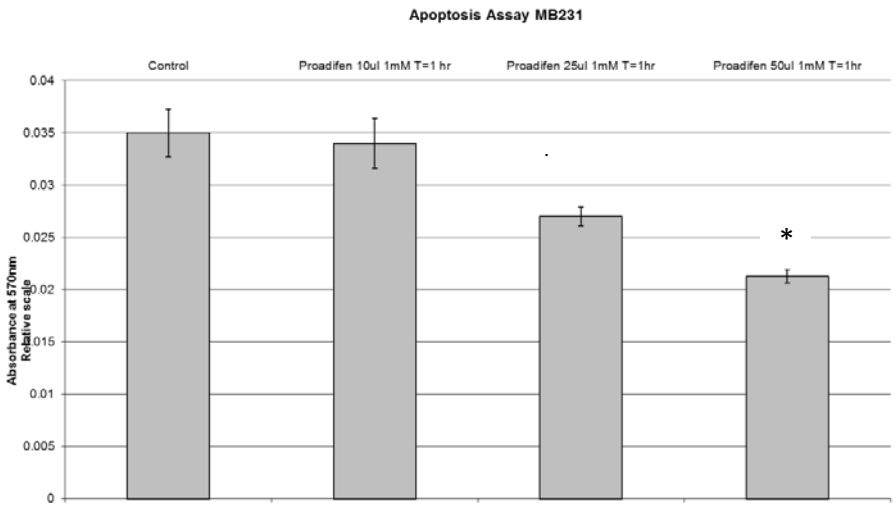

FIGURE 12: APOPTOSIS ASSAY MB231 CELLS TREATED WITH PROADIFEN TIME 0 HOUR

IN THE FOLLOWING GRAPHS (11-19) THE Y-AXIS SHOWS THE ABSORBANCE OF CHROMOPHORES THAT MEASURE APOPTOSIS AND NECROSIS. APOPTOSIS IS ONLY SIGNIFICANT AT THE HIGHEST DOSE OF PROADIFEN SUGGESTING THAT THE REDUCTION IN CELL ADHERENCE SEE IN FIGURE 10 IS REAL.

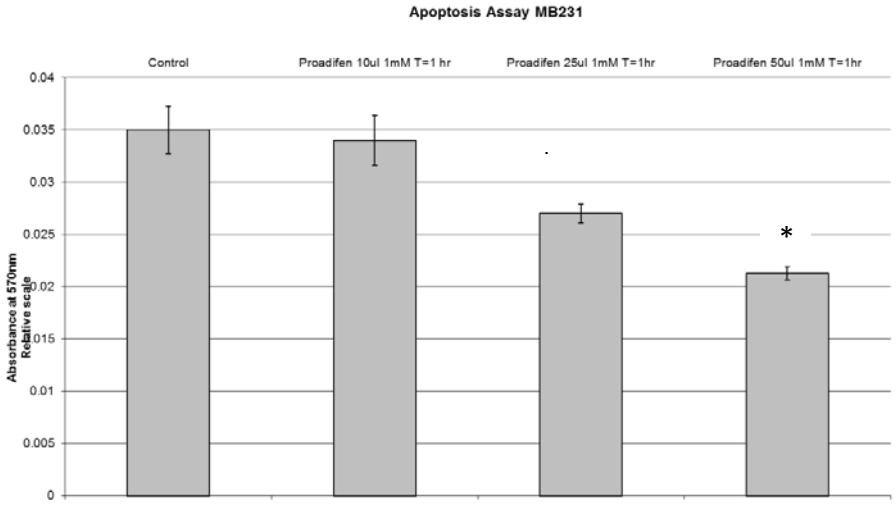

FIGURE 13: APOPTOSIS ASSAY MB231 CELLS TREATED WITH PROADIFEN TIME 1 HOUR

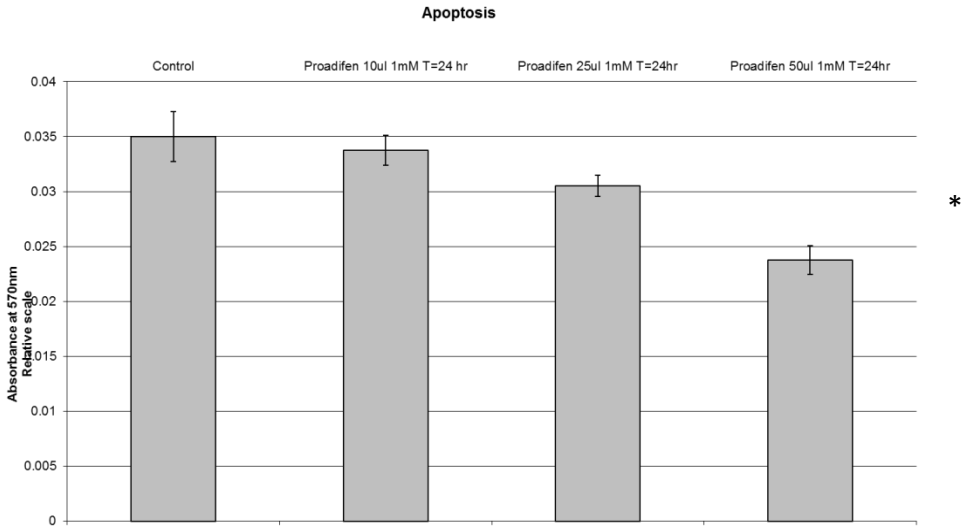

FIGURE 14: APOPTOSIS ASSAY MB231 CELLS TREATED WITH PROADIFEN TIME 24 HOUR

FIGURES 12 AND 13. EXPOSURE TIME DOES NOT APPEAR TO SIGNIFICANTLY ALTER THE LEVELS OF APOPTOSIS CAUSED BY PROADIFEN

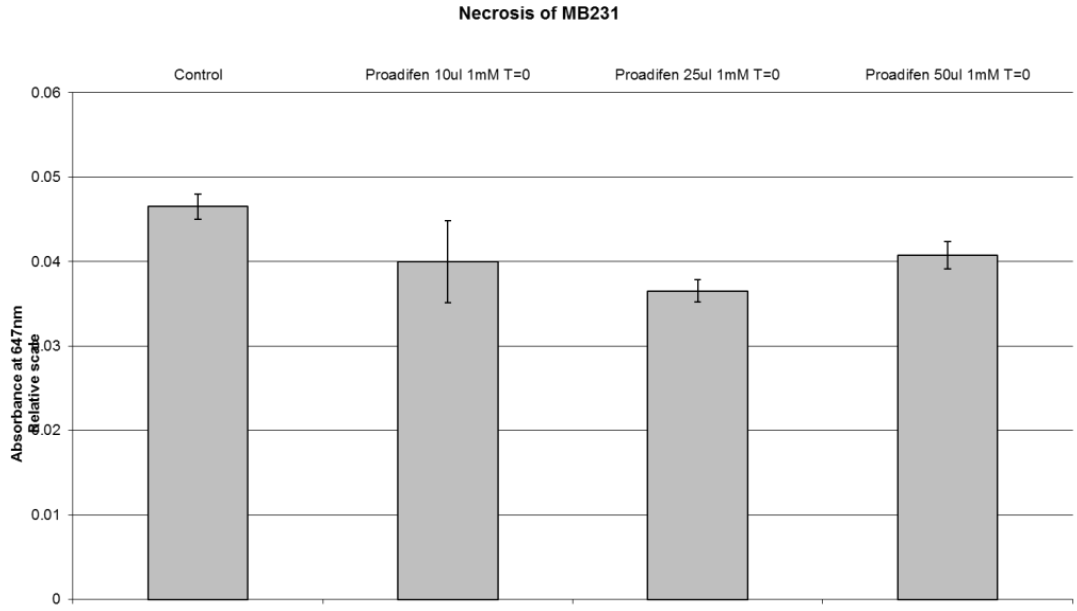

FIGURE 15: NECROSIS IN MDA-MB-231 CELLS TREATED WITH PROADIFEN TIME 0 HOURS

THERE IS LITTLE DIFFERENCE BETWEEN THE TREATED AND CONTROL GROUPS IN TERMS OF NECROSIS.

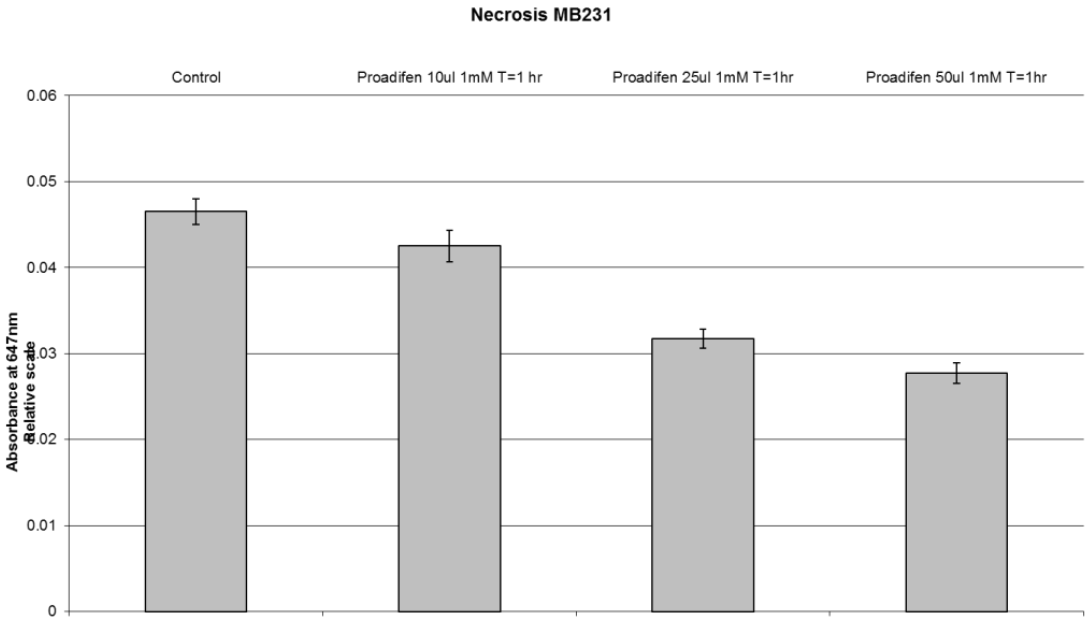

FIGURE 16: NECROSIS IN MDA-MB-231 CELLS TREATED WITH PROADIFEN TIME 1 HOURS

THERE APPEARS TO BE A DOSE RESPONSE BUT THE DATA IS NOT SIGNIFICANT AT P<0.05.

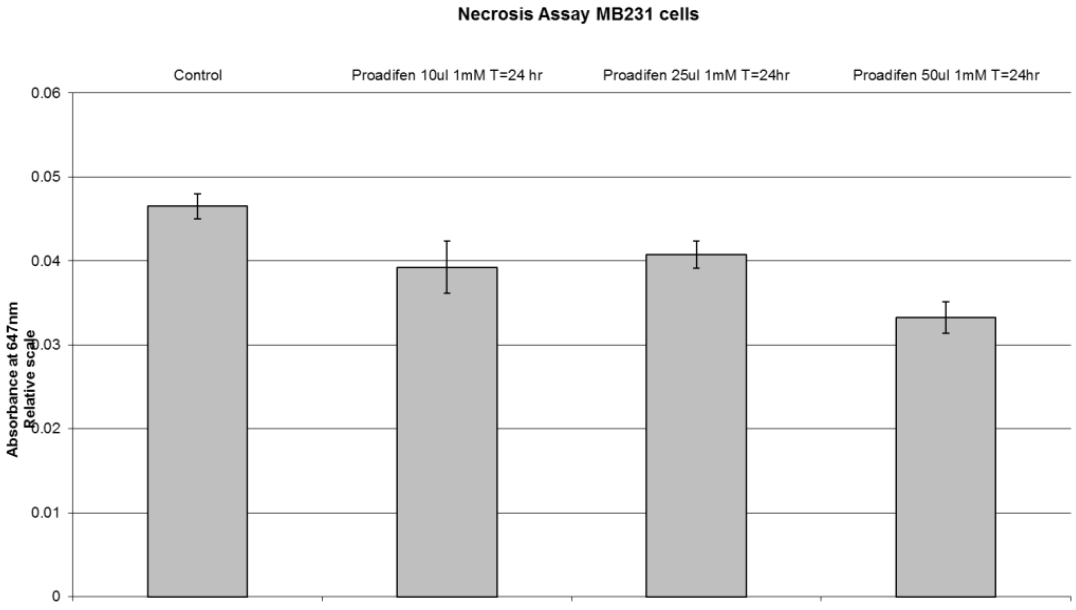

FIGURE 17: NECROSIS IN MDA-MB-231 CELLS TREATED WITH PROADIFEN TIME 24 HOURS

FIGURES 15 AND 16. EXPOSURE TIME DOES NOT APPEAR TO SIGNIFICANTLY ALTER THE LEVELS OF NECROSIS CAUSED BY PROADIFEN

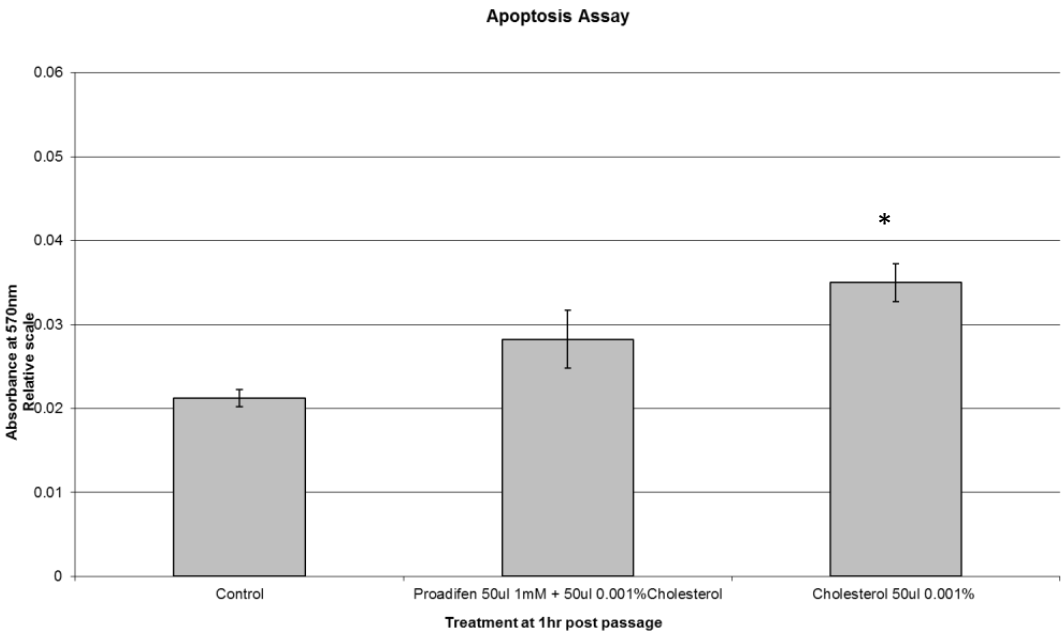

FIGURE 18: APOPTOSIS ASSAY IN MDA-MB-231 CELLS TREATED WITH PROADIFEN AND CHOLESTEROL

CHOLESTEROL INDUCES APOPTOSIS WITHIN 1 HOUR OF SUB-CULTURE AND THIS RESULT IS SIGNIFICANT P<0.05.

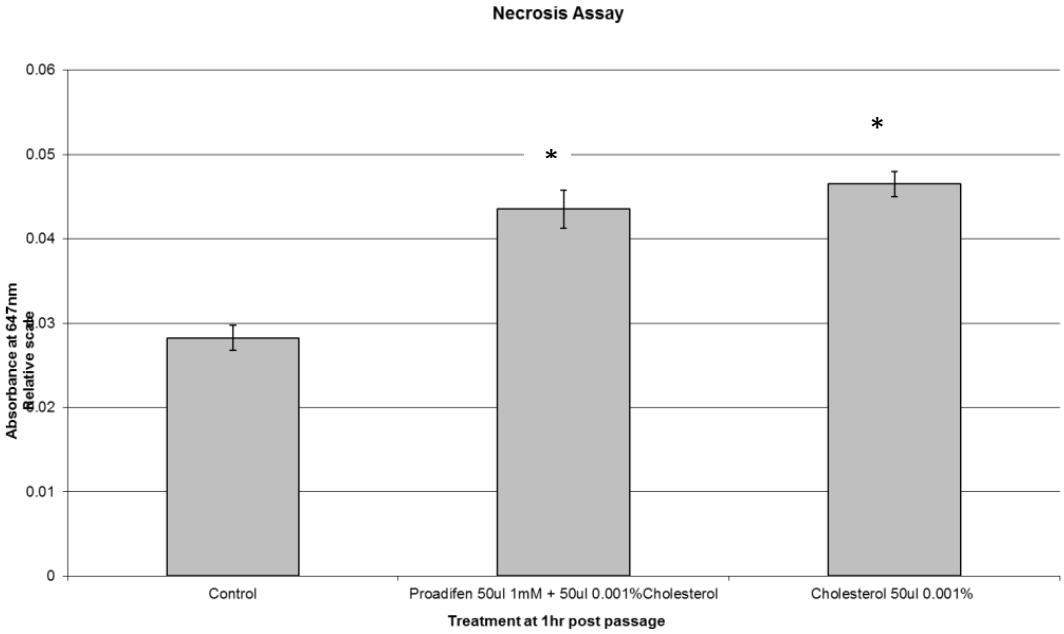

FIGURE 19: NECROSIS ASSAY IN MDA-MB-231 CELLS TREATED WITH PROADIFEN AND CHOLESTEROL

NECROSIS WAS DETECTED IN BOTH TREATMENTS SUGGESTING THAT CHOLESTEROL CAUSES APOPTOSIS AND NECROSIS WHILE PROADIFEN DOES NOT.

Proadifen reduces the ability of MDA-MB-231 cells to attach to the flask surface but no clear response is visible between 10µl 1mM and 50µl 1mM exposures at time zero. At

1hr, the result is profound with only ~20% of the treated cells remaining attached. A dose-response profile is now apparent but not statistically ($p<0.05$) valid (see Figure 9). Proadifen appears to cause some limited apoptosis and this is not time dependant (see Figure 11). Necrosis was simultaneously measured and increased slightly over time, presumably following the trend of apoptosis already recorded (see Figure 15).

Cell viability (along with apoptosis and necrosis) was measured to exclude the de-attachment of dead cells caused by treatment toxicity. In fact, and in accordance with the proteomic analysis (apoptotic marker set), apoptosis was reduced in the treated groups in a dose and time dependant manner. Necrosis results were broadly in line with apoptosis as might be expected. Overall viability of cells exposed to Proadifen is reduced by ~15%. Likewise, 50µl 0.001%w/v cholesterol reduces overall viability by 10% and cholesterol appears to induce high rates of apoptosis and necrosis. It is interesting to note that both exogenous ceramide and cholesterol are known to induce apoptosis.

Adhesion assays – specifically those involving cleared areas of substrate - were found to be very problematic. Several commercially available kits were evaluated and proved to be useless with these treatments and these cell lines. Proadifen rapidly induces de-attachment and free floating cells are able to re-attach on cleared areas and proliferate. Anchorage dependence of mammalian cells decreases upon tumourogenicity (Shin et al., 1975).

However, re-attachment of migrating cells is one of the final steps in successful metastasis. Oncogenesis overcomes the natural checkpoint of integrin mediated

attachment and is correlated to both activation of oncogenes and metastatic potential (Schwartz, 1997) Pozo and Schwartz showed that the growth regulatory pathways Rac, Erk and Ptdlns-3 kinase mediate anchorage independence (Del Pozo and Schwartz, 2007). Rac is found in caveolae and is under the control of integrins (del Pozo et al., 2000).

The proteomic analysis confirmed that Proadifen decreased Rac and Erk so two experiments were devised to measure the re-attachment and sustained attachment post-passage of MDA-MB-231 and cell-cell aggregation of BJAB cells. It was anticipated that Proadifen would decrease attachment to the extracellular matrix (ECM) if caveolae based integrin signalling was reduced. The results of this experiment were intriguing: if Proadifen is introduced at time zero (that is, simultaneously with the cell suspension following trypsinisation and centrifugation) then a modest dose-dependant reduction in re-attachment was observed (Figure 9). However, introduction of Proadifen 1hr after seeding dramatically reduced the attachment (Figure 10). MDA-MB-231 cells in the media and conditions described typically take 4-6 hours to adhere.

Exogenous cholesterol was also tested in the same way and significantly increased apoptosis (and necrosis) but did not impact attachment as recorded in the viability assay (Figure 17). The combination of Proadifen and cholesterol appears to mitigate the apoptosis-inducing effects of exogenous cholesterol. Again, necrosis closely tracked apoptosis.

3.2.6 RESULTS OF 656 PROTEIN ARRAY SEGREGATED BY PROTEIN FUNCTION

THE FIGURES BELOW SHOW MEAN OF TRIPLICATE VALUES FROM MORE THAN ONE EXPERIMENT. ERROR BARS DENOTE ± STANDARD ERRORS AND * DENOTES STATISTICAL SIGNIFICANCE AT P<0.05 (ANNOVA TWO TAILED TEST FOR DIFFERENCE FROM THE CONTROL). THE DIRECT OUTPUT OF THE SCANNER (FIGURE 20) REVEALS THE INTENSITY OF THE ANTIBODY-CONJUGATION AND IS A VISUAL CHECK THAT THERE WAS SUFFICIENT PROTEIN PRESENT FOR THE EXPERIMENT TO BE VALID.

BJAB control sample

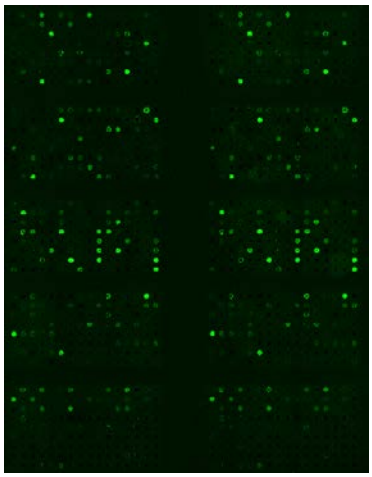

BJAB treated sample

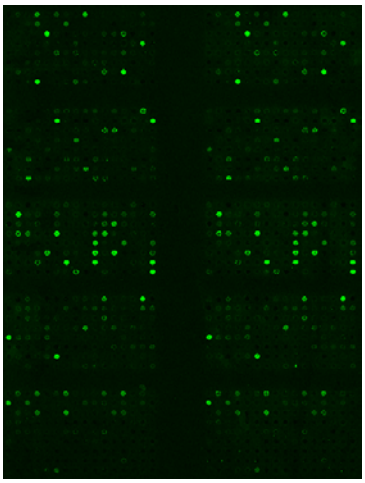

MDA-MB-231 control sample

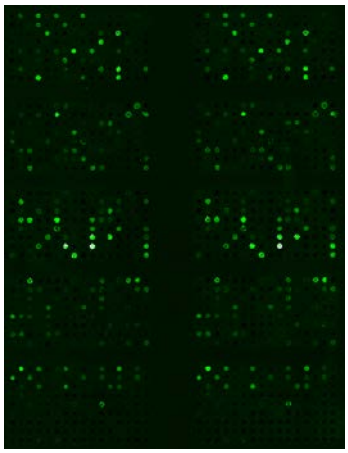

MDA-MB-231 treated sample

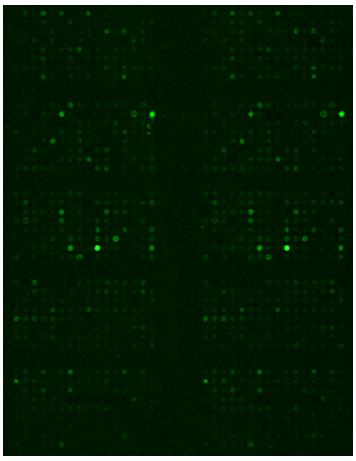

FIGURE 20: SPOT INTENSITIES

IT IS CLEAR FROM THESE IMAGES THAT SPOT INTENSITIES WERE GENERALLY LOWER IN THE TREATED GROUPS BUT TO BETTER UNDERSTAND THE DATA IS PRESENTED AS SPREAD SHEET OF SPOT INTENSITIES FOR EACH OF THE 656 ANTIBODIES WITH THE

COEFFICIENT OF VARIATION FOR THE MEAN OF THE REPLICATES. THESE DATA WERE THEN PLOTTED USING EXCEL SOFTWARE IN GROUPS BY PROTEIN FUNCTION.

3.2.6.1 RESULTS IN MDA-MB-231

THE FOLLOWING FIGURES SHOW THE CHANGE IN PROTEIN EXPRESSION (Y-AXIS) AS A PERCENTAGE CHANGE FROM THE CONTROL DATA. THE ERROR BARS INDICATE ±SE AND THE STANDARD ERROR IS CALCULATED FROM THE COEFFICIENT OF VARIATION OF THE SPOT INTENSITIES. THE DATA HAS BEEN SEGREGATED ON THE BASIS OF PROTEIN FUNCTION DIVIDED INTO ANGIOGENESIS, IMMUNE RESPONSE MARKERS, PROLIFERATION MARKERS AND APOPTOTIC MARKERS. THE ASSIGNMENT OF THE PROTEINS INTO THESE SUB-GROUPS IS BASED ON COMMERCIAL ARRAYS SUPPLIED BY SIGMA-ALDRICH FOR THESE PARTICULAR MARKER GROUPS..

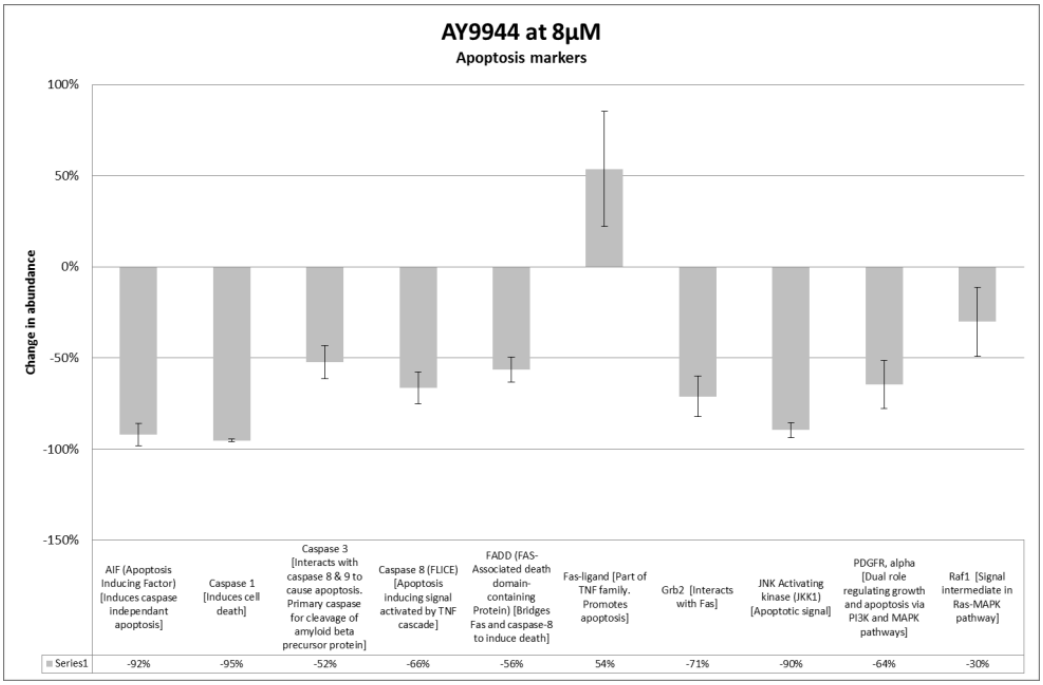

FIGURE 21: EFFECTS OF AY9944 ON APOPTOTIC MARKERS IN PROTEIN ASSAY

ALL APOPTOTIC MARKERS ARE REDUCED EXCEPT FOR FAS-LIGAND WHICH IS UP-REGULATED. FAS-LIGAND IS A TRANSMEMBRANE PROTEIN THAT IS UPSTREAM IN THE DISC CASCADE TO CASPASES 2,3 AND 8.

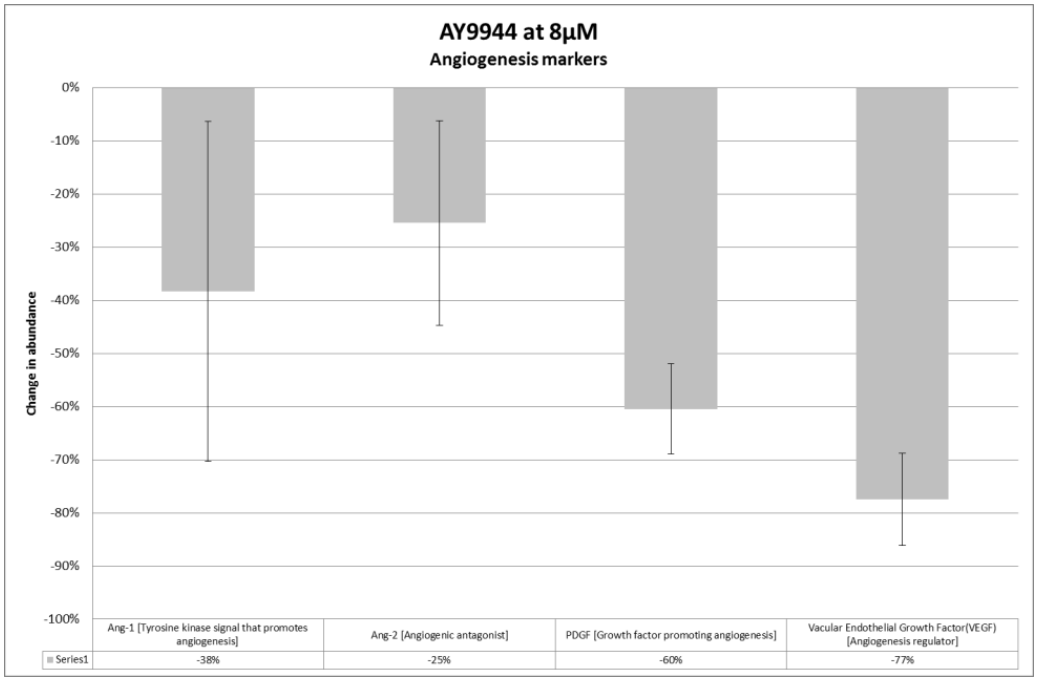

FIGURE 22: EFFECTS OF AY9944 ON ANGIOGENESIS MARKERS IN PROTEIN ASSAY

THE Δ-7 REDUCTASE INHIBITOR CAUSES A REDUCTION IN ALL THE MARKER PROTEINS FOR ANGIOGENESIS.

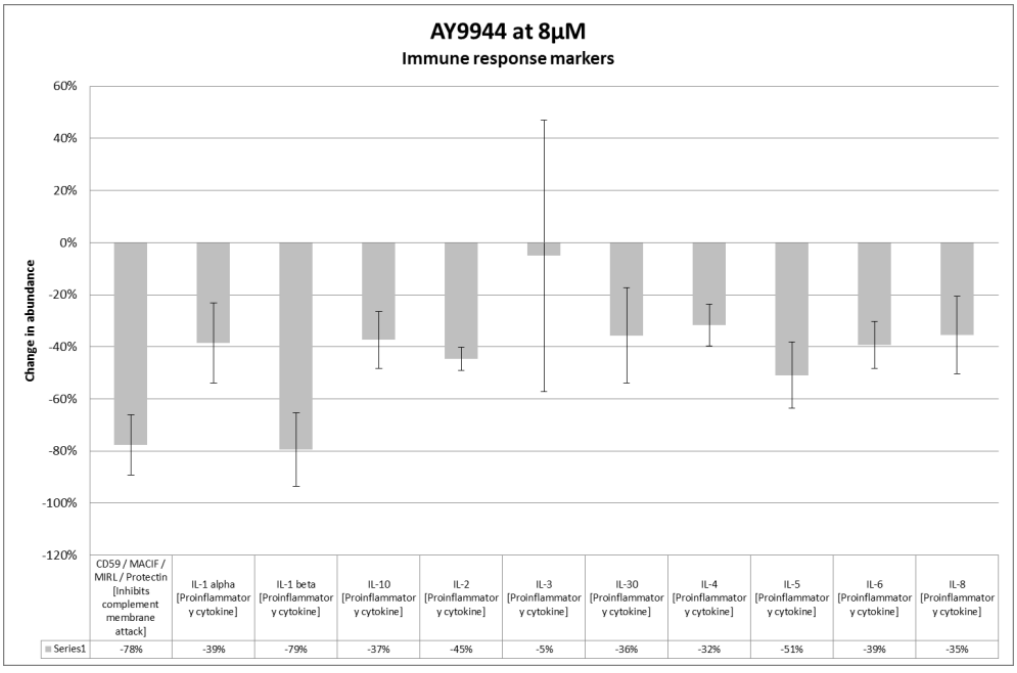

FIGURE 23: EFFECTS OF AY9944 ON IMMUNE RESPONSE MARKERS IN PROTEIN ASSAY

INTERLEUKIN-3 RESULT HAS A HIGH SE. IL-3 NORMALLY STIMULATES PROLIFERATION OF MYELOID AND MYELOID PROGENITOR CELLS.

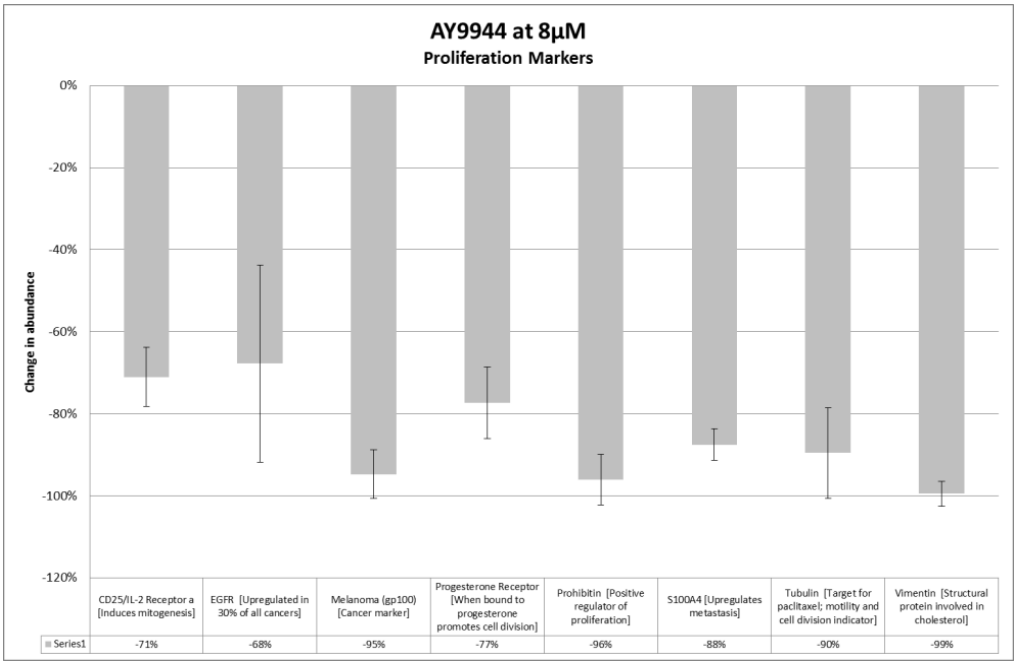

FIGURE 24: EFFECTS OF AY9944 ON PROLIFERATION MARKERS IN PROTEIN ASSAY

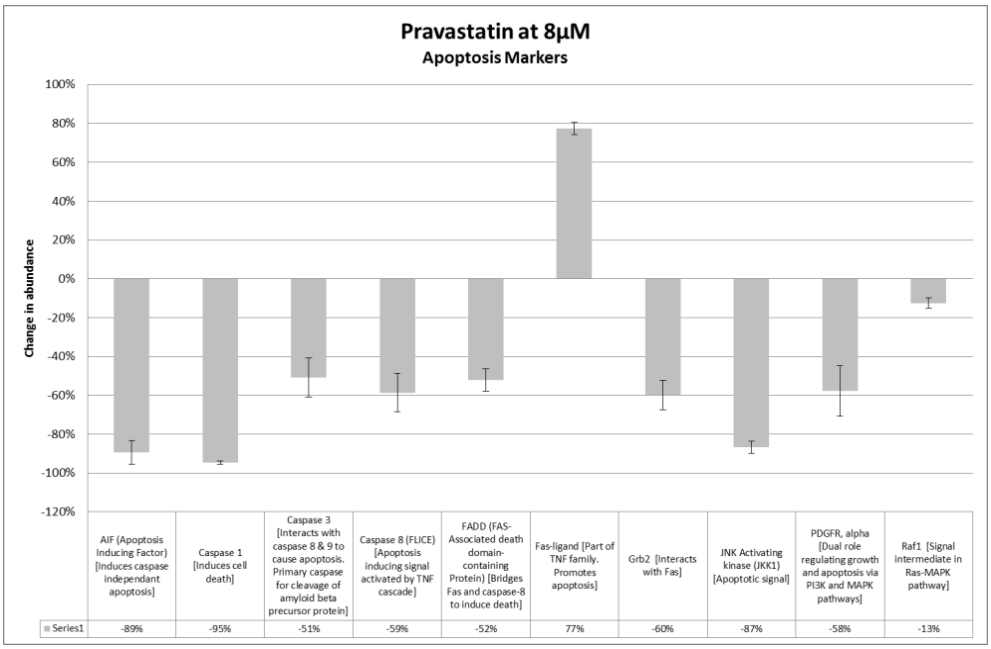

FIGURE 25: EFFECTS OF PRAVASTATIN ON APOPTOTIC MARKERS IN PROTEIN ASSAY

THIS IS A SIMILAR PATTERN OF RESPONSE TO THAT SEEN WITH AY9944 TREATMENT WHERE THERE IS ALSO A SIGNIFICANT INCREASE IN EXPRESSION OF FAS-LIGAND

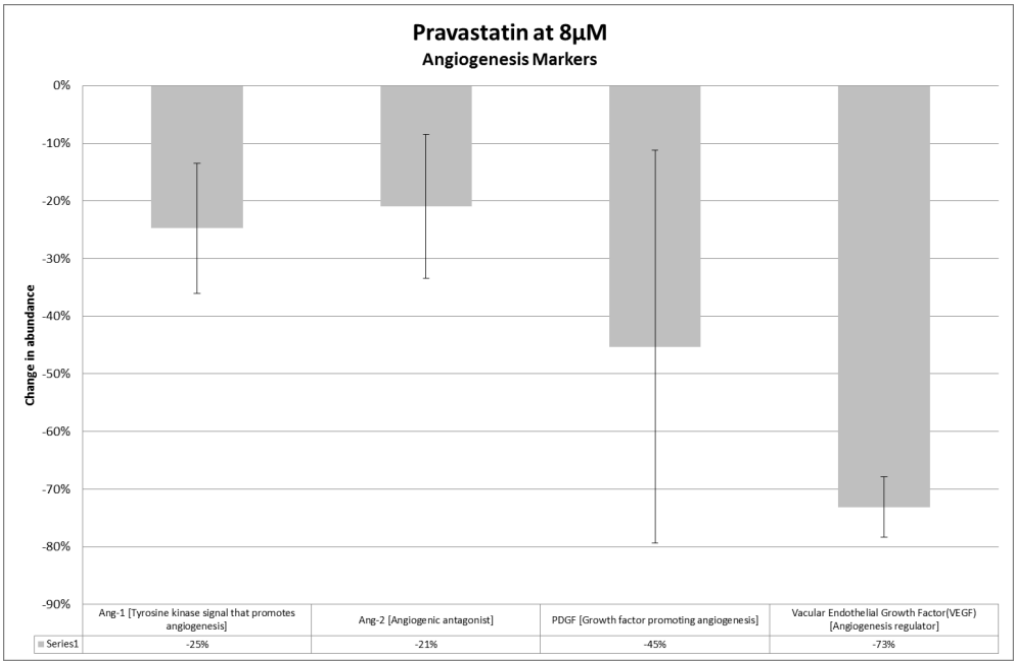

FIGURE 26: EFFECTS OF PRAVASTATIN ON ANGIOGENESIS MARKERS IN PROTEIN ASSAY

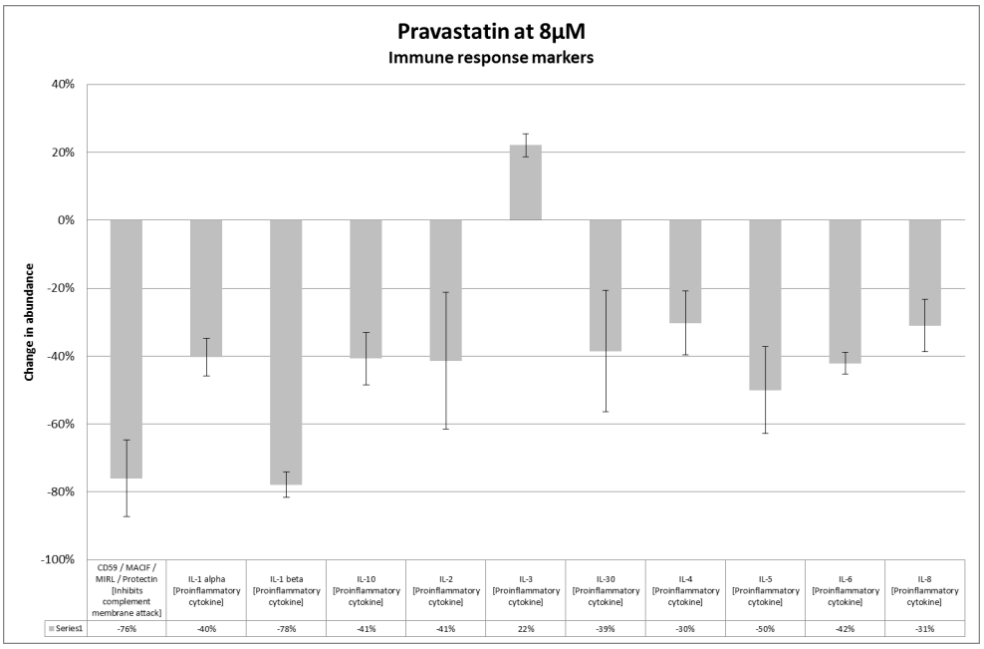

FIGURE 27: EFFECTS OF PRAVASTATIN ON IMMUNE RESPONSE MARKERS IN PROTEIN ASSAY

INTERLEUKIN-3 IS AGAIN EXCEPTIONAL IN THIS RESULT, PERHAPS SIMILAR TO THE AY9944 RESULT.

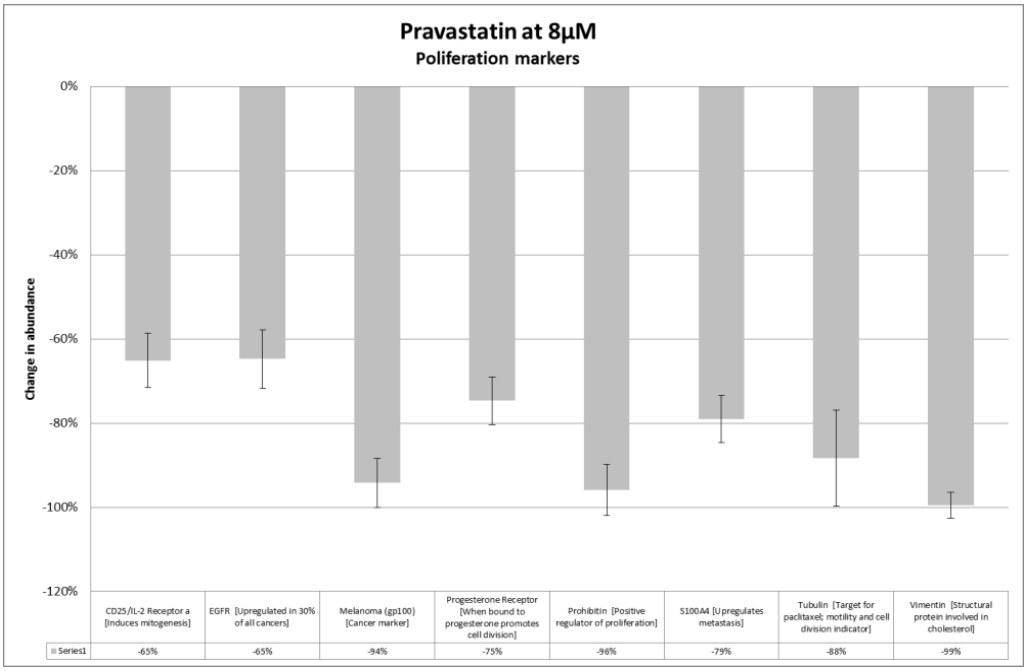

FIGURE 28: EFFECTS OF PRAVASTATIN ON PROLIFERATION MARKERS IN PROTEIN ASSAY

A SIGNIFICANT DOWN-REGULATION OF THESE MARKER PROTEINS IS EVIDENT.

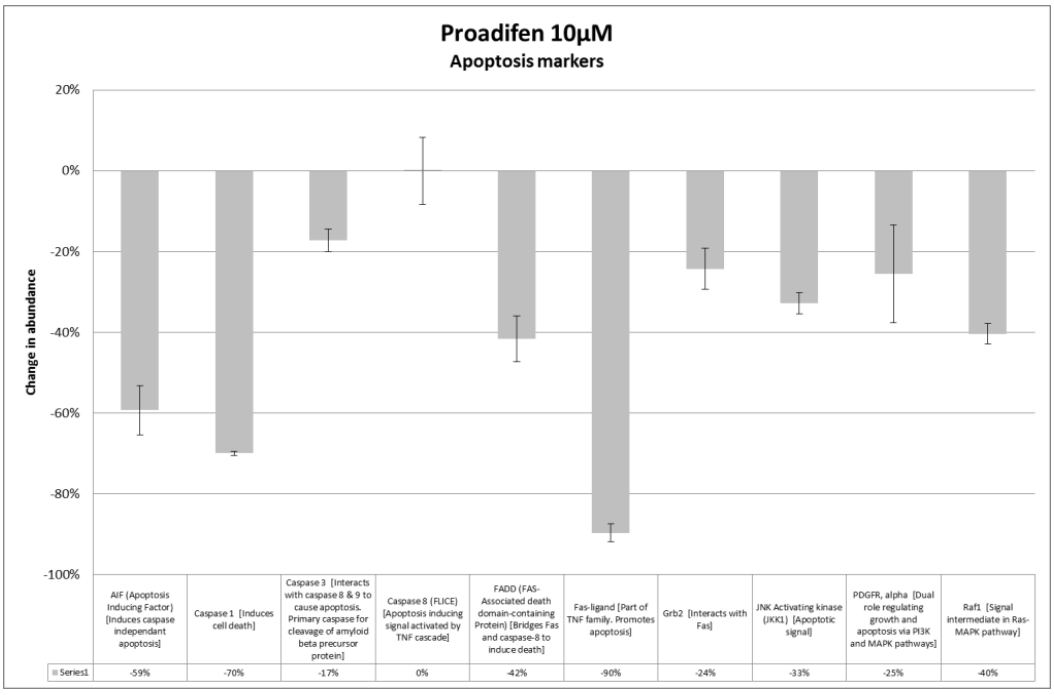

FIGURE 29: EFFECTS OF PROADIFEN ON APOPTOTIC MARKERS IN PROTEIN ASSAY

PROADIFEN RESULTED IN NO UP-REGULATION OF ANY OF THE SELECTED MARKERS.

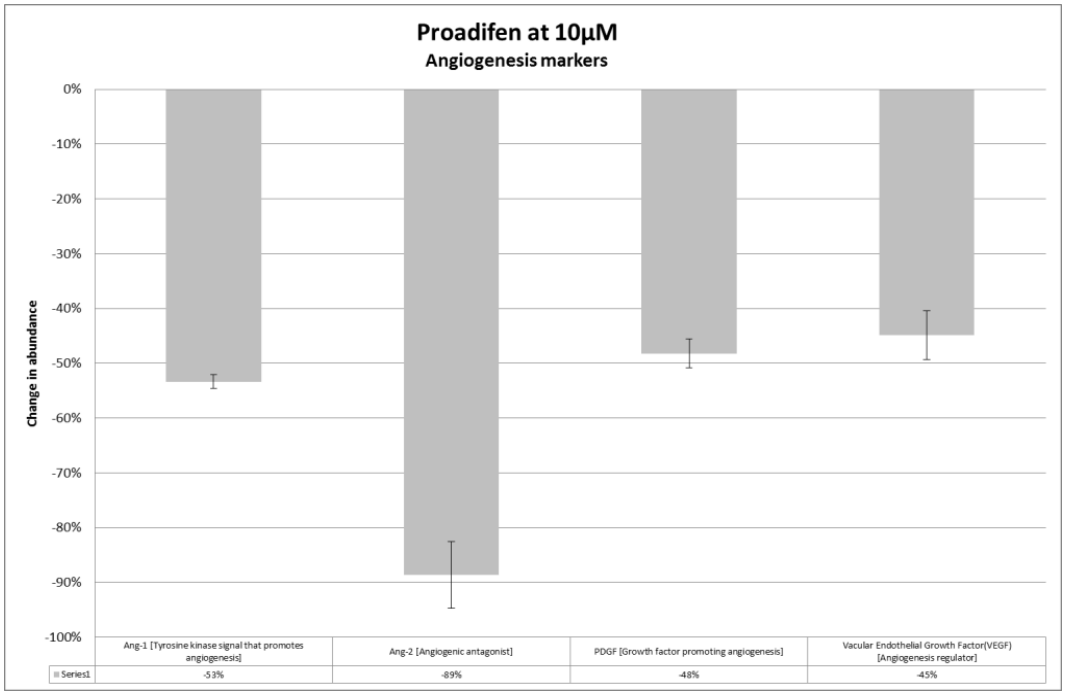

FIGURE 30: EFFECTS OF PROADIFEN ON ANGIOGENESIS MARKERS IN PROTEIN ASSAY

A SIGNIFICANT DOWN-REGULATION OF THESE MARKER PROTEINS IS EVIDENT.

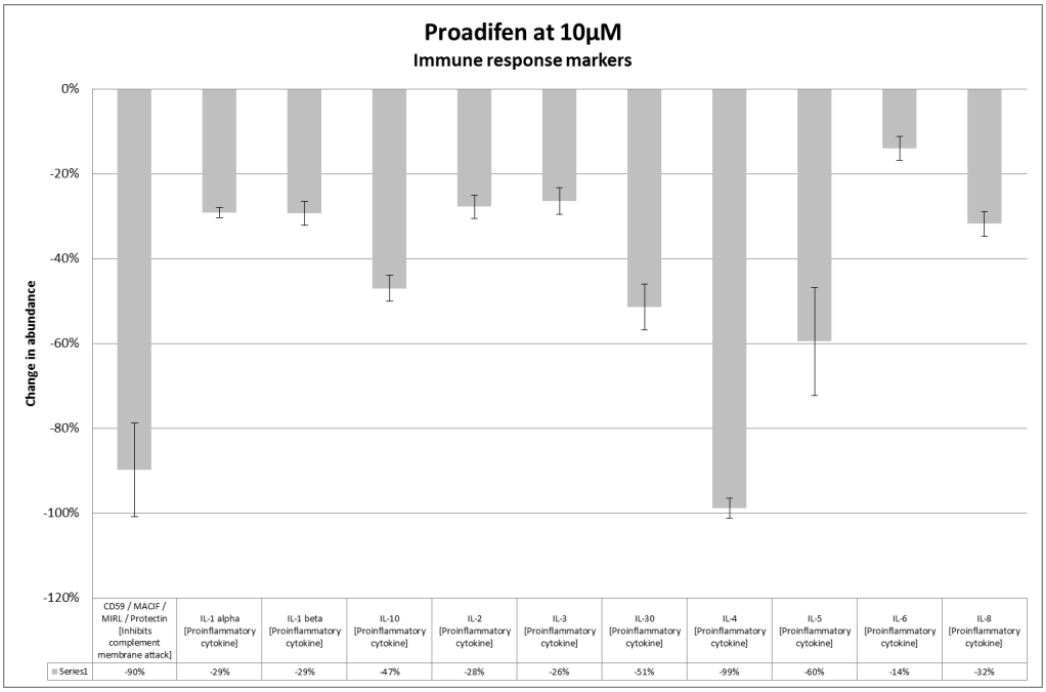

FIGURE 31: EFFECTS OF PROADIFEN ON IMMUNE RESPONSE MARKERS IN PROTEIN ASSAY

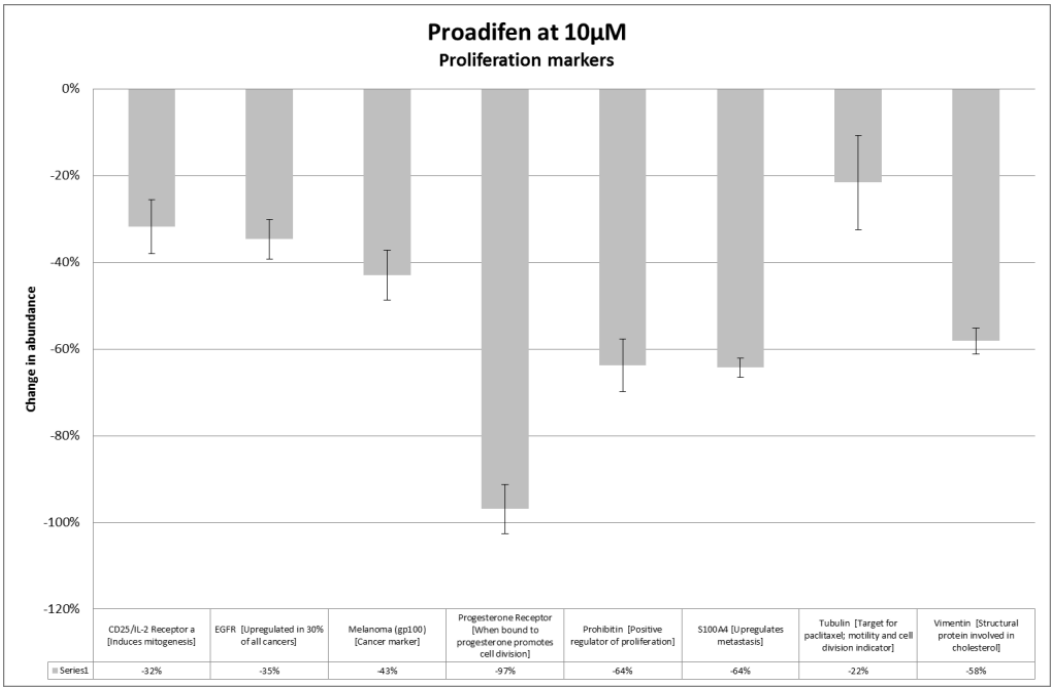

FIGURE 32: EFFECTS OF PROADIFEN ON PROLIFERATION MARKERS IN PROTEIN ASSAY

A SIGNIFICANT DOWN-REGULATION OF THESE MARKER PROTEINS IS EVIDENT.

Comparative Effect of Proadifen on MDA-MB-231 and BJAB cells

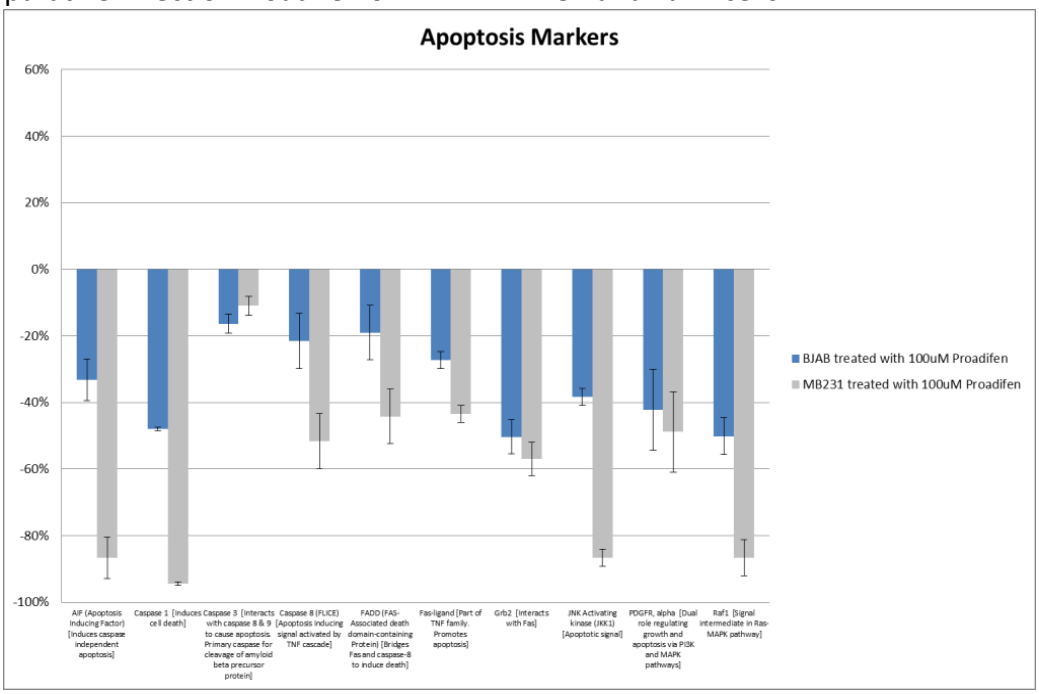

FIGURE 33: COMPARISON OF EFFECTS OF PROADIFEN ON APOPTOSIS MARKERS IN MDA-MB-231 AND BJAB CELLS

BOTH CELL LINES RESPOND IN A SIMILAR MANNER FOR THIS SUB-SET OF PROTEINS WITH ALL BEING DOWN-REGULATED.

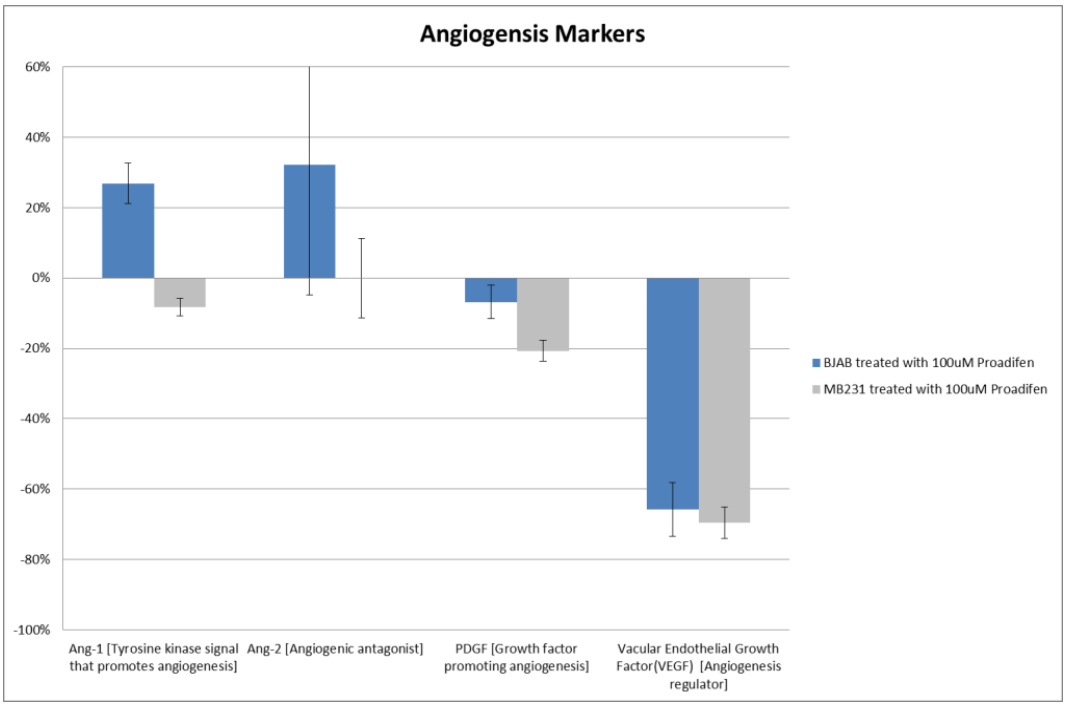

FIGURE 34: COMPARISON OF EFFECTS OF PROADIFEN ON ANGIOGENESIS MARKERS IN MDA-MB-231 AND BJAB CELLS

GROWTH FACTORS ARE DOWN REGULATED IN BOTH CELL LINES BUT ANG-1 IS UPREGULATED IN BJAB.

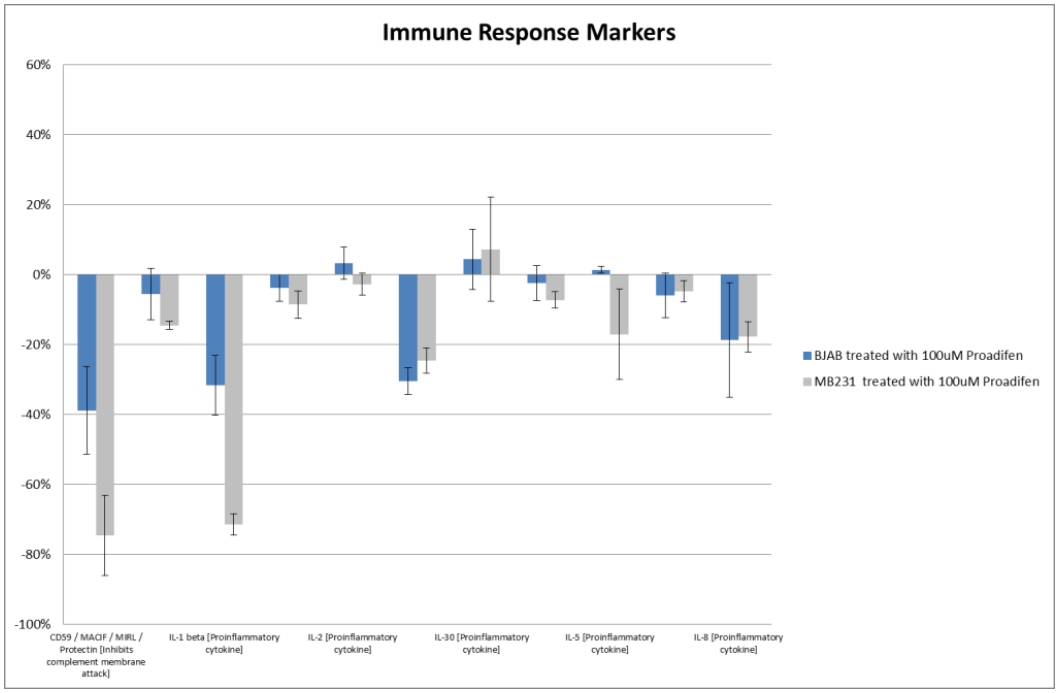

FIGURE 35: COMPARISON OF EFFECTS OF PROADIFEN ON IMMUNE RESPONSE MARKERS IN MDA-MB-231 AND BJAB CELLS

MARKER PROTEINS THAT ARE MOST DOWN-REGULATED ARE COMMON TO BOTH CELL LINES.

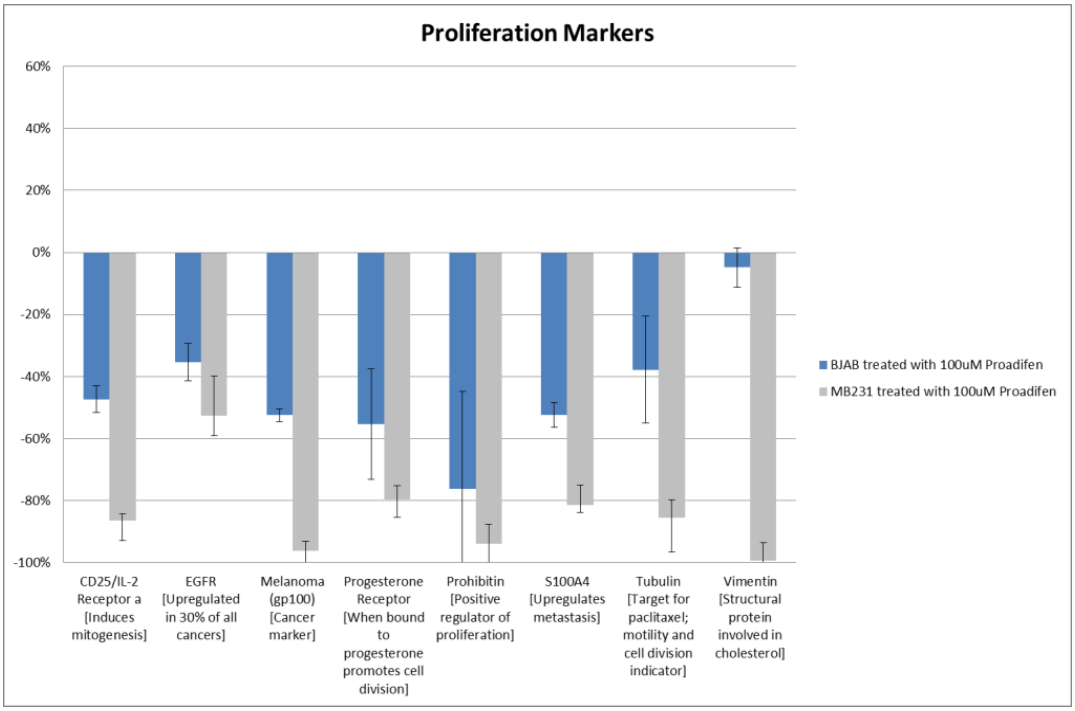

FIGURE 36: COMPARISON OF EFFECTS OF PROADIFEN ON PROLIFERATION MARKERS IN MDA-MB-231 AND BJAB CELLS

VIMENTIN EXPRESSION IS DIFFERENTLY AFFECTED BY THE TREATMENT IN BJAB CELLS. VIMENTIN MAY NOT BE A SUITABLE INDICATOR FOR PROLIFERATION IN NON-ADHERENT CELLS.

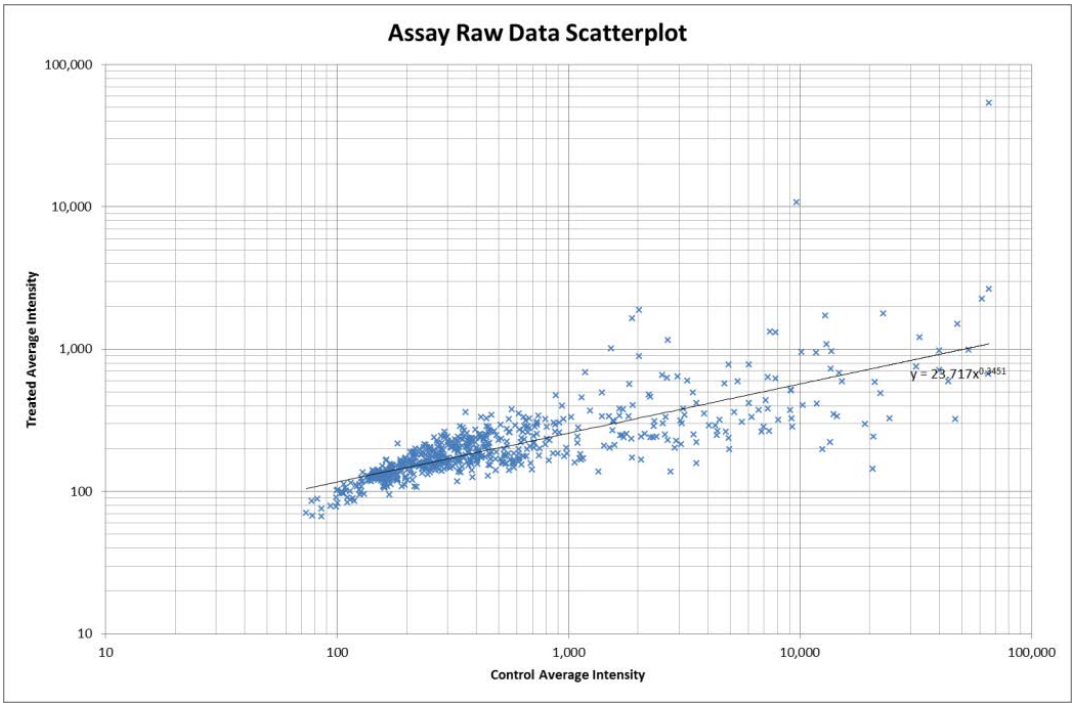

FIGURE 37: MDA-MB-231 CELLS SHOW GENERAL DOWN-REGULATION OF PROTEINS AFTER TREATMENT WITH PROADIFEN

BOTH MDA-MB-231 AND CALU-1 CELL LINES RESPONDED TO THE TREATMENT BY DOWN-REGULATING PROTEINS. IN THE CASE OF MDA-MB-231 CELLS, 294 PROTEINS WERE DOWN REGULATED COMPARED WITH 350 THAT WERE UP-REGULATED OR UNCHANGED.

TABLE 6: SUMMARY OF IMPACTS ON PROTEIN EXPRESSION IN MDA-MB-231 CELLS TREATED WITH STATIN, PROADIFEN AND AY9944

This table shows the three treatments of MDA-MB-231 where all the proteins are considered and the 24 proteins most impacted in a positive direction are ranked. Proteins that appear in more than one list are shaded.

Treatment = AY9944	% Change over control	***Treatment = Pravastatin***	% Change over control	**Treatment = Proadifen High dose**	% Change over control
Integrin beta5	313%	Integrin beta5	287%	Caspase 8 (FLICE)	0%
Histone H1	58%	Histone H1	169%	Thomsen-Friedenreich Antigen	-5%
Fas-ligand	54%	Vinculin	95%	Heat Shock Protein 90a/hsp86	-7%
TGF beta 3	43%	Fas-ligand	77%	Hepatic Nuclear Factor-3B	-9%
HPV 16-E7	42%	TGF beta 3	67%	Catenin alpha	-10%
Vinculin	34%	S100A6	63%	Cystic Fibrosis Transmembrane Regulator	-11%
S100A6	19%	HPV 16-E7	48%	Phosphotyrosine	-14%
CD57	18%	TGF-beta 2	28%	PSCA	-14%
Epithelial Membrane Antigen (EMA / CA15-3 / MUC-1)	14%	CD57	24%	IL-6	-14%
CD94	12%	IL-3	22%	CD105	-14%
Retinoic Acid Receptor (b)	5%	Epithelial Membrane Antigen (EMA / CA15-3 / MUC-1)	20%	Alkaline Phosphatase (AP)	-15%
Human Sodium Iodide Symporter (hNIS)	1%	Superoxide Dismutase	16%	B-cell Linker Protein (BLNK)	-15%
Bovine Serum Albumin	0%	Apolipoprotein D	15%	Insulin Receptor	-17%
TGF-beta 2	0%	Retinoic Acid Receptor (b)	14%	Hepatocyte	-17%
Laminin B2/g1	-1%	ER Ca+2 ATPase2	14%	Caspase 3	-17%
ER Ca+2 ATPase2	-2%	CD94	12%	Synaptophysin	-18%
Amyloid A	-4%	Human Sodium Iodide Symporter (hNIS)	10%	Negative Control for Mouse IgG2a	-18%
IL-3	-5%	Laminin B2/g1	9%	EMA/CA15-3/MUC-1	-19%
Superoxide Dismutase	-9%	Heregulin	4%	Heat Shock Protein 27/hsp27	-19%
Surfactant Protein A	-9%	Glicentin	4%	HDAC1	-19%
CITED1	-9%	Surfactant Protein A	1%	b-2-Microglobulin	-19%
Ret Oncoprotein	-11%	Bovine Serum Albumin	0%	Tyrosinase	-20%
Apolipoprotein D	-12%	Amyloid A	0%	Estradiol	-20%
Glicentin	-13%	Ret Oncoprotein	-2%	DcR2 / TRAIL-R4 / TRUNDD	-20%

3.2.7 DISCUSSION OF PROTEIN ASSAYS (ANTIBODY ARRAY)

To better assess the effects of the treatments, a small number of proteins (33) of the 656 assayed were isolated from the data according to their role in cancer. According to the detailed descriptions provided by a manufacturer of similar protein array (Sigma-Aldrich Ltd, UK), they were segregated by functional implication - immune response, angiogenesis proteins, proteins involved in proliferation and those involved in apoptosis. The effects on cancer of their up/down regulation is specific to the proteins so that not all down-regulation of proliferation markers is desirable outcome nor is all up-regulation of apoptotic markers. They do however provide a manageable data set.

Table 6: Summary of impacts on protein expression in MDA-MB-231 cells treated with statin, Proadifen and AY9944 reveals that AY9944 and statin treatments share many of the most affected proteins while the Proadifen treatment shares none with the other treatments. This is quite suggestive and it is tempting to theorize that the effects of Proadifen upon the proteome are caused by a different mechanism to those seen in the cells treated with other types of cholesterol inhibitor. It is most likely that the statin and the Δ-7 reductase inhibitor leave the isoprenoid branch of the mevalonate pathway unaffected and that these positive shifts in protein expression are the response to interference with this important pathway.

Li *et al* (Li Y., 2010) compared the proteomics of benign and malignant human osteosarcomas using 2-D gel electrophoresis and Western blotting to compare the expression levels of proteins. They found 30 alterations in the malignant cells using

these techniques of which 18 were identified and of these 12 were up-regulated and 6 down-regulated. Their results suggested that vimentin and tubulin were of special importance to the propensity of the cells to metastasize. These two cytoskeleton proteins work together to form and stabilize microtubules that are involved in cell-cell interaction and reattachment processes. It is also known that destabilizing actin fibres and microtubules with drugs prevents reattachment of circulating colon carcinoma (Korb et al., 2004) and so reduce the cancer's ability to successfully spread. There is also evidence that elevated levels of tubulin in patients with breast cancer are positively correlated with poor prognosis (Mialhe et al., 2001).

AY9944 and Pravastatin caused very significant reduction in these proteins – nearly 100% (Figure 24) – while Proadifen reduced tubulin and vimentin by 21% and 59% respectively (Figure 36).

Two partial cancer related signalling pathways can be examined using the 100uM Proadifen treatments of -MDA-MB-231 and BJAB cells proteomic data:

APOPTOTIC PATHWAY AT CHOLESTEROL RICH RAFT, LEADING TO CELL DEATH

Signal pathway	**Fas**	**FASL**	**Ezrin**	**FAS-DISC**
Change % post treatment MDA-MB-231	-	-43	-12	-44
Change % post treatment BJAB	-	-27	-19	-19

TABLE 7: EXTRACTION OF PROTEIN DATA TO ONE APOPTOTIC PATHWAY

PROLIFERATION PATHWAY BASED AT CHOLESTEROL RICH RAFT:

Signal pathway	EGF	EGFR	Grb2	Ras	Raf	MEK	Erk	Elk-1
Change % post treatment MDA-MB-231	--	-53	-57	-87	-87	-49	-56	-
Change % post treatment BJAB	-	-35	-50	-35	-50	-35	-21	-

TABLE 8: EXTRACTION OF PROTEIN DATA TO ONE PROLIFERATION PATHWAY

- Indicates not assayed

The treatment affected these pathways in the two cell lines in the same direction (down) but to varying degrees. Ezrin (known to be associated with rafts, Table 12) was the only exception and showed a slightly larger decrease in the BJAB assay.

A high dose of Δ-7 reductase inhibitor (A9944) appears to significantly reduce the expression of all but one of the proteins in the marker selection. This exception is Fas-ligand which promotes apoptosis, although the proteins downstream of this apoptotic pathway are, in fact, all down-regulated. A reduction of Δ-7 should theoretically lead to the accumulation of 5,7,24-cholesatrien-3β-ol, 4,4-dimethylcholesta-8(9)-1,4-dien-3b-ol and 7-dehydrocholesterol. In the presence of a Δ-24 inhibitor the route to 7-dehydrocholesterol is blocked.

Statin treatment caused a very similar effect in the protein marker set, except that there was a 22% rise in interleukin-3 cytokine. IL-3 stimulates the immune response by provoking the differentiation of pluripotent stem cells into lymphoid progenitor cells. Statin treatment resulted in a generally greater down-regulation of apoptotic markers compared with Proadifen or AY9944, but this is not unexpected given that statins truncate the cholesterol pathway at a very early stage of the mevalonate-cholesterol

pathway, and isoprenylation of the marker proteins is also reduced. This means that it is possible there is little feedstock lanosterol for the ultimate steps of cholesterol synthesis and it is known that the enzyme-substrate affinities of the transferases involved in prenylation are higher than those involved in sterol synthesis (Goldstein and Brown, 1990). Total inhibition of synthesis of cholesterol by statins is unlikely.

There were some marked differences in response to Proadifen in BJAB cells compared to MDA-MB-231 cells. Notably, the cytokines Ang-1 and Ang-2, respectively an angiogenesis promoter and inhibitor, were affected differently in the two lines by Proadifen treatment. Ang-1 expression was increased in BJAB cells but reduced in MDA-MB-231 cells. Generally, however, BJAB cells followed the same pattern as MDA-MB-231 cells but with a much reduced response. When the entire data set was ranked by impact for the three treatments in MDA-MB-231 cells there was a very clear correlation between AY9944 and statin treatments in terms of the proteins most affected. Proadifen, however, shared none of the top 24 most affected proteins compared to AY9944 (18) and statin (20) (see table 4).

This does suggest that Δ-24 reductase inhibition – as opposed to Δ-7 reductase inhibition - causes a very different response in terms of protein profile. It seems possible that the extent and nature of the protein regulation is correlated to whatever cholesterol intermediate is the ultimate compound in the synthetic pathway. That is to say, AY9944 may reduce the overall amount of cholesterol in the membrane through a build-up 7-Dehydrocholesterol – a compound very closely related to cholesterol. It is

possible that this sterol can form rafts whereas other intermediates cannot. The build-up of dehydrocholesterol by AY9944 and the reduction of mevalonate feedstock by statin, appears to cause 12 of 21 proteins in the marker selection to be up-regulated respectively, whereas no proteins were up-regulated in the Proadifen treatments. This effect on the marker group by Proadifen is not reflected in the entire data set where for Proadifen almost half of the responding proteins are up-regulated. This is a clear distinction in the impact of Proadifen compared with the Δ-7 reductase inhibitors. Alternatively, one possible hypothesis could be that AY9944 and the statins cause a reduction in the number of viable membrane rafts while Proadifen alters the nature of those rafts. It is conceivable that cholesterol-rich rafts are reduced in number by both sorts of inhibitor but that caveolae are principally affected by the Proadifen. Perhaps rafts can assemble from lanosterol and desmosterol but caveolae cannot. There is evidence that desmosterol cannot replace cholesterol to form functional rafts (Vainio et al., 2006). It is thus more likely that the organisation of caveolae takes precedence to the formation of cholesterol-rich rafts: the affinity of cholesterol with Cav-1 is conceivably higher than the affinity of cholesterol with itself or with sphingosines.

In an earlier study, using antisense oligonucleotide DNA probes, Slaton *et al* (Slaton et al., 2001) determined that the expression levels of vascular endothelial growth factor, IL-8 and MMP-2 and -9 were significantly higher in metastatic renal cell carcinoma (RCC). All three treatments caused IL-8 to be reduced. In particular they identified the ratio of the surface glycoprotein E-cadherin to MMP-9 as a significant predictor of metastatic potential in RCC. Other reports also indicate a predictive value to the

expression levels of E-cadherin (Yasui W., 1991), (Buehler H., 2001) which is known to mediate cell-cell adherence and re-attachment (Takeichi, 1991). Integrin-controlled Rac activation signalling is another positively correlated factor in metastasis (McLean et al., 2005) and Rac and Ras binding is known to be localized in cholesterol rafts (Guan, 2004), (Del Pozo and Schwartz, 2007) and internalized in caveolae in a process triggered by GM1, at least in detached cells. The levels of integrin are dependent on the cells anchorage and determine the internalization of receptors or the activation of down-stream signals involved in cancer promotion and metastasis.

Given that expression levels of vimentin, tubulin, IL-8, MMP-2, E-cadherin, integrin and Rac are positively correlated to proliferation it seems reasonable to assume that a reduction in these proteins would result in a reduction in proliferation.

In general BJAB and MDA-MB-231 cells responded in a similar manner to Proadifen treatment with BJAB cells showing a reduced response (Figure 35). There are, however, three clear exceptions: the pro-inflammatory IL-2 and IL-2 and Angiopoietin-1 are each up-regulated in BJAB but down-regulated in MDA-MB-231. The reason for this is unclear.

3.3 RESULTS OF GENE EXPRESSION ASSAYS

Note: the raw dataset is available at: : WWW://WWW.NCBI.NLM.NIH.GOV/GEO/ and has the accession number GSE47463.

3.3.1.1 MDA-MB-231 GENE EXPRESSION

The statistical significance threshold chosen for functional enrichment analyses was adjusted to $p<0.01$. Functional enrichment analyses were undertaken for each comparison that had loci significant at this threshold. Up- and down-regulated loci were assessed separately.

An overview of the underlying biological changes occurring within each comparison can be obtained by functional enrichment analysis. This was performed from two perspectives, namely KEGG pathway membership and Gene Ontology (GO) terms. The level of statistical significance for functional analysis would normally be chosen to be the most stringent level at which 1% of the array features were, on average, significant (which would have been adjusted $p<0.0001$). In this instance, as the number of significant genes across the 15 comparisons was quite skewed, the significance threshold was manually chosen to be adjusted $p<0.01$.

3.3.1.2 KEGG PATHWAYS

Probesets on the array may have been annotated as being a member of a KEGG pathway (www.kegg.jp). Although there is always a degree of overlap between functional annotations from different sources, each set has information/applications

not available in the others, and thus it is generally beneficial to consider more than one. Significant genes (adjusted p<0.01) from each comparison were analysed for enrichment of KEGG pathway membership using a hypergeometric test. Enrichment ($p < 0.05$) was assessed for up-regulated and down-regulated genes separately.

3.3.1.3 GO TERMS

As described at www.geneontology.org, the Gene Ontology (GO) project is a collaborative effort to address the need for consistent descriptions of gene products in different databases. The GO project has developed three structured controlled vocabularies (ontologies) that describe gene products in terms of their associated biological processes, cellular components and molecular functions in a species-independent manner. The use of GO terms by collaborating databases facilitates uniform queries across them. The controlled vocabularies are structured so that they can be queried at different levels: for example, you can use GO to find all the gene products in the human genome that are involved in signal transduction, or you can zoom in on all the receptor tyrosine kinases. It should be noted that not all GO terms assigned to a given gene are manually attached; many are IEA, i.e. inferred from electronic annotation. Although rigorous thresholds are typically applied before assignment, the caveat remains. Probesets on the array may have been annotated with GO terms from any or all of the three ontologies. Within any grouping of genes, chosen on any given criterion (e.g. statistical significance), one can assess, using a hypergeometric test, whether any of the GO terms attached to the chosen genes are over-represented relative to the "universe" of genes, and hence associated terms, that

are present on the array. Significant genes (adjusted p<0.01) from each comparison were analysed for enrichment of GO terms across all three GO ontologies using a hypergeometric test. Enrichment ($p < 0.001$) was assessed for up-regulated and down-regulated genes separately.

THE FOLLOWING GRAPHS (FIGURES 38 TO 52) ARE VOLCANO PLOTS WHERE THE LOG2 FOLD CHANGE IN GENE EXPRESSION IS PLOTTED AGAINST THE SIGNIFICANCE. THE X-AXIS IS THE LOG2 FOLD CHANGE IN GENE EXPRESSION WHILE THE Y-AXIS SHOWS THE –LOG10 ADJUSTED P VALUE. IN EACH CASE, THE TREATMENTS ARE FIRST COMPARED WITH THE NEGATIVE CONTROL AND THEN, IN TURN, WITH EACH OTHER. THIS ENABLES VERY EASY COMPARISONS BETWEEN TREATMENTS AS TO THEIR OVERALL EFFECTS ON GENE EXPRESSION. THE AREAS OF GREATEST INTEREST ARE THE UPPER RIGHT AND LEFT QUADRANTS SINCE THESE ARE THE MOST SIGNIFICANT AND MOST AFFECTED GENES THAT HAVE BEEN UP- OR DOWN- REGULATED RESPECTIVELY. CELLS WERE EXPOSED TO THE TREATMENTS FOR 24 HOURS PRIOR TO RNA EXTRACTION.

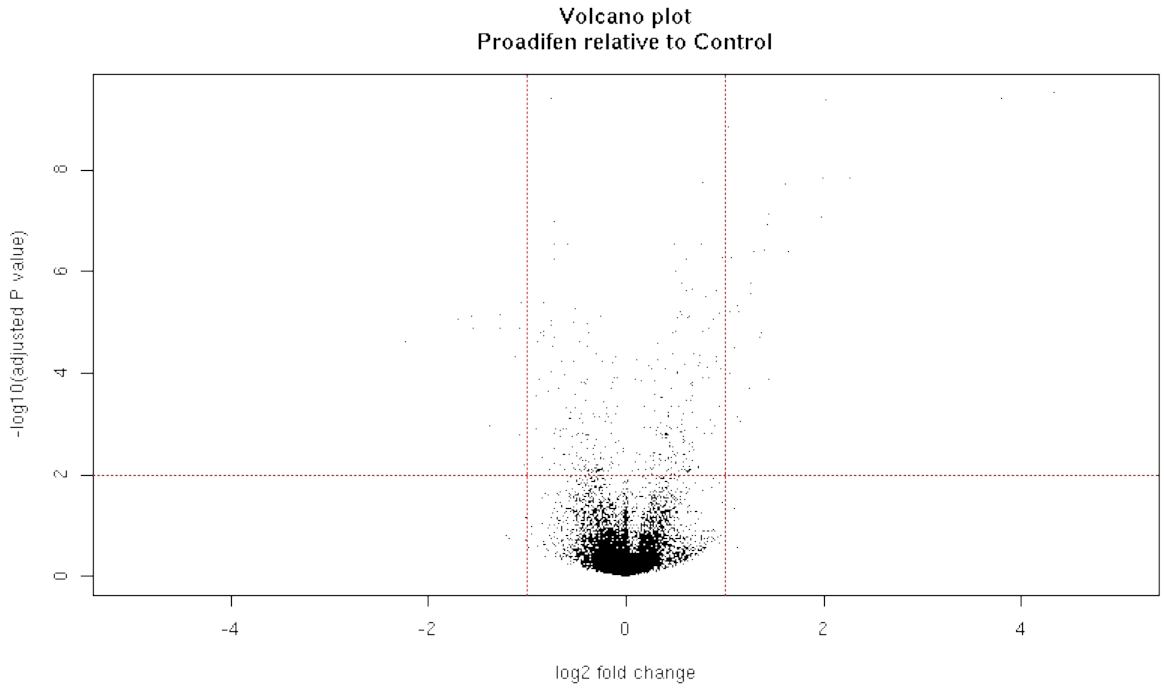

FIGURE 38: VOLCANO PLOT PROADFIEN (10µM) RELATIVE TO CONTROL (MDA-MB-231)

PROADIFEN CAUSES A MIXTURE OF UP- AND DOWN- GENE REGULATIONS, MANY OF WHICH ARE SIGNIFICANT.

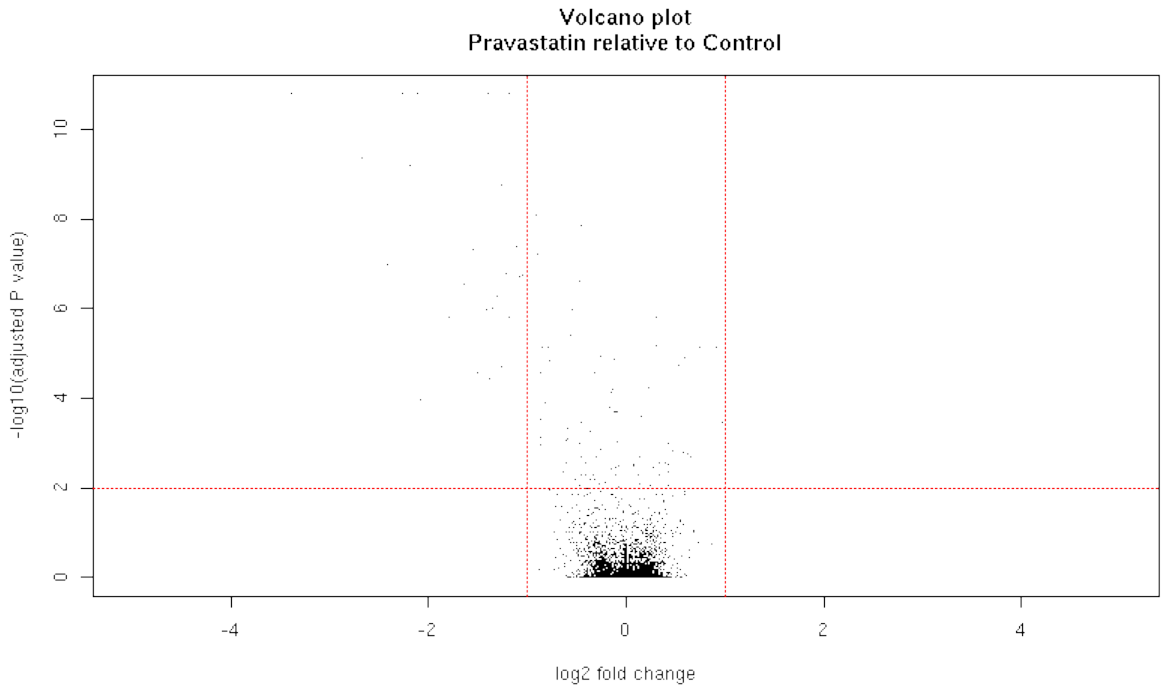

FIGURE 39: VOLCANO PLOT PRAVASTATIN (8.0µM) RELATIVE TO CONTROL (MDA-MB-231)

THE STATIN CAUSES MAINLY DOWN-REGULATIONS. THIS IS REFLECTED IN GENE DATA ISOLATED FOR INVOLVEMENT IN THE MEVALONATE PATHWAY (SEE TABLE 10)

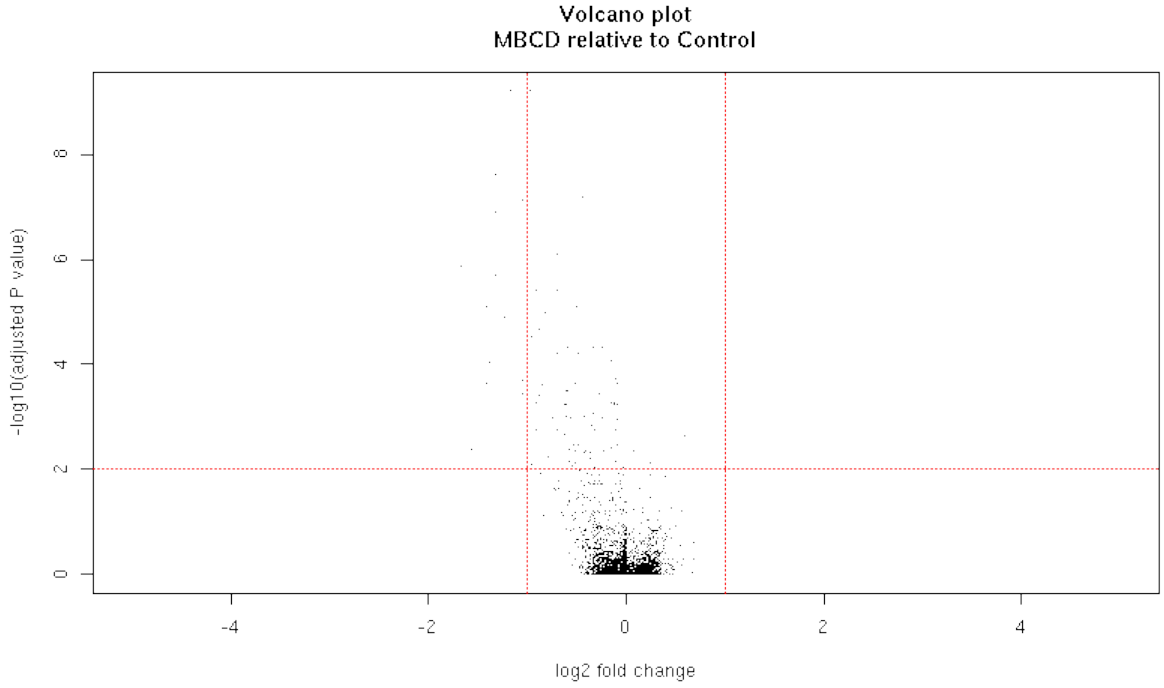

FIGURE 40: VOLCANO PLOT MBCD (0.0008% W/V) RELATIVE TO CONTROL (MDA-MB-231)

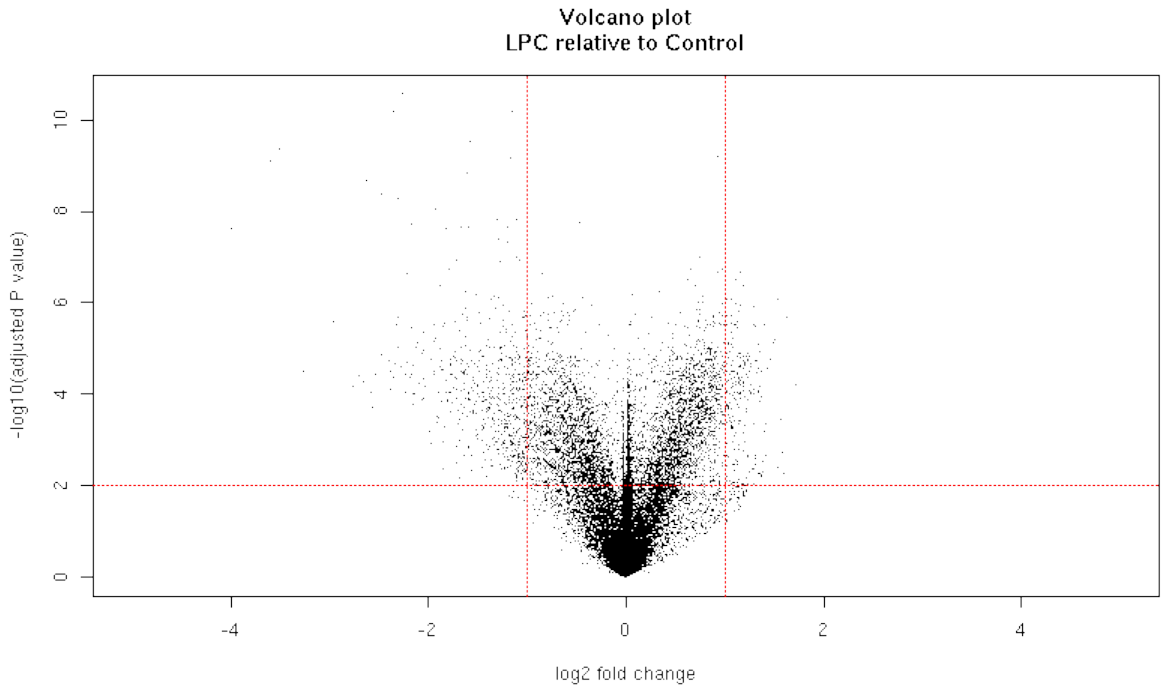

FIGURE 41 VOLCANO PLOT LPC (100µM) RELATIVE TO CONTROL (MDA-MB-231)

LPC CAUSED A WIDESCALE DISRUPTION TO NORMAL GENE EXPRESSION WITH BOTH UP AND DOWN REGULATIONS THAT ARE LARGE IN SIZE AND HIGHLY SIGNIFICANT. THIS MAY BE DUE TO THE FLUIDIZING EFFECTS OF THE MOLECULE WHEN IT INTERDIGITATES WITH THE MEMBRANE CAUSING SIGNAL PROTEINS TO LOSE THEIR ANCHORAGE IN RAFTS AND OTHER MICRODOMAINS.

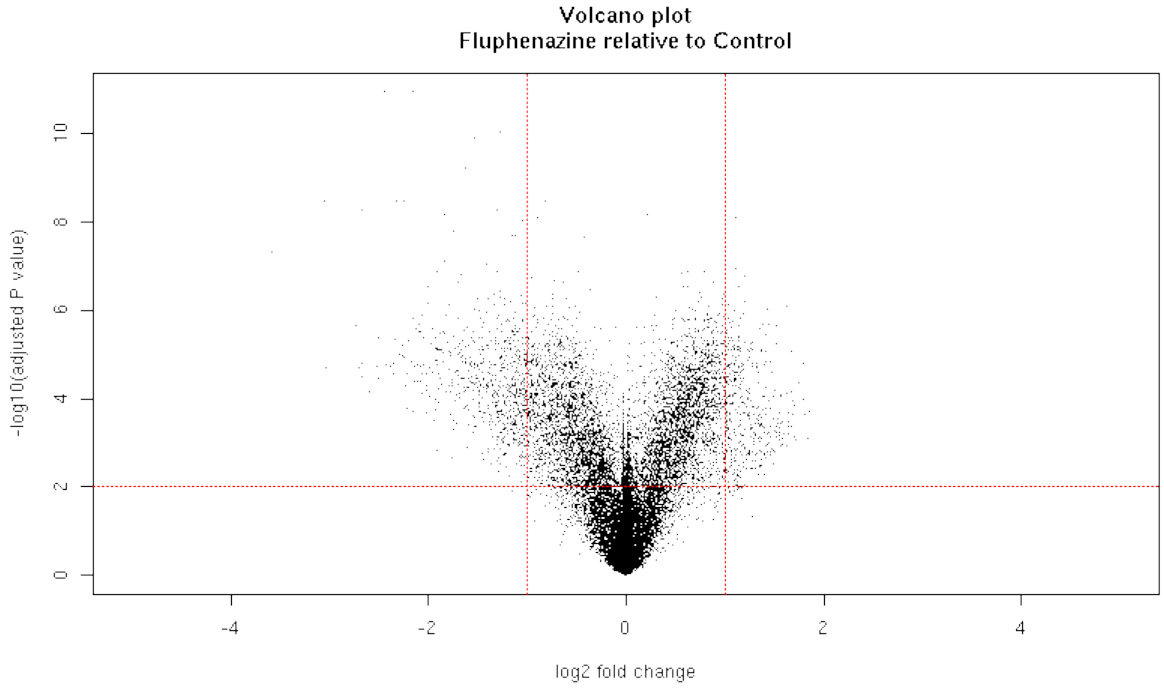

FIGURE 42: VOLCANO PLOT FLUPHENAZINE (100µM) RELATIVE TO CONTROL (MDA-MB-231)

LIKE LPC, FLUPHENAZINE IS ALSO KNOWN TO BE A MEMBRANE FLUIDIZING AGENT AND THE RESPONSE IN TERMS OF GENE EXPRESSION IS PROFOUND.

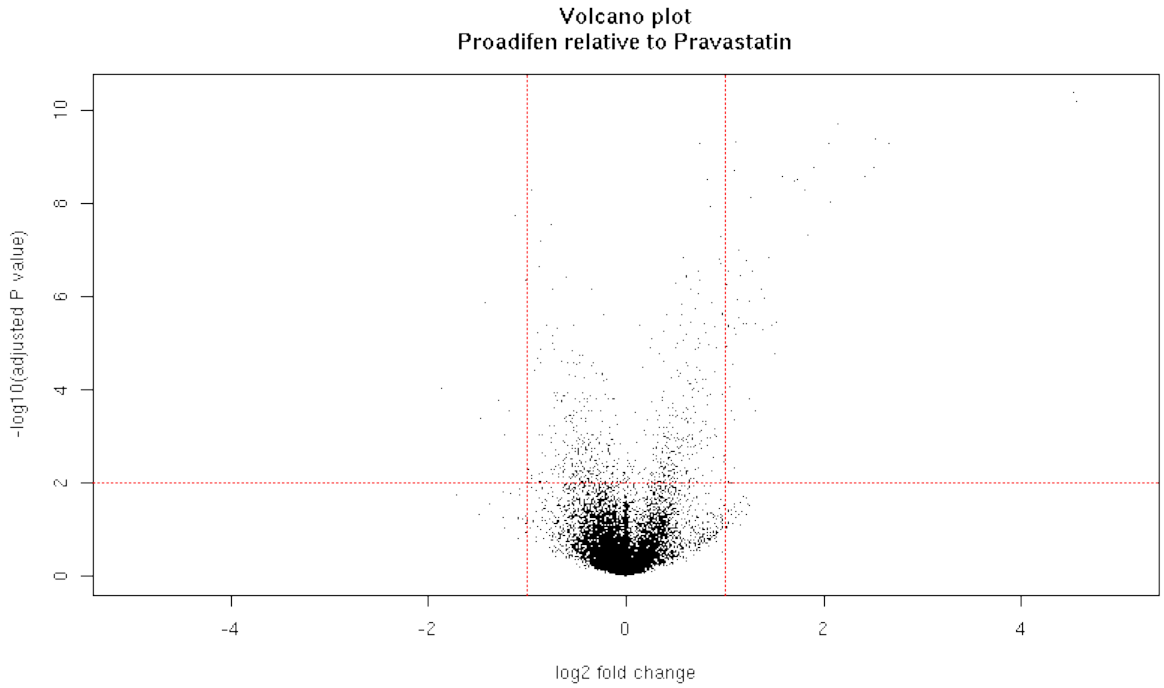

FIGURE 43: VOLCANO PLOT PROADIFEN (10µM) RELATIVE TO PRAVASTATIN 8.0µM (MDA-MB-231)

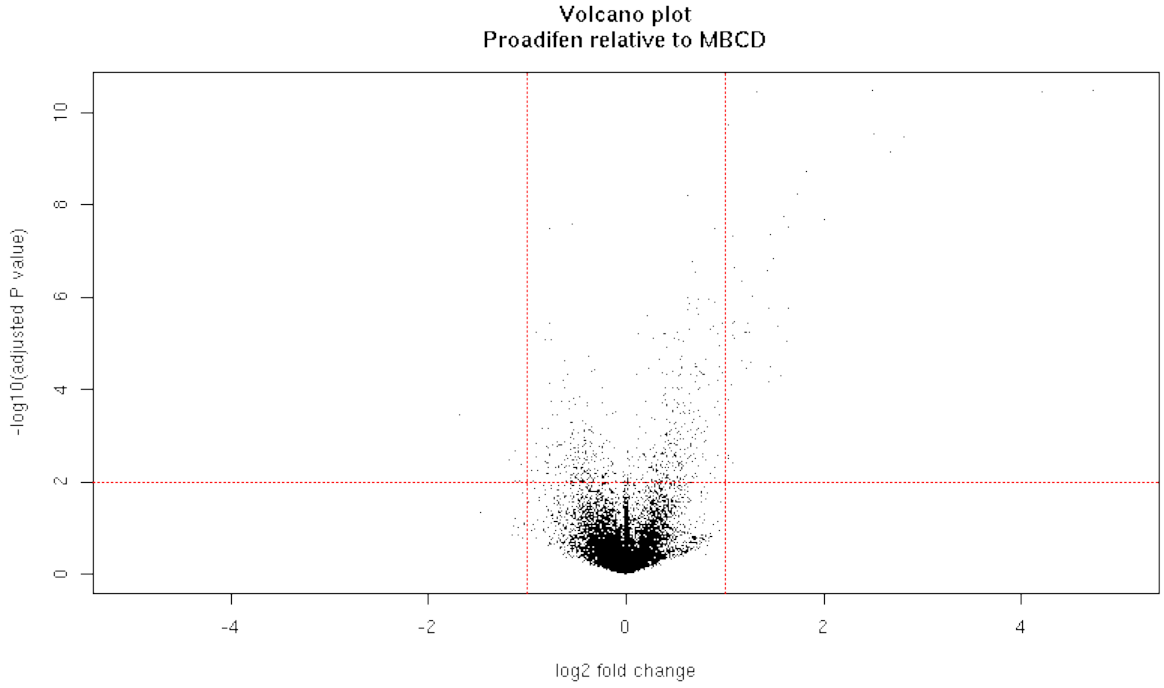

FIGURE 44: VOLCANO PLOT PROADIFEN (10µM) RELATIVE TO MBCD 0.0008% W/V (MDA-MB-231)

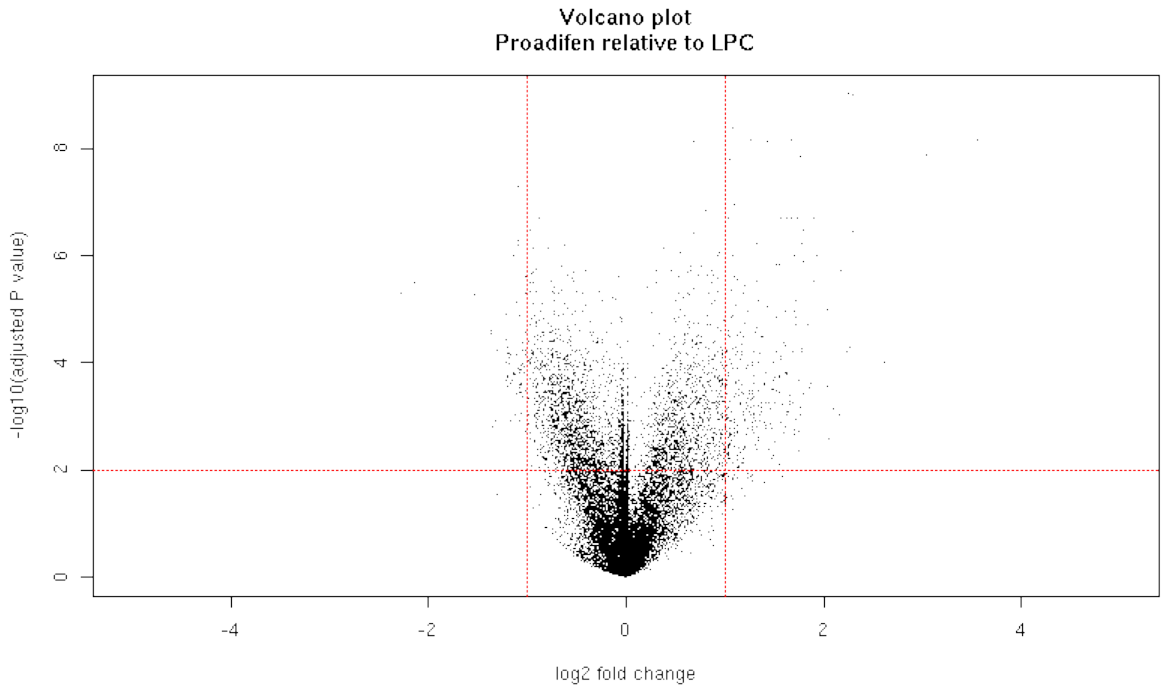

FIGURE 45: VOLCANO PLOT PROADIFEN (10µM) RELATIVE TO LPC (100µM) (MDA-MB-231)

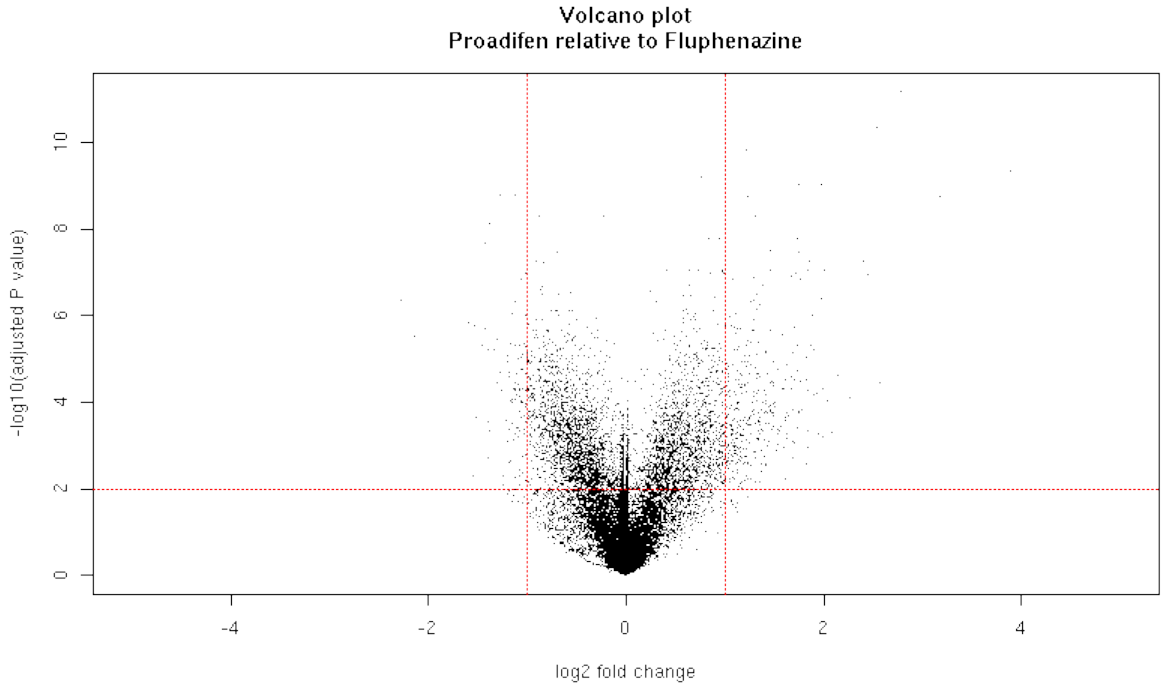

FIGURE 46: VOLCANO PLOT PROADIFEN (10µM) RELATIVE TO FLUPHENAZINE (100µM) (MDA-MB-231)

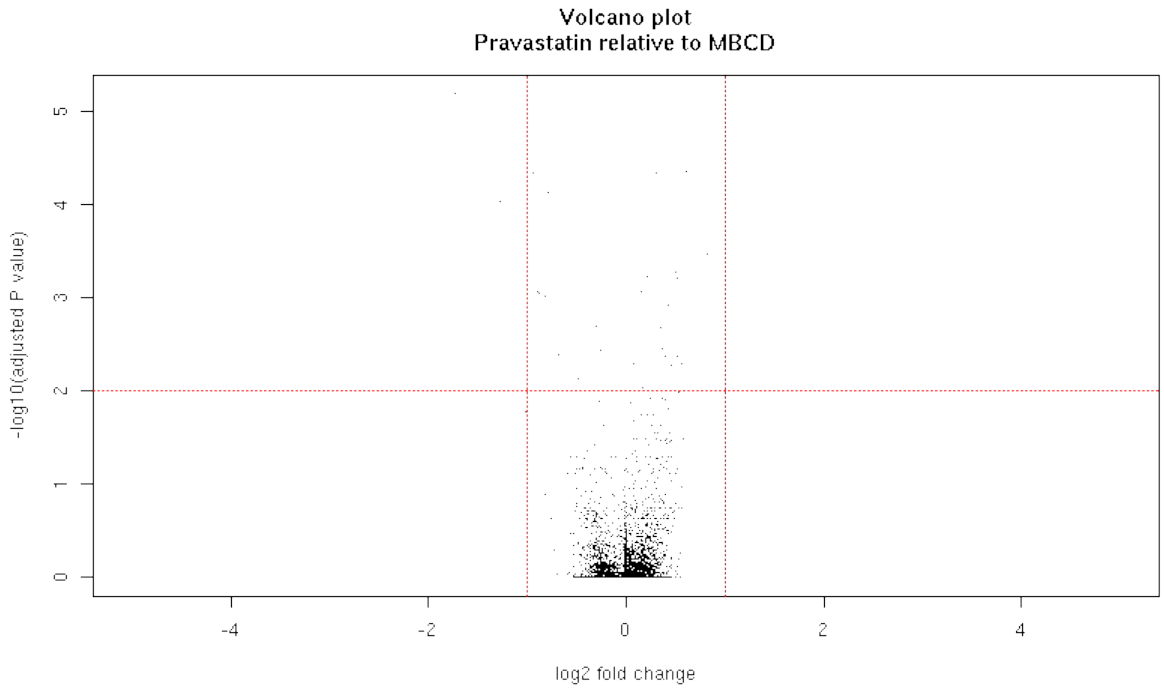

FIGURE 47: VOLCANO PLOT PRAVASTATIN 8.0µM RELATIVE TO MBCD 0.0008% W/V (MDA-MB-231)

FIGURE 47 SUGGESTS THAT THERE IS ALMOST NO DIFFERENCE (IN TERMS OF GENE EXPRESSION) BETWEEN THESE TWO TREATMENTS AND CONFIRMS THE EQUIVALENCE OF A STATIN AND CHOLESTEROL SEQUESTERING DRUG. IT SUGGESTS ALSO THAT THE REMOVAL OF CHOLESTEROL FROM THE CELL MEMBRANE IS WHAT THEN CAUSES CHANGES TO GENE EXPRESSION RATHER THAN SOME DIRECT EFFECT OF THE STATIN.

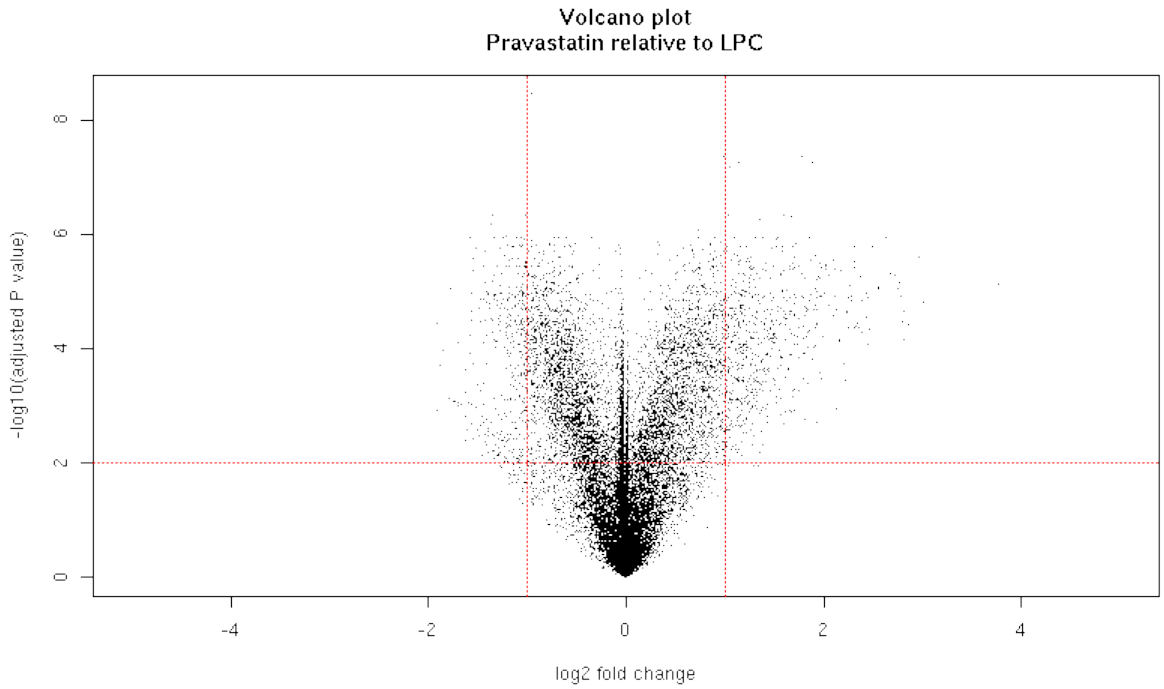

FIGURE 48: VOLVANO PLOT PRAVASTATIN 8.0µM RELATIVE TO LPC 100µM (MDA-MB-231)

THERE IS A CLEAR DIFFERENCE IN EFFECT OF THESE TWO TREATMENTS.

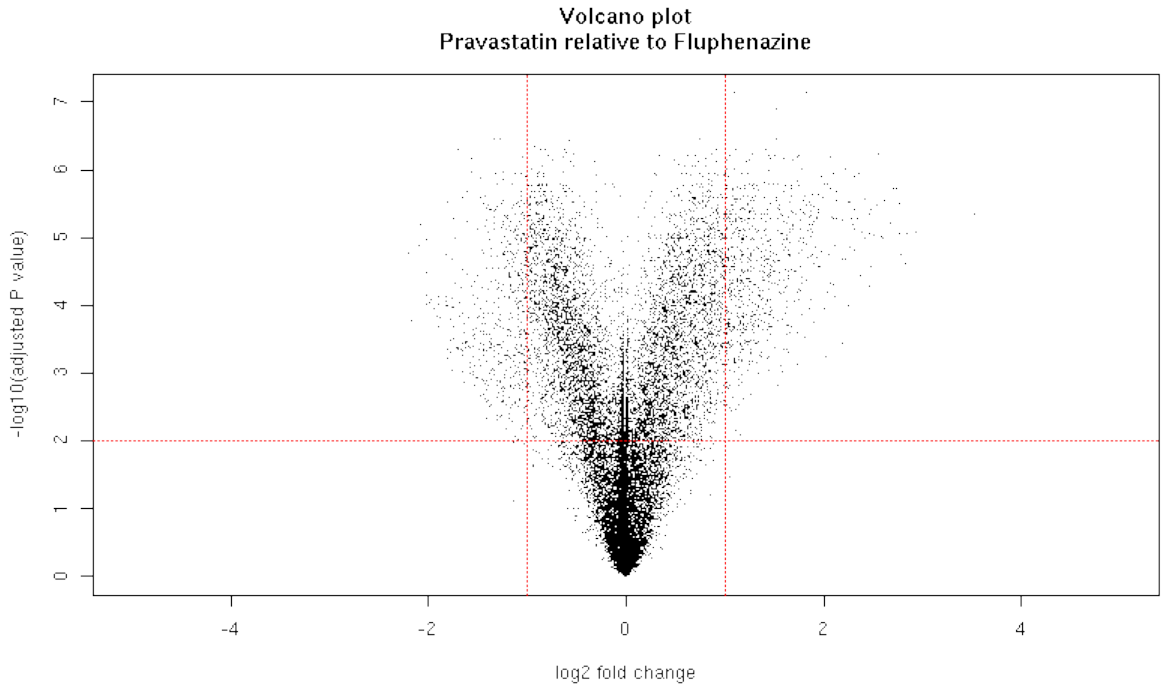

FIGURE 49: VOLCANO PLOT PRAVASTATIN 8.0µM RELATIVE TO FLUPHENAZINE 100µM (MDA-MB-231)

THERE IS A CLEAR DIFFERENCE IN EFFECT OF THESE TWO TREATMENTS.

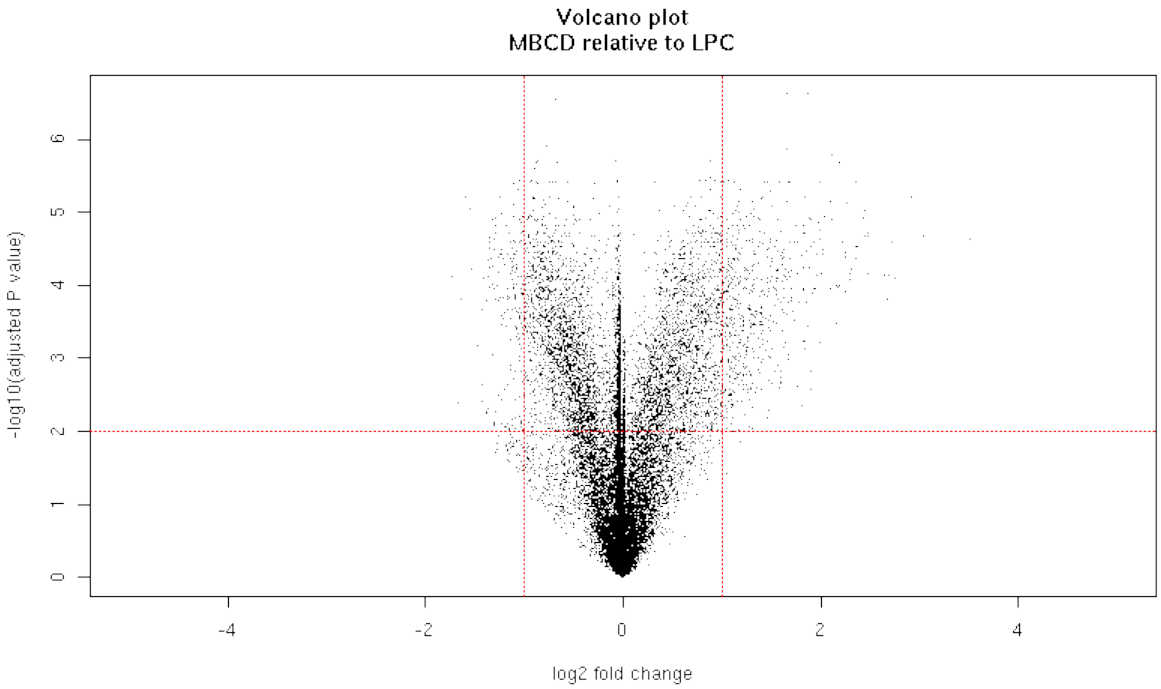

FIGURE 50: VOLCANO PLOT MBCD 0.0008% W/V RELATIVE TO LPC 100µM (MDA-MB-231)

THERE IS A CLEAR DIFFERENCE IN EFFECT OF THESE TWO TREATMENTS SUGGESTING THAT REMOVAL OF CHOLESTEROL IS NOT EQUIVALENT TO INCREASING MEMBRANE FLUIDITY/POROSITY. THIS DESPITE THE FACT THAT CHOLESTEROL IS THOUGHT TO BE A REGULATOR OF MEMBRANE RIGIDITY.

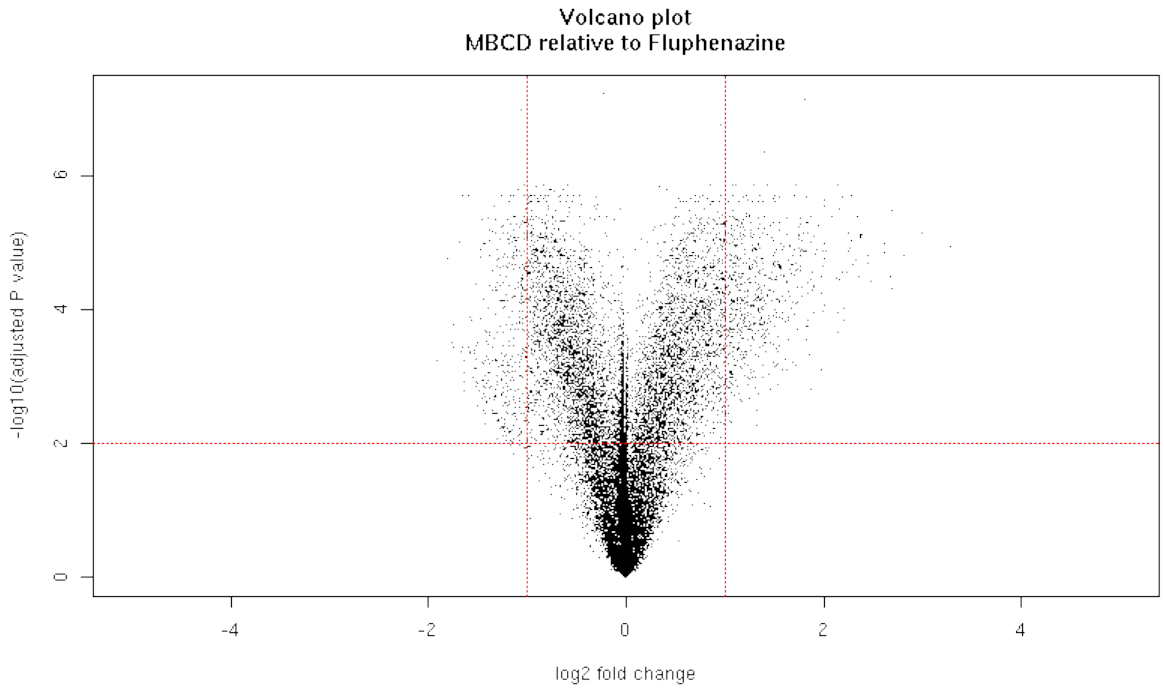

FIGURE 51: VOLCANO PLOT MBCD (0.0008% W/V) RELATIVE TO FLUPHENAZINE (100µM) (MDA-MB-231)

THERE IS A CLEAR DIFFERENCE IN EFFECT OF THESE TWO TREATMENTS.

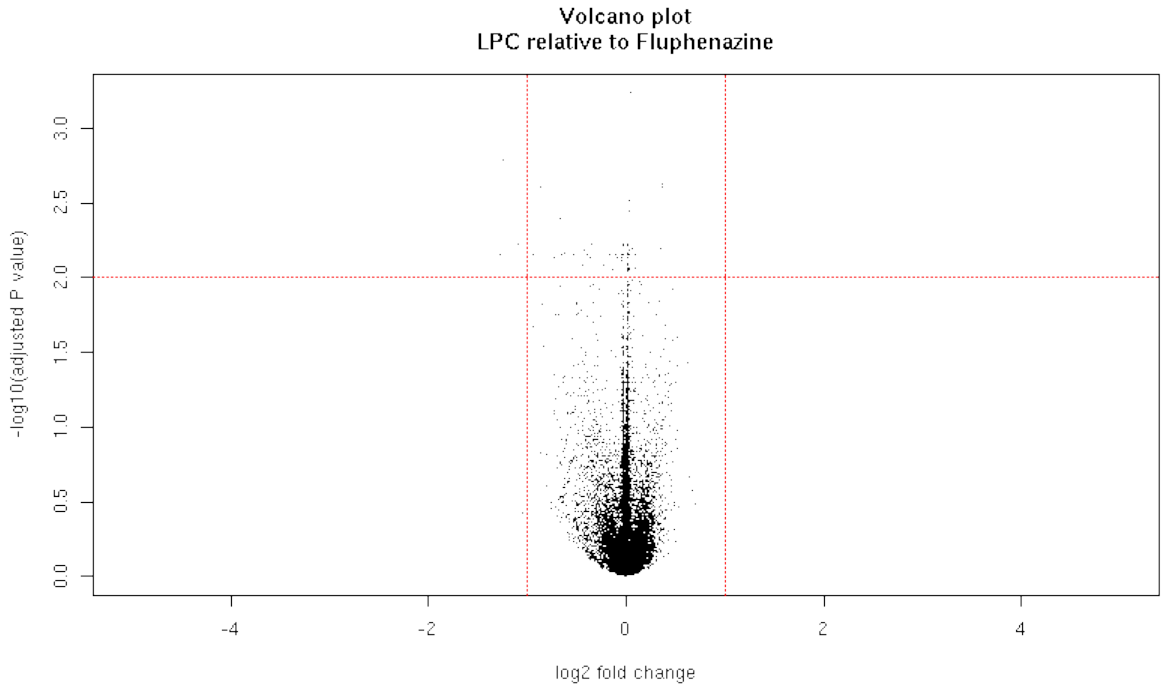

FIGURE 52: VOLCANO PLOT LPC (100µ) RELATIVE TO FLUPHENAZINE (100µM) (MDA-MB-231)

THESE TREATMENTS HAVE MATCHING PATTERNS ENTIRELY WITHIN ±2 LOG2 FC INDICATING VERY SIMILAR EFFECTS ON GENE EXPRESSION.

It is noteworthy that the response of the cell to LPC and Fluphenazine is very similar suggesting a similar mode of action.

KEGG PATHWAY ENRICHMENT IN MDA-MB-231 CELLS

Ribosome pathway was strongly up-regulated with Pravastatin and MBCD versus either LPC or Fluphenazine. Spliceosome, cell cycle and pyruvate metabolism were also up-regulated in these comparisons. Steroid biosynthesis, lysosome, terpenoid backbone biosynthesis and metabolic pathways were up-regulated with Proadifen versus control, Pravastatin or MBCD. p53 signalling pathway was down-regulated by Proadifen and both Pravastatin or MBCD. Cytokine-cytokine receptor interaction and NOD-like receptor signalling pathways were down-regulated with MBCD, Proadifen and Pravastatin versus control.

mTOR signalling, lysine degradation and chronic myeloid leukaemia pathways were down-regulated between Pravastatin and either MBCD or Fluphenazine. Protein binding pathway was over-represented in all comparisons except for Proadifen versus control, Pravastatin or MBCD, which had sterol and cholesterol biosynthesis process pathways in common. Cytokine activity was down-regulated with Pravastatin, MBCD and Proadifen versus control.

It is significant that the four loci with the greatest fold change are all associated with cancer:

NUPR1 (Nuclear protein 1) is up-regulated in metastatic cancer and plays a key role in malignant breast [and other] cancers, protecting them from apoptosis (Chowdhury et al., 2009). Both isoforms are actually enhanced by Pravastatin, MβCD and Proadifen, with the latter having the greatest impact.

GDF15 (Growth Differentiation Factor) codes for a cardioprotective protein that regulates inflammatory and apoptotic pathways (Ago and Sadoshima, 2006).These are all overwhelmingly increased with Proadifen having the greatest impact. CTGF (Connective Tissue Growth Factor) up-regulates MMPs and their inhibitors and

promotes cell growth, migration and adhesion. It is implicated in angiogenesis (Brigstock, 1999). This gene is the most down-regulated by the statin, MβCD and most of all Proadifen.

Two additional cancer related loci that are included in the 16-fold change data are COL1A1 which is down-regulated by Proadifen. This gene codes for collagen. ATF3 which represses MMP-2 (Yan et al., 2002) is up-regulated by Proadifen and to a lesser extent by the other treatments. Overall, steroid biosynthesis is up-regulated with Proadifen, MβCD and Pravastatin. Furthermore, aminoacyl-tRNA biosynthesis, Biosynthesis of unsaturated fatty acids and terpenoid backbone biosynthesis are up-regulated with MβCD and Pravastatin.

The following graphs are volcano plots (as before) but this time the cell type is CaLu-1 instead of MDA-MB-231, allowing comparison with Figures 38-50.

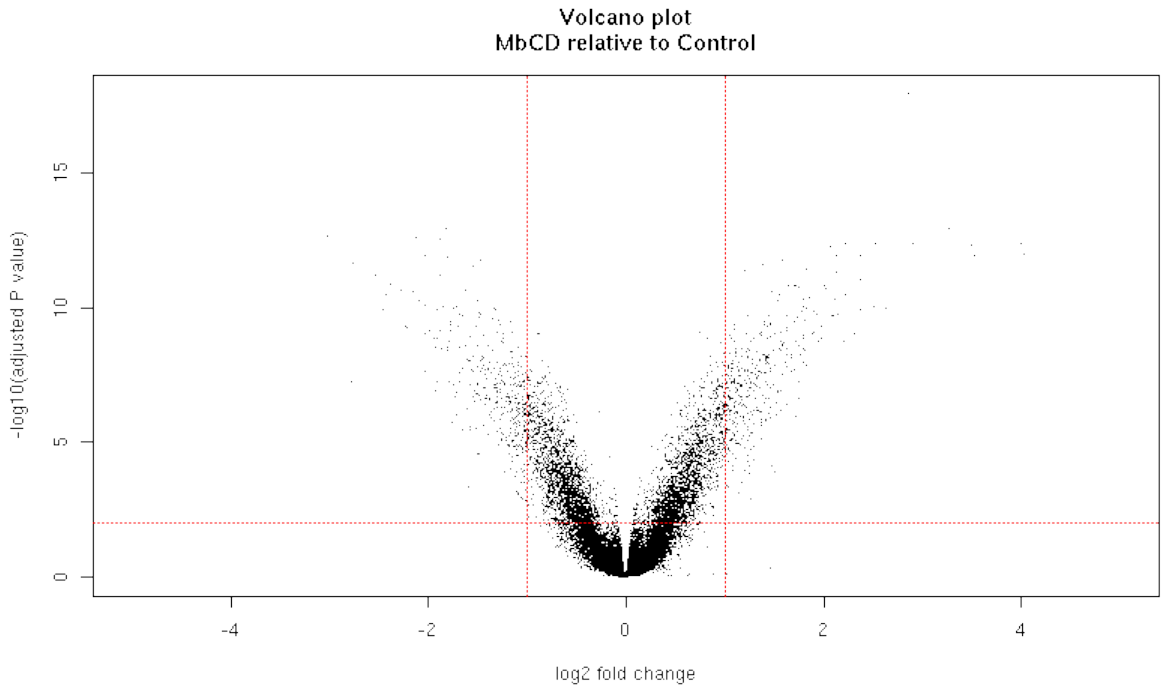

FIGURE 53: VOLCANO PLOT MBCD 0.0008% W/V RELATIVE TO CONTROL (CALU-1)

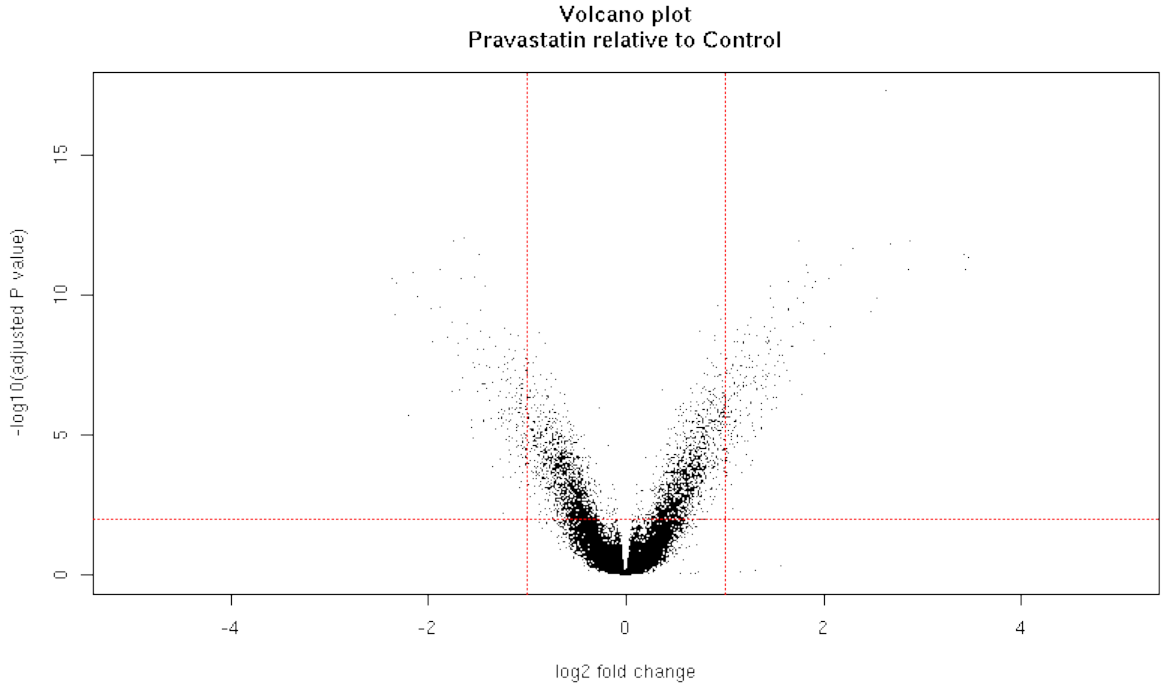

FIGURE 54: HEATMAP PRAVASTATIN 8.0µM RELATIVE TO CONTROL (CALU-1)

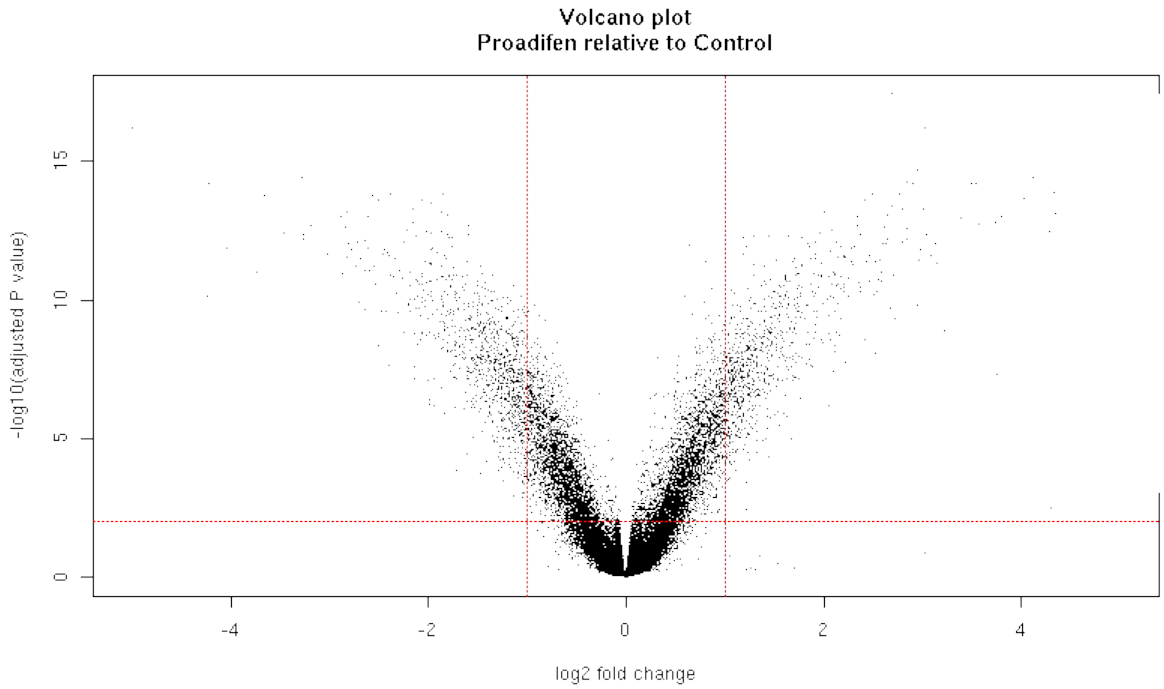

FIGURE 55: VOLCANO PLOT PROADIFEN (10µM) RELATIVE TO CONTROL (CALU-1)

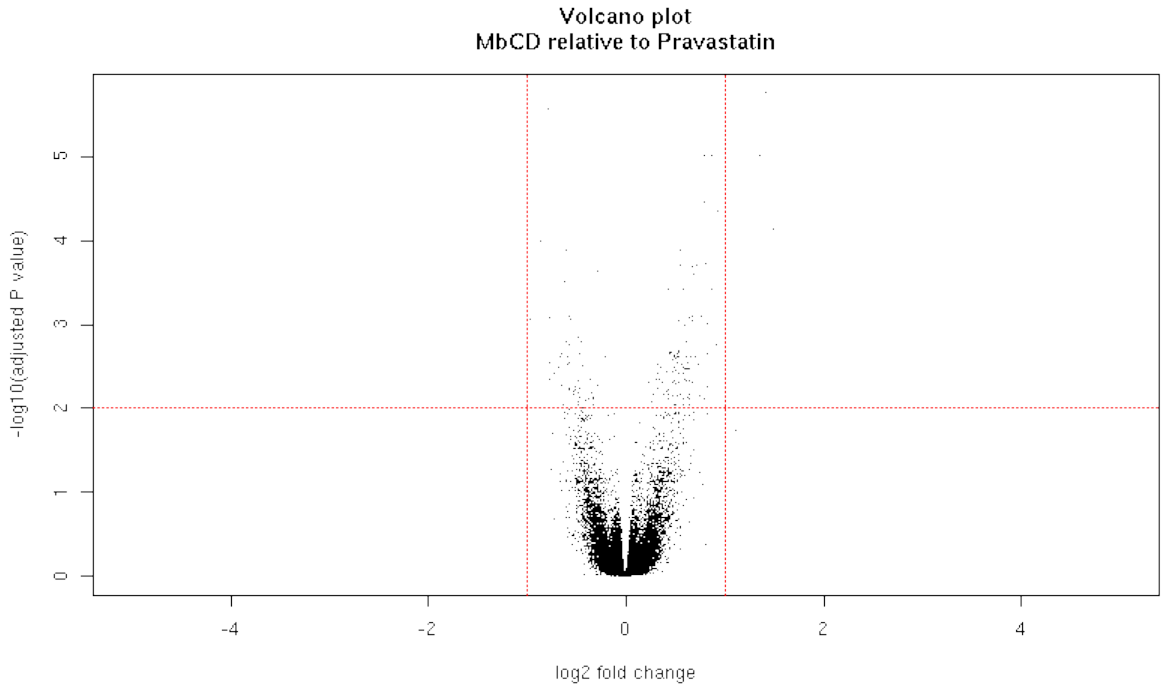

FIGURE 56: VOLCANO PLOT MBCD (0.0008%) RELATIVE TO PRAVASTATIN (8.0µM) (CALU-1)

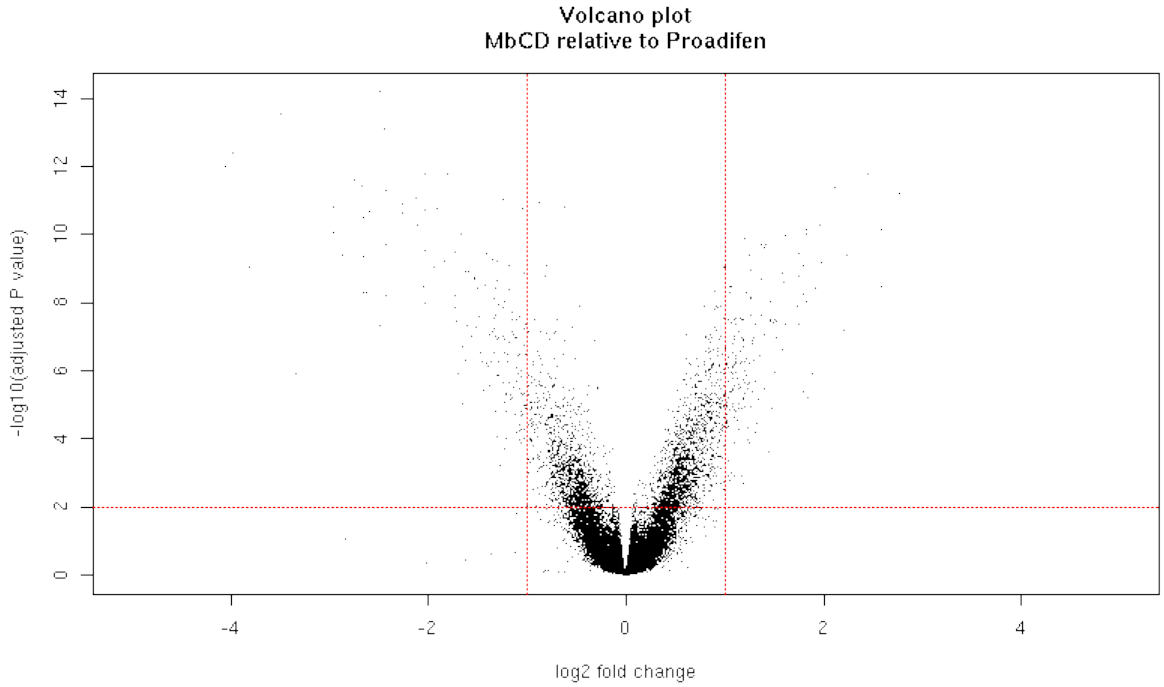

FIGURE 57: VOLCANO PLOT MBCD (0.0008%) RELATIVE TO PROADIFEN (10µM) (CALU-1)

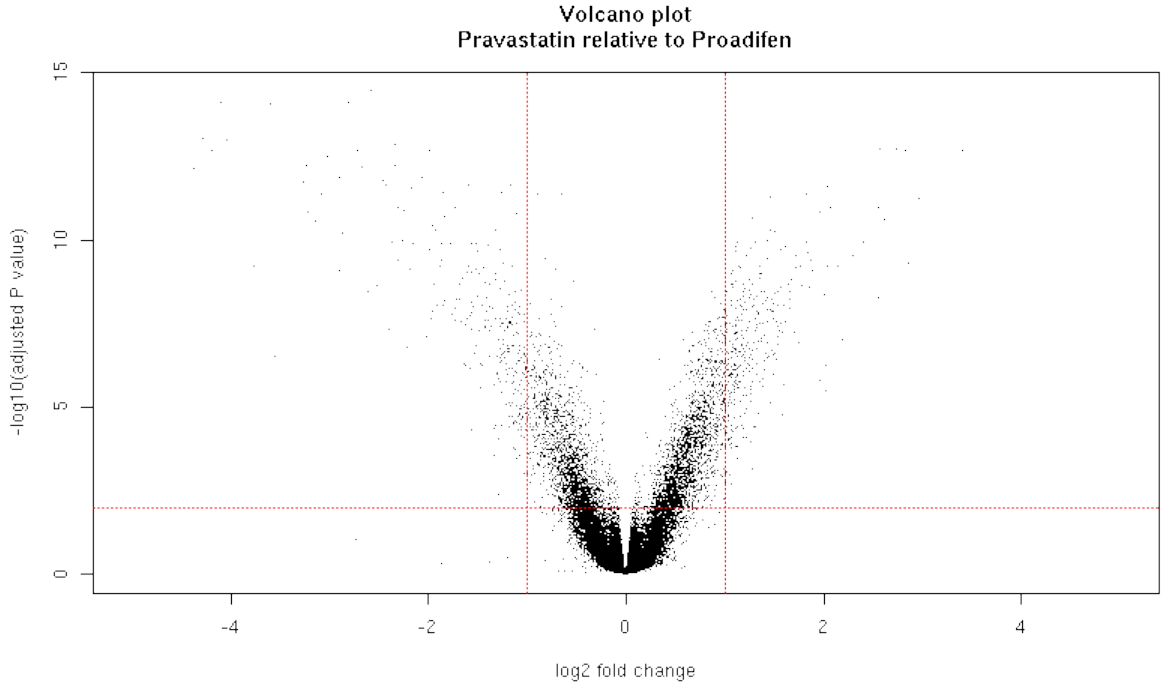

FIGURE 58: VOLCANO PLOT PRAVASTATIN (8.0µM) RELATIVE TO PROADIFEN (10µM) (CALU-1)

FIGURES 54 TO 61 ARE QUALITATIVELY VERY SIMILAR TO THOSE VOLCANO PLOTS FOR THE SAME TREATMENTS IN MDA-MB-231. HOWEVER, CALU-1 APPEARS TO BE CONSIDERABLY MORE SENSITIVE TO THESE TREATMENTS .

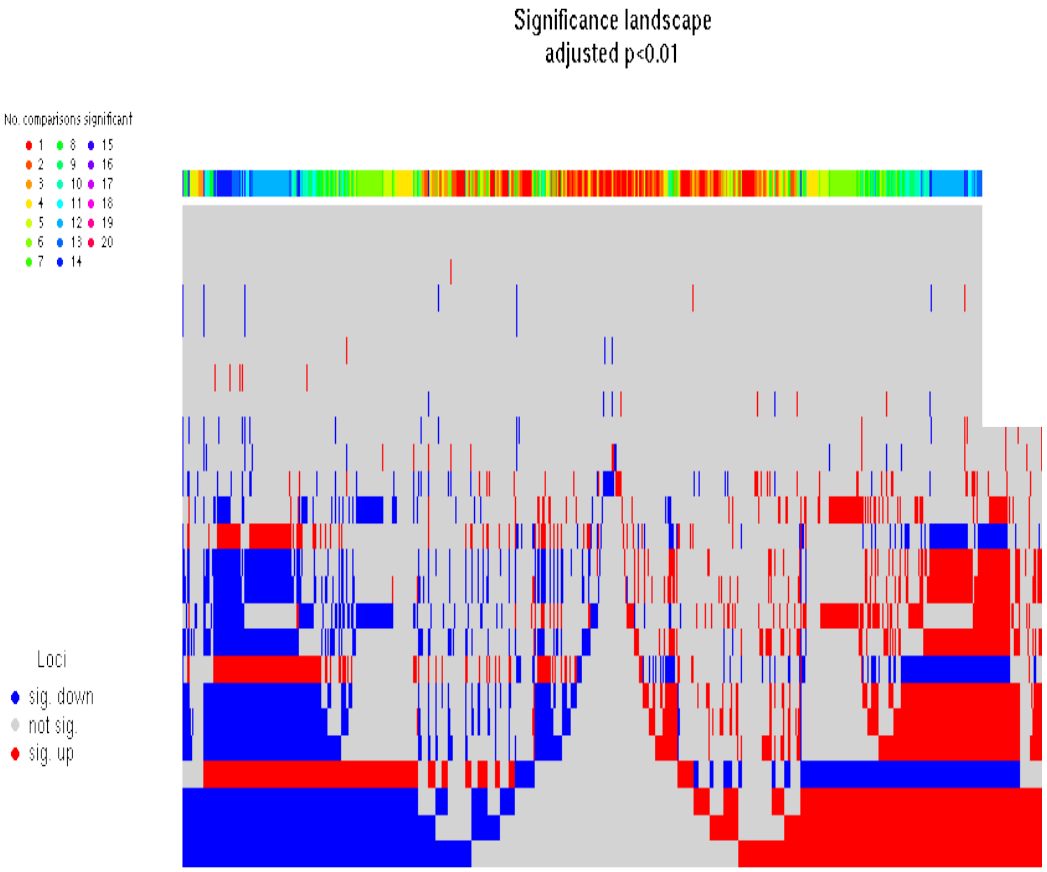

FIGURE 59: SIGNIFICANCE LANDSCAPE (CALU-1)

A significance landscape for array features significant at adjusted p<0.01 in one or more of the 25 comparisons was generated In the plot below, the non-redundant set of 11942 significant genes (X-axis) is broken down by comparisons (Y-axis; the number of significant genes in each comparison are shown in parentheses after the comparison description); comparisons with no significant genes were removed. This enables one to gain a rapid insight into which array features are significant in which comparisons, and if so, were they up-regulated (red) or down-regulated (blue). The comparisons are ordered in the plot such that the one with the highest number of significant changes is shown at the bottom. Loci that were not significant in a given comparison are shown in grey

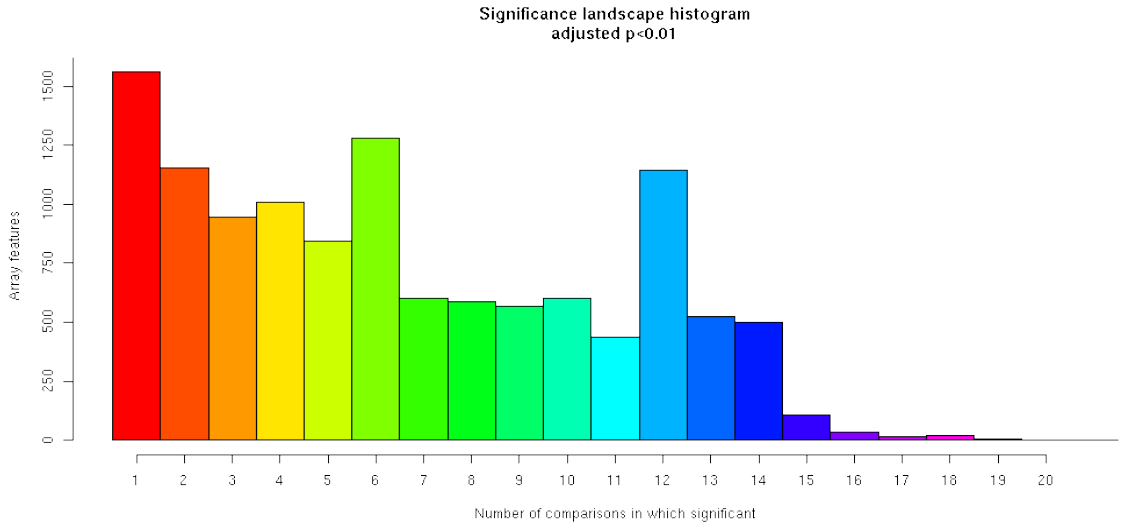

FIGURE 60: SIGNIFICANCE HISTOGRAM (CALU-1)

The significance landscape view of the data provides a direct visual representation of which array features were significant in which comparison, thus enabling "condition" specific and/or enriched loci to be rapidly identified. Groupings of comparison-specific/enriched loci are clearly visible, as are significant loci common to multiple comparisons (depicted in the histogram).

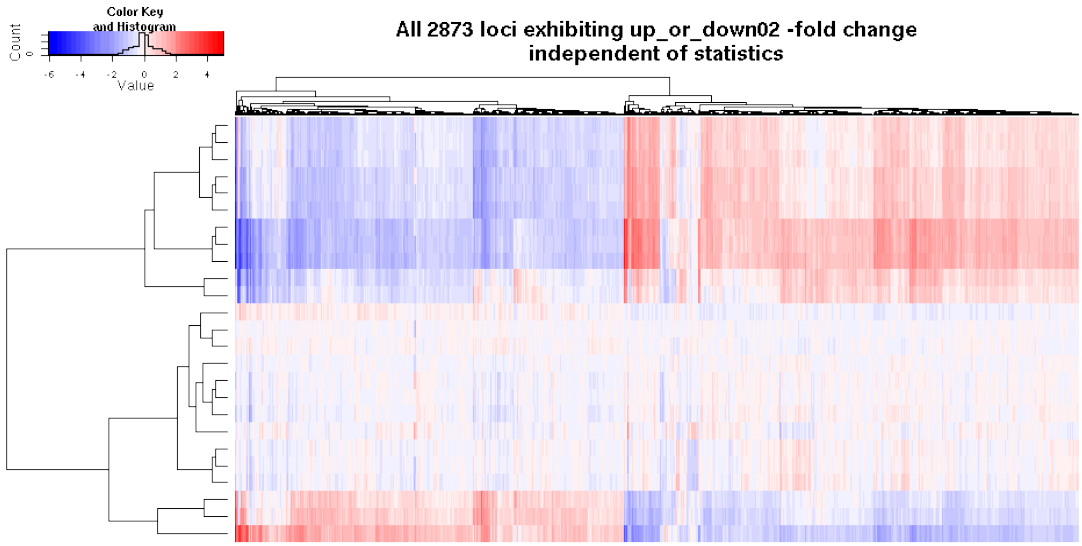

FIGURE 61: 2-FOLD CHANGES (CALU-1)

The figure 61 shows a heatmap of the fold change for all loci exhibiting an up or down 02-fold change in one or more of the comparisons. Array features are shown on the X-axis, with the comparisons on the Y axis. A red colour indicates up regulation and blue down regulation . Clustering of both array feature and comparison has been

performed. This heatmap and Figures 62-64 were used to quality assure the data since they provide a visual check on the clustering of replicates which appear in clear bands across the X-axis.

FIGURE 62: 8-FOLD CHANGES (CALU-1)

The figure above shows a heatmap of the fold change for all loci exhibiting an up or down 8-fold change in one or more of the comparisons. Array features are shown on the X-axis, with the treatment comparisons on the Y axis. A red colour indicates up regulation and blue down regulation . Clustering of both array feature and comparison has been performed.

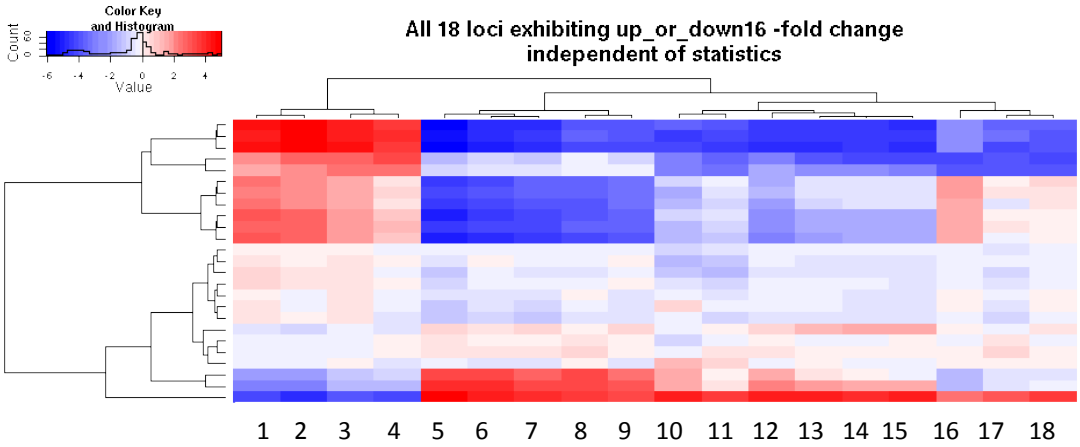

FIGURE 63: 16-FOLD CHANGES (CALU-1)

The figure above shows a heatmap of the fold change for all loci exhibiting an up or down 16-fold change in one or more of the comparisons. Array features are shown on the X-axis, with the treatment comparisons on the Y axis. A red colour indicates up regulation and blue down regulation . Clustering of both array feature and comparison has been performed.Details of the genes indicated by the feature numbers 1-18 are provided in Table 9 Part A.

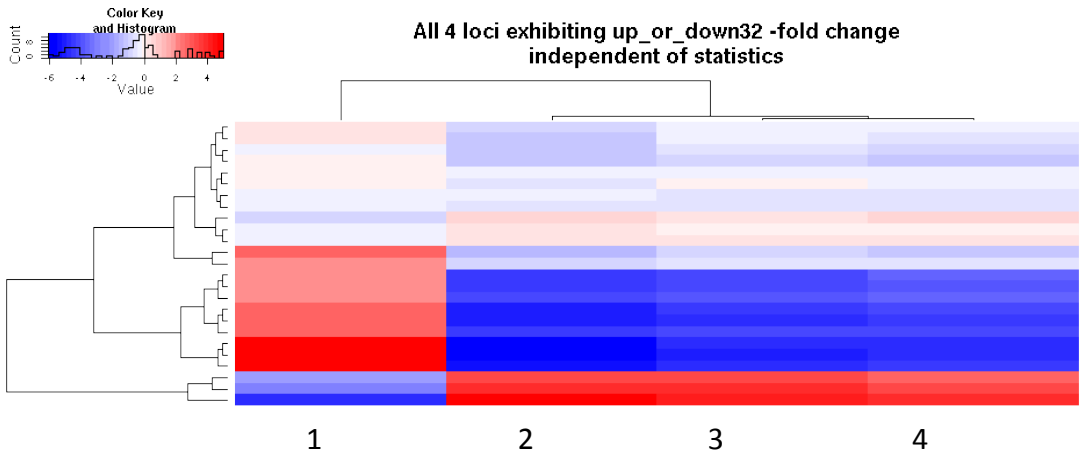

FIGURE 64: 32-FOLD CHANGES (CALU-1)

The figure above shows a heatmap of the fold change for all loci exhibiting an up or down 32-fold change in one or more of the comparisons. Array features are shown on the X-axis, with the treatment comparisons on the Y axis. A red colour indicates up regulation and blue down regulation . Clustering of both array feature and comparison has been performed. Details of the genes indicated by the feature numbers 1-4 are provided in Table 9 Part B

		Probe ID	Symbol	Description
Part A				
	1	QWq7Z1IXOOH7yUCHlE	GDF15	growth differentiation factor 15
	2	HdUm8EQDU6ks46Std4	ATF3	activating transcription factor 3
	3	um_PC1eV.sRFlbZxxY	RN18S1	RNA, 18S ribosomal 1
	4	9PSIoIJiqRpniEieiM	NUPR1	nuclear protein, transcriptional regulator, 1
	5	xJ5IPSIoIJiqRpniEg	NUPR1	nuclear protein, transcriptional regulator, 1
	6	WhV5j9VA7qAdh5MP7o	RNU1-3	RNA, U1 small nuclear 3
	7	BueFXmP1UDuoB2Hkw8	RNU1-5	RNA, U1 small nuclear 5
	8	l7nlXmP1UDuoB2Hkw8	RNU1-9	RNA, U1 small nuclear 9
	9	Z_QKopNLtfpKeP3Kyg	CTGF	connective tissue growth factor
	10	BS7X6Snj9ysoDusnRk	CTGF	connective tissue growth factor
	11	lS3DCed5V_50i6O86g	THBS1	thrombospondin 1
	12	u1dct7Xm13tVq.SIQc	COL1A1	collagen, type I, alpha 1
	13	uiSdXZ5jc_AtI3URCo		
	14	cTqn3heJFCvioSjyko	TRIB3	tribbles homolog 3 (Drosophila)
	15	0FCogUoBoBIutPVSVo	DDIT3	DNA-damage-inducible transcript 3
	16	uEGOv.TNPrbr7LW5iA	MIR1974	microRNA 1974
	17	oon0If5P1yz97_0vdA	HSPA1A	heat shock 70kDa protein 1A
	18	ct43aCcJKtqXryx_ho	RN5S9	RNA, 5S ribosomal 9
Part B				
	1	BS7X6Snj9ysoDusnRk	CTGF	connective tissue growth factor
	2	QWq7Z1IXOOH7yUCHlE	GDF15	growth differentiation factor 15
	3	9PSIoIJiqRpniEieiM	NUPR1	nuclear protein, transcriptional regulator, 1
	4	xJ5IPSIoIJiqRpniEg	NUPR1	nuclear protein, transcriptional regulator, 1

TABLE 9 LIST OF GENES AND LOCI ID FOR THE 16-FOLD AND 32-FOLD CHANGES

3.3.1.4 KEGG PATHWAY ENRICHMENT IN CALU-1 CELLS

Spliceosome, DNA replication and Cell cycle, as well as mismatch repair and ubiquitin mediated proteolysis, amongst several others are strongly down-regulated by MβCD, Pravastatin and Proadifen. Steroid Biosynthesis is up-regulated with Proadifen, MβCD and Pravastatin. Furthermore, Aminoacyl-tRNA biosynthesis, biosynthesis of unsaturated fatty acids and terpenoid backbone biosynthesis are up-regulated with MβCD and Pravastatin. Proadifen, MβCD and Pravastatin appear to have a narrow target range that includes pathways that may be involved in antimicrobial-based processes e.g. terpenoid backbone biosynthesis. Comparison of Proadifen, MβCD or Pravastatin relative to Control show enrichment of GO terms involved in regulatory processing e.g. regulation of macromolecule biosynthetic process.

Kegg pathway analysis revealed that Proadifen treatment up-regulated sterol synthesis. It seems likely that the enzymes for sterol synthesis are being manufactured but are ineffective in making cholesterol or that cholesterol is shunted from the membrane into the cytoplasm (not seen in these experiments). Another, more intriguing possibility is that Proadifen prevents the formation of caveolae and this in itself is sufficient for the cell to begin up-regulating cholesterol to counter this loss. These are, in essence, homeostatic negative feedback responses from the membrane to the nucleus to restore sterol balance. Why this should be the case for a Δ-24 inhibitor and not the case for a statin like Pravastatin is unknown but suggestive. Perhaps the earlier (biochemically speaking) intervention of the statins cannot trigger the same response or perhaps the

statins do not provoke the abolition of caveolae. Pravastatin and MβCD did not affect sterol synthesis pathways in this way but both these treatments caused significant up-regulation of ribosome and spliceosome pathways. HMGCS1, the gene associated with the production of HMG-CoA (the target for statin intervention) was typical of enzymes in this system.

3.3.2 Gene expression results for both cell types

HMGCS1 is significantly up-regulated by Proadifen but unaffected by all other treatments including Pravastatin. Likewise the tumour suppressor p53 was down regulated by Proadifen but unaffected by statin or MβCD. Proliferation related signalling was reduced by Proadifen as were cytokine and NOD-like receptor signalling. However, protein binding *per se* was not reduced by Proadifen unlike all other treatments.

Interleukins 1 and 6 were down regulated by -1.56 and -1.27 log fold respectively. IL-8 was down regulated by -1.69 to -2.23 log fold. These data are consistent with the reductions of interleukin expression seen in the antibody array experiment. The spread of negative and positive impacts on RNA expression was similar to that found in the protein assays as shown by the volcano plots and Figure 17 for a global comparison.

LPC and Fluphenazine increased pathway related signalling according to GO analysis while MβCD decreased cancer pathways. Exogenous LPC is able, due to the molecule's size and wedge-like shape, to interdigitate into the plasma membrane and typically causes an increase in fluidity and permeability of the bilayer. It was used here to check if

the effects of Proadifen were due to a simple fluidizing behaviour in the membrane since Proadifen is known to increase absorption of several pharmaceuticals. Proadifen-relative-to-LPC at $p<0.0001$ caused 10 times fewer significant changes to protein expression – clearly disturbing the fluidity of the membrane drastically affects RNA expression. LPC could be perturbing the rafts and/or caveolae. At the same level of confidence, there were no differences in the LPC-relative-to-Fluphenazine analyses, suggesting a similar response to these two treatments. Fluphenazine is also a membrane fluidiser. Sequestration of cholesterol by MβCD and HMG-CoA inhibition by the statin both caused minimal response at $p<0.0001$ (25 and 46 events respectively) and at $p<0.001$ both induced only <1000 RNA events. Does LPC make much contribution to direct effects on gene expression distinct from those effects on the organisation of the phospholipid bilayer? (A separate, but unreported, genome-wide analysis examining lysophosphatidylcholine, lysophosphatidylethanolamine, lysophosphatidylinositol and lysophosphatidic acid revealed that LPE has, by far, the greatest impact on gene expression compared to other lysolipids). Proadifen causes a reduction of cholesterol in the membrane and a concurrent up-regulation of cholesterol pathway enzymes. However, this up-regulation of sterol pathway does not result in a restoration of the membrane cholesterol. Why this pattern is not followed in treatments with statin is unknown but it would appear to confirm that the primary feedback originates distal in the pathway to squalene. If most of the Δ-24 oxoreductase action is normally on the lanosterol, zymosterol and desmosterol then when these routes are shut-down by Proadifen the build-up of intermediates is not sufficient to trigger any negative

feedback. The effects of Proadifen on cancer related signalling were mainly down-regulation, including p53 which is a tumour suppressor.

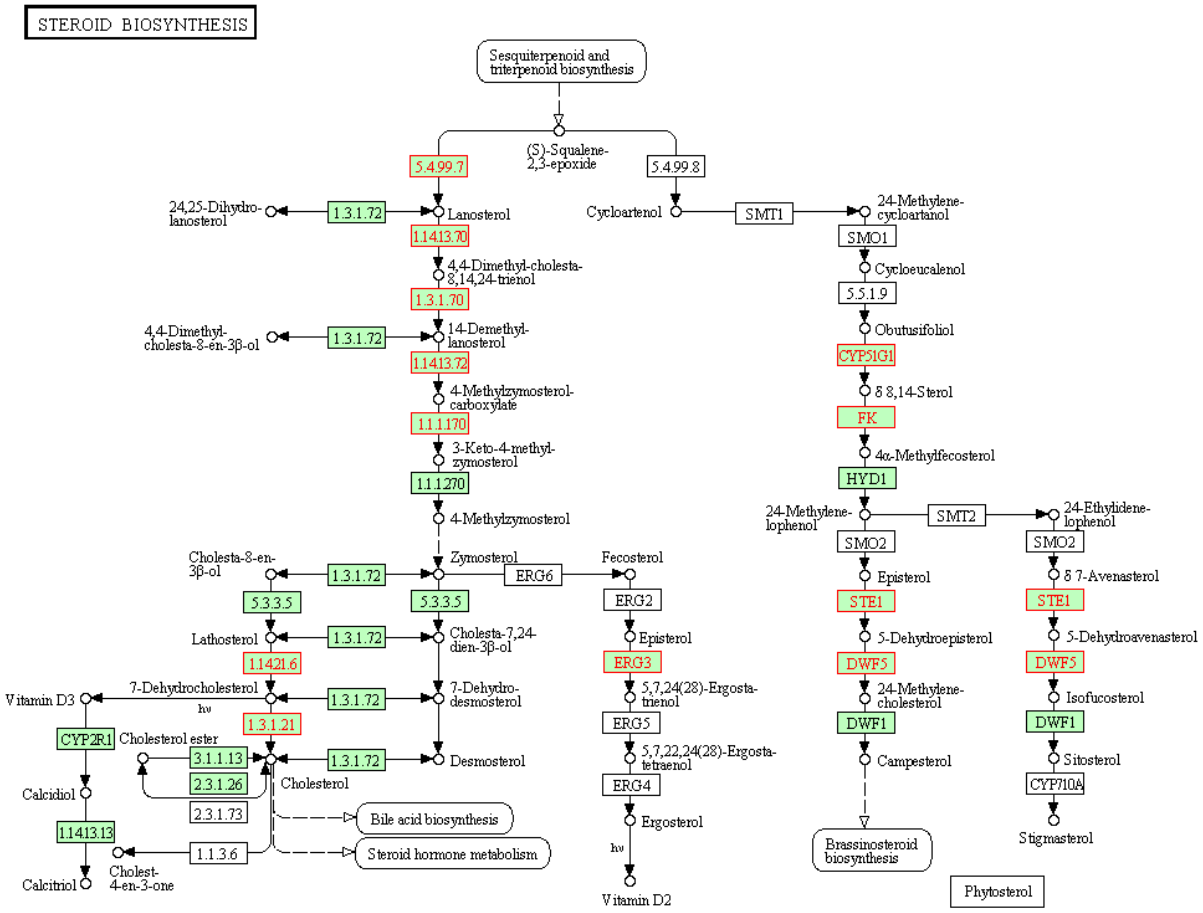

FIGURE 65: AN EXAMPLE OF A KEGG PATHWAY

USING KEGG PATHWAY ANALYSIS METHODS IT IS POSSIBLE TO SEE THE EFFECT ON MULTIPLE POINTS ALONG A BIOCHEMICAL PATHWAY. HOWEVER, THE TECHNIQUE IS DESIGNED FOR LARGE AMOUNTS OF GENOMIC DATA AND BECOMES LESS RELIABLE FOR SMALL PATHWAYS OF INTEREST OR PATHWAYS THAT BRANCH.

3.3.2.1 KEGG PATHWAY DETAILED ANALYSIS OF CANCER RELATED GENES IN MDA-MB-231

Treatment	KEGG	Pathway number	Pathway name	p value	Gene(s)
Fluphenazine-Control	Up	5213	Endometrial cancer	0.026379906	AKT1, ARAF, AXIN1, BAD, CCND1, ERBB2, FOXO3, GSK3B, HRAS, MAPK3, PIK3CD, PIK3R1, PIK3R2
Fluphenazine-Control	Up	5219	Bladder cancer	0.028575455	ARAF, CCND1, DAPK3, E2F2, E2F3, ERBB2, FGFR3, HRAS, MAPK3, PGF, TYMP
Fluphenazine-Control	Up	5215	Prostate cancer	0.041136016	AKT1, AR, ARAF, BAD, CCND1, CCNE1, CREB1, E2F2, E2F3, ERBB2, GSK3B, GSTP1, HRAS, INS, KLK3, MAPK3, PIK3CD, PIK3R1, PIK3R2
Pravastatin-Control	Down	5219	Bladder cancer	0.01550555	IL8, MMP1
MBCD-Control	Down	5219	Bladder cancer	0.001347276	IL8, MMP1, VEGFA
MBCD-Control	Down	5200	Pathways in cancer	0.006387016	IL6, IL8, LAMC2, MMP1, PTGS2, VEGFA
LPC-Control	Down	5213	Endometrial cancer	0.034873706	BAD, CDH1, CTNNB1, FOXO3, GRB2, ILK, LEF1, MAP2K1, MLH1, MYC, PDPK1, SOS1
LPC-Control	Down	5212	Pancreatic cancer	0.036719585	BAD, CDC42, JAK1, MAP2K1, MAPK9, RAC1, RAC2, RALA, RALGDS, SMAD4, STAT3, TGFA, TGFBR2, VEGFA, VEGFC
Fluphenazine-Control	Down	5211	Renal cell carcinoma	0.000324486	CDC42, CREBBP, CRK, CRKL, CUL2, EGLN1, EP300, EPAS1, ETS1, HIF1A, KRAS, MAP2K1, MET, NRAS, RAC1, RBX1, SLC2A1, SOS1, TCEB1, TGFA, VEGFA, VEGFC, VHL
Fluphenazine-Control	Down	5200	Pathways in cancer	0.008951591	BCL2L1, BID, BIRC2, CASP8, CBL, CCNA1, CDC42, CDKN1B, CHUK, CKS1B, CREBBP, CRK, CRKL, CTNNB1, CUL2, DVL3, EGFR, EGLN1, EP300, EPAS1, ETS1, FADD, FZD6, FZD7, HIF1A, HSP90AA1, HSP90B1, IGF1R, IL6, IL8, ITGA2, ITGAV, ITGB1, JAK1, KRAS, LAMA3, LAMB3, LAMC1, LAMC2, LEF1, MAP2K1, MAPK9, MET, MLH1, MMP1, MYC, NFKB1, NRAS, PTGS2, RAC1, RAC2, RALA, RALB, RARB, RBX1, SLC2A1, SMAD4, SOS1, STAT3, STAT5B, TCEB1, TFG, TGFA, TGFBR2, VEGFA, VEGFC, VHL, WNT5A
Fluphenazine-Control	Down	5212	Pancreatic cancer	0.011168505	BCL2L1, CDC42, CHUK, EGFR, JAK1, KRAS, MAP2K1, MAPK9, NFKB1, RAC1, RAC2, RALA, RALB, SMAD4, STAT3, TGFA, TGFBR2, VEGFA, VEGFC
Proadifen-Control	Down	5200	Pathways in cancer	0.047516463	CDKN1B, IL6, IL8, JUP, LAMC2, PTGS2, VEGFA

TABLE 10:KEGG PATHWAYS AND CANCER RELATED GENES IN MDA-MB-231

THIS TABLE PROVIDES THE EXTRACTED DATA FOR THE GENES ASSOCIATED WITH CANCERS. ONLY SIGNIFICANT (P<0.05) EVENTS ARE SHOWN.

3.3.2.2 KEGG PATHWAY DETAILED ANALYSIS OF CANCER RELATED GENES IN CALU-1

TABLE 11: KEGG PATHWAY AND CANCER RELATED GENES IN CALU-1

Treatment	KEGG	Pathway number	Pathway name	p value	Gene(s)
LPC-CONTROL	Down	5219	Bladder cancer	0.019255247	IL8, MMP2
LPC-CONTROL	Down	5200	Pathways in cancer	0.023254347	CCNE1, IL6, IL8, MMP2, PTGS2
MβCD-CONTROL	Down	5200	Pathways in cancer	0.003765599	ARNT2, AXIN2, BCL2L1, BID, BIRC2, BIRC3, BIRC5, BMP4, CASP3, CCND1, CCNE1, CDC42, CDK2, CDK6, COL4A1, COL4A6, CRK, CYCS, DAPK3, E2F2, FADD, FGF5, FGFR1, FH, FZD4, HDAC1, HDAC2, HSP90AA1, IL8, ITGA6, JUN, MECOM, MMP1, MMP2, MSH2, MSH6, MTOR, NKX3-1, PRKCA, RARA, RASSF1, RBX1, RUNX1, RXRA, SKP2, SMAD3, TCEB1, TCEB2, TGFA, TGFB2, TGFBR2, TRAF2, WNT5B, WNT7B
Pravastatin-CONTROL	Down	5200	Pathways in cancer	0.001593765	ARNT2, BCL2L1, BID, BIRC2, BIRC3, BIRC5, BMP4, CASP3, CCND1, CCNE1, CDK2, CDK6, CRK, DAPK3, E2F2, FGF5, FH, FZD4, HDAC1, HDAC2, HSP90AA1, IL6, IL8, ITGA6, JUN, MMP1, MSH2, MSH6, NKX3-1, PRKCA, PTGS2, RARA, RASSF1, RBX1, RUNX1, RXRA, SKP2, TCEB1, TCEB2, TGFA, WNT5B, WNT7B
Pravastatin-CONTROL	Down	5222	Small cell lung cancer	0.017232385	APAF1, BCL2L1, BIRC2, BIRC3, CCND1, CCNE1, CDK2, CDK6, E2F2, ITGA6, PTGS2, RXRA, SKP2
Proadifen-CONTROL	Down	5222	Small cell lung cancer	0.00743923	APAF1, BCL2, BCL2L1, BIRC2, CCND1, CCNE1, CDK2, CDK6, COL4A1, COL4A6, CYCS, E2F2, E2F3, ITGA6, ITGAV, ITGB1, LAMC1, PIAS2, PIK3CB, PIK3R1, PTK2, RXRA, SKP2
Proadifen-CONTROL	Down	5211	Renal cell carcinoma	0.015640768	ARNT2, CDC42, CRK, EGLN1, EP300, FH, GRB2, MAP2K1, MAPK1, MET, PIK3CB, PIK3R1, PTPN11, RBX1, TCEB2, TGFA, TGFB2, VEGFC, VHL

Proadifen-CONTROL	Down	5215	Prostate cancer	0.028467316	BCL2, CCND1, CCNE1, CDK2, CREB1, CREB3L2, CREB5, E2F2, E2F3, EP300, ERBB2, GRB2, HSP90AA1, KLK3, MAP2K1, MAPK1, MTOR, NKX3-1, PDPK1, PIK3CB, PIK3R1, TGFA
MβCD-CONTROL	Up	5216	Thyroid cancer	0.005342649	CCDC6, CDH1, MAPK3, MYC, NRAS, PPARG, RXRB, TFG
MβCD-CONTROL	Up	5219	Bladder cancer	0.006075948	CDH1, CDKN2A, EGFR, MAPK3, MYC, NRAS, RPS6KA5, TYMP, VEGFA, VEGFB
MβCD-CONTROL	Up	5212	Pancreatic cancer	0.037240109	ARHGEF6, CDKN2A, EGFR, MAPK3, PIK3R2, RAC2, RALGDS, SMAD2, SMAD4, STAT1, VEGFA, VEGFB
Pravastatin-CONTROL	Up	5219	Bladder cancer	0.004455468	CDH1, CDKN2A, EGFR, MAPK3, MYC, RPS6KA5, TYMP, VEGFA, VEGFB
Pravastatin-CONTROL	Up	5212	Pancreatic cancer	0.044862777	ARHGEF6, CDKN2A, EGFR, MAPK3, PIK3R2, RAC2, RALGDS, STAT1, VEGFA, VEGFB
Proadifen-CONTROL	Up	5219	Bladder cancer	0.000339897	ARAF, BRAF, CDH1, CDKN1A, CDKN2A, EGFR, FGFR3, IL8, MAPK3, MYC, NRAS, RPS6KA5, TYMP, VEGFA, VEGFB
Proadifen-CONTROL	Up	5212	Pancreatic cancer	0.002739927	AKT3, ARAF, BAD, BRAF, CASP9, CDKN2A, EGFR, MAPK3, PIK3R2, PLD1, RAC2, RALA, RALGDS, SMAD2, SMAD4, STAT1, STAT3, VEGFA, VEGFB
Proadifen-CONTROL	Up	5213	Endometrial cancer	0.003979299	AKT3, ARAF, AXIN1, BAD, BRAF, CASP9, CDH1, EGFR, GSK3B, ILK, MAPK3, MYC, NRAS, PIK3R2, PTEN
Proadifen-CONTROL	Up	5216	Thyroid cancer	0.014507544	BRAF, CCDC6, CDH1, MAPK3, MYC, NRAS, PAX8, PPARG, TFG
Proadifen-CONTROL	Up	5211	Renal cell carcinoma	0.029969488	AKT3, ARAF, BRAF, EGLN2, EPAS1, ETS1, FLCN, HIF1A, MAPK3, NRAS, PAK1, PIK3R2, SLC2A1, VEGFA, VEGFB, VHL
Proadifen-CONTROL	Up	5210	Colorectal cancer	0.044639572	AKT3, ARAF, AXIN1, BAD, BRAF, CASP9, GSK3B, MAPK3, MYC, PIK3R2, RAC2, RALGDS, SMAD2, SMAD4

THIS TABLE PROVIDES THE EXTRACTED DATA FOR THE GENES ASSOCIATED WITH CANCERS. ONLY SIGNIFICANT ($P<0.05$) EVENTS ARE SHOWN. WHEN COMPARED TO THE DATA SET FOR MDA-MB-231 IS CAN BE CLEARLY SEEN THAT CALU-1 IS MORE SENSITIVE TO THE TREATMENTS WITH MANY MORE CANCER RELATED GENES AFFECTED.

3.3.2.3 KEGG PATHWAY DETAILED ANALYSIS OF GENES INVOLVED IN STEROID SYNTHESIS

TABLE 12 KEGG PATHWAYS AND STEROID SYNTHESIS

Treatment	KEGG	Pathway number	Pathway name	p value	Gene(s)
CaLu-1					
MβCD-CONTROL	Up	100	Steroid biosynthesis	9.11E-06	CYP51A1, DHCR7, FDFT1, LSS, NSDHL, SC4MOL, SC5DL, SQLE, TM7SF2
Pravastatin-CONTROL	Up	100	Steroid biosynthesis	9.36E-08	CYP51A1, DHCR7, FDFT1, LIPA, LSS, NSDHL, SC4MOL, SC5DL, SQLE, TM7SF2
Proadifen-CONTROL	Up	100	Steroid biosynthesis	0.005590514	CYP51A1, DHCR7, FDFT1, NSDHL, SC4MOL, SC5DL, TM7SF2
MDA-MB-231					
Proadifen-Control	Up	100	Steroid biosynthesis	1.11E-17	CYP51A1, DHCR24, DHCR7, EBP, FDFT1, LSS, NSDHL, SC4MOL, SC5DL, SQLE, TM7SF2
LPC-Control	Up	100	Steroid biosynthesis	0.011254582	CEL, DHCR24, DHCR7, LSS, NSDHL, TM7SF2

IT IS INTERESTING THAT IN CONTRAST TO THE SPECIFIC GENES (TABLE 10) THE KEGG PATHWAYS FOR CHOLESTEROL SYNTHESIS ARE EXCLUSIVELY UP-REGULATED. WHY THIS IS THE CASE IS UNKNOWN.

3.3.3 GENE EXPRESSION OF THE MARKER PROTEINS USED IN PROTEIN ARRAY ASSAY

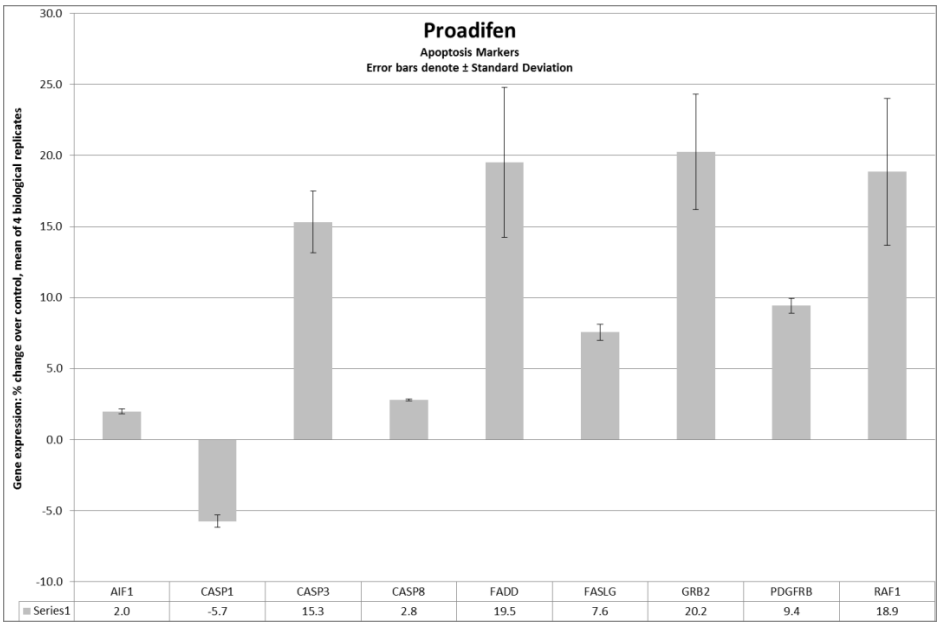

FIGURE 66: GENE EXPRESSION OF APOPTOTIC MARKERS IN MDA-MB-231 TREATED WITH PROADIFEN

FOR COMPARISON TO ACTUAL PROTEIN EXPRESSED SEE FIGURE 29

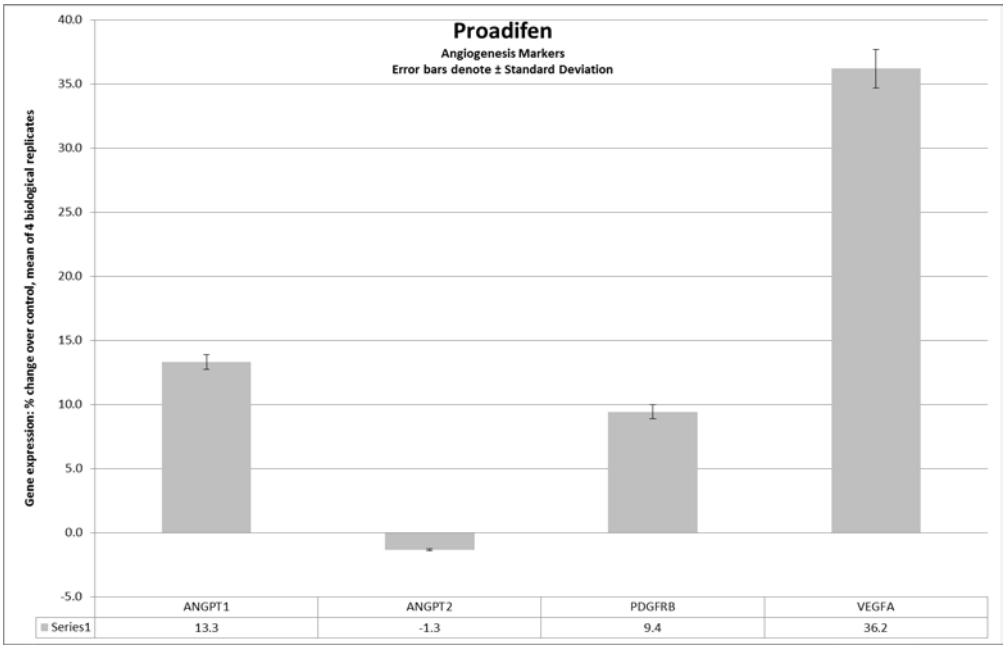

FIGURE 67: GENE EXPRESSION OF ANGIOGENESIS MARKERS IN MDA-MB-231 TREATED WITH PROADIFEN

FOR COMPARISON TO ACTUAL PROTEIN EXPRESSED SEE FIGURE 30

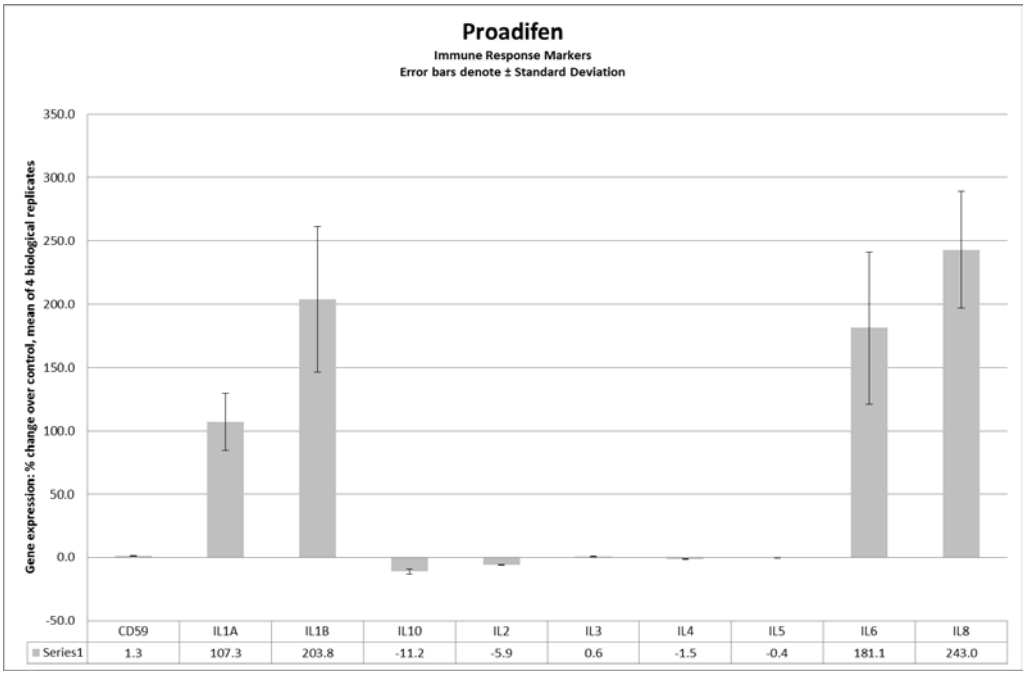

FIGURE 68: GENE EXPRESSION OF IMMUNE RESPONSE MARKERS IN MDA-MB-231 TREATED WITH PROADIFEN

FOR COMPARISON TO ACTUAL PROTEIN EXPRESSED SEE FIGURE 31

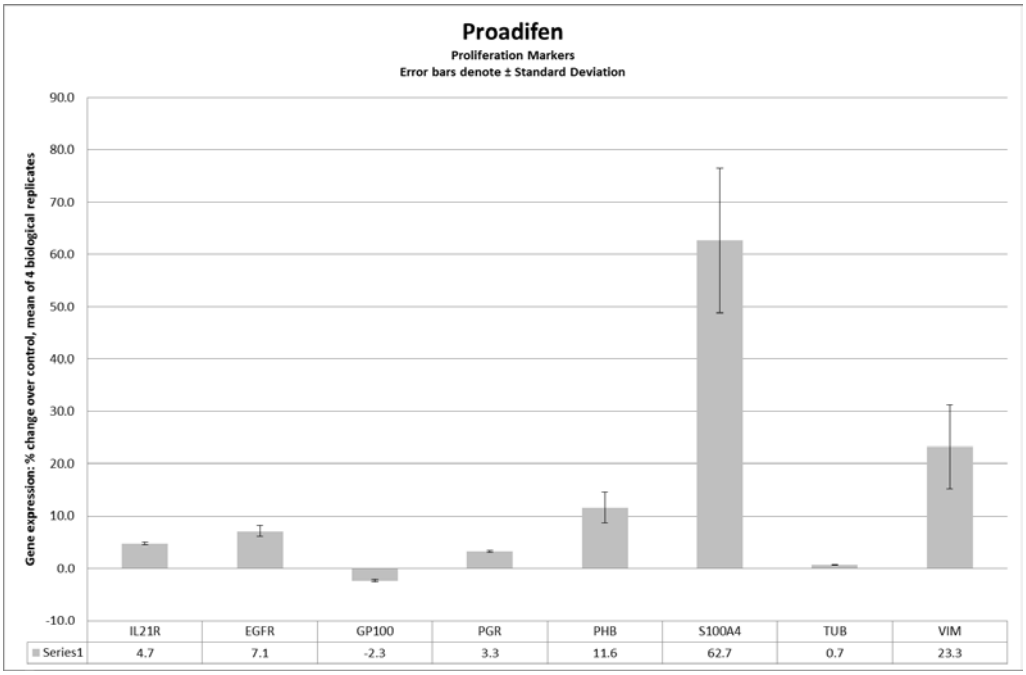

FIGURE 69: GENE EXPRESSION OF PROLIFERATION MARKERS IN MDA-MB-231 TREATED WITH PROADIFEN

FOR COMPARISON TO ACTUAL PROTEIN EXPRESSED SEE FIGURE 32

ISOLATION OF THE GENES INVOLVED IN THE MEVALONATE PATHWAY REVEALS THAT MOST OF THE TREATMENTS CAUSED DOWN-REGULATIONS OF THESE GENES (SHOWN IN RED). A NOTABLE EXCEPTION IS PROADIFEN WHICH ONLY CAUSED UP-REGULATIONS.

% Change in Mean Averages of mRNA spot intensity by cholesterol pathway genes

Target	Proadifen	Pravastatin	MβCD	LPC	Fluphenazine
HMGCS1	224.8056	-12.46216842	-27.8767	-7.09948	-19.6962
HMGCR	200.6086	-5.818088499	-10.804	-24.8451	-33.9883
MVK	144.1146	4.290899663	-0.32409	-6.54222	-17.9803
FDPS	200.1963	-15.10127375	-7.75527	0.485836	-12.9881
FDFT1	178.1766	2.398725153	-12.2486	-51.4775	-58.5775
SQLE	149.0991	3.303303303	-12.4249	-55.7057	-59.9944
LSS	164.4272	2.641767251	-6.35391	-17.2702	-24.9146
TM7SF2	159.9011	-6.973245944	-17.5352	-10.1751	-20.1676
CYP51A1	155.8444	-14.2267498	-8.09695	-22.555	-34.5394
SC4MOL	244.8134	-10.25277915	-17.5954	-39.1347	-52.064
DHCR24	159.5037	-21.05399976	-4.65556	6.591043	-19.3596
EBP	138.3187	-2.112855866	-0.1149	-43.4699	-46.4381
DHCR7	217.3947	-18.31700865	-18.1847	-3.89648	-27.9796

TABLE 13 CHANGES TO REGULATION OF GENES ASSOCIATED WITH CHOLESTEROL SYNTHESIS (NOT FILTERED BY SIGNIFICANCE)

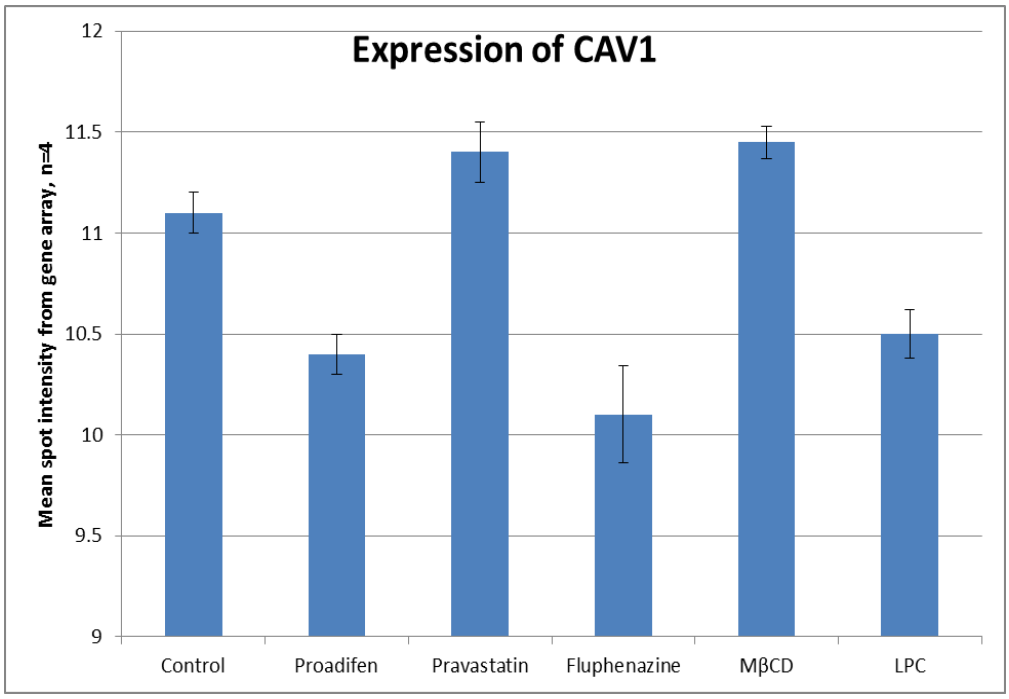

FIGURE 70: CAV1 RNA EXPRESSION IN MDA-MB-231

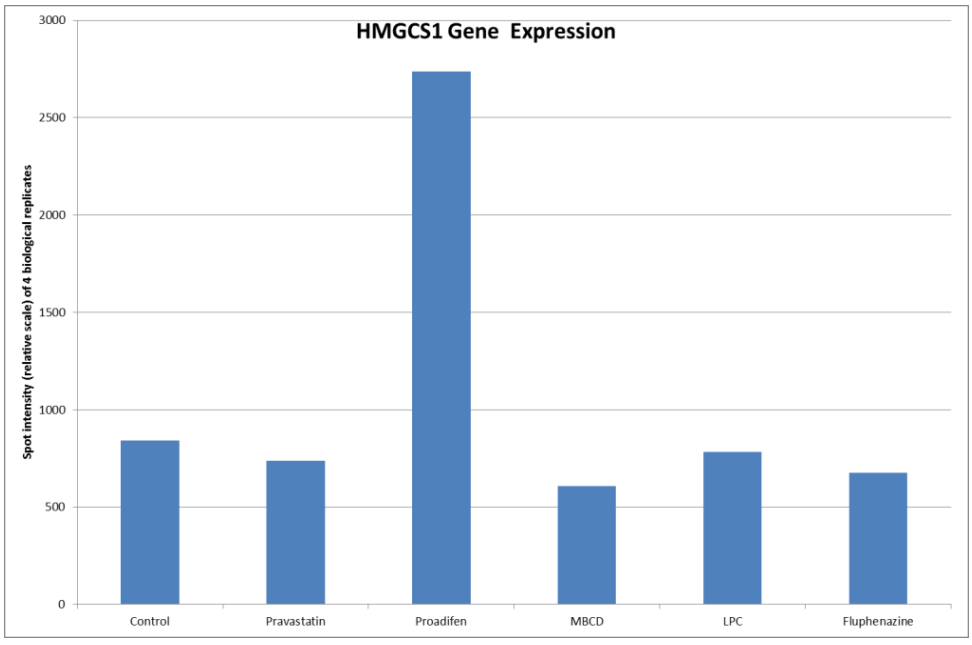

FIGURE 71: HMGCS1 CODES FOR THE ENZYME THAT CALALYSES ACETOACETYL-COA INTO HMG-COA.

3.3.4 RESULTS OF ANTIBODY ASSAYS

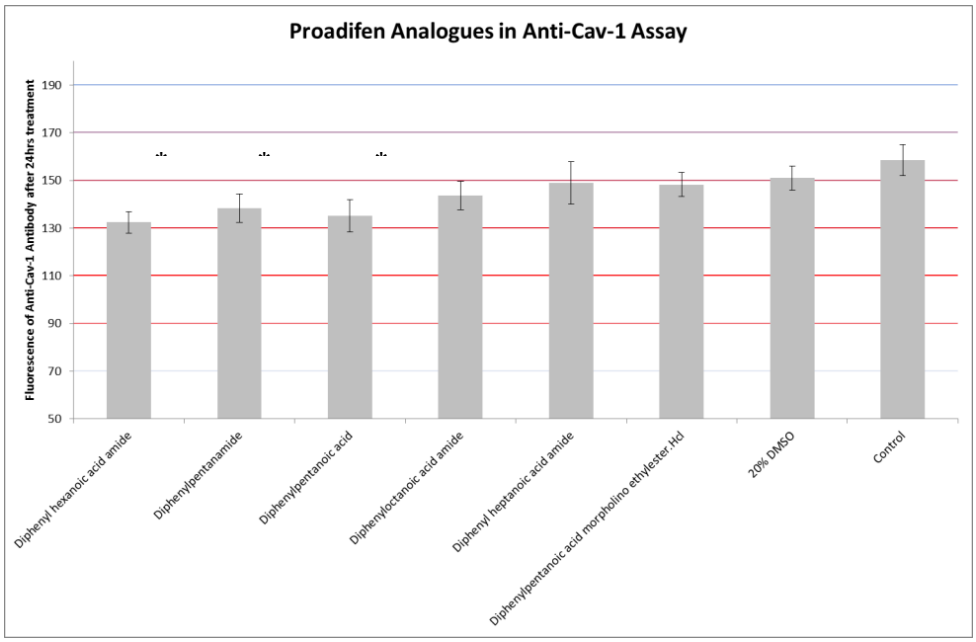

FIGURE 72: CAV-1 ASSAY WITH MULTIPLE PROADIFEN ANALOGUES

THE FIGURES 72-88 SHOW MEAN OF TRIPLICATE VALUES FROM MORE THAN ONE EXPERIMENT. ERROR BARS DENOTE ± STANDARD ERRORS AND * DENOTES STATISTICAL SIGNIFICANCE AT $P<0.05$ (ANNOVA TWO TAILED TEST FOR DIFFERENCE FROM THE CONTROL). Y-AXIS SHOWS THE BINDING OF ANTI-CAV-1 ANTIBODY TO MEMBRANE CAV-1 AND IS MEASURED ON A SCALE RELATIVE TO THE NEGATIVE CONTROL. INCREASING ACYL CHAIN LENGTH OF THE MODEL DIPHENYLVALERATE COMPOUNDS CAUSES MODEST DECREASE IN CAV-1 EXPRESSION.

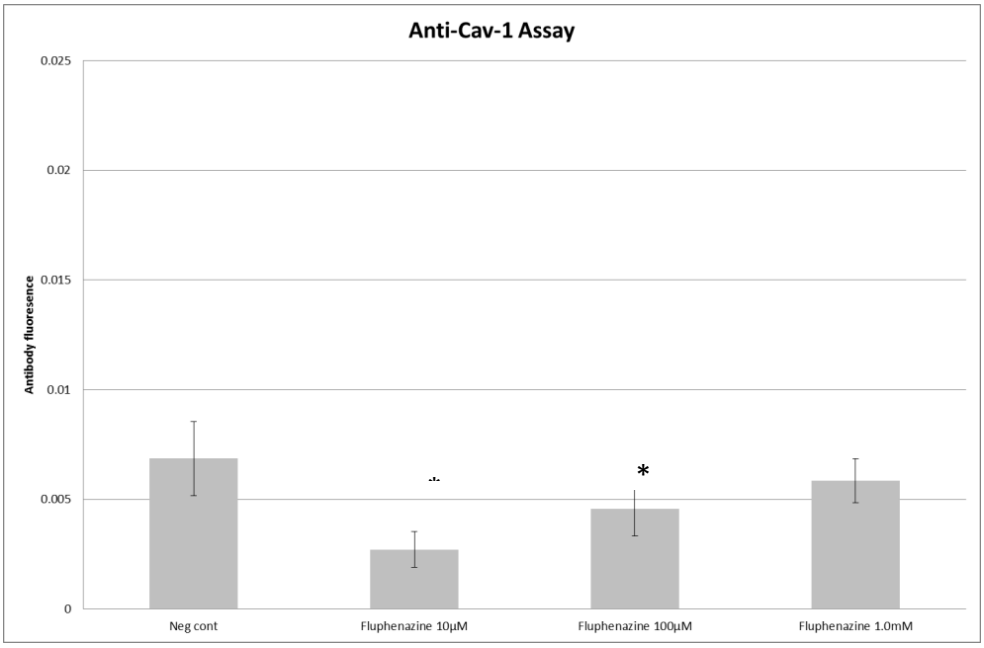

FIGURE 73: CAV-1 ASSAY FLUPHENAZINE

ALL FLUPHENAZINE TREATMENTS CAUSED A STATISTICALLY SIGNIFICANT REDUCTION IN CAV-1 EXPRESSION BUT THIS RESPONSE WAS NON-LINEAR.

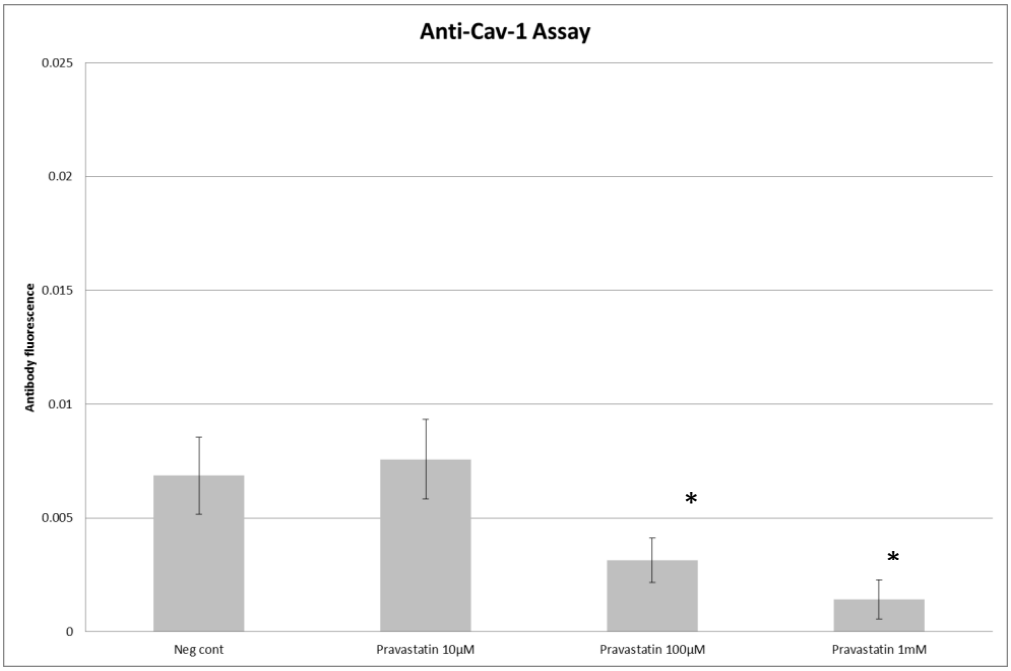

FIGURE 74: CAV-1 ASSAY PROADIFEN

THIS FIGURE SHOWS A CLEAR DOSE-RESPONSE REDUCTION OF CAV-1 EXPRESSION.

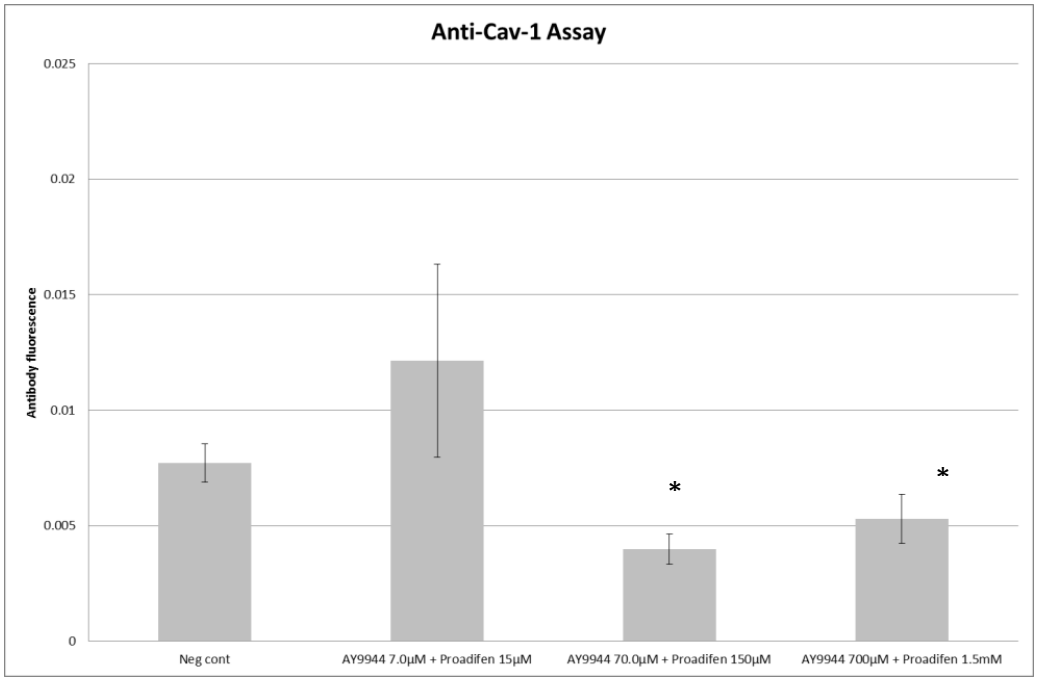

FIGURE 75 CAV-1 ASSAY AY9944

PROADIFEN AND AY9944 SHOWED NO INCREASE IN CAV-1 REDUCTION WHEN COMBINED (ALSO SEE FIGURE 81 AND FIGURE 82)

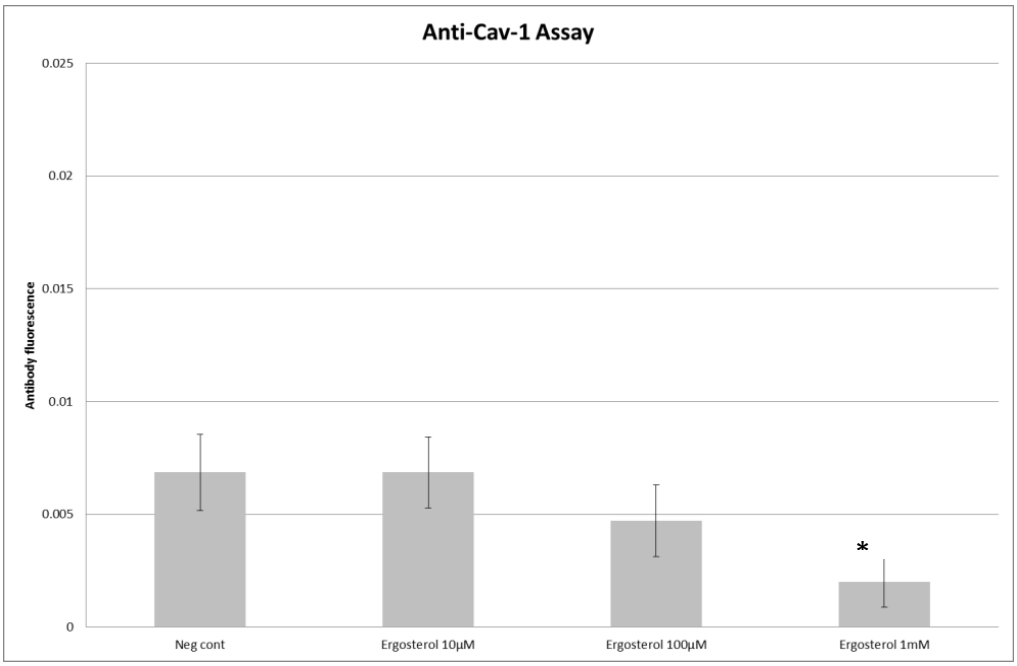

FIGURE 76: CAV-1 ASSAY ERGOSTEROL

ERGOSTEROL IS USED TO SIMULATE A Δ24 DESATURASE BLOCKADE AND DOES APPEAR TO REDUCE CAV-1 AT HIGH DOSES (SEE ALSO FIGURE 78**)**

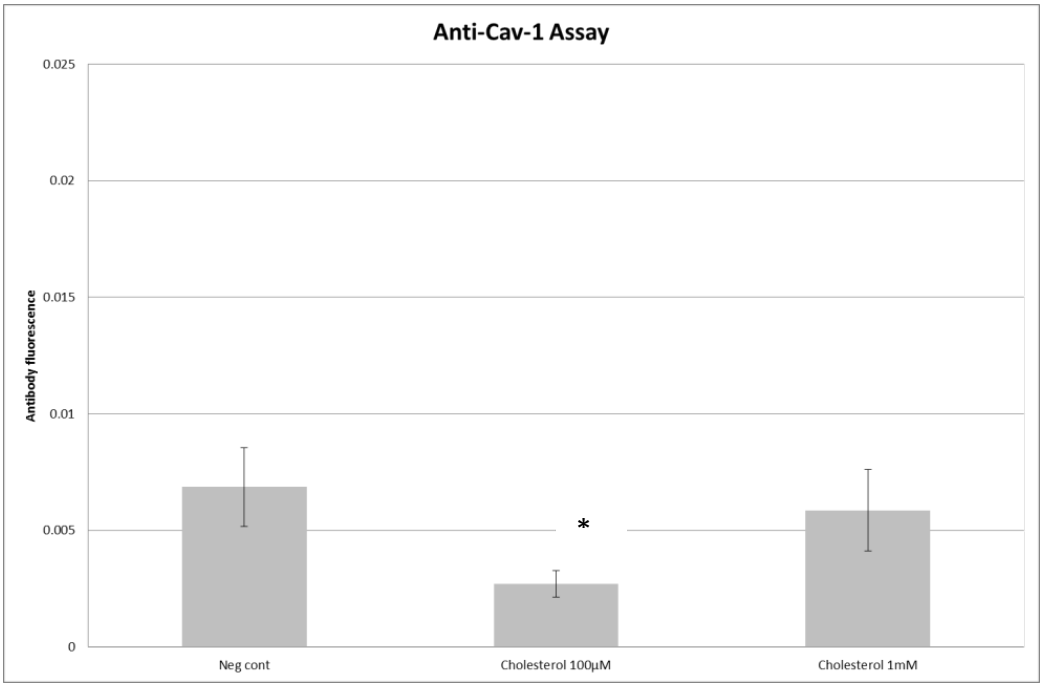

FIGURE 77: CAV-1 ASSAY CHOLESTEROL

THE RESULTS OF CHOLESTEROL TREATMENTS ON CAV-1 EXPRESSION WERE NOT STATISTICALLY SIGNIFICANT.

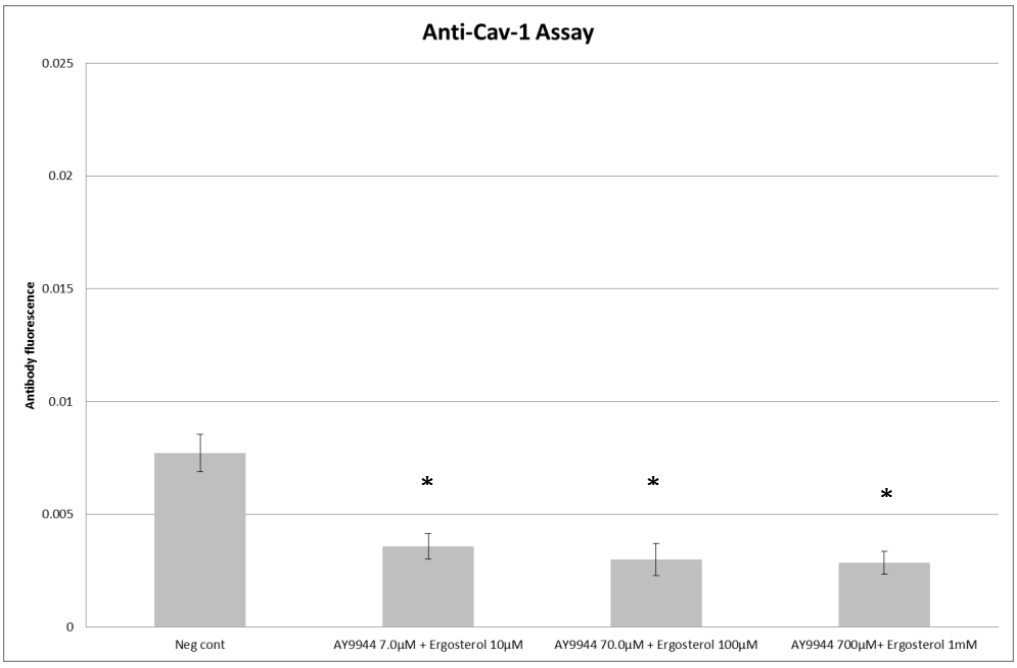

FIGURE 78: CAV-1 ASSAY ERGOSTEROL AND AY9944 COMBINED TREATMENTS

COMBINED TREATMENTS OF AY9944 AND ERGOSTEROL DO NOT APPEAR TO BE SYNERGISTIC IN TERMS OF CAV-1 EXPRESSION. ERGOSTEROL IS USED HERE FOR COMPETITIVE INHIBITION OF THE Δ-24 DESATURASE TO SEE IF THE RESPONSE TO COMBINED TREATMENT WITH Δ-7 INHIBITOR IS SIMILAR TO THAT WITH PROADIFEN. SEE FIGURE 87.

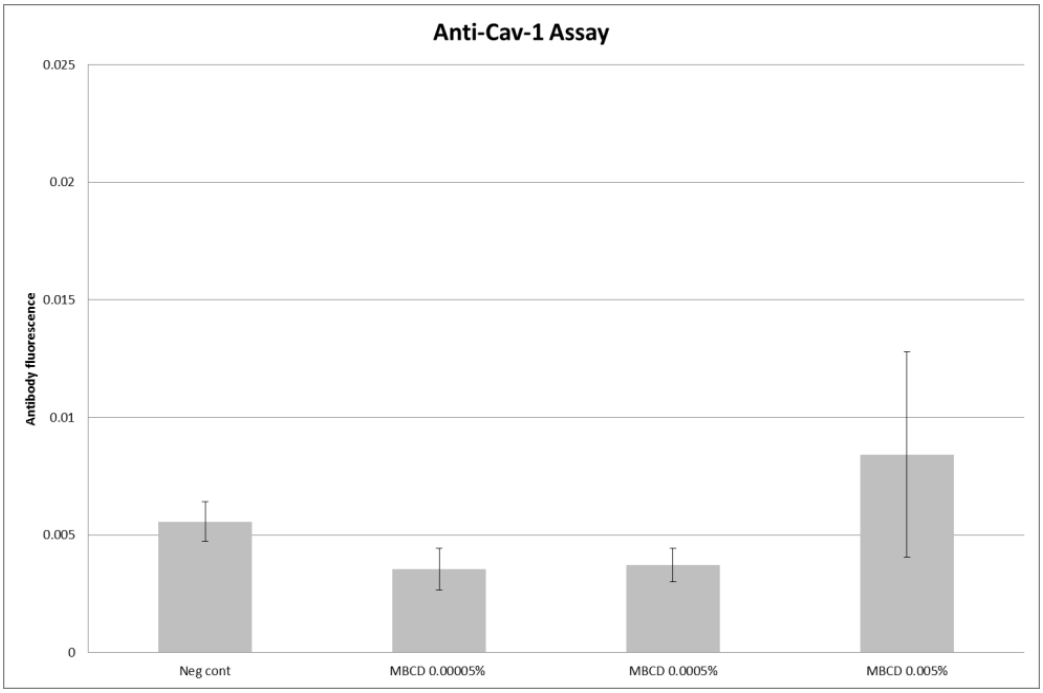

FIGURE 79: CAV-1 ASSAY MBCD TREATMENT

SEQUESTRATION BY MBCD OF MEMBRANE CHOLESTEROL HAS A MODEST IMPACT ON CAV-1 EXPRESSION.

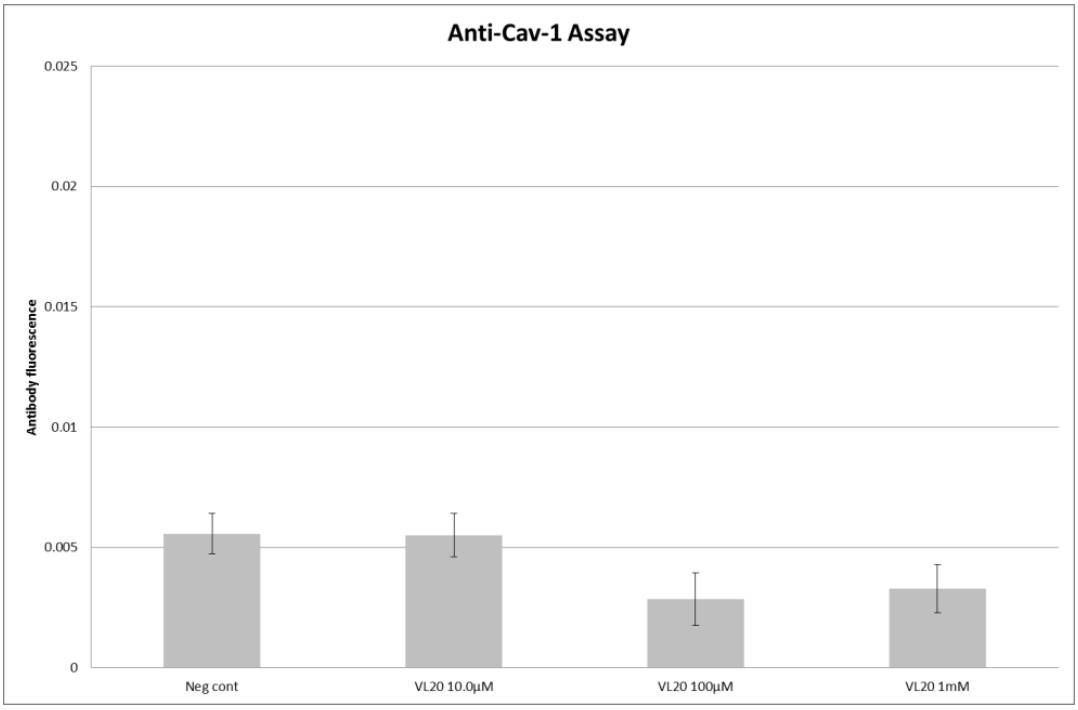

FIGURE 80: CAV-1 ASSAY "VL20" ANALOGUE

NO ADDITIONAL REDUCTION OF CAV-1 WAS SEEN FOLLOWING THE INSERTION OF AN EXTRA METHYL GROUP BETWEEN THE PHENYL MOIETIES.

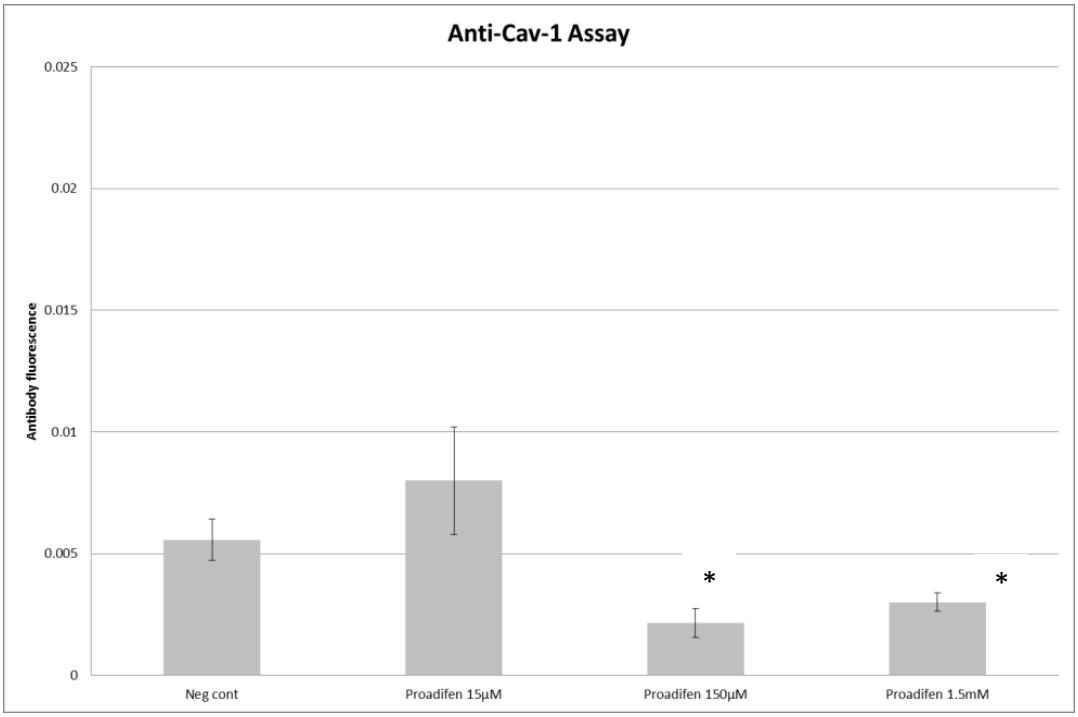

FIGURE 81: CAV-1 ASSAY PROADIFEN

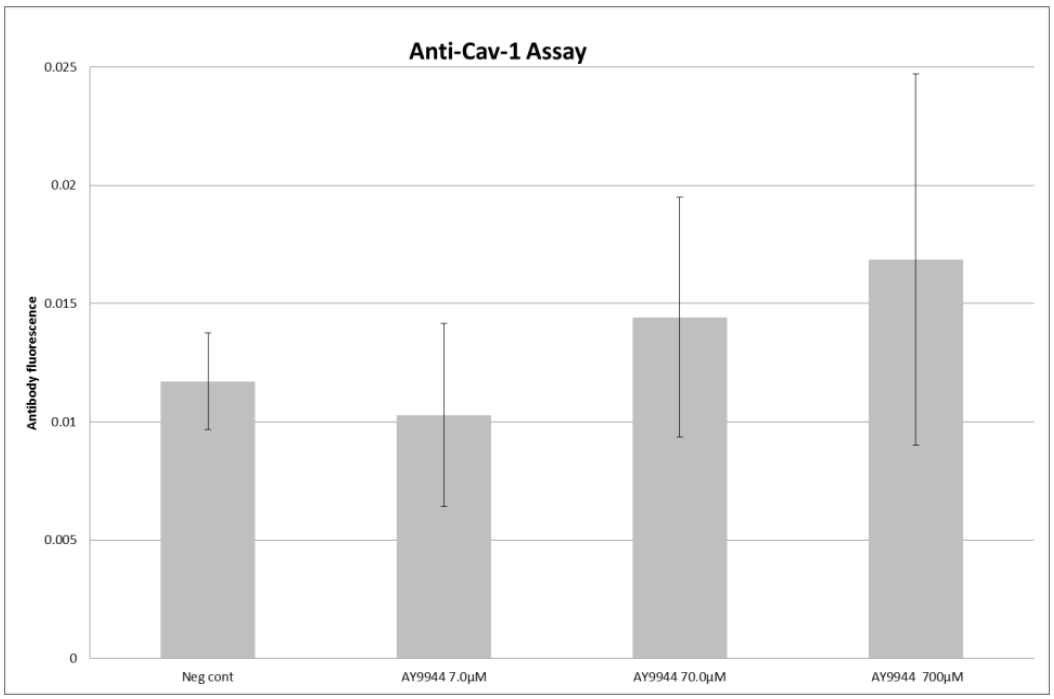

FIGURE 82: CAV-1 ASSAY AY9944 TREATMENT

AY9944 DOES NOT APPEAR TO REDUCE CAV-1 EXPRESSION BUT DOES REDUCE OVERALL RAFT PREVALENCE (SEE ALSO FIGURE 91)

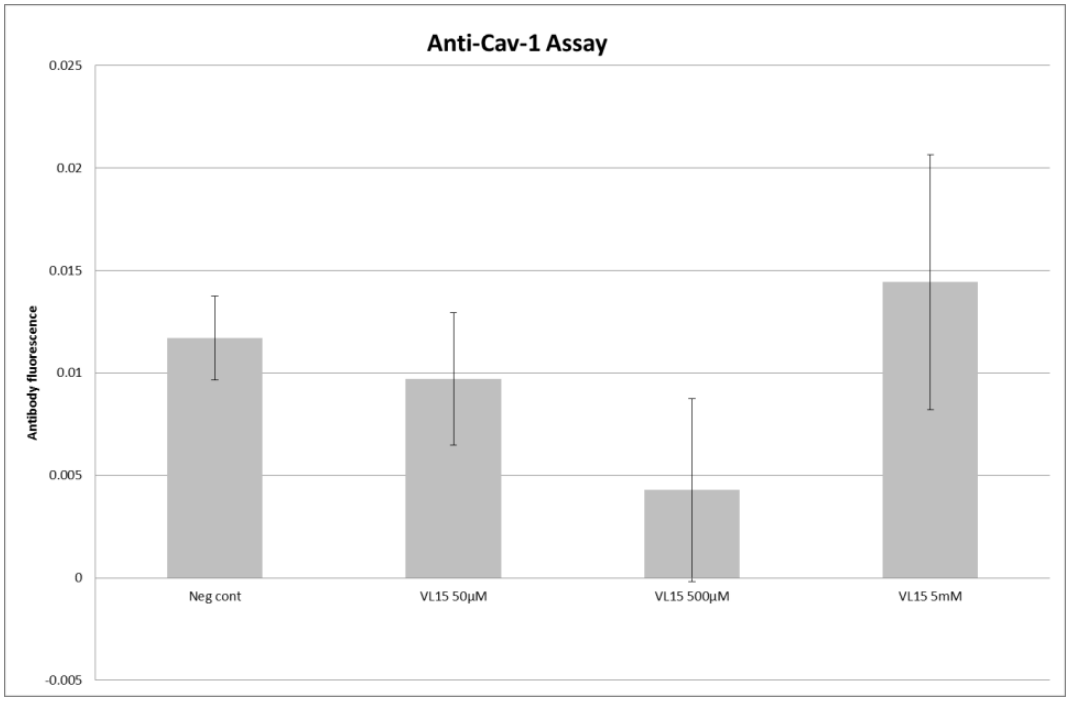

FIGURE 83: CAV-1 ASSAY "VL15" ANALOGUE

REMOVAL OF THE TERMINAL ETHYL GROUPS FROM THE PROADIFEN STRUCTURE REDUCES THE EFFECT ON CAV-1 EXPRESSION.

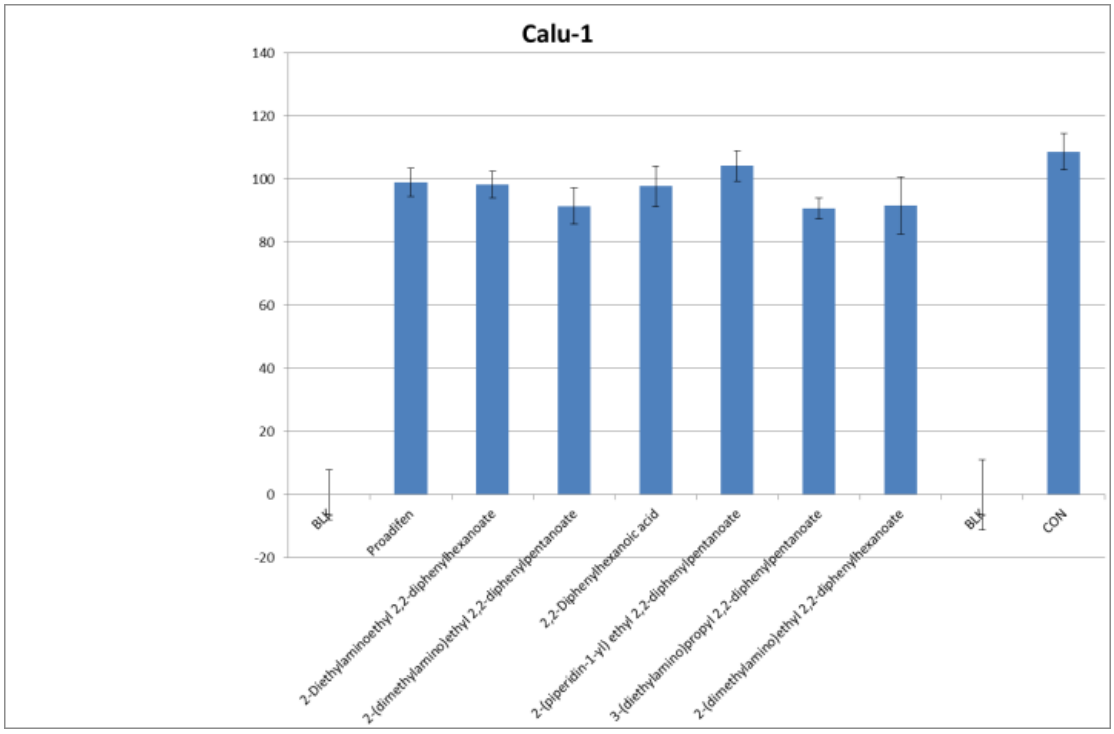

FIGURE 84: CAV-1 ASSAY MULTIPLE ANALOGUES TESTED ON CALU-1 CELLS

THERE IS LITTLE DIFFERENCE BETWEEN PROADIFEN AND ITS ANALOGUES ON CAV-1 EXPRESSION.

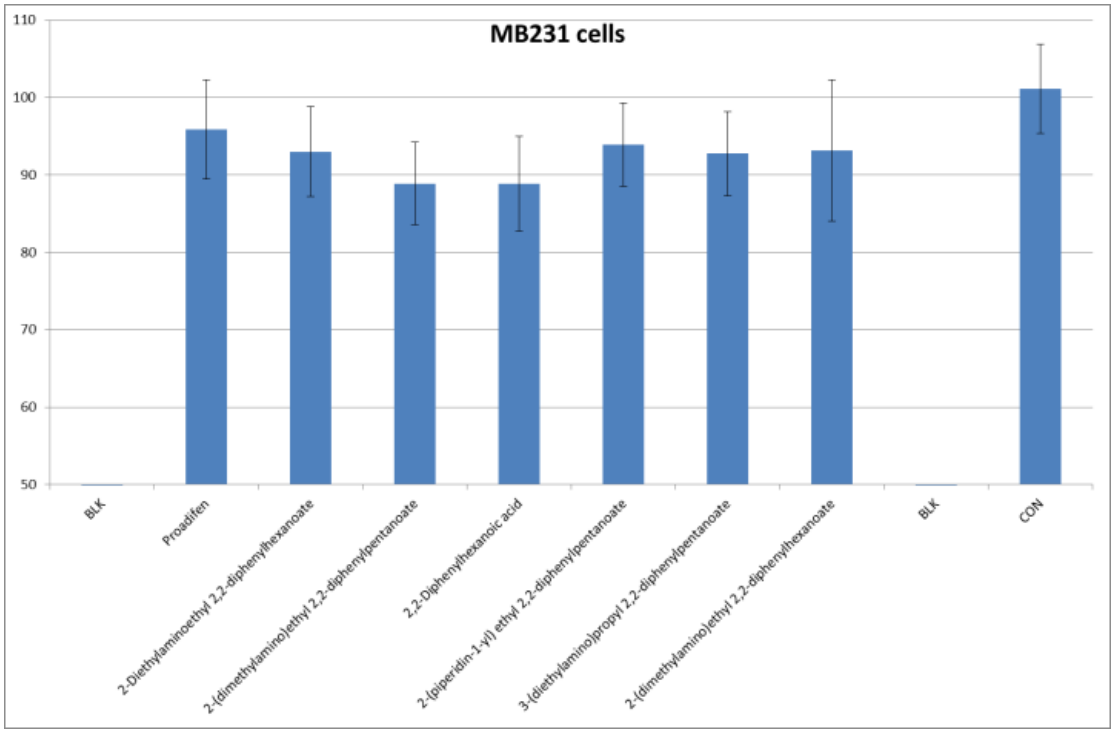

FIGURE 85: CAV-1 ASSAY ADDITIONALPROADIFEN ANALOGUES TESTED ON MDA-MB-231 CELLS

THERE IS LITTLE DIFFERENCE BETWEEN PROADIFEN AND ITS ANALOGUES ON CAV-1 EXPRESSION.

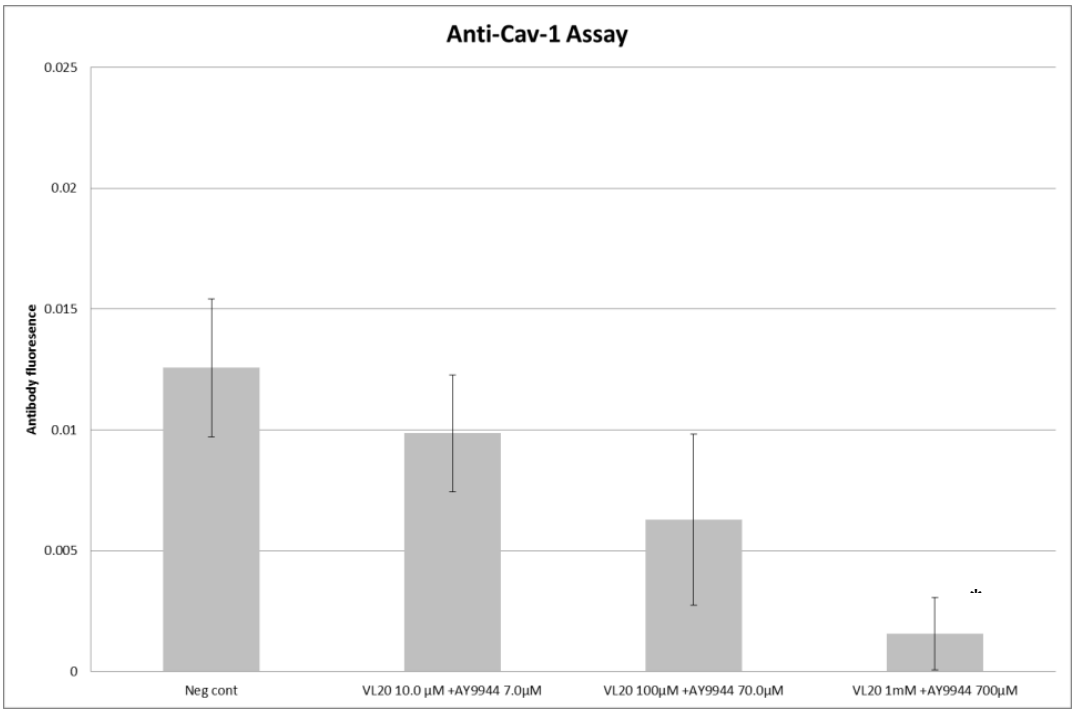

FIGURE 86: CAV-1 ASSAY COMBINED TREATMENT VL20 AND AY9944

A COMBINED TREATMENT OF VL20 AND AY9944 AT HIGH DOSES APPEARS TO SIGNIFICANTLY REDUCE CAV-1 EXPRESSION (SEE ALSO FIGURE 80 AND FIGURE 82 FOR COMPARISON.

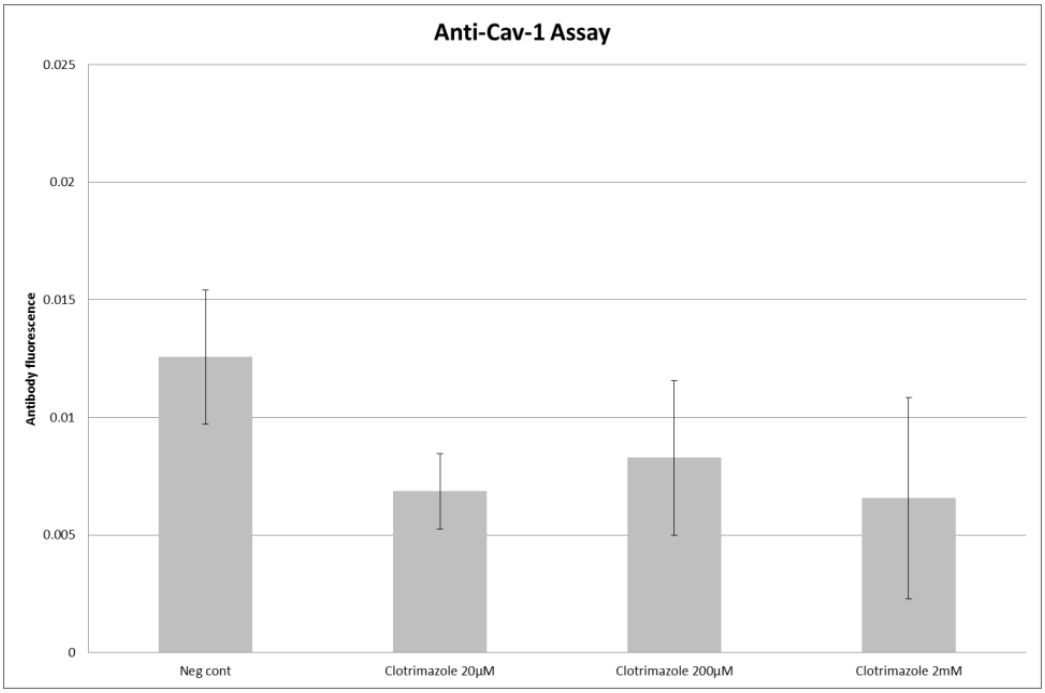

FIGURE 87: CAV-1 ASSAY CLOTRIMAZOLE

CLOTRIMAZOLE DOES NOT APPEAR TO REDUCE CAV-1 EXPRESSION

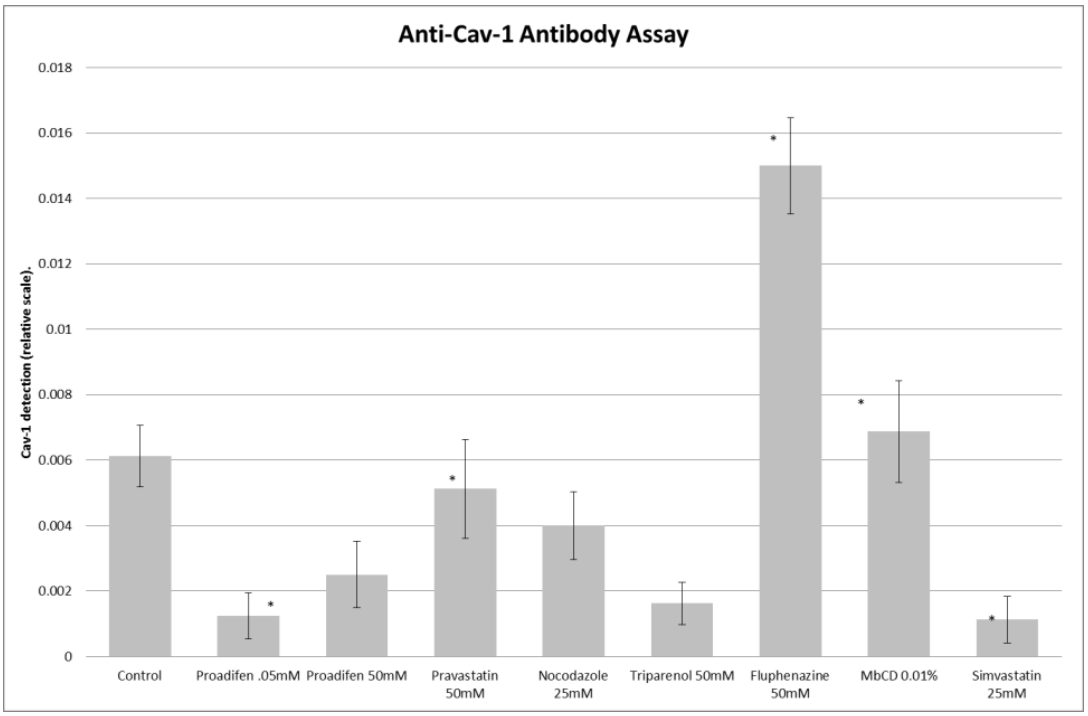

FIGURE 88: COMPARISON OF SEVERAL TREATMENTS IN CAV-1 ASSAY

PRAVASTATIN, SIMVASTATIN, PROADIFEN, MBCD AND TRIPARENOL ALL REDUCE CAV-1

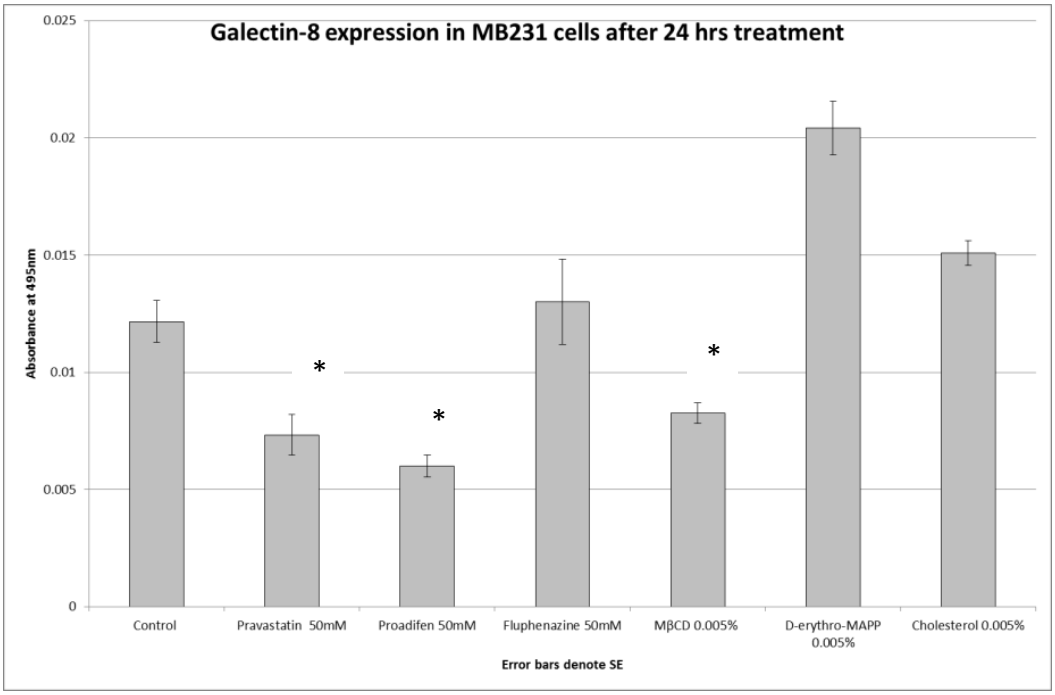

FIGURE 89: COMPARISON OF SEVERAL TREATMENTS IN GAL-8 ASSAY

FIGURES 89-91 SHOW THE BINDING OF A FLUORESCENT TAGGED ANTIBODY TO MEMBRANE GLECTIN-8, TUBULIN-1 AND FLOTILIN-1 RESPECTIVELY. Y-AXIS SHOWS ANTIBODY BINDING. GALACTINS ARE SECRETED CARBOHYDRATE-BINDING PROTEINS THAT MODULATE CELL-MATRIX ADHESION. GAL-8 FORMS COMPLEXES WITH INTEGRINS TO INHIBIT CELL ADHESION AND INDUCE APOPTOSIS (HADARI ET AL., 2000).

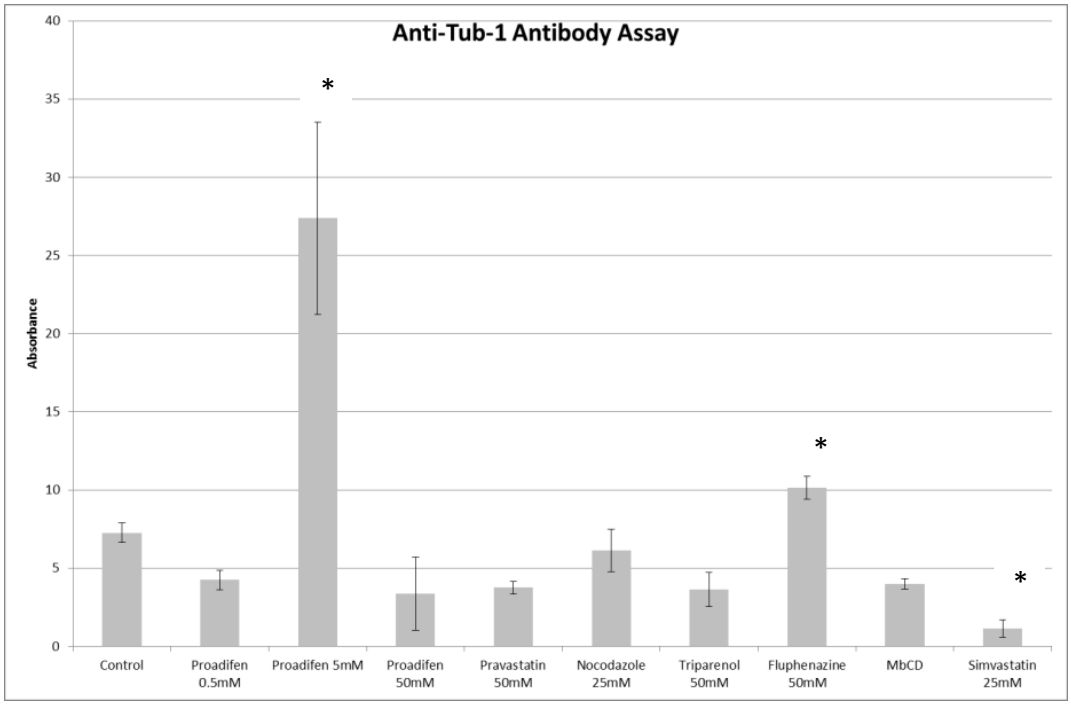

FIGURE 90: COMPARISON OF SEVERAL TREATMENTS IN TUB-1 ASSAY

TUBULIN IS A MARKER OF CYTOSKELETON REARRANGEMENT. A DECREASE IN TUB-1 IS CORRELATED TO REDUCED MOTILITY.

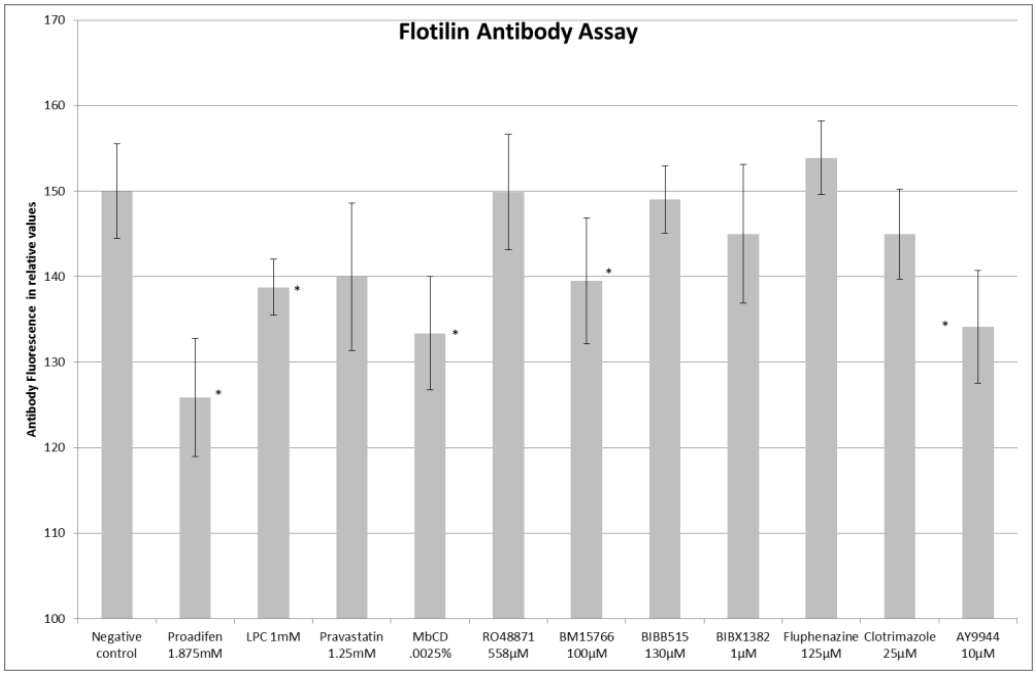

FIGURE 91: COMPARISON OF SEVERAL TREATMENTS IN ANTI-FLOTILLIN ASSAY

These assays were conducted to examine in more detail the effects of Proadifen and its analogues on these key metastatic markers and to compare them with other inhibitors of the mevalonate pathway. Introduction of cholesterol resulted in elevated Cav-1 in contrast to the reduction of Cav-1 caused by Proadifen or the cholesterol sequestering agent MβCD. Tubulin (Tub-1) was also assayed to permit a comparison with the protein microarray data as caveolins were not screened in that assay. Proadifen appeared to reduce the expression of tubulin in MDA-MB-231 (↓18% at 50µl 1mM) and this reduction is predicted by the microarray assay (↓56% at 100µl 1mM). Interestingly, both cholesterol and MβCD also reduced tubulin expression.

Proadifen, Pravastatin, ergosterol and MβCD all significantly reduced Cav-1 expression in these assays. Pravastatin, Proadifen and ergosterol display a dose-response profile. Combining AY9944 with Proadifen made no difference to the results for Proadifen as a

discreet treatment. It may be that Δ-7 inhibition alone produces an accumulation of a cholesterol intermediate suitable for complexing with Cav-1 (dehydrocholesterol) while the products of the Δ-24 inhibitor (lanosterol and desmosterol) are unsuitable for caveolae formation. If this is true then Proadifen could be used to target only caveolae mediated signal transduction. Various close analogues of Proadifen were tested in this assay with unremarkable results. A slight reduction in Cav-1 was seen with increasing acyl chain length but the insertion of an extra methyl group or removal of both ethyl groups has no observable effect on activity as measured in this assay. Of the other compounds tested, clotrimazole made no significant impact on Cav-1 expression but Pravastatin, Simvastatin, Fluphenazine and MβCD all reduced the amount of caveolin-1 visible to the labelled antibody in the assay.

Gal-8 expression was measured in a similar experiment and here, Pravastatin, Proadifen and MβCD reduced Gal-8 expression but interestingly Fluphenazine and D-erythro-MAPP did not. Tub-1 was also assayed and here again, Proadifen and the Pravastatin caused significant reduction in Tub-1 expression. Flotillin, the general marker for the presence of rafts was statistically significant reduced in treatments with Proadifen, LPC, MβCD, AY9944 and BM15766.

3.3.5 RESULTS FROM COMBINED PROTEOLYSIS AND MOTILITY EXPERIMENT

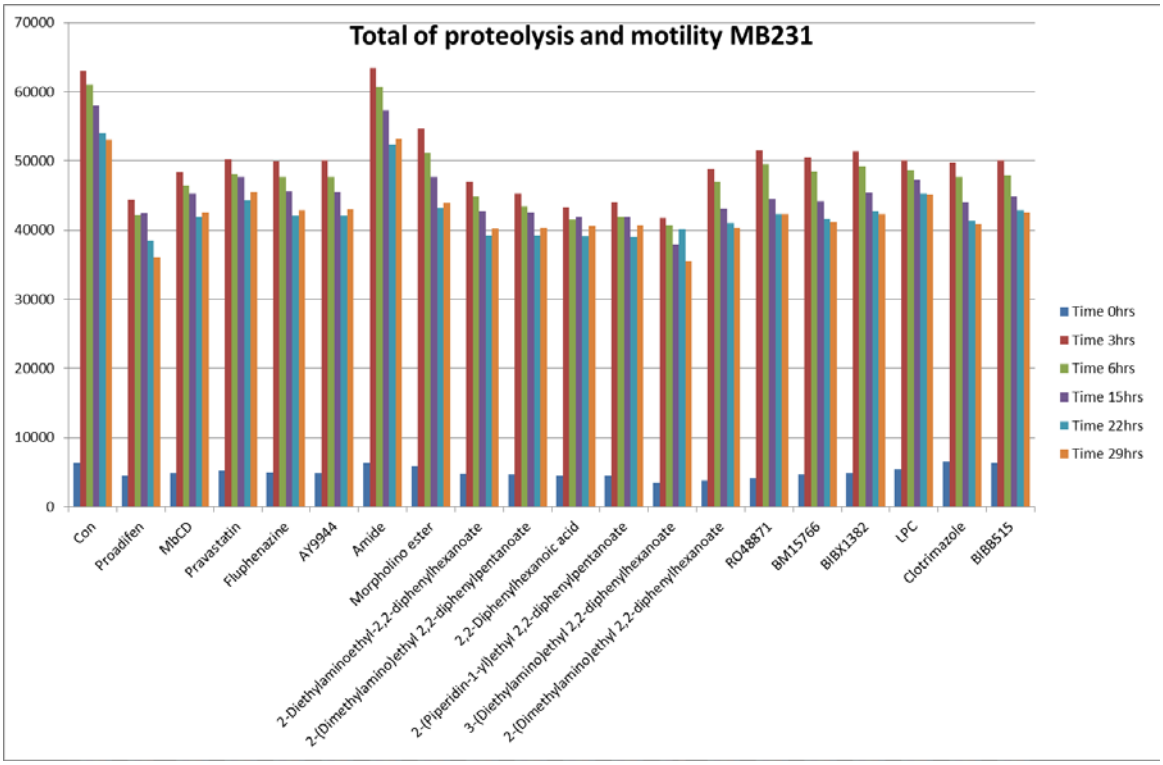

FIGURE 92: PROTEOLYSIS AND MOTILITY DATA MDA-MB-231

FIGURES 92. THIS EXPERIMENT SOUGHT TO MEASURE THE EFFECT OF THE COMPLETE RANGE OF DRUG TREATMENTS, INCLUDING ALL OF THE NEWLY SYNTHESIZED PROADIFEN ANALOGUES, ON THE PROTEOLYSIS CAPACITY OF MDA-MB-231 AND CALU-1 CELLS. A SIMPLE TEST OF ENZYME DIGESTION OF FLUORESCENT-QUENCHED GELATIN WAS USED. TO SEE THE EFFECT OF RESTRICTING THE CELLS MOVEMENT ON THE DEGREE OF PROTEOLYSIS THE MOTILITY INHIBITOR CYTOCHALISIN B WAS USED IN REPEATED EXPERIMENTS. THE EXPERIMENT WAS RUN OVER 29 HOURS BUT THE REPEATED EXPOSURE OF THE PLATES TO LIGHT DURING THE INTERVALS TO TAKE READINGS IN THE PLATE READER AND VARIOUS MICROSCOPE EXAMINATIONS OF THE CELLS SEEMS TO HAVE CAUSED THE GELATIN CONJUGATE TO BE LOSE ITS FLUORESCENCE AFTER JUST 3 HOURS. DATA AFTER 3 HOURS CAN BE IGNORED AND IS PRESENTED HERE ONLY FOR THE SAKE OF COMPLETENESS. FIGURES 92-97 SHOW RESULTS THAT ARE SCALED BY TRYPAN BLUE VIABILITY DATA AND HAVE AN ARBITRARY Y-AXIS SCALE.

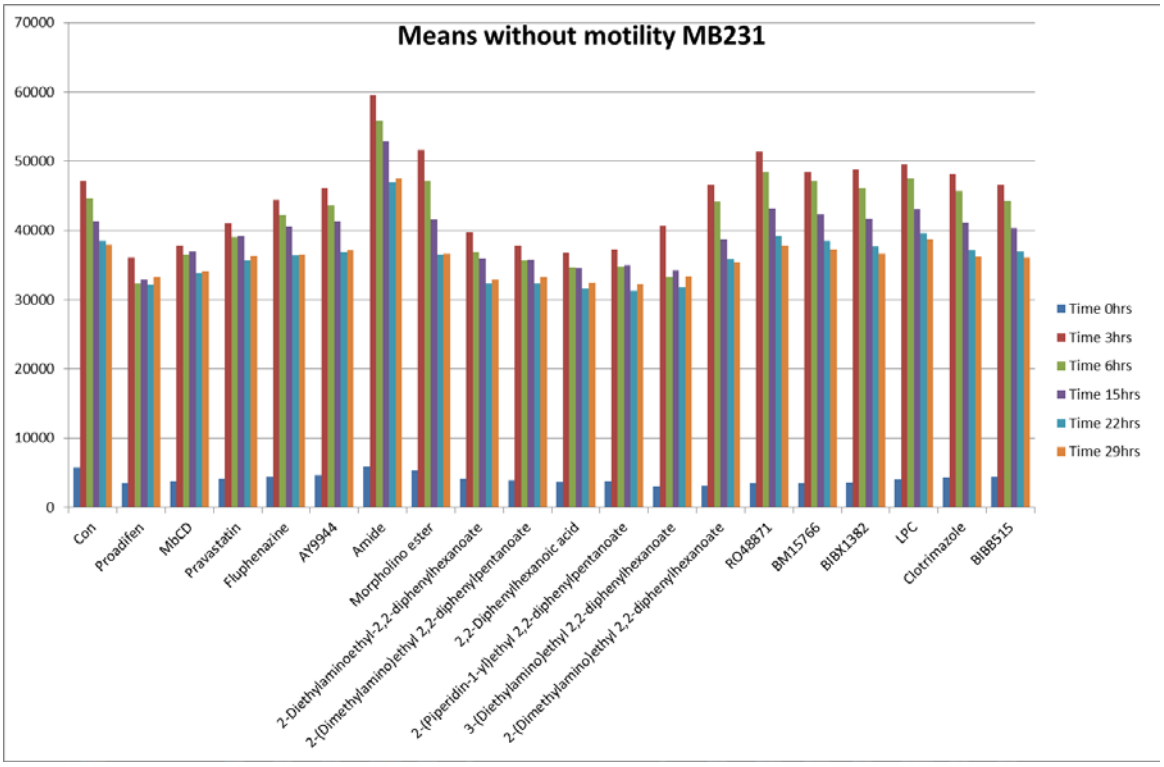

FIGURE 93: PROTEOLYSIS DATA MDA-MB-231

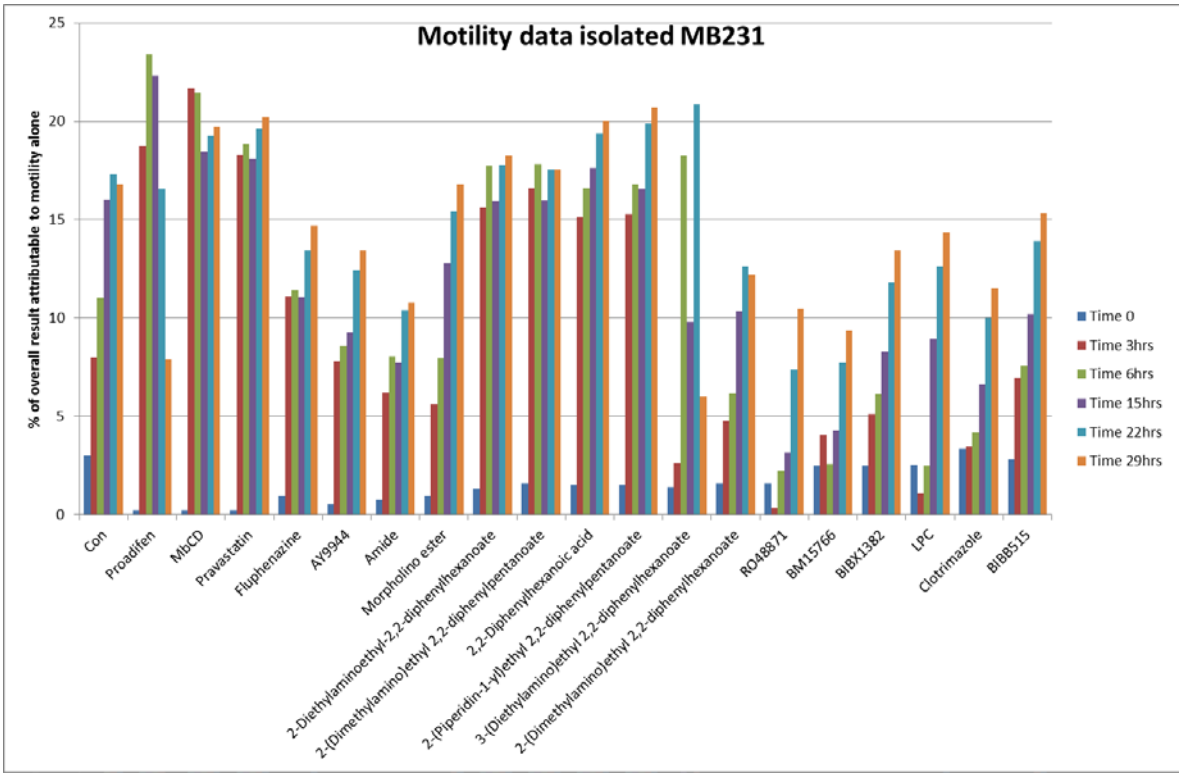

FIGURE 94: MOTILITY DATA MDA-MB-231

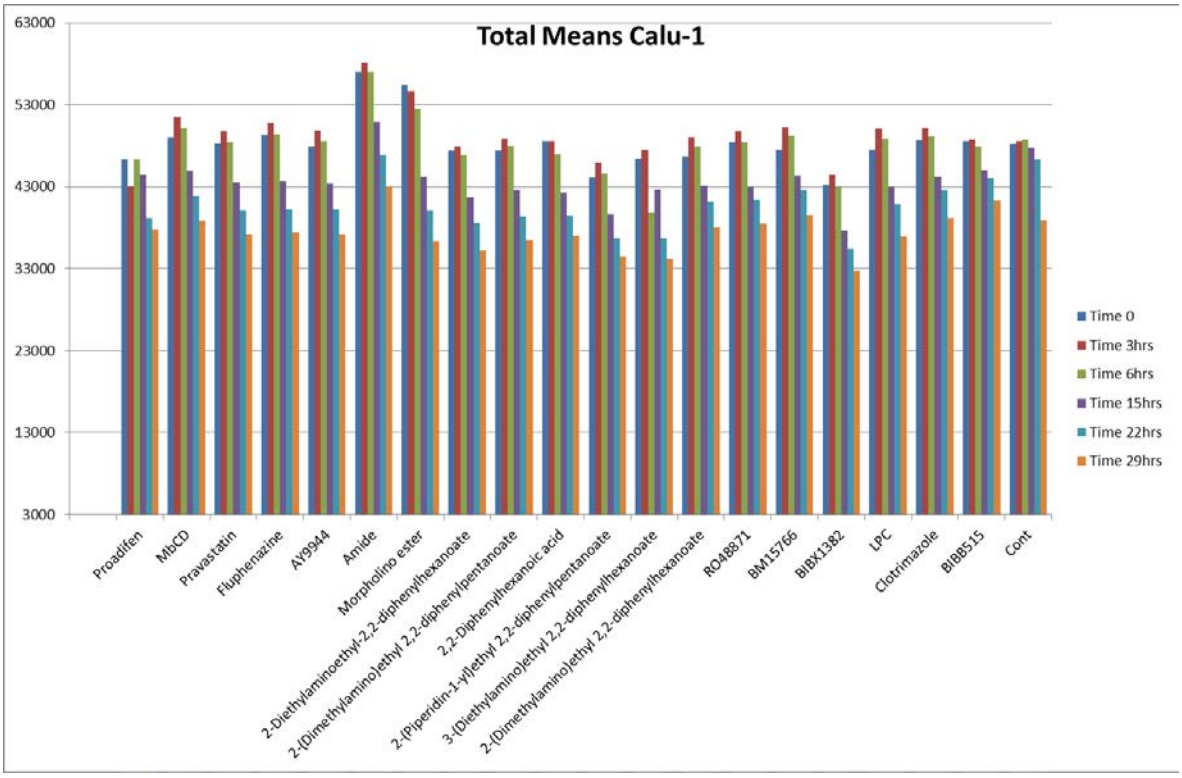

FIGURE 95: PROTEOLYSIS AND MOTILITY DATA CALU-1

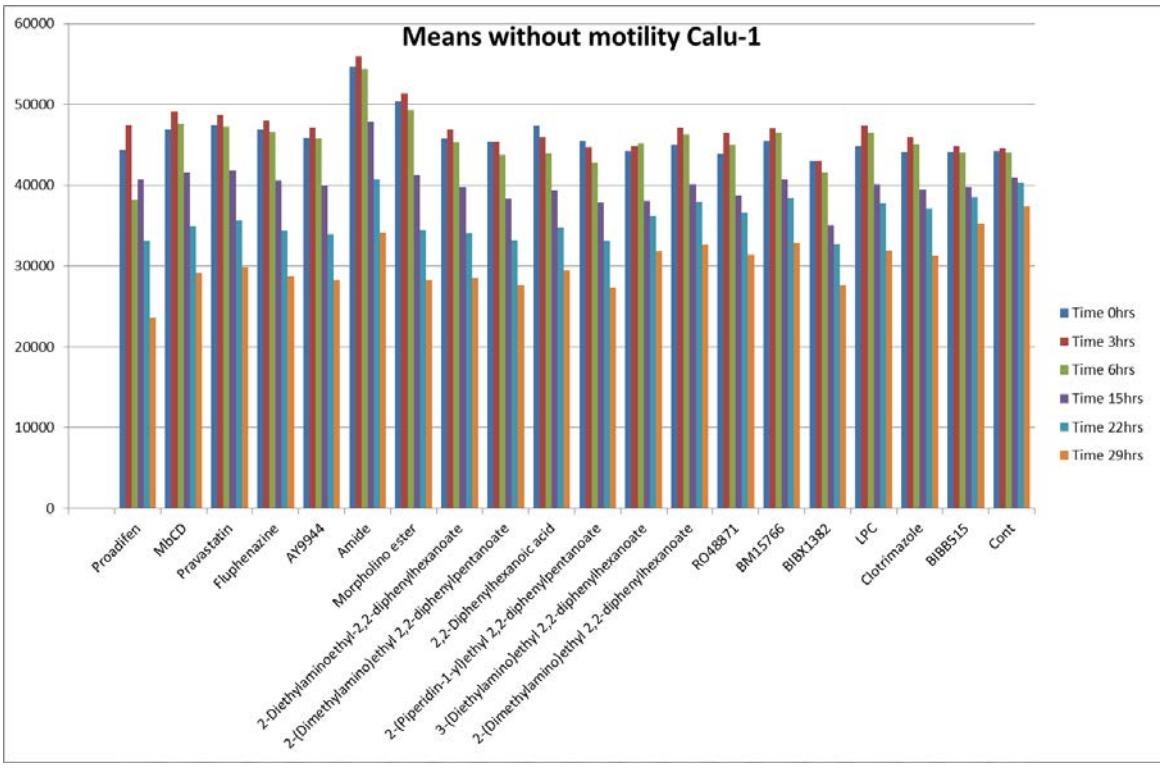

FIGURE 96: PROTEOLYSIS DATA CALU-1

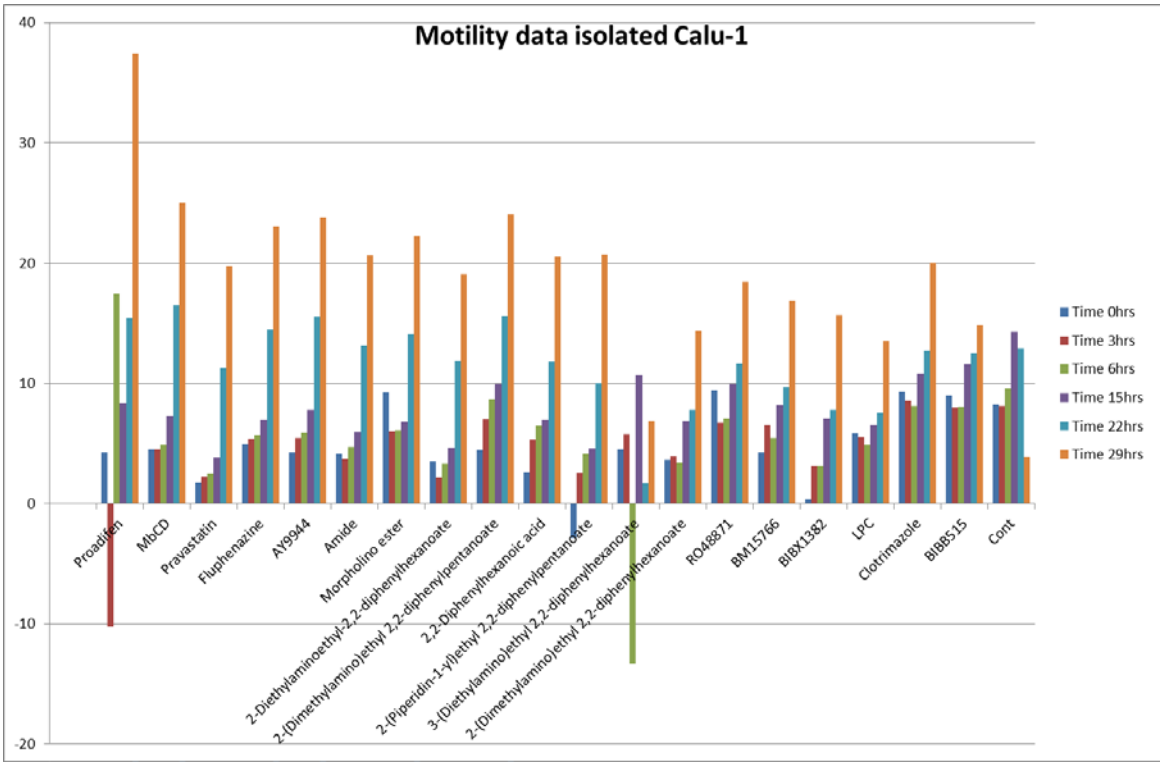

FIGURE 97: MOTILITY DATA CALU-1

Treatment with cytochalsin B reduced the proteolysis by 25-30% presumably because the cell exhausts the local media of conjugated protein. The data indicates that all treatments (except the 2,2-diphenylpentanamide “amide”) caused a reduction of fluorescence. 2-(Diethylamino)ethyl-2,2-diphenylhexanoate appears to the slightly more potent than Proadifen itself suggesting a minor increase in efficacy is related to the addition of the C6 moiety. Pravastatin and methyl-β-cyclodextrin had very similar effects on proteolysis and the statin treatment appeared to be slightly less affected by the cytochalisin. In general, CaLu-1 appears to very rapidly exhaust all available gelatin-conjugate and none of the treatments proved very effective in reducing proteolysis in this cell line. The motility data when isolated from the total proteolysis data suggests that in MDA-MB-231 particularly, Proadifen and its analogues all have a measurable

impact on motility but AY9944 does not. The other cholesterol inhibitors tested also had little effect on motility.

3.3.6 RESULTS OF CHOLESTEROL ASSAYS CONDUCTED IN MDA-MB-231 CELLS.

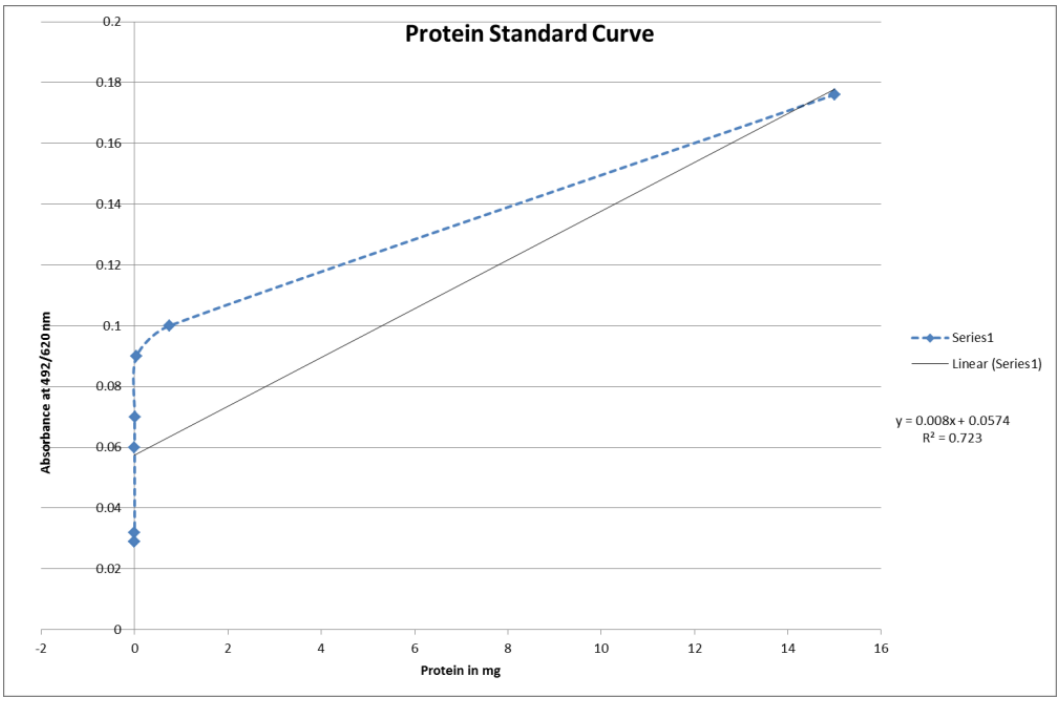

FIGURE 98: PROTEIN STANDARD CURVE

TO ESTABLISH TEST LINEARITY OF PROTEIN DETECTION BEFORE START OF EXPERIMENT

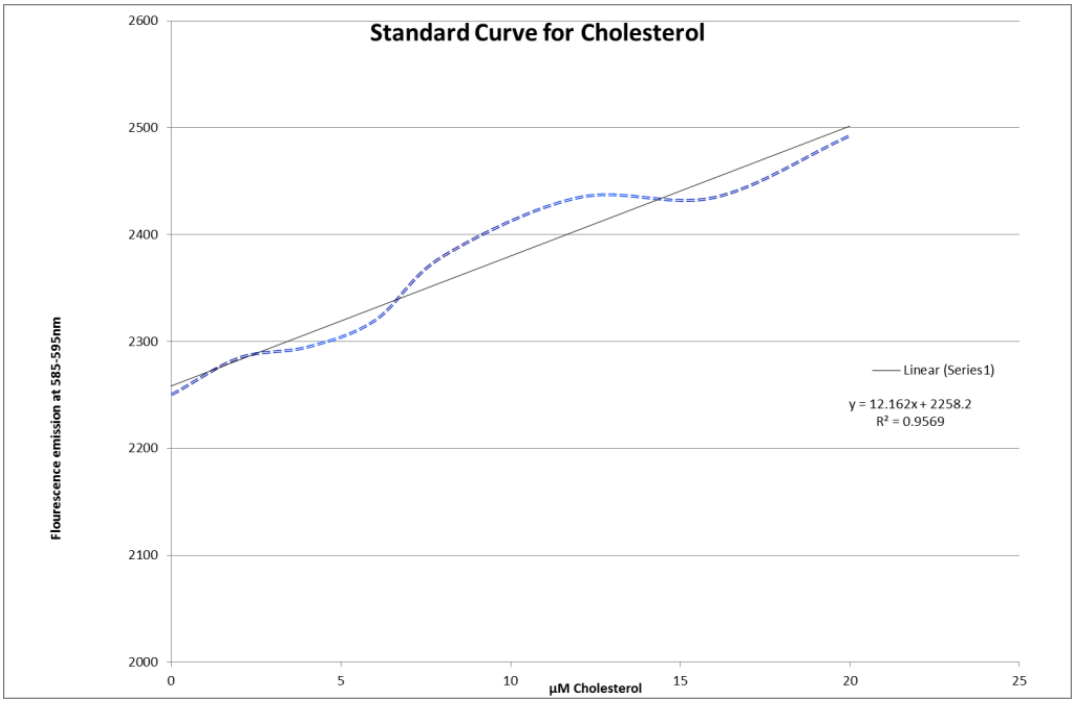

FIGURE 99: CHOLESTEROL STANDARD CURVE

TO VERIFY LINEARITY OF CHOLESTEROL DETECTION BEFORE START OF EXPERIMENT

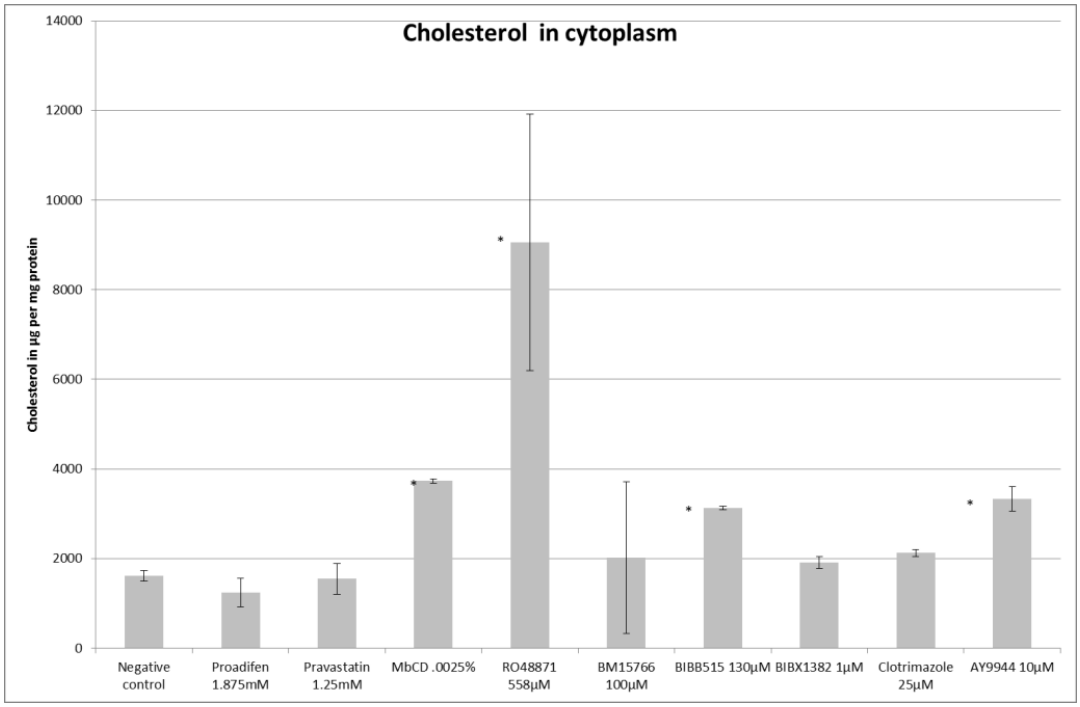

FIGURE 100: CHOLESTEROL IN CYTOPLASM

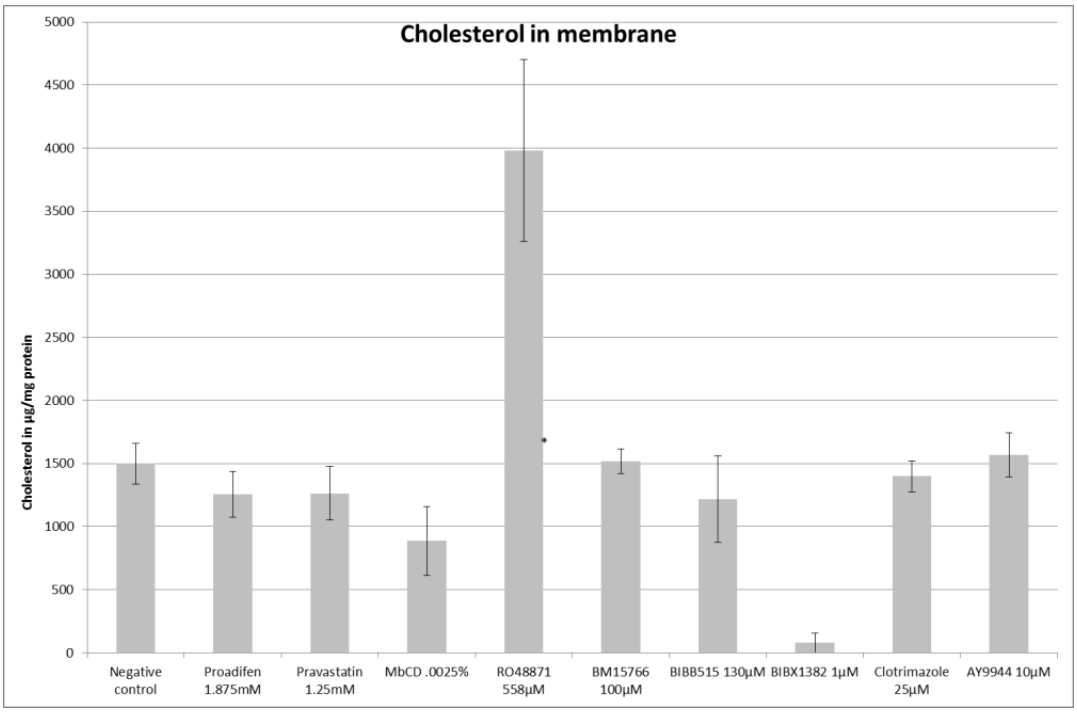

FIGURE 101: CHOLESTEROL IN MEMBRANE

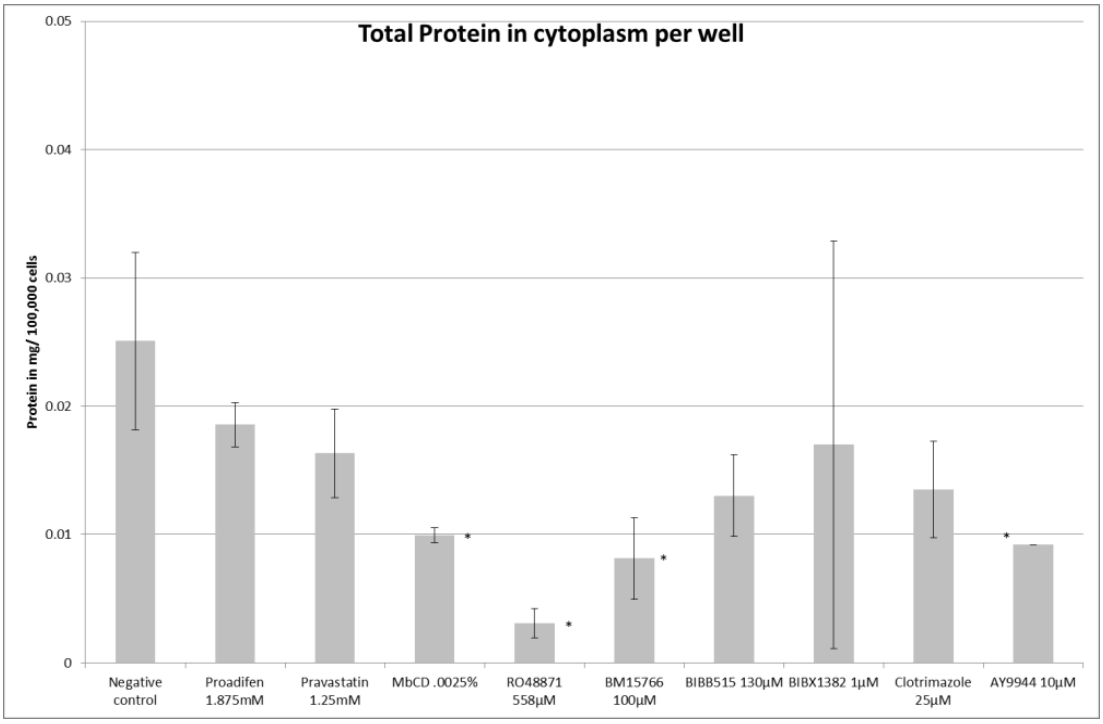

FIGURE 102: TOTAL PROTEIN IN CYTOPLASM PER WELL

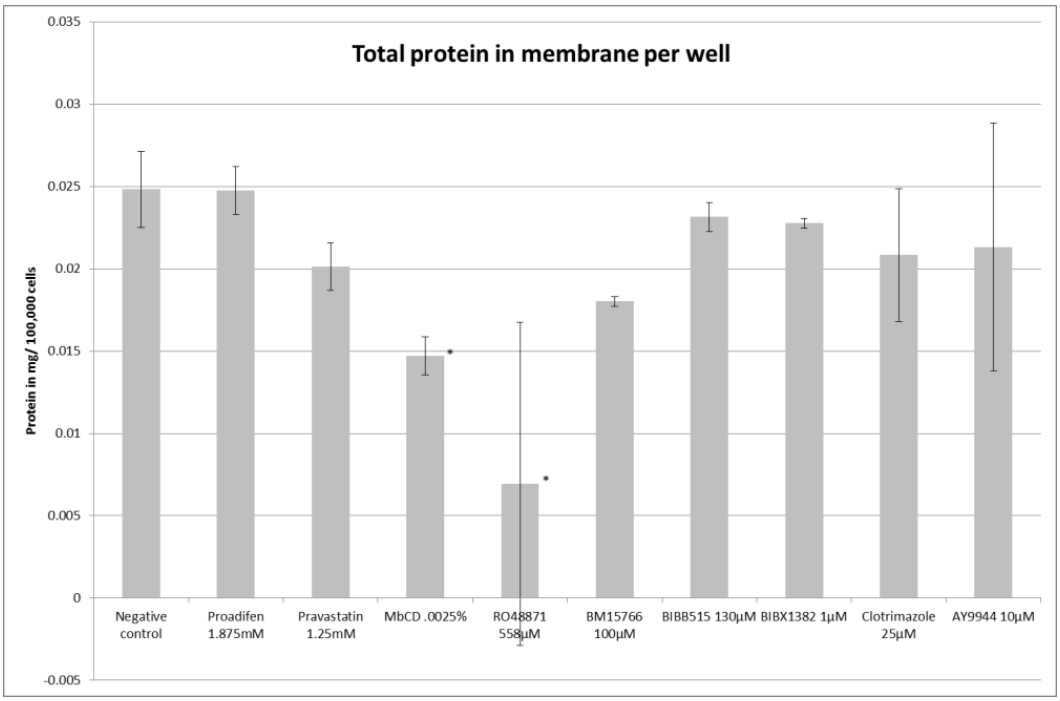

FIGURE 103: TOTAL PROTEIN IN MEMBRANE PER WELL

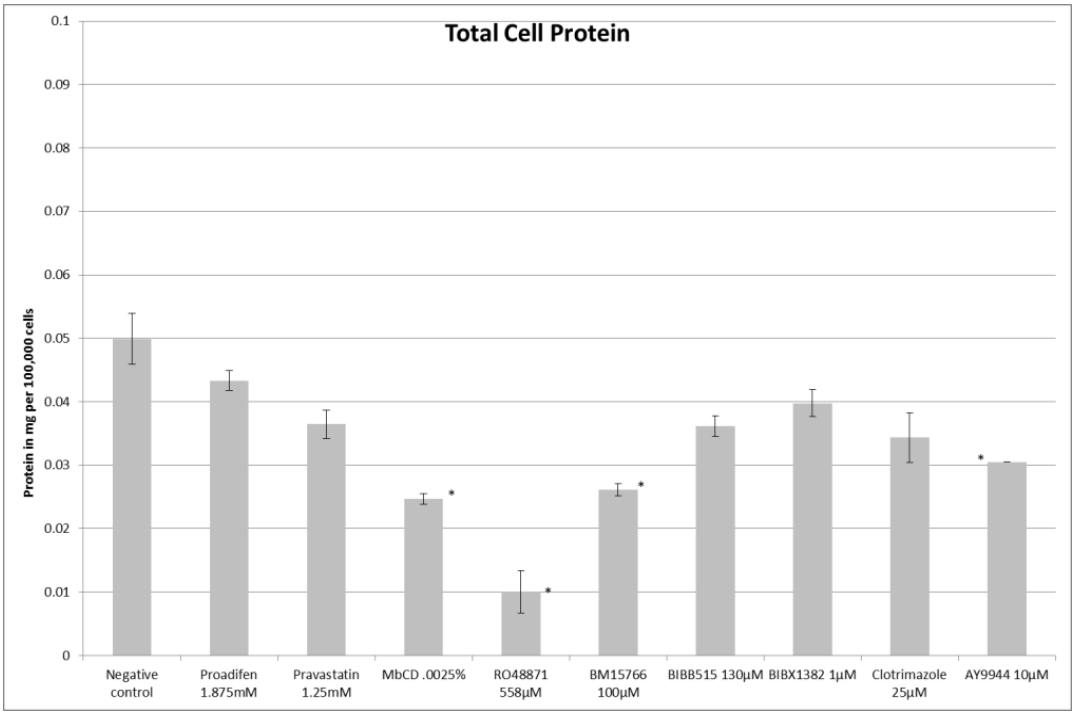

FIGURE 104: TOTAL CELL PROTEIN

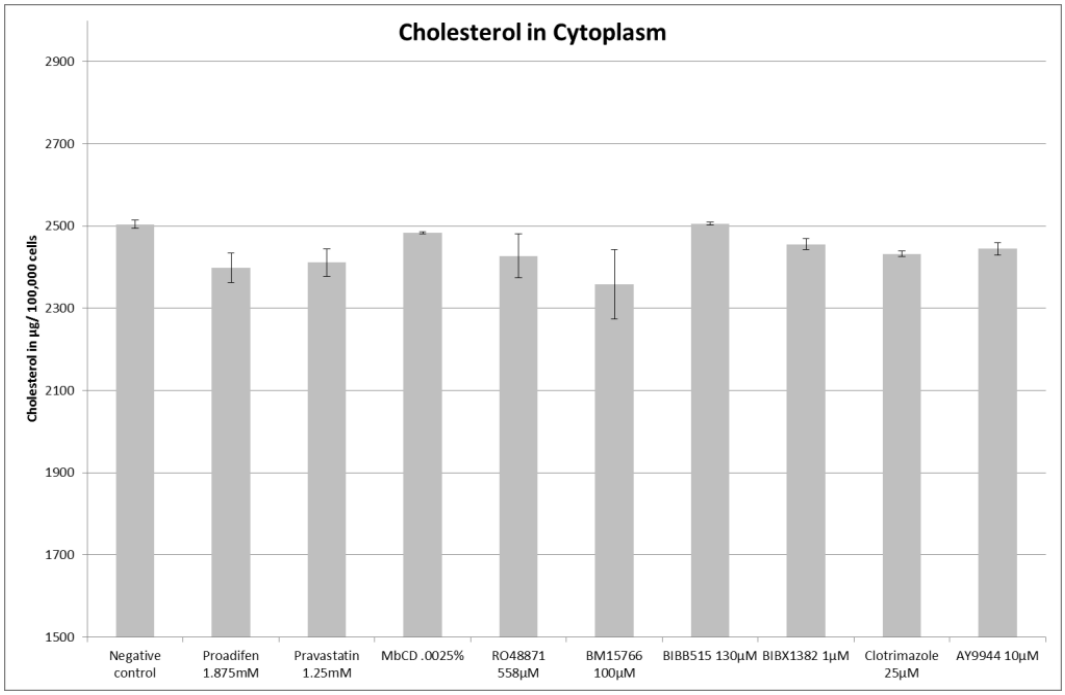

FIGURE 105: CHOLESTEROL IN CYTOPLASM

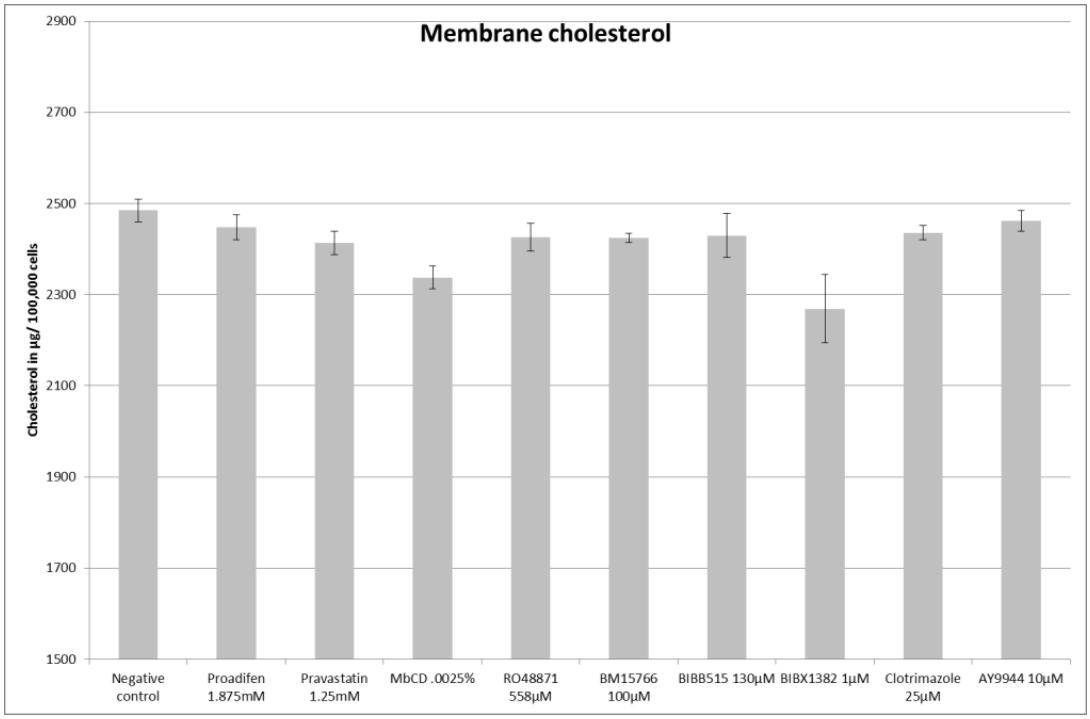

FIGURE 106: MEMBRANE CHOLESTEROL

FIGURES 100-106 SHOW THE LEVELS OF CHOLESTEROL AS ACTUAL WEIGHT % OF CHOLESTEROL PER MG PROTEIN OR 100,000CELLS FOR WHOLE CELLS, CYTOPLASM AND THE CELL MEMBRANE FRACTION. THE CHOLESTEROL TEST WAS DEVISED USING A COMMERCIALLY AVAILABLE CHOLESTEROL DETECTION KIT IN A 96 WELL PLATE FORMAT. USING THIS TEST AND CENTRIFUGE-SEPARATED CELLS, MEMBRANES AND THE CELL CONTENTS WERE SEPARATELY ANALYSED FOLLOWING VARIOUS TREATMENTS TOGETHER WITH TOTAL CELL PROTEIN. THERE WERE SOME INTERESTING FINDINGS WHEN CHOLESTEROL WAS EXPRESSED IN µG/MG PROTEIN. THESE CHOLESTEROL INHIBITORS (WITH THE MARKED EXCEPTIONS OF BIBX1382 AND RO48871 AND THE SEQUESTERING AGENT MBCD) DID NOT APPEAR TO HAVE DRAMATIC IMPACT ON MEMBRANE CHOLESTEROL BUT DID REDUCE TOTAL CELL PROTEIN. MBCD DID REDUCE MEMBRANE CHOLESTEROL AS EXPECTED BUT RESULTED IN AN UNEXPECTED UPLIFT IN CYTOPLASMIC CHOLESTEROL. IF TOTAL PROTEIN CONTENT IS AN INDICATOR OF CELL HEALTH, THEN PROADIFEN AND PRAVASTATIN, BM15766 AND BIB515 WERE THE LEAST DETRIMENTAL TREATMENTS, WHILE PROVIDING SIGNIFICANT REDUCTION IN CHOLESTEROL. MBCD AND RO48871 CAUSED THE MOST SERIOUS REDUCTION OF TOTAL PROTEIN.

4 CONCLUSIONS

Proadifen blocks the cholesterol pathway at multiple points (see Figure 107) but the RNA expression assay reveals that at each position on the pathway Proadifen also up-regulates the enzyme involved. Proadifen reduces both cytoplasmic and membrane cholesterol. Treatment of cells with Proadifen reduces the amount of Cav-1 (and, presumably, caveolae *per se*) but this is not a direct result of lowered cholesterol since, unlike statins and MβCD, Proadifen also directly down-regulates mRNA *CAV1* gene expression. Two processes appear to be at work in this system: statins reduce cholesterol by inhibition of the HMG-CoA enzyme and MβCD sequestrates cholesterol into its hydrophobic core and effectively removes the sterol from the membrane as a clathrate-type species. Neither of these treatments caused *CAV1* mRNA production to be down- regulated but both achieved a reduction in Cav-1 expression at the membrane. However, Proadifen did down-regulate *CAV1* mRNA and caused a commensurate reduction in Cav-1 expression in the membrane.

MβCD and LPC both up-regulated cancer pathways while Proadifen and statin down regulated cancer pathways. MβCD did not reduce Cav-1 in the membrane but did reduce the generic raft marker protein, Flotillin (as did LPC treatment). It is tempting to hypothesize that MβCD and LPC cause a similar perturbation in the membrane through physico-chemical effects. These have consequences for the health of the cell but do not

impact the formation of caveolae. The reduction of Cav-1 in the membrane caused by statin must therefore be due solely to the reduction of cholesterol – that is to say, a reduction in the recruitment of Cav-1 to raft inclusions. Proadifen, like Fluphenazine, must act to induce or repress mRNA expression irrespective of their effects on cholesterol and raft/caveolae formation.

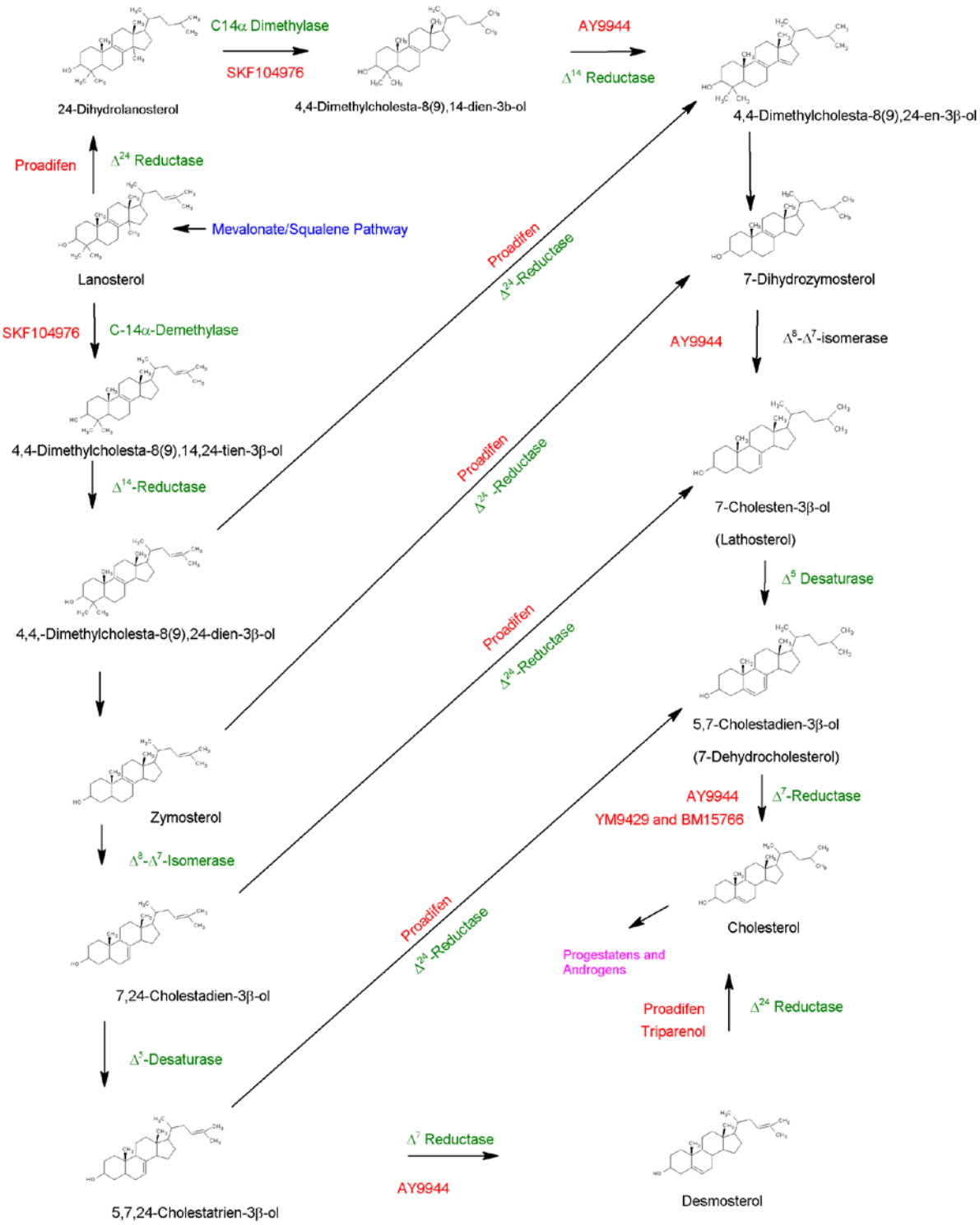

FIGURE 107: CHOLESTEROL BIOSYNTHESIS PATHWAY

Cancer signalling is likely to be affected by a reduction of signal-bearing rafts; for example, Fluphenazine caused an increase in the actual amount of Cav-1 and is also associated with up-regulation of cancer pathways. Fluphenazine does not increase the amount of flotillin detected, suggesting that these cancer-related pathway proteins are indeed caveolae –as opposed to raft – based signals.

It is known that statins can induce apoptosis by down-regulating the expression of Bcl-2 and activation of ErbB2 and this effect is independent of cholesterol inhibition (Herrero-Martin and Lopez-Rivas, 2008). Likewise, an RNA-based theory to explain anti-artherogenic activity of statins through up-regulation of low-density lipoprotein-receptor related protein 1 has been proposed (Moon et al., 2011). The mechanism requires isoprenylation of the relevant proteins, despite a reduced supply of the necessary farnesyl pyrophosphate. However, it is possible that these effects on gene expression may be secondary effects originating from the cells inability to assemble rafts and perform raft-mediated signalling.

Diagram showing the cholesterol synthesis pathway with gene involvement, adapted from Polymeropoulos *et al* (Polymeropoulos et al., 2009)

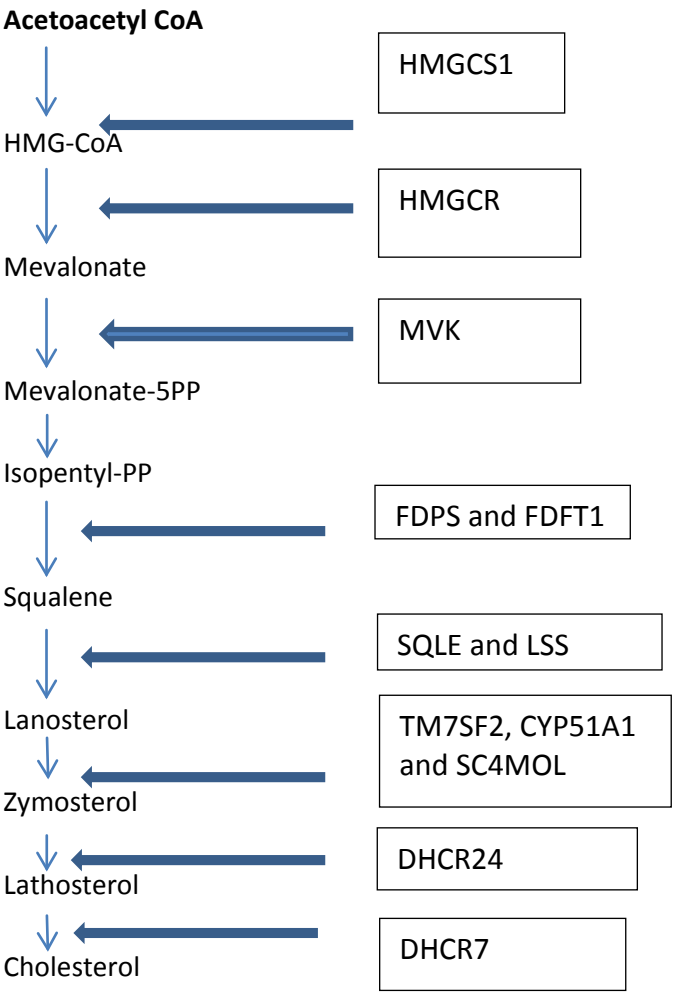

Figure 108: Cholesterol pathway with genes coding for enzymes

4.1.1 Molecular structures and activity

A group of membrane-active phenylvalerate derivatives of the research tool Proadifen were synthesized in this study and, like Proadifen, are likely to impact membrane fluidity (Garnett, 2001). Structurally, they resemble the sphingosine-1-phosphate (S1P) agonists currently being investigated for multiple drug activities, notably multiple sclerosis. Pro-drugs from the S1P agonists family of compounds are believed to control membrane integrity (permeability) by modulating G-protein coupled receptors located on lipid rafts. S1P can rescue endothelial cell membranes from thrombin induced lysis and yet some members of this drug family also demonstrate viral cognate docking inhibition, possibly by raft disruption.

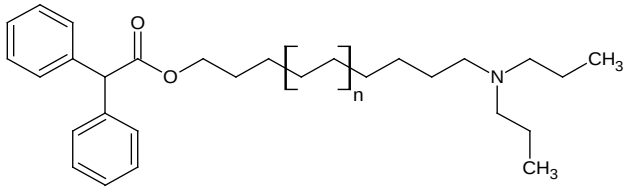

Example of 2-(N,N-diethylamino)ethyl 2,2-diphenylethanoates

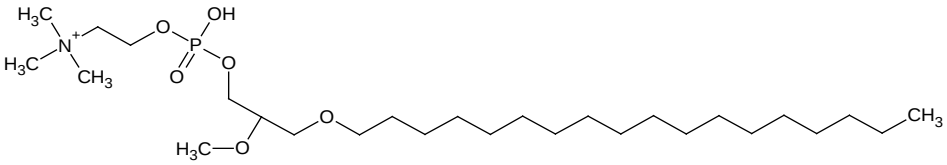

Edelfosine

FIGURE 109: STRUCTURES OF MODEL PROADIFEN TYPE Δ-24 INHIBITOR AND EDELFOSINE

These disparate actions could be related to either their membrane effects on raft formation and stability or perhaps as direct ligands that are involved upstream in raft formation. There is evidence that both may be true and this indicates that molecules possessing short C4-C8 acyl chains can have both membrane stabilizing effects through (for example) S1P receptor activation and subsequent recruitment to lipid rafts; or membrane permeabilizing effects that can lead to cell injury. These actions can have alternate outcomes dependant on the pathological status of the cells for example, S1P can increase permeability and expression of adhesion molecules that stimulate the innate immune response leading to inflammation and or cell death. These findings further suggest that control of raft mediated receptor-ligand binding may have therapeutic relevance.

4.1.2 TRIPARENOL AND OTHER REDUCTASE INHIBITORS

Triparenol, for example, also blocks 24-dehydrocholesterol reductase. It appears to down-regulate the Hegehog (Hh) pathway activation associated with certain cancers and has been shown to reduce tumour cell proliferation both *in vitro* and *in vivo* models. It has been proposed as a new therapeutic (Bi X., 2012) . Pokjak *et al* performed some interesting experiments with Triparenol in rat hepatoma cells using radiolabelled mevalonate to study the conversion process to cholesterol (Popjak et al., 1989). They found that Triparenol completely blocks the synthesis of cholesterol and inhibits the growth of H4 cells even at very low (4.5µM) concentrations. Triparenol acted as an effective Δ-24 reductase inhibitor and also partially prevented the isomerization of the 8(9)-double bond giving rise to an accumulation of the normally trace sterol, zymosterol. They propose that cell growth reduction is due to the presence of zymosterol which may adversely affect membrane integrity.

A decrease in membrane fluidity by the non-steroidal anti-inflammatory (NSAID) drug Licofelone has been shown to both inhibit EGFR signalling and to cause apoptosis in colon cancer cells. The pro-apoptotic effects of Licofelone are independent of the drugs cyclooxygenase and 5-lipoxygenase activity but are associated with changes to the levels of mono and poly-unsaturated lipids in the cell membrane that significantly lower membrane fluidity. It is claimed that the membrane rigidity prevents phosphorylation of EGFR and consequently MAPK and AKT cascades that stimulate oncogenesis and that disruption of these pathways induces apoptosis (Tavolari et al., 2012).

Donatello *et al* have described how methyl β- cyclodextrin can be used to disrupt the association of the raft localised protein CD44 and cause it to co-precipitate with ezrin to induce cell migration. They also report that knock-down of Cav-1 did not increase cell migration (Donatello et al., 2012). No such effects on cell migration were observed in these studies by any of the agents used to disrupt or inhibit rafts, including MβCD.

It is known that in MDA-MB-231 cells Simvastatin is able to prevent phosphorylation of Akt kinase and so reduce cancer cell growth (Ghosh-Choudhury et al., 2010).

4.1.3 STATINS

One study by Brown *et al* demonstrated that Atorvastatin, Mevastatin, Simvastatin and Rosuvastatin all reduced the invasive potential of PC-3 prostate cells. They reported that the drugs treated cell colonies all displayed altered morphology, describing the cells as "more compact" and "containing cells of more epithelial phenotype". This is in agreement with the observations in this study where cells became rounded with fewer cilia and invasapodia. However, they report that Pravastatin had no effect up to 100μM on the ability of the cells to invade bone marrow stroma (Brown M., 2011). Lovostatin has also been shown to reduce the invasiveness of pleural mesothelioma cells (Yamauchi et al., 2011).

4.1.4 FATTY ACIDS AND THE ISOPRENOID PATHWAY

Fatty acid synthase (FASN) over-expression is a common indicator of malignancy. It is thought that this is because rapidly dividing cells have an increased requirement for

fatty acids for the generation of new membranes (Swinnen et al., 2002). It is also true that fatty acids have a generally fluidising effect on the membranes when they are applied to a membrane exogenously so it is tempting to speculate that FASN activation is an early event in the coordination of raft formation: as the preponderance of lipids and phospholipids increases there is a recruitment to local microdomains of cholesterol and sphingolipids, made possible by increasingly fluid conditions. Di Vizio *et al* have concluded that FASN up-regulation is dependent upon the presence of Cav-1 during cancer progression (Di Vizio et al., 2007) – strongly implicating caveolae for such signalling. This could be a valuable model system for the control of caveolae (independently of other rafts) to manipulate mRNA transcription in cancer.

Inhibition by the bisphosphonates of farnesyl pyrophosphate synthase has not attracted much research interest despite the fact that zoledronic acid is a widely prescribed drug (in the treatment of bone conditions). The use of bisphosphonates to inhibit synthesis of farnesyl pyrophosphate and gerenylgeranyl pyrophosphate and so prevent isoprenylation of the GTP-ases such as Ras and prevent it from correctly binding to its site of action may be another clinical possibility to impede metastasis through the mevalonate pathway. It also illustrates the attractiveness of targeting steps in the distal end of the pathway – the bisphosphonates specifically inhibit farnesylpyrophosphate synthase some five (and also six) steps further forwards, when compared to the statins, and they are known to be well tolerated drugs, while 5% of patients using statins suffer from toxic muscle damage (Hamilton-Craig, 2001).

All four of the Ras isoforms are modified by farnesyl isoprenylation to become oncogenically active forms of the protein but this process can be prevented using geranylgeranyl protein transferase inhibitors (GGPTIs) that are able to inhibit tumour growth in mice. However, this treatment also killed the mice (Lobell et al., 2001). However, if Ras isoprenylation can be prevented using cholesterol inhibitors there would be wider scope for doses and reduced mortality. Certainly, farnesyl transferase inhibitors and GGPTIs are currently an exciting group of new drug candidates (Buhaescu and Izzedine, 2007).

Campbell *et al* examined the effects of statins on the growth of breast cancer cells. They found that only the lipophilic statins caused a reduction in the proliferation of the MB-231 cells whereas Pravastatin had little effect on growth (Campbell et al., 2006). This response is supported by the data presented here – at the concentrations used there was no observable reduction in proliferation by Pravastatin but effects on motility were apparent and consistent. It could be that for anti-proliferative action to manifest the drug concentration in the cells must be higher than required to produce more subtle effects on metastatic behaviours. The reported mode of actions for anti-cancer effects of statins *in vitro* are multifold (Sassano and Platanias, 2008). Statins are often described as pleiotropic in nature (Zhou and Liao, 2010) [see also Appendix 1]. Their cancer related effects include prevention of geranylgeranylation (Ras, Rac, Rab and RhoA GTP-ases are all subject to post translational prenylation); inhibition of EGFR; activation of Map kinase pathways; induced nitric oxide synthase (eNOS) and arginase dependent pathways; caspase-9 activation and inhibition of MMP synthesis. However,

Dulak and Jozkowicz point out that some of these studies on the effects of statins on cancer cell growth have used very high concentrations (10μM - 100μM) to observe an effect (Dulak and Jozkowicz, 2005). What is rarely proposed in these studies are mechanistic hypotheses for the effects on a molecular level. Some mevalonate-pathway based interactions are readily understood, not least because raised cholesterol is known to be associated with gastric (Caruso et al., 2002), breast (Kucharska-Newton et al., 2008) and leukaemia (Tatidis et al., 2001) cancers, and cholesterol can increase the aggressiveness of cancers *in vivo* (Goldstein and Brown, 1990). Many others are obscure. However, it is plausible that some are a result of up- and down- regulation of protein expression resulting from the effects of statins on raft-based signal transduction.

4.1.5 THE MEVALONATE PATHWAY

Cholesterol is produced in the cell by the mevalonate pathway but also enters the cell from plasma in the form of low-density lipoprotein. In order to maintain the optimal level of cholesterol production, the cell must balance these two sources and it performs this function through a number of negative feedback systems including down-regulation of transcription of HMG-CoA reductase and squalene synthase (Goldstein and Brown, 1990). This is achieved by the sterol regulatory element (SRE-1) but even when the cell is saturated with sterol, attenuation of the mRNA transcription of the HMG-CoA reductase is incomplete. In this case approximately 12% of the transcription continues the supply of HMG-CoA reductase enzyme. This is because the mevalonate pathway

also feeds pyrophosphate intermediates into the farnesylation pathways regardless of the cells requirement for cholesterol [see also Appendix 2].

4.1.6 RESEARCH OVERVIEW

This research looked at a number of cholesterol inhibitors – including some novel compounds – to see the effects they have on cholesterol synthesis and indirectly on raft related signalling. The involvement of cholesterol in cancer pathogenesis is not straightforward: for example, it has long been known that (*in vitro*) macrophages (Devries-Seimon et al., 2005) and other cells (Lu et al., 2011) become apoptotic when challenged with exogenous cholesterol and yet, recent meta-studies in the USA have revealed a negative correlation between the consumption of cholesterol-lowering drugs (statins) and the incidence of cancer related morbidity and mortality (Dale et al., 2006). These two behaviours of cholesterol appear to be at odds, since most clinical treatments of cancer seek to promote apoptosis. One explanation may be that cholesterol has different attributes dependent upon its location in the cell (or indeed in the body) or even that cholesterol can have multiple roles in cancer dependent on the type of cancer cell, staging of the cancer and environmental co-factors. This notwithstanding, statins themselves have been implicated in advancing apoptosis in breast cancer and other cells by mechanisms independent of cholesterol inhibition (Herrero-Martin and Lopez-Rivas, 2008).

As part of this research, the effects of cholesterol inhibitors on the expression of one particular membrane inclusion protein, caveolin-1, are investigated. An examination is made of the effects of blockades at three different points: HMG-CoA, Δ-7 and Δ-24. These points of inhibition cause HMG-CoA, 7-dehydrocholesterol (and 5,7,24-cholestatrienol) and desmosterol to accumulate respectively. This study shows that

Proadifen is most effective at preventing the formation of caveolae while the statin and AY9944 share with Proadifen an ability to reduce the prevalence of rafts in general. This implies that Cav-1 is not able to intercalate with desmosterol but can coordinate to form caveolae with 7-dehydrocholesterol. In the case of the statin, there is simply reduced feedstock entering the mevalonate pathway and this reduction in membrane cholesterol probably explains the reduction in raft formation seen in this study.

An array of signalling proteins are quantified under different treatments, as is the composition of the membrane. The downstream consequences of perturbation of the signals cannot be fully assessed but an effort is made to correlate signalling inhibition with metastatic potential *in vitro*. The upstream effects on the proteome – that is to say, the way that the signalling protein levels are attributable to the canonical pathways or possibly induction/suppression of protein expression, is tested using mRNA profiling. The global effects on cellular morphology are also recorded by optical and electron microscopy.

The project began with a series of assays to determine the metastatic behaviours of the human breast cancer cell line MDA-MB-231 treated with a variety of agents believed to impact cholesterol, but early experiments based on colonization of cleared areas in the tissue culture plates were unsuccessful. One of the effects of Proadifen is pronounced de-attachment of the cells leading to growth from *within* the cleared patch rather than *into* it from the margins. A number of similar assays were examined but all were vulnerable to this phenomenon. Cell adherence was also measured. One assay, the

phagokinetic track assay wherein the cells are visualised clearing a track through a gold colloid was effective but did not produce unequivocal data with the equipment available. It did however indicate that Proadifen does affect motility. Total cholesterol and membrane cholesterol was measured in the treated cells to check the effects of the agent on the amount and location of cholesterol being produced.

A separate strand of research involved the assay of the cells for Cav-1 protein and this assay was used to test all of the analogues synthesised. There was clearly a need to correlate the expression of this protein to metastatic potential and ultimately this was achieved using a fluorescence based gel-invasion test that combined motility and expression of digestive enzymes by the cancer cells. From these experiments it was clear that Cav-1 expression is correlated to motility and proteolysis. Using a combination of the Cav-1 assay and the gel invasion assay the analogues could be ranked in terms of efficacy.

It was hypothesized that a reduction of cholesterol leads to a reduction of caveolae, and to a lesser extent, a reduction of rafts *per se*. This appears to be true but the experiments indicate an inhibition of Δ-24 reductase is a specific route to this reduction. To better understand the implications of lowered levels of caveolae on the cell and to examine how caveolae are implicated in metastasis, gene expression was measured using whole genome mRNA profiling. This data, coupled with protein array data, provides a comprehensive picture of wide scale changes caused by the cholesterol inhibitors. As an interesting comparison, the lymphoma line BJAB was used in the

protein array experiment as this line is non-adherent and does not spread through the body using the normal metastasis tools of de-attachment, intravasation and re-attachment. BJAB appears to be less sensitive to the inhibitors although any morphological changes caused by the drugs could not be imaged by e.m. because BJAB cell line lives in suspension.

Morphological changes in MDA-MB-231 are evident during exposure to Proadifen and these were imaged using scanning and transmission microscopy. Light microscopy also reveals some differences in the shape of the cells. A number of additional assays were performed to measure changes to the raft marker Flotilin and to several other cancer markers. The data indicates 1.875mM of Proadifen can reduce by half the Flotilin available to the antibody but was not the most *potent* inhibitor of rafts: AY9944 at a dose of 10µM reduced Flotilin by 30%. AY9944 does not however impact Cav-1 availability and has a membrane cholesterol lowering approximating that of Pravastatin at 1.25mM. It is, however, quite toxic.

Cholesterol measurements from both whole cells and cell membrane fractions were taken with a number of treatments. The membrane cholesterol lowering potentials of the statin and Proadifen are similar in magnitude. To check that the effects of Proadifen were not unique to MDA-MB-231 cells, a second cell line (lung cancer, CaLu-1) was used in identical mRNA and gel invasion experiments. The results showed that there were differences in the magnitude of effects but the response between treatments was very similar.

Throughout the experiments, Pravastatin was used as a model hydrophilic type HMG-CoA reductase inhibitor and provides a baseline for the anti-cholesterol effects of other types of cholesterol inhibitor. Statins are reported to be anti-metastatic although their mode of action remains uncertain [see Appendix 2]. Proadifen and its analogues blockade the cholesterol synthetic pathway at the penultimate sterol Desmosterol although they can also inhibit other synthetic steps in the pathway that are reliant on Δ-24 reductases. This is in contrast to the statins that have their effects at the proximal end of the pathway. If the effects on cancer metastasis are to be enhanced without deleterious effects on other cell systems, the specificity of the molecule to the distal (but upstream of the isoprenoid branch) part of the pathway may be a useful development. It is well known that statins cause moderate side effects *in vivo* and the mRNA data indicates profound changes to gene expression resulting from their use. Subsequent alterations to the proteome may contribute to this pathology.

4.1.7 PROADIFEN VERSUS PRAVASTATIN

This research has revealed that unlike statins, Proadifen inhibits cholesterol synthesis through Δ-24 reductase activity and yet increases mRNA expression of Δ-24 reductase as well as all other enzymes involved in the synthesis of cholesterol. The consequent net reduction in membrane cholesterol is concurrent with a decrease in Cav-1 protein but whether this is due to the reduction of sterol in the membrane or to the direct down-regulation of *CAV1* is unknown. Cholesterol synthesis and caveolae formation are linked because Cav-1 requires cholesterol to form its oligomer which determines the shape of the membrane inclusion. Previous research in this field has focussed on the recruitment

of Cav-1 into cholesterol-rich domains that become caveolae. This work has shown that there is a RNA involvement either caused by depletion of cholesterol or cholesterol intermediates or caused by reduction of caveolae with their associated signalling. Inhibition of the HMG-CoA reductase, the Δ-7 reductase and the Δ-24 reductase all caused wholesale shifts in gene expression but while the statin and the Δ-7 reductase had many overlaps the Proadifen caused a very different set of responses. Generally however, the result of Proadifen treatment is lower cholesterol, fewer rafts, lower Cav-1, reduced expression of *CAV1*, and so presumably fewer caveolae.

Proadifen – like the statins – appears to impact the behaviours of cancer cells. In particular, cell-ECM adhesion is dramatically reduced and it is hypothesized that this is due to a reduction in adhesion factors found on membrane structures such as cilia and flagella. The cells studied are normally quite motile but as adhesion is lost, so too is motility. Microscope images of the treated cells confirm that Proadifen causes the cell to lose almost all its peri-membrane structures outside of the bilayer. It seems likely that this is caused by the reduction of cholesterol. Indeed, electron microscopy reveals drastic changes to the surface of the cells and these changes to the external structures could explain the loss of adhesion seen in the adherence assays. Interestingly, R.A Cooper noticed that the contours of erythrocytes grown in cholesterol enriched media became "redundant and folded"[41] whereas the corollary is also true: in this study reduction of cholesterol appears to have a generally smoothing effect on the membranes. Another significant effect of Proadifen treatment is the change to the proteome. Many proteins – including those associated with proliferation, angiogenesis

and apoptosis are simultaneously reduced -and this is also seen at the mRNA level. Other proteins are found in elevated concentrations. It is conceivable that the reduction in cholesterol is the driver for these protein changes since signal transduction may be mediated by cholesterol-rich rafts. It is possible that a homeostatic mechanism involving sequestration of additional signals to the membrane is a response to cholesterol depletion.

The differences observed between the Proadifen and the statin treatments may be due to a specific reduction in caveolae upon exposure to Proadifen. If this is the case then Proadifen may be used to target caveolae signal transduction. Certainly, the mRNA expression profiling data supports the hypothesis that statins are able to reduce rafts *per se* but that an additional action is involved with Proadifen that (also) reduces the prevalence of caveolae. The mechanisms may well be different despite an apparent overlap of activity against cholesterol synthesis. Interestingly, Proadifen was not the only treatment found to down-regulate the expression of *CAV1*: Fluphenazine and LPC also caused a lower expression of this gene. It is unclear if this is due to the sterol intermediates that accumulate as a result of treatment, producing unfavourable environments for raft or caveolae formation. Perhaps cholesterol or its intermediates are involved in a feedback system to *CAV1*. That a reduction of specific types of rafts then causes gene expression to alter is speculative but would account for the differences seen in the data. Generally, the levels of proteins detected tracked the gene expression profile.

Certainly, cancer cells treated with Proadifen behave differently *in vitro,* have a very different signal protein composition and are morphologically distinct. Proadifen and its analogues effectively reduce cholesterol *in vitro* and have measurable impacts on *in vitro* cancer cell behaviour, similar in magnitude to the statins. The site of action of Proadifen is very different to the HMG-CoA reductase inhibitors and this may present both opportunities and problems. Further work in a mouse or rat model would be invaluable to assess if the *in vitro* responses translate to an *in vivo* situation and would also quickly reveal if toxicity is an issue.

4.1.8 FUTURE RESEARCH

The control of cancer metastasis by suppression of caveolae-mediated signalling *in vivo* may be possible but the consequences of using Proadifen or similar enzyme inhibitors to achieve this end may entail significant negative effects on 'innocent' cell systems.

Historical work with Proadifen in the 1970's revealed problematic p450 activity and this contributed to the decision (by Smith, Kline & French Ltd.) to abandon further work with the compound. However, Triparenol – currently a putative drug - suffers from the same issues. Some of the new Proadifen analogues synthesised for this study may offer improved toxicological profiles - by greater specificity in binding to the Δ-24 reductase enzyme - but they do not offer greatly improved anti-cancer characteristics.

Cav-1 knockdown cells (or rodent model) offer a good opportunity to examine the effects of caveolae separate to other signalling platforms and would be a valuable next step for this research. Also, the gene expression profiling in this study produced a very

large data set and this project concentrated on a tiny minority of genes: the data suggests that many metabolic and other systems are impacted by statins and further data mining may yield useful information on the pleiotropic effects of statins. The microplate assay developed to examine proteolysis and motility is crude but has the potential to be a useful experimental protocol if refined since it is applicable to the testing of agents that cause almost immediate de-attachment of cells from the plate and gives unequivocal data on motility that otherwise tends to be subjective. It may be improved by using a better fluorophore ligand or by a single reading at 6 or 12 hours to prevent photobleaching of the gelatin-conjugate substrate.

Many signal transduction systems are found on raft entities and the ability to specifically target caveolae formation may be useful to combat pathologies where caveolae-mediated protein interactions are essential to disease progression. Some non-statin cholesterol inhibitors appear to offer this tantalising prospect. Perhaps the most immediate application could be against cancers where elevated Cav-1 is implicated in pathology and already used as a prognostic marker.

5 REFERENCES

AGARWAL, B., BHENDWAL, S., HALMOS, B., MOSS, S. F., RAMEY, W. G. & HOLT, P. R. 1999. Lovastatin augments apoptosis induced by chemotherapeutic agents in colon cancer cells. *Clin Cancer Res,* 5**,** 2223-9.

AHMED, S. N., BROWN, D. A. & LONDON, E. 1997. On the origin of sphingolipid/cholesterol-rich detergent-insoluble cell membranes: physiological concentrations of cholesterol and sphingolipid induce formation of a detergent-insoluble, liquid-ordered lipid phase in model membranes. *Biochemistry,* 36**,** 10944-53.

ALPHONSE, G., ALOY, M. T., BROQUET, P., GERARD, J. P., LOUISOT, P., ROUSSON, R. & RODRIGUEZ-LAFRASSE, C. 2002. Ceramide induces activation of the mitochondrial/caspases pathway in Jurkat and SCC61 cells sensitive to gamma-radiation but activation of this sequence is defective in radioresistant SQ20B cells. *Int J Radiat Biol,* 78**,** 821-35.

AMUNDSON, D. M. & ZHOU, M. 1999. Fluorometric method for the enzymatic determination of cholesterol. *J Biochem Biophys Methods,* 38**,** 43-52.

ANDELA, V. B., PIRRI, M., SCHWARZ, E. M., PUZAS, E. J., O'KEEFE, R. J., ROSENBLATT, J. D. & ROSIER, R. N. 2003. The mevalonate synthesis pathway as a therapeutic target in cancer. *Clin Orthop Relat Res***,** S59-66.

ANDERS, M. W. & MANNERING, G. J. 1966. Inhibition of drug metabolism. IV. Induction of drug metabolism by 2-diethylaminoethyl 2,2-diphenylvalerate HC1 (SKF 525-A) and 2,4-dichloro-6-phenylphenoxyethylamine HBr (Lilly 18947) and the effect of induction on the inhibitory properties of SKF 525-A type compounds. *Mol Pharmacol,* 2**,** 341-6.

ARELLANO-REYNOSO, B., LAPAQUE, N., SALCEDO, S., BRIONES, G., CIOCCHINI, A. E., UGALDE, R., MORENO, E., MORIYON, I. & GORVEL, J. P. 2005. Cyclic beta-1,2-glucan is a Brucella virulence factor required for intracellular survival. *Nat Immunol,* 6**,** 618-25.

BARBOUR, S., EDIDIN, M., FELDING-HABERMANN, B., TAYLOR-NORTON, J., RADIN, N. S. & FENDERSON, B. A. 1992. Glycolipid depletion using a ceramide analogue (PDMP) alters growth, adhesion, and membrane lipid organization in human A431 cells. *J Cell Physiol,* 150**,** 610-9.

BEN-BASSAT, H., POLLIAK, A., ROSENBAUM, S. M., NAPARSTEK, E., SHOUVAL, D. & INBAR, M. 1977. Fluidity of membrane lipids and lateral mobility of concanavalin A receptors in the cell surface of normal lymphocytes and lymphocytes from patients with malignant lymphomas and leukemias. *Cancer Res,* 37**,** 1307-12.

BERGAMO, A., MASI, A., PEACOCK, A. F., HABTEMARIAM, A., SADLER, P. J. & SAVA, G. 2010. In vivo tumour and metastasis reduction and in vitro effects on invasion

assays of the ruthenium RM175 and osmium AFAP51 organometallics in the mammary cancer model. *J Inorg Biochem,* 104**,** 79-86.

BI X., H. X., ZHANG F., HE M., ZHANG Y., ZHI X-Y., ZHAO H. 2012. Triparenol supresses human tumour growth in vitro and in vivo. *Biochem Biophys Res Comm,* 425**,** 5.

BIELAWSKA, A., GREENBERG, M. S., PERRY, D., JAYADEV, S., SHAYMAN, J. A., MCKAY, C. & HANNUN, Y. A. 1996. (1S,2R)-D-erythro-2-(N-myristoylamino)-1-phenyl-1-propanol as an inhibitor of ceramidase. *J Biol Chem,* 271**,** 12646-54.

BIOSCIENCE, F. M.

BIST, A., FIELDING, P. E. & FIELDING, C. J. 1997. Two sterol regulatory element-like sequences mediate up-regulation of caveolin gene transcription in response to low density lipoprotein free cholesterol. *Proc Natl Acad Sci U S A,* 94**,** 10693-8.

BREMER, E. G., HAKOMORI, S., BOWEN-POPE, D. F., RAINES, E. & ROSS, R. 1984. Ganglioside-mediated modulation of cell growth, growth factor binding, and receptor phosphorylation. *J Biol Chem,* 259**,** 6818-25.

BREMER, E. G., SCHLESSINGER, J. & HAKOMORI, S. 1986. Ganglioside-mediated modulation of cell growth. Specific effects of GM3 on tyrosine phosphorylation of the epidermal growth factor receptor. *J Biol Chem,* 261**,** 2434-40.

BRETSCHER, M. S. 1976. Directed lipid flow in cell membranes. *Nature,* 260**,** 21-3.

BRODIE, B. B., GILLETTE, J. R. & LA DU, B. N. 1958. Enzymatic metabolism of drugs and other foreign compounds. *Annu Rev Biochem,* 27**,** 427-54.

BROWN, D. A. 2006. Lipid rafts, detergent-resistant membranes, and raft targeting signals. *Physiology (Bethesda),* 21**,** 430-9.

BROWN, D. A. & LONDON, E. 2000. Structure and function of sphingolipid- and cholesterol-rich membrane rafts. *J Biol Chem,* 275**,** 17221-4.

BROWN M., H. C., TAWADROS T., CLARKE N. 2011. Statins reduce the risk of prostate cancer progression: an in vitro study in the mechanism of metastasis. *Eur Urology Suppl,* 10**,** 2.

BRUSSELMANS, K., TIMMERMANS, L., VAN DE SANDE, T., VAN VELDHOVEN, P. P., GUAN, G., SHECHTER, I., CLAESSENS, F., VERHOEVEN, G. & SWINNEN, J. V. 2007. Squalene synthase, a determinant of Raft-associated cholesterol and modulator of cancer cell proliferation. *J Biol Chem,* 282**,** 18777-85.

BUEHLER H., B. C., FUCHS I., BANGERMAN N., SCHALLER G. 2001. The up-regulation of cellular adhesion proteins following transfection of the keratin-18 gene into human breast cancer cells is accampanied by a dramatic increase of invasion and metastasis in vitro and in vivo. *Eur J Cancer,* 37.

BUHAESCU, I. & IZZEDINE, H. 2007. Mevalonate pathway: a review of clinical and therapeutical implications. *Clin Biochem,* 40**,** 575-84.

CAI, C., ZHU, H. & CHEN, J. 2004. Overexpression of caveolin-1 increases plasma membrane fluidity and reduces P-glycoprotein function in Hs578T/Dox. *Biochem Biophys Res Commun,* 320**,** 868-74.

CAILLEAU, R., YOUNG, R., OLIVE, M. & REEVES, W. J., JR. 1974. Breast tumor cell lines from pleural effusions. *J Natl Cancer Inst,* 53**,** 661-74.

CAMPBELL, M. J., ESSERMAN, L. J., ZHOU, Y., SHOEMAKER, M., LOBO, M., BORMAN, E., BAEHNER, F., KUMAR, A. S., ADDUCI, K., MARX, C., PETRICOIN, E. F., LIOTTA, L. A., WINTERS, M., BENZ, S. & BENZ, C. C. 2006. Breast cancer growth prevention by statins. *Cancer Res,* 66**,** 8707-14.

CAMPBELL, S., GAUS, K., BITTMAN, R., JESSUP, W., CROWE, S. & MAK, J. 2004. The raft-promoting property of virion-associated cholesterol, but not the presence of virion-associated Brij 98 rafts, is a determinant of human immunodeficiency virus type 1 infectivity. *J Virol,* 78**,** 10556-65.

CARUSO, M. G., NOTARNICOLA, M., CAVALLINI, A. & DI LEO, A. 2002. 3-Hydroxy-3-methylglutaryl coenzyme A reductase activity and low-density lipoprotein receptor expression in diffuse-type and intestinal-type human gastric cancer. *J Gastroenterol,* 37**,** 504-8.

CHAPKIN, R. S., WANG, N., FAN, Y. Y., LUPTON, J. R. & PRIOR, I. A. 2008. Docosahexaenoic acid alters the size and distribution of cell surface microdomains. *Biochim Biophys Acta,* 1778**,** 466-71.

CHIGORNO, V., PALESTINI, P., SCIANNAMBLO, M., DOLO, V., PAVAN, A., TETTAMANTI, G. & SONNINO, S. 2000. Evidence that ganglioside enriched domains are distinct from caveolae in MDCK II and human fibroblast cells in culture. *Eur J Biochem,* 267**,** 4187-97.

COHEN, A. W., HNASKO, R., SCHUBERT, W. & LISANTI, M. P. 2004. Role of caveolae and caveolins in health and disease. *Physiol Rev,* 84**,** 1341-79.

COLLISSON, E. A., KLEER, C., WU, M., DE, A., GAMBHIR, S. S., MERAJVER, S. D. & KOLODNEY, M. S. 2003. Atorvastatin prevents RhoC isoprenylation, invasion, and metastasis in human melanoma cells. *Mol Cancer Ther,* 2**,** 941-8.

COLOMBAIONI, L. & GARCIA-GIL, M. 2004. Sphingolipid metabolites in neural signalling and function. *Brain Res Brain Res Rev,* 46**,** 328-55.

COOK, L., TONER, J. J. & FELLOWS, E. J. 1954. The effect of beta-diethylaminoethyl-diphenylpropylacetate hydrochloride (SKF No. 525-A) on hexobarbital. *J Pharmacol Exp Ther,* 111**,** 131-41.

COOPER, R. A. 1978. Influence of increased membrane cholesterol on membrane fluidity and cell function in human red blood cells. *J Supramol Struct,* 8**,** 413-30.

CUVILLIER, O., NAVA, V. E., MURTHY, S. K., EDSALL, L. C., LEVADE, T., MILSTIEN, S. & SPIEGEL, S. 2001. Sphingosine generation, cytochrome c release, and activation of caspase-7 in doxorubicin-induced apoptosis of MCF7 breast adenocarcinoma cells. *Cell Death Differ,* 8**,** 162-71.

DALE, K. M., COLEMAN, C. I., HENYAN, N. N., KLUGER, J. & WHITE, C. M. 2006. Statins and cancer risk: a meta-analysis. *JAMA,* 295**,** 74-80.

DASGUPTA, S., YANAGISAWA, M., KRISHNAMURTHY, K., LIOUR, S. S. & YU, R. K. 2007. Tumor necrosis factor-alpha up-regulates glucuronosyltransferase gene expression in human brain endothelial cells and promotes T-cell adhesion. *J Neurosci Res,* 85**,** 1086-94.

DE MARIA, R., LENTI, L., MALISAN, F., D'AGOSTINO, F., TOMASSINI, B., ZEUNER, A., RIPPO, M. R. & TESTI, R. 1997. Requirement for GD3 ganglioside in CD95- and ceramide-induced apoptosis. *Science,* 277**,** 1652-5.

DEFEO, D., GONDA, M. A., YOUNG, H. A., CHANG, E. H., LOWY, D. R., SCOLNICK, E. M. & ELLIS, R. W. 1981. Analysis of two divergent rat genomic clones homologous to the transforming gene of Harvey murine sarcoma virus. *Proc Natl Acad Sci U S A,* 78**,** 3328-32.

DEL POZO, M. A., PRICE, L. S., ALDERSON, N. B., REN, X. D. & SCHWARTZ, M. A. 2000. Adhesion to the extracellular matrix regulates the coupling of the small GTPase Rac to its effector PAK. *EMBO J,* 19**,** 2008-14.

DEL POZO, M. A. & SCHWARTZ, M. A. 2007. Rac, membrane heterogeneity, caveolin and regulation of growth by integrins. *Trends Cell Biol,* 17**,** 246-50.

DEMIERRE, M. F., HIGGINS, P. D., GRUBER, S. B., HAWK, E. & LIPPMAN, S. M. 2005. Statins and cancer prevention. *Nat Rev Cancer,* 5**,** 930-42.

DENG W., L. R., GUERRA M., LIU Y., LADISCH S. 2002. Transfection of glucosylceramide synthase antisense inhibits mouse melanoma formation. *Glycobiology,* 12**,** 7.

DENOYELLE, C., VASSE, M., KORNER, M., MISHAL, Z., GANNE, F., VANNIER, J. P., SORIA, J. & SORIA, C. 2001. Cerivastatin, an inhibitor of HMG-CoA reductase, inhibits the signaling pathways involved in the invasiveness and metastatic properties of highly invasive breast cancer cell lines: an in vitro study. *Carcinogenesis,* 22**,** 1139-48.

DEVRIES-SEIMON, T., LI, Y., YAO, P. M., STONE, E., WANG, Y., DAVIS, R. J., FLAVELL, R. & TABAS, I. 2005. Cholesterol-induced macrophage apoptosis requires ER stress pathways and engagement of the type A scavenger receptor. *J Cell Biol,* 171**,** 61-73.

DI BARTOLOMEO, S. & SPINEDI, A. 2001. Differential chemosensitizing effect of two glucosylceramide synthase inhibitors in hepatoma cells. *Biochem Biophys Res Commun,* 288**,** 269-74.

DI VIZIO, D., SOTGIA, F., WILLIAMS, T. M., HASSAN, G. S., CAPOZZA, F., FRANK, P. G., PESTELL, R. G., LODA, M., FREEMAN, M. R. & LISANTI, M. P. 2007. Caveolin-1 is required for the upregulation of fatty acid synthase (FASN), a tumor promoter, during prostate cancer progression. *Cancer Biol Ther,* 6**,** 1263-8.

DONATELLO, S., BABINA, I. S., HAZELWOOD, L. D., HILL, A. D., NABI, I. R. & HOPKINS, A. M. 2012. Lipid raft association restricts CD44-ezrin interaction and promotion of breast cancer cell migration. *Am J Pathol,* 181**,** 2172-87.

DULAK, J. & JOZKOWICZ, A. 2005. Anti-angiogenic and anti-inflammatory effects of statins: relevance to anti-cancer therapy. *Curr Cancer Drug Targets,* 5**,** 579-94.

DUNLAP, J. E., NICHOLS, W. S., HEBEBRAND, L. C., MATHES, L. E. & OLSEN, R. G. 1979. Mobility of lymphocyte surface membrane concanavalin A receptors of normal and feline leukemia virus-infected viremic felines. *Cancer Res,* 39**,** 956-8.

DYKSTRA, M., CHERUKURI, A., SOHN, H. W., TZENG, S. J. & PIERCE, S. K. 2003. Location is everything: lipid rafts and immune cell signaling. *Annu Rev Immunol,* 21**,** 457-81.

ECCLES, S. A. 2001. Basic principles for the study of metastasis using animal models. *Methods Mol Med,* 58**,** 161-71.

EDIDIN, M. 2003. The state of lipid rafts: from model membranes to cells. *Annu Rev Biophys Biomol Struct,* 32**,** 257-83.

EGAN, S. E., MCCLARTY, G. A., JAROLIM, L., WRIGHT, J. A., SPIRO, I., HAGER, G. & GREENBERG, A. H. 1987. Expression of H-ras correlates with metastatic potential: evidence for direct regulation of the metastatic phenotype in 10T1/2 and NIH 3T3 cells. *Mol Cell Biol,* 7**,** 830-7.

ENGLISH, D., BRINDLEY, D. N., SPIEGEL, S. & GARCIA, J. G. 2002. Lipid mediators of angiogenesis and the signalling pathways they initiate. *Biochim Biophys Acta,* 1582**,** 228-39.

FARINA, H. G., BUBLIK, D. R., ALONSO, D. F. & GOMEZ, D. E. 2002. Lovastatin alters cytoskeleton organization and inhibits experimental metastasis of mammary carcinoma cells. *Clin Exp Metastasis,* 19**,** 551-9.

FERNANDEZ, G., VILLARRUEL, M. C. & CASTRO, J. A. 1978. Mechanism of the drug-metabolizing enzymes' induction by 2-diethylaminoethyl-2-2-diphenylvalerate-HCl (SKF 525 A). *Toxicol Appl Pharmacol,* 46**,** 315-21.

FIELDING, C. J., BIST, A. & FIELDING, P. E. 1997. Caveolin mRNA levels are up-regulated by free cholesterol and down-regulated by oxysterols in fibroblast monolayers. *Proc Natl Acad Sci U S A,* 94**,** 3753-8.

FOSTER, L. J., DE HOOG, C. L. & MANN, M. 2003. Unbiased quantitative proteomics of lipid rafts reveals high specificity for signaling factors. *Proc Natl Acad Sci U S A,* 100**,** 5813-8.

FOUTS, J. R. & BRODIE, B. B. 1956. On the mechanism of drug potentiation by iproniazid (2-isopropyl-1-isonicotinyl hydrazine). *J Pharmacol Exp Ther,* 116**,** 480-5.

FUCHS, E. 1882. Das Sarkon des Uvealtrachtus. *Graefe's Archive fur Opthalmologie,* 12**,** 1.

FUTERMAN, A. H. & HANNUN, Y. A. 2004. The complex life of simple sphingolipids. *EMBO Rep,* 5**,** 777-82.

GAJATE, C., GONZALEZ-CAMACHO, F. & MOLLINEDO, F. 2009. Lipid raft connection between extrinsic and intrinsic apoptotic pathways. *Biochem Biophys Res Commun,* 380**,** 780-4.

GAJATE, C. & MOLLINEDO, F. 2005. Cytoskeleton-mediated death receptor and ligand concentration in lipid rafts forms apoptosis-promoting clusters in cancer chemotherapy. *J Biol Chem,* 280**,** 11641-7.

GALEOTTI, T., EBOLI, M. L., PALOMBINI, G., VAN ROSSUM, G. D. & KAPOOR, S. C. 1983. Inhibition of mitochondrial oxidative metabolism by SKF-525A in intact cells and isolated mitochondria. *Biochem Pharmacol,* 32**,** 3285-95.

GARNETT, D. J. 2001. Membrane models as they relate to inducers of fluidity.

GENNIS, R. B. 1989. *Biomembranes: molecular structure and function.,* New York, Springer-Verlag.

GHOSH-CHOUDHURY, N., MANDAL, C. C., GHOSH-CHOUDHURY, N. & GHOSH CHOUDHURY, G. 2010. Simvastatin induces derepression of PTEN expression via NFkappaB to inhibit breast cancer cell growth. *Cell Signal,* 22**,** 749-58.

GLIEMROTH, J., ZULEWSKI, H., ARNOLD, H. & TERZIS, A. J. 2003. Migration, proliferation, and invasion of human glioma cells following treatment with simvastatin. *Neurosurg Rev,* 26**,** 117-24.

GOLDSTEIN, J. L. & BROWN, M. S. 1990. Regulation of the mevalonate pathway. *Nature,* 343**,** 425-30.

GRAAF, M. R., BEIDERBECK, A. B., EGBERTS, A. C., RICHEL, D. J. & GUCHELAAR, H. J. 2004. The risk of cancer in users of statins. *J Clin Oncol,* 22**,** 2388-94.

GREAVES, M. 2000. *Cancer: the evolutionary legacy,* United Kingdom, OUP.

GRIFFONI, C., SPISNI, E., SANTI, S., RICCIO, M., GUARNIERI, T. & TOMASI, V. 2000. Knockdown of caveolin-1 by antisense oligonucleotides impairs angiogenesis in vitro and in vivo. *Biochem Biophys Res Commun,* 276**,** 756-61.

GUAN, J. L. 2004. Cell biology. Integrins, rafts, Rac, and Rho. *Science,* 303**,** 773-4.

HADARI, Y. R., ARBEL-GOREN, R., LEVY, Y., AMSTERDAM, A., ALON, R., ZAKUT, R. & ZICK, Y. 2000. Galectin-8 binding to integrins inhibits cell adhesion and induces apoptosis. *J Cell Sci,* 113 (Pt 13)**,** 2385-97.

HAGER, M. H., SOLOMON, K. R. & FREEMAN, M. R. 2006. The role of cholesterol in prostate cancer. *Curr Opin Clin Nutr Metab Care,* 9**,** 379-85.

HAIMOVITZ-FRIEDMAN, A., KAN, C. C., EHLEITER, D., PERSAUD, R. S., MCLOUGHLIN, M., FUKS, Z. & KOLESNICK, R. N. 1994. Ionizing radiation acts on cellular membranes to generate ceramide and initiate apoptosis. *J Exp Med,* 180**,** 525-35.

HAIT, N. C., OSKERITZIAN, C. A., PAUGH, S. W., MILSTIEN, S. & SPIEGEL, S. 2006. Sphingosine kinases, sphingosine 1-phosphate, apoptosis and diseases. *Biochim Biophys Acta,* 1758**,** 2016-26.

HAMILTON-CRAIG, I. 2001. Statin-associated myopathy. *Med J Aust,* 175**,** 486-9.

HAN M, L. S. M., KIM Y.L., KIM H.L, KIM K., SACKET S.J., JO J.Y., BAE Y.S., OKAJIMA F., IM D.S. 2008. Albumin and anti-oxidants inhibit swerum-deprived cell adhesion in hematopoietic cells. *Biomol Ther,* 16**,** 5.

HANCOCK, J. F. 2006. Lipid rafts: contentious only from simplistic standpoints. *Nat Rev Mol Cell Biol,* 7**,** 456-62.

HARROUN, T. A., KATSARAS, J. & WASSALL, S. R. 2006. Cholesterol hydroxyl group is found to reside in the center of a polyunsaturated lipid membrane. *Biochemistry,* 45**,** 1227-33.

HARROUN, T. A., KATSARAS, J. & WASSALL, S. R. 2008. Cholesterol is found to reside in the center of a polyunsaturated lipid membrane. *Biochemistry,* 47**,** 7090-6.

HEBERLE, F. A., BUBOLTZ, J. T., STRINGER, D. & FEIGENSON, G. W. 2005. Fluorescence methods to detect phase boundaries in lipid bilayer mixtures. *Biochim Biophys Acta,* 1746**,** 186-92.

HEERKLOTZ, H. 2002. Triton promotes domain formation in lipid raft mixtures. *Biophys J,* 83**,** 2693-701.

HEMLER, M. E. 2005. Tetraspanin functions and associated microdomains. *Nat Rev Mol Cell Biol,* 6**,** 801-11.

HENNEMAN, L., VAN CRUCHTEN, A. G., KULIK, W. & WATERHAM, H. R. 2011. Inhibition of the isoprenoid biosynthesis pathway; detection of intermediates by UPLC-MS/MS. *Biochim Biophys Acta,* 1811**,** 227-33.

HERRERO-MARTIN, G. & LOPEZ-RIVAS, A. 2008. Statins activate a mitochondria-operated pathway of apoptosis in breast tumor cells by a mechanism regulated by ErbB2 and dependent on the prenylation of proteins. *FEBS Lett,* 582**,** 2589-94.

HOLMES, W. L. & BENTZ, J. D. 1960. Inhibition of cholesterol biosynthesis in vitro by beta-diethylaminoethyl diphenylpropylacetate hydrochloride (SKF 525-A). *J Biol Chem,* 235**,** 3118-22.

INOKUCHI, J., KABAYAMA, K. 2007. *Comprehensive glycoscience,* Holland, Elsevier.

JACOBSON, K., MOURITSEN, O. G. & ANDERSON, R. G. 2007. Lipid rafts: at a crossroad between cell biology and physics. *Nat Cell Biol,* 9**,** 7-14.

JAYADEV, S., LIU, B., BIELAWSKA, A. E., LEE, J. Y., NAZAIRE, F., PUSHKAREVA, M., OBEID, L. M. & HANNUN, Y. A. 1995. Role for ceramide in cell cycle arrest. *J Biol Chem,* 270**,** 2047-52.

JEMAL, A., BRAY, F., CENTER, M. M., FERLAY, J., WARD, E. & FORMAN, D. 2011. Global cancer statistics. *CA Cancer J Clin,* 61**,** 69-90.

JOSEPH, C. K., BYUN, H. S., BITTMAN, R. & KOLESNICK, R. N. 1993. Substrate recognition by ceramide-activated protein kinase. Evidence that kinase activity is proline-directed. *J Biol Chem,* 268**,** 20002-6.

KENNEALEY P., S. E., DECAROLIS P., GEHA R., SHE Y., SCHWARTZ G., CHEN J.H., SINGER S. 2005. NMR detectable cholesterol is an early marker of tumour response to cytotoxic chemotherapy in colon cancer xenografts. *Surg Oncol,* 201.

KHANZADA U., P. O., MEIER C., DOWNWARD J., SECKL M., ARCARO A. 2005. Potent inhibition of small cell lung cancer cell growth simvastatin reveals selective function of Ras isoforms in growth factor signalling. *Oncogene,* 25**,** 9.

KIM, M. Y., LINARDIC, C., OBEID, L. & HANNUN, Y. 1991. Identification of sphingomyelin turnover as an effector mechanism for the action of tumor necrosis factor alpha and gamma-interferon. Specific role in cell differentiation. *J Biol Chem,* 266**,** 484-9.

KIM, W. H., CHOI, C. H., KANG, S. K., KWON, C. H. & KIM, Y. K. 2005. Ceramide induces non-apoptotic cell death in human glioma cells. *Neurochem Res,* 30**,** 969-79.

KORADE, Z. & KENWORTHY, A. K. 2008. Lipid rafts, cholesterol, and the brain. *Neuropharmacology,* 55**,** 1265-73.

KORB, T., SCHLUTER, K., ENNS, A., SPIEGEL, H. U., SENNINGER, N., NICOLSON, G. L. & HAIER, J. 2004. Integrity of actin fibers and microtubules influences metastatic tumor cell adhesion. *Exp Cell Res,* 299**,** 236-47.

KOROSEC, T., ACIMOVIC, J., SELISKAR, M., KOCJAN, D., TACER, K. F., ROZMAN, D. & URLEB, U. 2008. Novel cholesterol biosynthesis inhibitors targeting human lanosterol 14alpha-demethylase (CYP51). *Bioorg Med Chem,* 16**,** 209-21.

KOTAMRAJU, S., WILLIAMS, C. L. & KALYANARAMAN, B. 2007. Statin-induced breast cancer cell death: role of inducible nitric oxide and arginase-dependent pathways. *Cancer Res,* 67**,** 7386-94.

KOYBASI, S., SENKAL, C. E., SUNDARARAJ, K., SPASSIEVA, S., BIELAWSKI, J., OSTA, W., DAY, T. A., JIANG, J. C., JAZWINSKI, S. M., HANNUN, Y. A., OBEID, L. M. & OGRETMEN, B. 2004. Defects in cell growth regulation by C18:0-ceramide and longevity assurance gene 1 in human head and neck squamous cell carcinomas. *J Biol Chem,* 279**,** 44311-9.

KUCHARSKA-NEWTON, A. M., ROSAMOND, W. D., MINK, P. J., ALBERG, A. J., SHAHAR, E. & FOLSOM, A. R. 2008. HDL-cholesterol and incidence of breast cancer in the ARIC cohort study. *Ann Epidemiol,* 18**,** 671-7.

KUPER, H., BOFFETTA, P. & ADAMI, H. O. 2002. Tobacco use and cancer causation: association by tumour type. *J Intern Med,* 252**,** 206-24.

KUSAMA, T., MUKAI, M., IWASAKI, T., TATSUTA, M., MATSUMOTO, Y., AKEDO, H. & NAKAMURA, H. 2001. Inhibition of epidermal growth factor-induced RhoA translocation and invasion of human pancreatic cancer cells by 3-hydroxy-3-methylglutaryl-coenzyme a reductase inhibitors. *Cancer Res,* 61**,** 4885-91.

KUTZ, S. M., BENTLEY, D. L. & SINCLAIR, N. A. 1985. Improved fixation of cellulose-acetate reverse-osmosis membrane for scanning electron microscopy. *Appl Environ Microbiol,* 49**,** 446-50.

LACOUR, S., HAMMANN, A., GRAZIDE, S., LAGADIC-GOSSMANN, D., ATHIAS, A., SERGENT, O., LAURENT, G., GAMBERT, P., SOLARY, E. & DIMANCHE-BOITREL, M.

T. 2004. Cisplatin-induced CD95 redistribution into membrane lipid rafts of HT29 human colon cancer cells. *Cancer Res,* 64**,** 3593-8.

LANGE, Y. & RAMOS, B. V. 1983. Analysis of the distribution of cholesterol in the intact cell. *J Biol Chem,* 258**,** 15130-4.

LAVIE, Y., CAO, H., VOLNER, A., LUCCI, A., HAN, T. Y., GEFFEN, V., GIULIANO, A. E. & CABOT, M. C. 1997. Agents that reverse multidrug resistance, tamoxifen, verapamil, and cyclosporin A, block glycosphingolipid metabolism by inhibiting ceramide glycosylation in human cancer cells. *J Biol Chem,* 272**,** 1682-7.

LAVIE, Y., FIUCCI, G., CZARNY, M. & LISCOVITCH, M. 1999. Changes in membrane microdomains and caveolae constituents in multidrug-resistant cancer cells. *Lipids,* 34 Suppl**,** S57-63.

LE STUNFF, H., GALVE-ROPERH, I., PETERSON, C., MILSTIEN, S. & SPIEGEL, S. 2002. Sphingosine-1-phosphate phosphohydrolase in regulation of sphingolipid metabolism and apoptosis. *J Cell Biol,* 158**,** 1039-49.

LEE, Y. G., LEE, J. & CHO, J. Y. 2010. Cell-permeable ceramides act as novel regulators of U937 cell-cell adhesion mediated by CD29, CD98, and CD147. *Immunobiology,* 215**,** 294-303.

LI, M., YANG, C., TONG, S., WEIDMANN, A. & COMPANS, R. W. 2002. Palmitoylation of the murine leukemia virus envelope protein is critical for lipid raft association and surface expression. *J Virol,* 76**,** 11845-52.

LI, S., OKAMOTO, T., CHUN, M., SARGIACOMO, M., CASANOVA, J. E., HANSEN, S. H., NISHIMOTO, I. & LISANTI, M. P. 1995. Evidence for a regulated interaction between heterotrimeric G proteins and caveolin. *J Biol Chem,* 270**,** 15693-701.

LI Y., L. Q., WEN Y-Q., CHEN L-I., WANG L-T., LIU Y-I, LUO C-Q., LIANG H-Z., LI M-T., LI Z. 2010. Comparative proteomic analysis of human osteosarcomas and benign tumour of bone. *Cancer Gen Cytogen,* 198**,** 9.

LINDENTHAL, B., BERTSCH, T., FASSBENDER, K., STROICK, M., KUHL, S., LUTJOHANN, D. & VON BERGMANN, K. 2002. Influence of simvastatin, pravastatin, and BM 15.766 on neutral sterols in liver and testis of guinea pigs. *Metabolism,* 51**,** 492-9.

LIOTTA, L. A. 1988. *Oncogene Induction of Metastasis*, Ciba Foundation.

LIU, Y. Y., HAN, T. Y., YU, J. Y., BITTERMAN, A., LE, A., GIULIANO, A. E. & CABOT, M. C. 2004. Oligonucleotides blocking glucosylceramide synthase expression selectively reverse drug resistance in cancer cells. *J Lipid Res,* 45**,** 933-40.

LLAVERIAS, G., DANILO, C., MERCIER, I., DAUMER, K., CAPOZZA, F., WILLIAMS, T. M., SOTGIA, F., LISANTI, M. P. & FRANK, P. G. 2011. Role of cholesterol in the development and progression of breast cancer. *Am J Pathol,* 178**,** 402-12.

LOBELL, R. B., OMER, C. A., ABRAMS, M. T., BHIMNATHWALA, H. G., BRUCKER, M. J., BUSER, C. A., DAVIDE, J. P., DESOLMS, S. J., DINSMORE, C. J., ELLIS-HUTCHINGS, M. S., KRAL, A. M., LIU, D., LUMMA, W. C., MACHOTKA, S. V., RANDS, E., WILLIAMS, T. M., GRAHAM, S. L., HARTMAN, G. D., OLIFF, A. I., HEIMBROOK, D. C. & KOHL, N. E. 2001. Evaluation of farnesyl:protein transferase and geranylgeranyl:protein transferase inhibitor combinations in preclinical models. *Cancer Res,* 61**,** 8758-68.

LU, X., LIU, J., HOU, F., LIU, Z., CAO, X., SEO, H. & GAO, B. 2011. Cholesterol induces pancreatic beta cell apoptosis through oxidative stress pathway. *Cell Stress Chap,* 16**,** 539-48.

MA, D. W., SEO, J., DAVIDSON, L. A., CALLAWAY, E. S., FAN, Y. Y., LUPTON, J. R. & CHAPKIN, R. S. 2004a. n-3 PUFA alter caveolae lipid composition and resident protein localization in mouse colon. *FASEB J,* 18**,** 1040-2.

MA, D. W., SEO, J., SWITZER, K. C., FAN, Y. Y., MCMURRAY, D. N., LUPTON, J. R. & CHAPKIN, R. S. 2004b. n-3 PUFA and membrane microdomains: a new frontier in bioactive lipid research. *J Nutr Biochem,* 15**,** 700-6.

MACDONALD, J. L. & PIKE, L. J. 2005. A simplified method for the preparation of detergent-free lipid rafts. *J Lipid Res,* 46**,** 1061-7.

MALISAN, F. & TESTI, R. 2002. GD3 ganglioside and apoptosis. *Biochim Biophys Acta,* 1585**,** 179-87.

MANDALA, S. M., THORNTON, R., GALVE-ROPERH, I., POULTON, S., PETERSON, C., OLIVERA, A., BERGSTROM, J., KURTZ, M. B. & SPIEGEL, S. 2000. Molecular cloning and characterization of a lipid phosphohydrolase that degrades sphingosine-1-phosphate and induces cell death. *Proc Natl Acad Sci U S A,* 97**,** 7859-64.

MARTINEZ, G. V., DYKSTRA, E. M., LOPE-PIEDRAFITA, S. & BROWN, M. F. 2004. Lanosterol and cholesterol-induced variations in bilayer elasticity probed by 2H NMR relaxation. *Langmuir,* 20**,** 1043-6.

MATHIAS, S., PENA, L. A. & KOLESNICK, R. N. 1998. Signal transduction of stress via ceramide. *Biochem J,* 335 (Pt 3)**,** 465-80.

MCLEAN, G. W., CARRAGHER, N. O., AVIZIENYTE, E., EVANS, J., BRUNTON, V. G. & FRAME, M. C. 2005. The role of focal-adhesion kinase in cancer - a new therapeutic opportunity. *Nat Rev Cancer,* 5**,** 505-15.

MENGUBAS, K., FAHEY, A. A., LEWIN, J., MEHTA, A. B., HOFFBRAND, A. V. & WICKREMASINGHE, R. G. 1999. Killing of T lymphocytes by synthetic ceramide is by a nonapoptotic mechanism and is abrogated following mitogenic activation. *Exp Cell Res,* 249**,** 116-22.

MERRILL, A. H., JR., SCHMELZ, E. M., DILLEHAY, D. L., SPIEGEL, S., SHAYMAN, J. A., SCHROEDER, J. J., RILEY, R. T., VOSS, K. A. & WANG, E. 1997. Sphingolipids--the enigmatic lipid class: biochemistry, physiology, and pathophysiology. *Toxicol Appl Pharmacol,* 142**,** 208-25.

MEUILLET, E. J., MANIA-FARNELL, B., GEORGE, D., INOKUCHI, J. I. & BREMER, E. G. 2000. Modulation of EGF receptor activity by changes in the GM3 content in a human epidermoid carcinoma cell line, A431. *Exp Cell Res,* 256**,** 74-82.

MIALHE, A., LAFANECHERE, L., TREILLEUX, I., PELOUX, N., DUMONTET, C., BREMOND, A., PANH, M. H., PAYAN, R., WEHLAND, J., MARGOLIS, R. L. & JOB, D. 2001. Tubulin detyrosination is a frequent occurrence in breast cancers of poor prognosis. *Cancer Res,* 61**,** 5024-7.

MIRANTI, C. K. 2009. Controlling cell surface dynamics and signaling: how CD82/KAI1 suppresses metastasis. *Cell Signal,* 21**,** 196-211.

MIYAJI, M., JIN, Z. X., YAMAOKA, S., AMAKAWA, R., FUKUHARA, S., SATO, S. B., KOBAYASHI, T., DOMAE, N., MIMORI, T., BLOOM, E. T., OKAZAKI, T. & UMEHARA, H. 2005. Role of membrane sphingomyelin and ceramide in platform formation for Fas-mediated apoptosis. *J Exp Med,* 202**,** 249-59.

MODRAK, D. E., GOLD, D. V. & GOLDENBERG, D. M. 2006. Sphingolipid targets in cancer therapy. *Mol Cancer Ther,* 5**,** 200-8.

MOON, J. H., KANG, S. B., PARK, J. S., LEE, B. W., KANG, E. S., AHN, C. W., LEE, H. C. & CHA, B. S. 2011. Up-regulation of hepatic low-density lipoprotein receptor-related protein 1: a possible novel mechanism of antiatherogenic activity of hydroxymethylglutaryl-coenzyme A reductase inhibitor Atorvastatin and hepatic LRP1 expression. *Metabolism,* 60**,** 930-40.

MOYAD, M. A. & MERRICK, G. S. 2005. Statins and cholesterol lowering after a cancer diagnosis: why not? *Urol Oncol,* 23**,** 49-55.

MUNRO, S. 2003. Lipid rafts: elusive or illusive? *Cell,* 115**,** 377-88.

NA, H. K. & SURH, Y. J. 2008. The antitumor ether lipid edelfosine (ET-18-O-CH3) induces apoptosis in H-ras transformed human breast epithelial cells: by blocking ERK1/2 and p38 mitogen-activated protein kinases as potential targets. *Asia Pac J Clin Nutr,* 17 Suppl 1**,** 204-7.

NICOLSON, G. L. 1987. Tumor cell instability, diversification, and progression to the metastatic phenotype: from oncogene to oncofetal expression. *Cancer Res,* 47**,** 1473-87.

NIINAKA, Y., HAGA, A. & RAZ, A. 2001. Quantification of cell motility : gold colloidal phagokinetic track assay and wound healing assay. *Methods Mol Med,* 58**,** 55-60.

OBEID, L. M., LINARDIC, C. M., KAROLAK, L. A. & HANNUN, Y. A. 1993. Programmed cell death induced by ceramide. *Science,* 259**,** 1769-71.

OGRETMEN, B. & HANNUN, Y. A. 2004. Biologically active sphingolipids in cancer pathogenesis and treatment. *Nat Rev Cancer,* 4**,** 604-16.

OH, H. Y., LEEM, J., YOON, S. J., YOON, S. & HONG, S. J. 2010. Lipid raft cholesterol and genistein inhibit the cell viability of prostate cancer cells via the partial contribution of EGFR-Akt/p70S6k pathway and down-regulation of androgen receptor. *Biochem Biophys Res Commun,* 393**,** 319-24.

OLIVERA, A., KOHAMA, T., EDSALL, L., NAVA, V., CUVILLIER, O., POULTON, S. & SPIEGEL, S. 1999. Sphingosine kinase expression increases intracellular sphingosine-1-phosphate and promotes cell growth and survival. *J Cell Biol,* 147**,** 545-58.

ORSINI, F., CREMONA, A., AROSIO, P., CORSETTO, P. A., MONTORFANO, G., LASCIALFARI, A. & RIZZO, A. M. 2012. Atomic force microscopy imaging of lipid rafts of human breast cancer cells. *Biochim Biophys Acta,* 1818**,** 2943-9.

OSMAK, M. 2012. Statins and cancer: current and future prospects. *Cancer Lett,* 324**,** 1-12.

PAGET, S. 1889. The distribution of secondary growths in cancer of the breast. *Lancet,* 133**,** 3.

PAPADOPOULOS, G., DELAKAS, D., NAKOPOULOU, L. & KASSIMATIS, T. 2011. Statins and prostate cancer: molecular and clinical aspects. *Eur J Cancer,* 47**,** 819-30.

PARK, H. W., SONG, J. Y., KIM, K. S., HAN, Y., KIM, C. W., YI, S. Y. & YUN, Y. S. 2004. Enhancement of radiosensitivity by combined ceramide and dimethylsphingosine treatment in lung cancer cells. *Exp Mol Med,* 36**,** 411-9.

PATRA, S. K. 2008. Dissecting lipid raft facilitated cell signaling pathways in cancer. *Biochim Biophys Acta,* 1785**,** 182-206.

PAWELEK, J. M. & CHAKRABORTY, A. K. 2008. The cancer cell--leukocyte fusion theory of metastasis. *Adv Cancer Res,* 101**,** 397-444.

PCHEJETSKI, D., GOLZIO, M., BONHOURE, E., CALVET, C., DOUMERC, N., GARCIA, V., MAZEROLLES, C., RISCHMANN, P., TEISSIE, J., MALAVAUD, B. & CUVILLIER, O. 2005. Sphingosine kinase-1 as a chemotherapy sensor in prostate adenocarcinoma cell and mouse models. *Cancer Res,* 65**,** 11667-75.

PODAR, K. & ANDERSON, K. C. 2006. Caveolin-1 as a potential new therapeutic target in multiple myeloma. *Cancer Lett,* 233**,** 10-5.

POLLAK, M., BEAMER, W. & ZHANG, J. C. 1998. Insulin-like growth factors and prostate cancer. *Cancer Metastasis Rev,* 17**,** 383-90.

POLYMEROPOULOS, M. H., LICAMELE, L., VOLPI, S., MACK, K., MITKUS, S. N., CARSTEA, E. D., GETOOR, L., THOMPSON, A. & LAVEDAN, C. 2009. Common effect of antipsychotics on the biosynthesis and regulation of fatty acids and cholesterol supports a key role of lipid homeostasis in schizophrenia. *Schizophr Res,* 108**,** 134-42.

POPJAK, G., MEENAN, A., PARISH, E. J. & NES, W. D. 1989. Inhibition of cholesterol synthesis and cell growth by 24(R,S),25-iminolanosterol and triparanol in cultured rat hepatoma cells. *J Biol Chem,* 264**,** 6230-8.

PRALLE, A., KELLER, P., FLORIN, E. L., SIMONS, K. & HORBER, J. K. 2000. Sphingolipid-cholesterol rafts diffuse as small entities in the plasma membrane of mammalian cells. *J Cell Biol,* 148**,** 997-1008.

PRINETTI, A., PRIONI, S., LOBERTO, N., AURELI, M., CHIGORNO, V. & SONNINO, S. 2008. Regulation of tumor phenotypes by caveolin-1 and sphingolipid-controlled membrane signaling complexes. *Biochim Biophys Acta,* 1780**,** 585-96.

PUSHKAREVA, M., OBEID, L. M. & HANNUN, Y. A. 1995. Ceramide: an endogenous regulator of apoptosis and growth suppression. *Immunol Today,* 16**,** 294-7.

RAVID, D., LESER, G. P. & LAMB, R. A. 2010. A role for caveolin 1 in assembly and budding of the paramyxovirus parainfluenza virus 5. *J Virol,* 84**,** 9749-59.

RAVIS, W. R. & FELDMAN, S. 1979. Effect of enzyme-inducing and enzyme-inhibiting agents on drug absorption. II. Influence in proadifen on 3-O-methylglucose transport in rats. *J Pharm Sci,* 68**,** 945-9.

REINMUTH, N., LIU, W., FAN, F., JUNG, Y. D., AHMAD, S. A., STOELTZING, O., BUCANA, C. D., RADINSKY, R. & ELLIS, L. M. 2002. Blockade of insulin-like growth factor I receptor function inhibits growth and angiogenesis of colon cancer. *Clin Cancer Res,* 8**,** 3259-69.

RODAL, S. K., SKRETTING, G., GARRED, O., VILHARDT, F., VAN DEURS, B. & SANDVIG, K. 1999. Extraction of cholesterol with methyl-beta-cyclodextrin perturbs formation of clathrin-coated endocytic vesicles. *Mol Biol Cell,* 10**,** 961-74.

ROTHBERG, K. G., HEUSER, J. E., DONZELL, W. C., YING, Y. S., GLENNEY, J. R. & ANDERSON, R. G. 1992. Caveolin, a protein component of caveolae membrane coats. *Cell,* 68**,** 673-82.

SAMULI OLLILA, O. H., ROG, T., KARTTUNEN, M. & VATTULAINEN, I. 2007. Role of sterol type on lateral pressure profiles of lipid membranes affecting membrane protein functionality: Comparison between cholesterol, desmosterol, 7-dehydrocholesterol and ketosterol. *J Struct Biol,* 159**,** 311-23.

SANCHEZ-WANDELMER, J., DAVALOS, A., HERRERA, E., GIERA, M., CANO, S., DE LA PENA, G., LASUNCION, M. A. & BUSTO, R. 2009. Inhibition of cholesterol

biosynthesis disrupts lipid raft/caveolae and affects insulin receptor activation in 3T3-L1 preadipocytes. *Biochim Biophys Acta,* 1788**,** 1731-9.

SASSANO, A. & PLATANIAS, L. C. 2008. Statins in tumor suppression. *Cancer Lett,* 260**,** 11-9.

SCHLEGEL, A., ARVAN, P. & LISANTI, M. P. 2001. Caveolin-1 binding to endoplasmic reticulum membranes and entry into the regulated secretory pathway are regulated by serine phosphorylation. Protein sorting at the level of the endoplasmic reticulum. *J Biol Chem,* 276**,** 4398-408.

SCHWARTZ, M. A. 1997. Integrins, oncogenes, and anchorage independence. *J Cell Biol,* 139**,** 575-8.

SEBTI, S. M. 2005. Protein farnesylation: implications for normal physiology, malignant transformation, and cancer therapy. *Cancer Cell,* 7**,** 297-300.

SEGUI, B., ANDRIEU-ABADIE, N., JAFFREZOU, J. P., BENOIST, H. & LEVADE, T. 2006. Sphingolipids as modulators of cancer cell death: potential therapeutic targets. *Biochim Biophys Acta,* 1758**,** 2104-20.

SEKINE, Y., FURUYA, Y., NISHII, M., KOIKE, H., MATSUI, H. & SUZUKI, K. 2008. Simvastatin inhibits the proliferation of human prostate cancer PC-3 cells via down-regulation of the insulin-like growth factor 1 receptor. *Biochem Biophys Res Commun,* 372**,** 356-61.

SEO, J., BARHOUMI, R., JOHNSON, A. E., LUPTON, J. R. & CHAPKIN, R. S. 2006. Docosahexaenoic acid selectively inhibits plasma membrane targeting of lipidated proteins. *FASEB J,* 20**,** 770-2.

SHIN, S. I., FREEDMAN, V. H., RISSER, R. & POLLACK, R. 1975. Tumorigenicity of virus-transformed cells in nude mice is correlated specifically with anchorage independent growth in vitro. *Proc Natl Acad Sci U S A,* 72**,** 4435-9.

SIMONS, K. & IKONEN, E. 1997. Functional rafts in cell membranes. *Nature,* 387**,** 569-72.

SIMONS, K. & TOOMRE, D. 2000. Lipid rafts and signal transduction. *Nat Rev Mol Cell Biol,* 1**,** 31-9.

SINGER, S. J. & NICOLSON, G. L. 1972. The fluid mosaic model of the structure of cell membranes. *Science,* 175**,** 720-31.

SIVAPRASAD, U., ABBAS, T. & DUTTA, A. 2006. Differential efficacy of 3-hydroxy-3-methylglutaryl CoA reductase inhibitors on the cell cycle of prostate cancer cells. *Mol Cancer Ther,* 5**,** 2310-6.

SLATON, J. W., INOUE, K., PERROTTE, P., EL-NAGGAR, A. K., SWANSON, D. A., FIDLER, I. J. & DINNEY, C. P. 2001. Expression levels of genes that regulate metastasis and angiogenesis correlate with advanced pathological stage of renal cell carcinoma. *Am J Pathol,* 158**,** 735-43.

SLEEMAN, J. & STEEG, P. S. 2010. Cancer metastasis as a therapeutic target. *Eur J Cancer,* 46**,** 1177-80.

SONNINO, S. & PRINETTI, A. 2009. Sphingolipids and membrane environments for caveolin. *FEBS Lett,* 583**,** 597-606.

SOWA, G., PYPAERT, M. & SESSA, W. C. 2001. Distinction between signaling mechanisms in lipid rafts vs. caveolae. *Proc Natl Acad Sci U S A,* 98**,** 14072-7.

SWENSON E.S., C. W. J. 1992. Means to enhance penetration, (2) Intestinal permeability enhancement for proteins, peptides and other polar drugs: mechanisms and potential toxicity. *Adv Drug Del,* 8**,** 53.

SWINNEN, J. V., ROSKAMS, T., JONIAU, S., VAN POPPEL, H., OYEN, R., BAERT, L., HEYNS, W. & VERHOEVEN, G. 2002. Overexpression of fatty acid synthase is an early and common event in the development of prostate cancer. *Int J Cancer,* 98**,** 19-22.

SWINNEY, D. C., SO, O. Y., WATSON, D. M., BERRY, P. W., WEBB, A. S., KERTESZ, D. J., SHELTON, E. J., BURTON, P. M. & WALKER, K. A. 1994. Selective inhibition of mammalian lanosterol 14 alpha-demethylase by RS-21607 in vitro and in vivo. *Biochemistry,* 33**,** 4702-13.

TAHA, T. A., MULLEN, T. D. & OBEID, L. M. 2006. A house divided: ceramide, sphingosine, and sphingosine-1-phosphate in programmed cell death. *Biochim Biophys Acta,* 1758**,** 2027-36.

TAHIR, S. A., YANG, G., GOLTSOV, A. A., WATANABE, M., TABATA, K., ADDAI, J., FATTAH EL, M. A., KADMON, D. & THOMPSON, T. C. 2008. Tumor cell-secreted caveolin-1 has proangiogenic activities in prostate cancer. *Cancer Res,* 68**,** 731-9.

TAKEICHI, M. 1991. Cadherin cell adhesion receptors as a morphogenetic regulator. *Science,* 251**,** 1451-5.

TATIDIS, L., VITOLS, S., GRUBER, A., PAUL, C. & AXELSON, M. 2001. Cholesterol catabolism in patients with acute myelogenous leukemia and hypocholesterolemia: suppressed levels of a circulating marker for bile acid synthesis. *Cancer Lett,* 170**,** 169-75.

TAVOLARI, S., MUNARINI, A., STORCI, G., LAUFER, S., CHIECO, P. & GUARNIERI, T. 2012. The decrease of cell membrane fluidity by the non-steroidal anti-inflammatory drug Licofelone inhibits epidermal growth factor receptor signalling and triggers apoptosis in HCA-7 colon cancer cells. *Cancer Lett,* 321**,** 187-94.

THON, L., MOHLIG, H., MATHIEU, S., LANGE, A., BULANOVA, E., WINOTO-MORBACH, S., SCHUTZE, S., BULFONE-PAUS, S. & ADAM, D. 2005. Ceramide mediates caspase-independent programmed cell death. *FASEB J,* 19**,** 1945-56.

TOKUYAMA S., M. S., TANIGUCHI S., YASUI A., MIYAZAKI J., ORIKASA S., MIYAGI T. 1997. Supression of pulmonary metastasis in murine B16 melanoma cells by transfection of a sialidase cDNA. *Int J Cancer,* 73**,** 5.

TONOLI, H. & BARRETT, J. C. 2005. CD82 metastasis suppressor gene: a potential target for new therapeutics? *Trends Mol Med,* 11**,** 563-70.

VAINIO, S., JANSEN, M., KOIVUSALO, M., ROG, T., KARTTUNEN, M., VATTULAINEN, I. & IKONEN, E. 2006. Significance of sterol structural specificity. Desmosterol cannot replace cholesterol in lipid rafts. *J Biol Chem,* 281**,** 348-55.

VAN DEURS, B., ROEPSTORFF, K., HOMMELGAARD, A. M. & SANDVIG, K. 2003. Caveolae: anchored, multifunctional platforms in the lipid ocean. *Trends Cell Biol,* 13**,** 92-100.

VANDERKOOI, J., FISCHKOFF, S., CHANCE, B. & COOPER, R. A. 1974. Fluorescent probe analysis of the lipid architecture of natural and experimental cholesterol-rich membranes. *Biochemistry,* 13**,** 1589-95.

VEATCH, S. L. & KELLER, S. L. 2005. Seeing spots: complex phase behavior in simple membranes. *Biochim Biophys Acta,* 1746**,** 172-85.

VELDMAN, R. J., MAESTRE, N., ADUIB, O. M., MEDIN, J. A., SALVAYRE, R. & LEVADE, T. 2001. A neutral sphingomyelinase resides in sphingolipid-enriched microdomains and is inhibited by the caveolin-scaffolding domain: potential implications in tumour necrosis factor signalling. *Biochem J,* 355**,** 859-68.

VIRCHOW, R. 1863. Ueber bewegliche thierische Zellen. *Virchows Arch,* 28**,** 1.

WALKER, K. A., KERTESZ, D. J., ROTSTEIN, D. M., SWINNEY, D. C., BERRY, P. W., SO, O. Y., WEBB, A. S., WATSON, D. M., MAK, A. Y., BURTON, P. M. & ET AL. 1993. Selective inhibition of mammalian lanosterol 14 alpha-demethylase: a possible strategy for cholesterol lowering. *J Med Chem,* 36**,** 2235-7.

WANG, C. Y., LIU, P. Y. & LIAO, J. K. 2008. Pleiotropic effects of statin therapy: molecular mechanisms and clinical results. *Trends Mol Med,* 14**,** 37-44.

WANG, J., MEGHA & LONDON, E. 2004. Relationship between sterol/steroid structure and participation in ordered lipid domains (lipid rafts): implications for lipid raft structure and function. *Biochemistry,* 43**,** 1010-8.

WASSALL, S. R. & STILLWELL, W. 2009. Polyunsaturated fatty acid-cholesterol interactions: domain formation in membranes. *Biochim Biophys Acta,* 1788**,** 24-32.

WATANABE, R., OHYAMA, C., AOKI, H., TAKAHASHI, T., SATOH, M., SAITO, S., HOSHI, S., ISHII, A., SAITO, M. & ARAI, Y. 2002. Ganglioside G(M3) overexpression induces apoptosis and reduces malignant potential in murine bladder cancer. *Cancer Res,* 62**,** 3850-4.

WEBER, L. W., BOLL, M. & STAMPFL, A. 2004. Maintaining cholesterol homeostasis: sterol regulatory element-binding proteins. *World J Gastroenterol,* 10**,** 3081-7.

WECHSLER, A., BRAFMAN, A., SHAFIR, M., HEVERIN, M., GOTTLIEB, H., DAMARI, G., GOZLAN-KELNER, S., SPIVAK, I., MOSHKIN, O., FRIDMAN, E., BECKER, Y., SKALITER, R., EINAT, P., FAERMAN, A., BJORKHEM, I. & FEINSTEIN, E. 2003. Generation of viable cholesterol-free mice. *Science,* 302**,** 2087.

WEINBERG, R. A. 1990. The retinoblastoma gene and cell growth control. *Trends Biochem Sci,* 15**,** 199-202.

WEIS, M., HEESCHEN, C., GLASSFORD, A. J. & COOKE, J. P. 2002. Statins have biphasic effects on angiogenesis. *Circulation,* 105**,** 739-45.

WILLIAMS, T. M. & LISANTI, M. P. 2004. The caveolin proteins. *Genome Biol,* 5**,** 214.

WILLIAMS, T. M. & LISANTI, M. P. 2005. Caveolin-1 in oncogenic transformation, cancer, and metastasis. *Am J Physiol Cell Physiol,* 288**,** C494-506.

WILLIS, R. A. 1952. *The spread of tumours in the human body.,* London, Butterworth & Co.

XIA, Z., TAN, M. M., WONG, W. W., DIMITROULAKOS, J., MINDEN, M. D. & PENN, L. Z. 2001. Blocking protein geranylgeranylation is essential for lovastatin-induced apoptosis of human acute myeloid leukemia cells. *Leukemia,* 15**,** 1398-407.

YAMAUCHI, Y., IZUMI, Y., ASAKURA, K., FUKUTOMI, T., SERIZAWA, A., KAWAI, K., WAKUI, M., SUEMATSU, M. & NOMORI, H. 2011. Lovastatin and valproic acid additively attenuate cell invasion in ACC-MESO-1 cells. *Biochem Biophys Res Commun,* 410**,** 328-32.

YANG, G., TRUONG, L. D., WHEELER, T. M. & THOMPSON, T. C. 1999. Caveolin-1 expression in clinically confined human prostate cancer: a novel prognostic marker. *Cancer Res,* 59**,** 5719-23.

YANG, X., CLAAS, C., KRAEFT, S. K., CHEN, L. B., WANG, Z., KREIDBERG, J. A. & HEMLER, M. E. 2002. Palmitoylation of tetraspanin proteins: modulation of CD151 lateral interactions, subcellular distribution, and integrin-dependent cell morphology. *Mol Biol Cell,* 13**,** 767-81.

YASUI W., K. H., AKAMA Y., KITAHARA K., NAGAFUCHI A., ISHIHARA S., TSUKITA S., TAHARA E. 1991. Expression of E-cadherin, a- b- catenins in human gastric carcinoma: correlation with histology and tumour progression. *Science,* 251**,** 4.

YOO, S. H., PARK, Y. S., KIM, H. R., SUNG, S. W., KIM, J. H., SHIM, Y. S., LEE, S. D., CHOI, Y. L., KIM, M. K. & CHUNG, D. H. 2003. Expression of caveolin-1 is associated with poor prognosis of patients with squamous cell carcinoma of the lung. *Lung Cancer,* 42**,** 195-202.

ZEISIG, R., KOKLIC, T., WIESNER, B., FICHTNER, I. & SENTJURC, M. 2007. Increase in fluidity in the membrane of MT3 breast cancer cells correlates with enhanced cell adhesion in vitro and increased lung metastasis in NOD/SCID mice. *Arch Biochem Biophys,* 459**,** 98-106.

ZENG, G., LI, D. D., GAO, L., BIRKLE, S., BIEBERICH, E., TOKUDA, A. & YU, R. K. 1999. Alteration of ganglioside composition by stable transfection with antisense vectors against GD3-synthase gene expression. *Biochemistry,* 38**,** 8762-9.

ZHOU, Q. & LIAO, J. K. 2010. Pleiotropic effects of statins. - Basic research and clinical perspectives. *Circ J,* 74**,** 818-26.

ZHU, J., LIU, M., KENNEDY, R. H. & LIU, S. J. 2006. TNF-alpha-induced impairment of mitochondrial integrity and apoptosis mediated by caspase-8 in adult ventricular myocytes. *Cytokine,* 34**,** 96-105.

ZHU W., O. M., VENEGAS B. TRAN S., CHONG P. 2009. Role of membrane cholesterol content in the activity of cyclooxygenase-2 (Cox-2) IN mcf-7 HUMAN BREAST CANCER CELLS. *Biophys J,* 96.

ZHUANG, L., KIM, J., ADAM, R. M., SOLOMON, K. R. & FREEMAN, M. R. 2005. Cholesterol targeting alters lipid raft composition and cell survival in prostate cancer cells and xenografts. *J Clin Invest,* 115**,** 959-68.

ZIDOVETZKI, R. & LEVITAN, I. 2007. Use of cyclodextrins to manipulate plasma membrane cholesterol content: evidence, misconceptions and control strategies. *Biochim Biophys Acta,* 1768**,** 1311-24.

APPENDIX 1:

(*Gene Expression*, Vol. 15, pp. 225–234, 2013

1052-2166/13 $90.00 + .00
DOI: http://dx.doi.org/10.3727/105221613X13571653093240
E-ISSN 1555-3884

Statins cause profound effects on gene expression in human cancer cells in vitro: the role of membrane microdomains

David John Garnett and Trevor James Greenhough

Structural Biology Research Group, Institute of Science Technology in Medicine, Keele University, Keele, Staffordshire, ST5 5BG United Kingdom

Telephone: 01782 554718

Fax: 01782 734637

Corresponding author email d.garnett@istm.keele.ac.uk

Abstract

There is increasing evidence that statin treatment can be beneficial in certain cancer patients. To determine if these benefits are a direct result of the cholesterol lowering effects of statins or a result of secondary, protein transcription effects, the impacts of Pravastatin and a cholesterol sequestrating agent methyl–β-cyclodextrin (MβCD) on mRNA expression in the breast cancer cell MDA-MB-231 and the lung carcinoma cell Calu-1 have been compared by microarray techniques. The effects of these agents on cholesterol-rich rafts and caveolae, which have significance in cancer signalling, have also been examined. Both treatments caused a general down-regulation of not only signal transduction including cancer pathway proteins, but also apoptosis and chemokine pathways, with statins impacting 35 genes by 2-fold or greater in MDA-MB-231 and >300 genes in Calu-1. These manifold dysregulations could also explain the various side-effects reportedly caused by statins. MβCD produced far fewer statistical events than Pravastatin in the breast cancer line but many more in the lung cell line. Pravastatin increased expression of CAV1 but caveolae density decreased and overall raft density was unaffected. MβCD also caused an increase in CAV1 expression and reduced the prevalence of both rafts and caveolae. It is proposed that sequestration of cholesterol from the membrane by MβCD is not equivalent to blockade of the cholesterol pathway and causes different effects on microdomain mediated signal transduction dependant on the cell line. The profound effects of statins on mRNA expression can be explained by the failure of caveolin-1 to properly complex with cholesterol in an altered sterol environment, with caveolae acting as the main loci for signalling directed towards those transcription processes unaffected by MβCD. Targeted inhibition of the post-mevalonate pathway could offer an opportunity to specifically reduce

caveolae-based signalling in cancer cells. The observed impact of Pravastatin on gene expression may explain the pleiotropic effects of statins when they are used as adjuvants in chemotherapy and suggests impact on gene expression as a possible cause of side-effects from statin use.

Keywords: cancer, gene expression, pravastatin, rafts, caveolae

Introduction

Statins inhibit the in vivo expression of inflammatory cytokines[1,] C-reactive protein (CRP)[2,3] interleukins, tumour necrosis factor (TNF) and matrix metalloproteins (MMP)[4]. These inflammatory mediators are involved in many different diseases[5] including coronary disease[6], type-2 diabetes[7,8] and Alzheimer's[9]. The possible clinical benefits of statin use outside the normal lipid lowering applications have been reported and these pleiotropic effects have attracted considerable interest[10]. The use of statins to control cancer has also been explored[11,12] with some studies showing beneficial use in prostate cancer recurrence after surgery[13] and radiation therapy[14]; colorectal cancer[15,16] and ovarian cancer[17]. Others, notably cancers in the lung and bladder[18], do not respond[19]. Some researchers have postulated that statin use could even promote tumour growth[20,21] through up-regulation of proteins involved in angiogenesis[22], although the evidence is by no means conclusive.

Several putative models have been proposed for the pro-apoptotic and anti-metastatic effects of statins including the direct down-regulation of specific genes such as survivin in prostate cancer cells[23] and in breast cancer cells, and transcription factor activation of c-Jun, part of the mitogen activated protein kinase group that induce apoptosis and inhibit

growth[24]. In contrast, two mechanisms that are closely linked to the mevalonate pathway inhibited by statins are i) reduction in geranylgeranylpyrophosphate and farnesylpyrophosphate that cause isoprenylation and activation of RhoA, Ras and other pro-oncogenic proteins[25,26] and ii) reduction of caveolin-1 and cholesterol dependent endocytosis leading to non-canonical signalling and tumour development in colon cells[27], presumably through reduction of the complexing of Cav-1 with cholesterol to form caveolae in a reduced cholesterol environment Direct down-regulation of CAV1 expression is another route to fewer caveolae and generally reduced signal transduction. It is possible that more than one mechanism is involved in the manifold effects of statins on cancer progression.

Statins are known to affect gene expression in calcium regulatory (eg SERCA3) and membrane repair systems and this has been postulated as a cause of statin associated peripheral myopathy[28]. These 'extensive' changes in protein turnover have also been found in non-myopathic patients receiving statins[29]. Although the *in vivo* effects of statins on gene expression have been studied in aortic cells[30] and carotid explants[31] there have been few, if any, attempts to measure genome-wide mRNA changes following exposure to statins in human cancer cells despite the plethora of data suggesting involvement by statins in cancer pathways. It is difficult to discriminate between the cholesterol related effects of the statin and other effects the molecule may have on the proteome.

The objective of this study was to investigate the impact on gene expression by microarray based techniques using the ER-negative and p53-mutant human cell line MDA-MB-231 as a model invasive breast cancer and the human lung carcinoma line Calu-1 as an example of an aggressive lung cancer. Much of the epidemiological work linking statin use with reduced morbidity and mortality has alluded to possible anti-metastatic effects. For this reason these

two highly invasive cell lines were tested to examine if genes associated with metastasis were affected. Pravastatin was chosen as a model HMG-CoA reductase inhibitor. To examine if the observed effects on gene expression were caused by a reduction of cholesterol per se, methyl-β-cyclodextrin, a cyclic oligomer of glucose that is able to entrap cholesterol in its hydrophobic core and specifically sequester the sterol from the membrane[32], was used for comparison since it mimics only the ultimate cholesterol lowering effects of the statin.

Rafts and caveolae are morphologically and chemically distinct platforms that rely on high concentrations of cholesterol and, once assembled, serve as platforms for multiple signalling systems. To determine if these cholesterol-rich domains were disrupted by the treatments, flotillin was used as a general indicator of overall raft density and caveolin-1 as a specific marker of caveolae. Both were assayed using immuno-fluorescence techniques.

Experimental.

Materials and Methods

Sources: MDA-MB-231 and Calu-1 cells were obtained from Cell Lines Service, Eppenheim, Germany. Explorer protein microarrays were purchased from Full Moon Biosciences Inc, California. Illumina HumanHT12_V4_0_R2_15002873_B human expression microarray was purchased from Gen-Probe Ltd, UK. RNeasy Maxi Kit was purchased from Qiagen Ltd. All other reagents were sourced from Sigma Aldrich Ltd, UK except where noted.

Treatments: The final concentrations of Pravastatin and MβCD in culture flasks were 8.0μM and 0.00085% (w/v) respectively, dissolved in DMEM plus 10% v/v serum. The dose of

Pravastatin was chosen because low millimolar serum levels are attainable in vivo at high doses of other statins (Lovastatin)[33]. Treatment exposure was for 24 hours beginning after cells reached 80% confluence. The same treatment regime was used in the antibody assays at a range of doses were used

All treatments and controls were conducted in quadruplicate and the microarray was performed using these four biological replicates. There were no technical replicates. Cells were treated in 174ml culture flasks (Nunc) containing 40ml of Dulbeco's DMEM with 10% (v/v) FBS per treatment. Negative control flasks contained only the FBS supplemented media. Treatments were 24 hours and treatment start time was 24 hours after sub-culture. Incubation was at 37oC with 5.0% CO2. Cells from each treatment were harvested with 0.5g/L porcine trypsin w/v and 0.2g/L w/v EDTA in Dulbecco phosphate buffer and immediately spun down to a cell pellet. The cells were then re-suspended in PBS containing 0.1% of Sigma Protease inhibitor cocktail and then re-centrifuged. The resultant cell pellet was then stored in LN2 prior to RNA or protein extraction.

mRNA expression profiling. Array analysis was performed in accordance with the manufacturer's guidance. Each treatment was conducted in quadruplicate and there were no technical replicates in this study.

Protein assay. Treatments and controls were prepared as above. Each Explorer array slide has 656 protein probes in duplicate. Mean spot intensities and coefficient of variations were recorded to provide standard errors.

Immuno-fluorescence Assays. A conjugate of fluorescein isothiocyanate (Ex495 and Em525) and anti-Flotillin antibody was prepared using the Sigma Fluorotag kit and affinity isolated

anti-Flotillin-1 produced in rabbit. The second antibody used in the experiment was anti-Caveolin-1 that was purchased pre-conjugated to the cyanine dye Cy3 (Ex550nm and Em570nm). 1.25ml of phosphate buffer solution was added to 1mg of lyophilised protein and the light-protected tube vortexed for 1 minute. It was used without further preparation. Both antibodies were used at 1µg/ml in 96 x 100µl plates (Sterilin). Readings were taken using a Biochrom 480 fluorescence plate reader after 1 hour exposure post treatment followed by three gentle washes with phosphate buffer pH 7.4.

Statistical Treatment

Raw array data were assessed for quality, and outliers removed. The remaining arrays were normalised and array features annotated. A threshold for significance was adjusted to $p<0.01$ and significant loci in each comparison were assessed for functional enrichment of KEGG pathways, and GO terms, based on their annotation information. p values were adjusted using Benjamini & Hochberg method for multiple testing, to 0.001 for the comparison of significant array features.

Normalisation of the 47,319 features across all arrays was achieved using robust spline normalisation after data were subjected to a variance stabilizing transformation. Raw data were transformed using a variance stabilizing transformation (VST) method prior to normalisation across all arrays using the robust spline normalisation (RSN) method. Expression measures (summarised intensities) are in log base 2.

Probesets on the array may have been annotated as being a member of a KEGG pathway (www.kegg.jp). Significant genes (adjusted $p<0.01$) from each comparison were analysed for enrichment of KEGG pathway membership using a hypergeometric test. Enrichment ($p <$

0.05) was assessed for up-regulated and down-regulated genes separately. Significant genes (adjusted p<0.01) from each comparison were analysed for enrichment of GO terms across all three GO ontologies using a hypergeometric test. Enrichment ($p < 0.001$) was assessed for up-regulated and down-regulated genes separately.

Pravastatin treatment relative to negative control

101 array features were statistically significant at p<0.01; (27 up-regulated, 74 down-regulated). Within the significant features, ANGPTL2, COL5A1, COPS2, DST, FOS, GAS2L1, GPR56, GPRC5C, ID1 and ID2 were up-regulated. Within the significant features, ABCA1, ADM, ANGPTL4, C10orf10, C13orf15, C15orf48, C7orf68, CCL20, CCL26 and CDCP1 were down-regulated.

The predominant (number of p<0.01 features are in parenthesis) up-regulated pathways include those associated with TGF-beta signalling (3), focal adhesion (2) and ECM-receptor interactions (2).

The predominant down-regulated pathways include those associated with cytokine-cytokine receptor interactions (9), chemokine signalling (5), NOD-like receptor signalling (5), cancer (4) and MAPK signalling (3). In terms of observed fold change (independent of statistical threshold), no features exhibited >2-fold up-regulation, while 24 features exhibited >2-fold down-regulation. Fold changes ranged from 2-fold up to 10.4-fold down

20 KEGG pathways were statistically enriched. Members of ECM-receptor interaction pathways were amongst those enriched in up-regulated loci. Members of cytokine-cytokine receptor interaction and NOD-like receptor signalling pathways were amongst those enriched in down-regulated loci. CAV1 was up-regulated by 10%, FLOT1 by 1% and overall gene expression was down-regulated by 0.55% compared to the control group. In Calu-1

cells, 5107 array features were statistically significant (2535 up-regulated, 2572 down-regulated). The predominant up-regulated pathways include metabolic pathways (154), pathways in cancer (37), endocytosis (35), insulin signalling pathway (29), MAPK signalling pathway (28), lysosome (26), cytokine-cytokine receptor interaction (22) The predominant down-regulated pathways include metabolic pathways (126), pathways in cancer (57),

In terms of observed fold change (independent of statistical threshold), 219 features exhibited >2-fold up-regulation, while 174 features exhibited >2-fold down-regulation. Fold changes ranged from 11.1-fold up to 5.1-fold down. Within the biggest change loci, NUPR1, GDF15, TRIB3, RNF165, DDIT3, ASNS, DDIT4, PDE5A, CTH and PCK2 were up-regulated. Within the biggest change loci, TXNIP, MMP3, STC1, CTGF, GLIPR1, NPPB, BMPER, EDN1, MAP2K3 and CYP24A1 were down-regulated. FLOT1 was up-regulated with a log2 fold change of 0.51 (p=0.0024). CAV1 was also up-regulated but this was not statistically significant.

59 KEGG pathways and 408 GO terms were statistically enriched. Members of steroid biosynthesis were enriched in up-regulated loci. Members of spliceosome, cell cycle and DNA replication pathways were amongst those enriched in down-regulated loci.

MβCD treatment relative to negative control

There were 79 statistically significant (3 up-regulated, 76 down-regulated) array features. Within the significant features, MARCH4, NQO1 and SNX6 were up-regulated and ABCA1, ADAM8, ADM, AGR2, ANGPTL4, C10orf10, C13orf15, C15orf48, C7orf68 and CCL20 were down-regulated. The predominant down-regulated pathways include those associated with

cytokine-cytokine receptor interactions (9), cancer (6), chemokine signalling (5), NOD-like receptor signalling (5), MAPK signalling (3), Toll-like receptor signalling (3), Type I diabetes mellitus (3), bladder cancer (3), metabolism(2), Apoptosis (2) and VEGF signalling (2).

In terms of observed fold change (independent of statistical threshold), no features exhibited >2-fold up-regulation, while 13 features exhibited >2-fold down-regulation. Fold changes ranged from 1.6-fold up to 3.2-fold down. Within the biggest change loci, THBS1, AMY1C, FTLP2, NQO1, ID3, FLNC, CAV1, RPL35, SLC7A5 and PSMC1 were up-regulated. Cytokine-cytokine receptor interaction and NOD-like receptor signalling pathways were down-regulated loci. CAV1 was up-regulated by 25% and the entire treatment caused a global increase in gene expression of 8.64% compared to the control group. FLOT1 was not significantly affected (increasing by 1.9%).

In Calu-1 cells, 6868 array features were statistically significant (3417 up-regulated, 3451 down-regulated). The predominant up-regulated pathways include metabolic pathways (173), pathways in cancer (50), endocytosis (39), MAPK signalling pathway (37), insulin signalling pathway (34), lysosome (30), cytokine-cytokine receptor interaction (29). The predominant down-regulated pathways include metabolic pathways (174), pathways in cancer (73), spliceosome (61) and cell cycle (53). In terms of observed fold change (independent of statistical threshold), 393 features exhibited >2-fold up-regulation, while 349 features exhibited >2-fold down-regulation. Fold changes ranged from 16.4-fold up to 8.1-fold down. Within the biggest change loci, GDF15, NUPR1, TRIB3, DDIT3, RNF165, ASNS, PDE5A, CTH, DDIT4 and FBXO32 were up-regulated. Within the biggest change loci, CTGF, STC1, NPPB, BMPER, CYP24A1, GLIPR1, TXNIP, MMP3, EDN1 and MARCH4 were down-regulated. FLOT1 was up-regulated by log2 fold change of 0.56 (p=0.00069) but CAV1 was

not affected. 66 KEGG pathways were statistically enriched. Members of steroid biosynthesis were amongst those enriched in up-regulated loci. Members of spliceosome, cell cycle and DNA replication pathways were amongst those enriched in down-regulated loci.

500 GO terms were statistically enriched with members annotated with intracellular, intracellular part and membrane-bounded organelle GO terms amongst those up-regulated loci. Members annotated with organelle part, intracellular organelle part and organelle GO terms were amongst those enriched in down-regulated loci.

Pravastatin relative to MBCD: There were 27 statistically significant array features (16 up-regulated, 11 down-regulated). Within the significant features, ANGPTL2, GAS2L1, GPR56, GPRC5C, ID1, ID2, IGFBP6, ITGB4, MALL and MXD4 were up-regulated while ABCA1, CRY1, FST, IGFBP3, IL11, LOX, MMP1, PTGER4 and PTGS2 were down-regulated. The predominant up-regulated pathways include TGF-beta signalling (2). The predominant down-regulated pathways include pathways in cancer (2). In terms of observed fold change (independent of statistical threshold), no features exhibited >2-fold up-regulation, while 3 features exhibited >2-fold down-regulation. Fold changes ranged from 1.8-fold up to 3.3-fold down. Six KEGG pathways and 21 gene ontology terms were statistically enriched. Genes annotated with regulation of localization, negative regulation of transport and negative regulation of hormone secretion gene ontology terms were amongst those enriched in down-regulated loci.

In Calu-1, 382 array features were statistically significant (210 up-regulated, 172 down-regulated). The predominant up-regulated pathways include metabolic pathways (8),

cytokine-cytokine receptor interaction (7) and protein processing in endoplasmic reticulum (6). The predominant down-regulated pathways include metabolic pathways (17), cell cycle (8), pathways in cancer (7), DNA replication (6).

23 KEGG pathways were statistically enriched with members of prion diseases, protein processing in endoplasmic reticulum and NA pathways among those up-regulated loci. Members of DNA replication, cell cycle and pancreatic cancer pathways were amongst those enriched in down-regulated loci.

113 GO terms were statistically enriched. Members annotated with cellular response to stress, response to stress and cellular response to stimulus GO terms were amongst those enriched in up-regulated loci. Members annotated with cell division, DNA replication and organelle fission GO terms were amongst those enriched in down-regulated loci.

Discussion.

The response in mRNA expression caused by the two agents suggests some, but not total, commonality in mechanism. The volcano plots of mRNA events in MB231 cells reveal that in the statin treatment the there is a bias towards down-regulation [Figures 1-2]. MβCD versus statin [Figure 3] shows that both treatments cause similar responses, with some additional down-regulations caused by the statin. In Calu-1 cells the response is very different with a symmetrical distribution of statistical events in both treatments [Figures 4-6] and some additional up-regulations caused by the statin. In these two cell lines both the statin and MβCD showed considerable crossover in impact on ABCA1, ADM, ANGPTL4, C10orf10, C13orf15, C15orf48, C7orf68, CCL20 and this suggests a similar mode of action. Significantly, ABCA1 is a cholesterol efflux regulator[34], while C13orf15 and ANGPTL4 control the cell

cycle[35,36,37] and increase tumour growth respectively. A direct DNA suppression of these latter genes by both agents seems unlikely so an indirect cholesterol raft-mediated mechanism is an intriguing possibility. The results suggest that removal of cholesterol by either statin or MβCD causes changes in gene expression unfavourable to cancer development, with both treatments causing cancer pathways specifically to be down-regulated. However, apoptotic pathways are also down-regulated. In MDA-MB-231 cells MβCD produced fewer events at $p<0.001$ (regardless of impact) than pravastatin, with many fewer genes up-regulated. At the doses used in this research MβCD invoked down-regulation of the proteins involved in cholesterol synthesis to a greater extent than pravastatin suggesting that normal lipid homeostasis is secondary to cholesterol-raft based signal transduction directed at the genome. In Calu-1 MβCD had a drastic effect on gene regulation with 742 features exhibiting a fold change of >2. This suggests that Calu-1 is more than 20 times as susceptible to the effects of MβCD as the breast cancer cell line but the genes most affected are up-regulated and are not related to cancer pathways. The global gene events caused by the treatments are given in Table 1. Further analysis of the data set reveals that many of these features are highly significant but have a low fold change value and are therefore unlikely to affect cell health. In MDA-MB231 cells Pravastatin down-regulated 4 cancer pathways and increased CAV1 expression by 10% and FLOT1 by 1% ($p<0.05$). Overall gene expression was reduced by 0.55%. In Calu-1 cells 37 cancer pathways were up-regulated and 57 were down-regulated. MβCD treatment, in contrast, caused 6 cancer pathways in MDA-MB231 cells to be down-regulated and CAV1 expression to be up-regulated by 25%. Overall gene expression in this experiment was increased by 8.64% ($p<0.05$). However, in Calu-1 cells 37 cancer pathways were up-regulated and 57 were down-regulated by statin treatment and mirrored the result of MβCD treatment (50 up-

regulated and 73 down-regulated). When the two treatments in MDA-MB-231 cells are compared [Table 2] 2 genes specifically related to cancer are significantly affected by statin but not MβCD: PTGS2 (Log FC -1.73; p = 6.50E-06) and IL8 (Log FC -1.01; p=0.017). In Calu-1 cells 7 cancer related genes have low p values but the fold-change is minimal. These include IL-6, CCND1 and SMAD3. The data from the MβCD relative to Pravastatin treatments suggests that removing cholesterol from the bilayer is not biologically equivalent to inhibition of the mevalonate pathway.

MDA-MB-231 was analysed for differences in the densities of cholesterol-rich rafts and caveolae following treatment with Pravastatin and MβCD as determined by immuno-fluorescence [Figure 7-8]. The results indicate that both treatments cause a reduction of available Cav-1 at the membrane – despite the observed up-regulation of CAV1, with Pravastatin causing a significantly greater reduction. This difference in response to the treatments was not seen in Flot-1 availability suggesting that Pravastatin causes a specific reduction in caveolae but not rafts per se. Caveolae have unique signalling functionality in cancer that can vary by cell type and stage of disease progression[38] and caveolae require cholesterol for their formation. Pravastatin causes depletion of available sterol to perform this function but also causes significant reduction in membrane Cav-1 (as assayed by immunofluorescence) favouring the formation of rafts rather than caveolae with any available cholesterol. This is despite an up-regulation in CAV1 gene expression. Indeed, rafts containing other sterol intermediates are likely to be viable signalling platforms whereas caveolae may have a specific requirement for cholesterol so that the Cav-1 protein can oligomerize and coordinate with the other lipids correctly. However, the statin is able to significantly reduce membrane Cav-1 at higher doses. Neither treatment caused any change

to the amount of flotillin actually being transcribed by RNA so it seems likely that the changes in membrane flotillin and caveolin are not driven by transcription events but rather they are a down-stream result of the reduction of cholesterol. Statins are known to induce COX-2 gene expression in a manner consistent with farnesyl transferase inhibitors, geranylgeranyltransferase inhibition and impairment of G-protein prenylation[39] but this does not explain the breadth of response at the mRNA level. It has been suggested that statins specifically antagonise a set of genes modulated by L-NAME induced hypertension *in vivo*[40] but the results presented here reveal that 35 genes are modulated >2-fold by pravastatin in breast cancer cells and more than 300 are affected >2-fold in lung cancer cells.

Statins are among the most prescribed pharmaceuticals and have undoubted health benefits not limited to lipid lowering indications. However, membrane repair genes are activated during statin treatment irrespective of clinical myopathy and this could be due to cholesterol deprived membranes becoming more permeable to ion leakage as the bilayer becomes fluidised without sufficient sterol re-enforcement. Calcium leakage is associated with myopathy. It has been reported that 5% of patients using statins suffer from toxic muscle damage[41]. Common side-effects of statin treatment include peripheral myopathy and mood disturbance[42], but multiple others can be expected given the profound alterations that statins cause to both membrane microdomains and gene expression.

While the anti-inflammatory and anti-oncogenic characteristics of some statin treatments are unexpected but welcome it is possible that rebound effects on gene expression following termination of long-term statin use – similar to those seen in inflammatory

response[43] - might result in reduced or reversed biochemical impact in cancer patients benefiting from statin treatment.

The overall effect on cancer of statin treatment may be either deleterious or beneficial depending on the cell type, cancer phenotypes and tissue environment. Cholesterol is, after all, primarily a structural component of the plasma membrane and it seems reasonable to assume that its effects can be measured by the density of those microdomains that are rich in this sterol - be they predominantly cholesterol-lipid or cholesterol-protein in nature. Many of the anti-cancer and anti-inflammatory effects noted by other researchers could be explained by a diminution of either raft or caveolae based canonical pathways leading to mRNA dysregulation or abortive non-canonical signalling.

Conflict of interest.

D. Garnett's work has been funded by Brightwater Research LLP. T. Greenhough declares no potential conflict of interest.

Figures

MDA-MB-231 Volcano Plots

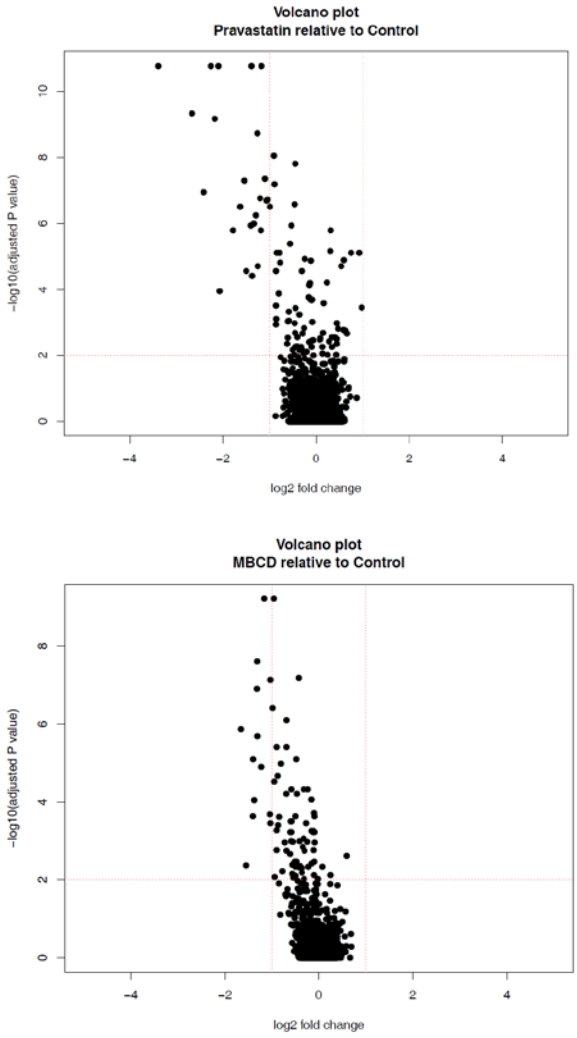

FIGURE 1-2 PRAVASTATIN CAUSES MANY MORE AND GREATER INTENSITY DOWN-REGULATIONS COMPARED TO MBCD. THE DIFFERENT RESPONSE IN TERMS OF GENE EXPRESSION COULD BE A RESULT OF THE TYPE OF MEMBRANE DOMAIN AFFECTED BY THE TWO TREATMENTS

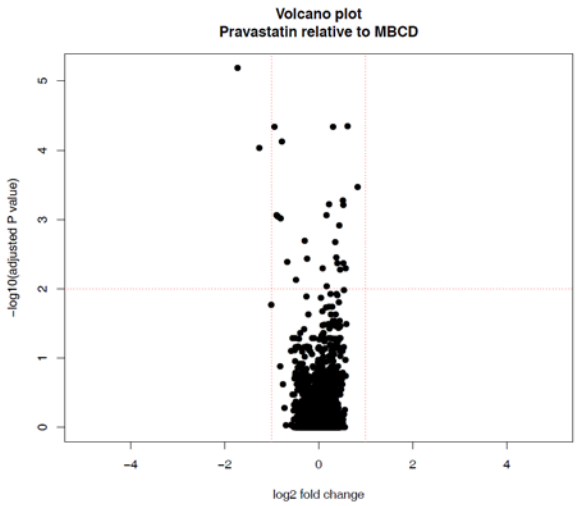

FIGURE 3 VOLCANO PLOT OF PRAVASTATIN RELATIVE TO MBCD. THE TREATMENTS DO NOT HAVE EQUIVALENT EFFECTS ON MRNA EXPRESSION

Calu-1 Volcano Plots

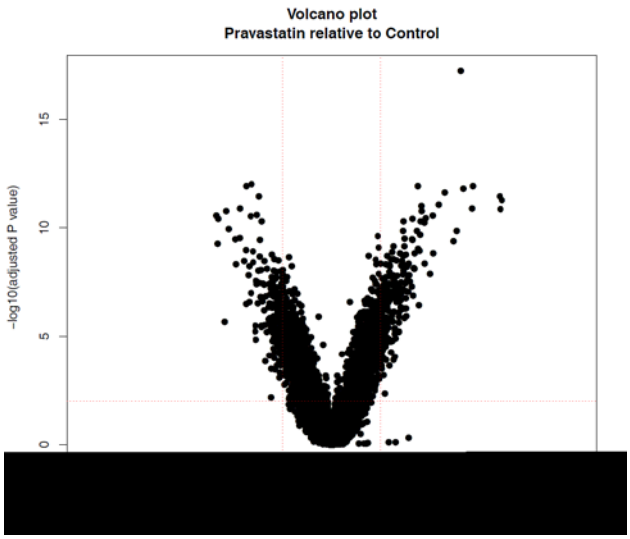

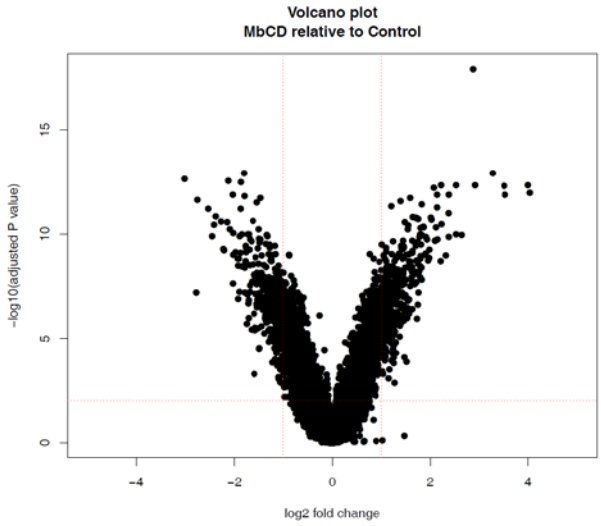

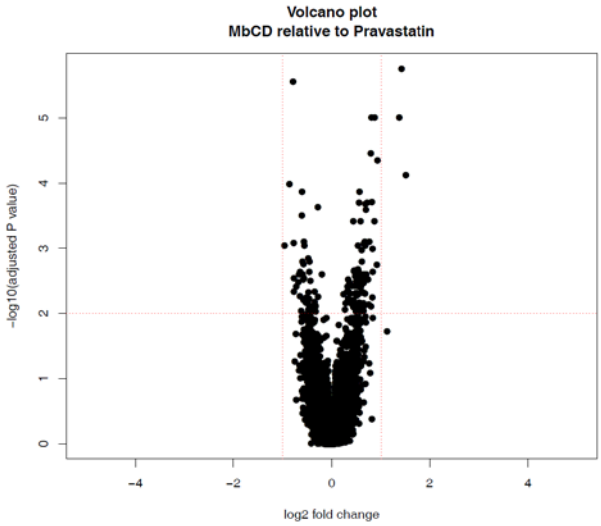

FIGURE 4-6 VOLCANO PLOTS OF FOLD CHANGES AND SIGNIFICANCE IN CALU-1 LUNG CELLS.

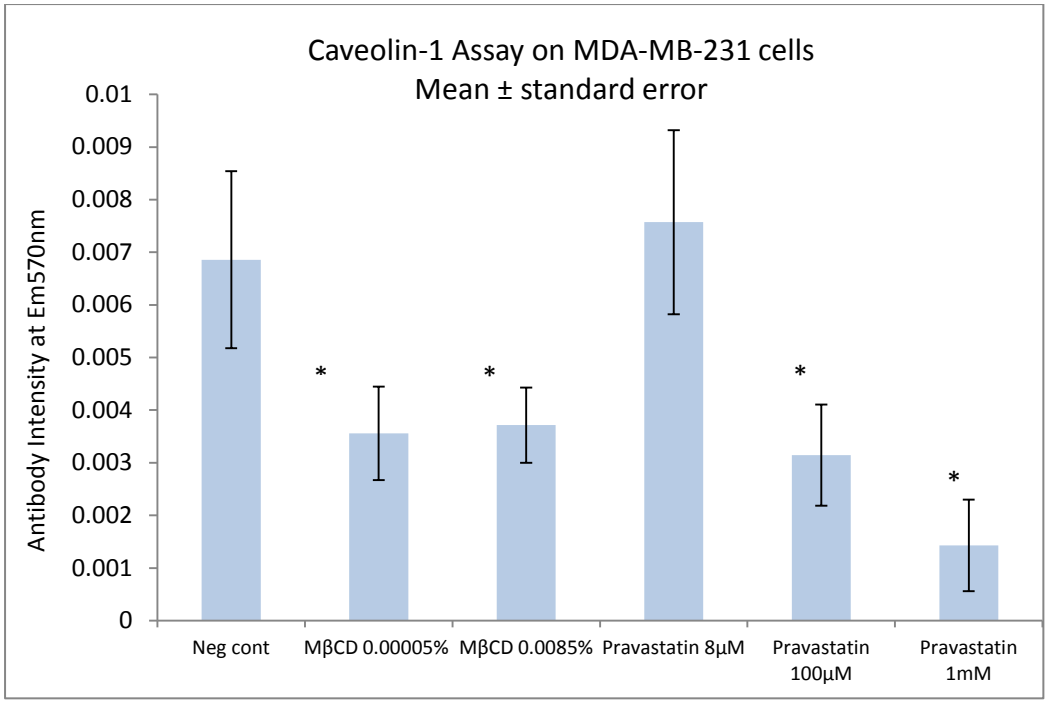

FIGURE 7 THE EFFECTS OF PRAVASTATIN AND MBCD ON CAVEOLIN-1 PROTEIN DETECTION BY IMMUNOFLUORESCENCE ASSAY.

MβCD caused a reduction in Caveolin-1 concentrations at both doses tested. The statin did not reduce cav-1 at 8µM but at much higher concentrations did reduce levels of the protein with a clear dose response. * indicates statistical significant difference $p<0.05$ between treatment and control data by Annova Two-tailed test, n=3.

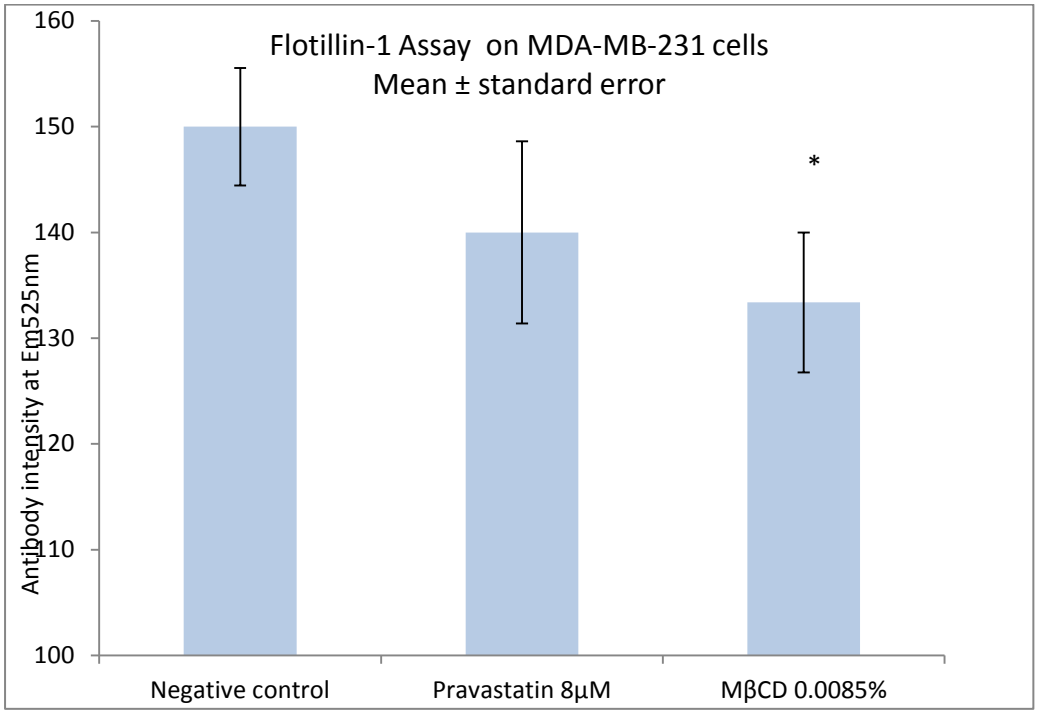

FIGURE 8 THE EFFECT OF PRAVASTATIN AND MBCD ON FLOTILLIN-1 PROTEIN DETECTION BY IMMUNOFLUORESCENCE ASSAY.

Pravastatin did not reduce Flotillin concentrations indicating that statins may not reduce prevalence of cholesterol-rich rafts in MB231. MβCD did reduce raft density. * indicates statistical significant difference $p<0.05$ between treatment and control data by Annova Two-tailed test, n=3.

Tables

Table 1 Changes to array features by treatment with Pravastatin and MβCD

Cell Type	Comparison	Significant array features at p<0.001 (corrected using Benjamini and Hochberg method for multiple testing	Features >2 fold change
MDA-MB-231	Pravastatin relative to Control	101	35
MDA-MB-231	MβCD relative to Control	79	34
MDA-MB-231	Pravastatin relative to MβCD	27	8
Calu-1	Pravastatin relative to Control	2013	393
Calu-1	MβCD relative to Control	3149	742
Calu-1	Pravastatin relative to MβCD	30	4

Table 2 Most significantly affected genes

Treatment	Cell Type	Gene Identifier	Log Fold Change	Adjusted Significance
Pravastatin-Control	MDA-MB-231	PTGS2[1]	-2.10	1.62E-11
MβCD-Control	MDA-MB-231	Lipocalin-2[2]	-0.96	6.19E-10
Pravastatin-MβCD	MDA-MB-231	PTGS2	-1.73	6.50E-06
Pravastatin-Control	Calu-1	ASNS[3]	2.63	5.43E-18
MβCD-Control	Calu-1	ASNS	2.87	1.18E-18
Pravastatin-MβCD	Calu-1	RNU1-5[4]	1.42	1.75E-06

When the 50 genes with the highest fold-change are ranked according to adjusted statistical significance these four genes are most impacted.

[1] Prostaglandin-endoperoxide synthase-2 is a component of the Pathways in Cancer and Small Cell Lung Cancer pathways
[2] Steroid transport protein
[3] Asparagine synthase
[4] snRNA component of the spliceosome

[1] Lyngdoh T, Vollenweider P, Waeber G, Marques-Vidal P.Association of statins with inflammatory cytokines: a population-based Colaus study. Athersclerosis; 219: 253-258;2011

[2] Marz W, Winkler K, Nauck M, Bohm B.O., Winkelmann .R. Effects of statins on C-reactive protein and interleukin-6 (the Ludwigshafen Risk and Cardiovascular health study). Am. J. Cardiol. 92: 305-308; 2003

[3] Voleti B, Agrawal A. Statins and nitric oxide reduce C-reactive protein production while inflammatory conditions persist. Mol. Immunol.;43:891-896; 2006

[4] Bellosta S, Via D, Canavesi M. Pfister P. Fumagalli R. Pauletti R et al. HMG-CoA reductase inhibitors reduce MMP-9 secretion by macrophages.. Arterioscler. Thromb. Vasc. Biol.;18:1671-1678; 1998

[5] Forrester J. S and Libby P.L. The inflammation hypothesis and its potential relevance to statin therapy. American Journal of Cardiology; 99:732-738; 2007

[6] Libby P.L. Inflammation in atherosclerosis. Nature; 420:868-874; 2002

[7] Yamagishi S, Matsui T., Sato T, Takeuchi M. Protective role of pravastatin in the pathogenesis of the metabolic syndrome. Medical Hypotheses; 66: 609-611; 2006

[8] Lang C.H., Dobrescu C., Bagby G.J. Tumour necrosis factor impairs insulin action on peripheral glucose disposal and hepatic glucose output. Endocrinology; 130: 43-52; 1992

[9] Koistinaho M, Koistinaho J. Interactions between Alzheimer's disease and cerebral ischemia – focus on inflammation. Brain Res Rev.;48: 240-250; 2005

[10] Almuti K, Rimawi R, Spevack D. Ostfeld R.J. Effects of statins beyond lipid lowering: potential for clinical benefits. Int. J. Cardio.;109: 7-15; 2006

[11] Dale K.M., Coleman C.I., Henyan N.N., Kluger J. and White C.M. Statins and cancer risk: a meta-analysis. JAMA. 295:74-80; 2006

[12] Kuoppala J, Lamminpaa A, Pukkala E. Statins and cancer: A systematic review and meta-analysis. Eur. J. Cancer. 44:2122-2132; 2008

[13] Mondul A.M., Han M., Humphreys E.B. Association of station use with pathological tumour characteristics and prostate cancer recurrence after surgery. European Urology. 60: 867-871; 2011

[14] Gutt R., Tonlaar N., Kunnavakkam R., Karrison T., Weichselbaum R.R., Liauw S.L. Statin use and risk of prostate cancer recurrence in men treated with radiation therapy. J. Clin. Oncol. 28: 2653-2659; 2010

[15] Bardou M, Barjun A.N., Martel M. Prolonged statin use weakly decreases the risk of colorectal cancer (CRC): a meta-analysis of 21 observational studies totalling more than 1.6 million patients Gastroenterology. 138:S-349-S350; 2010

[16] Katz M.S., Minsky B.D., Saltz L.B., Riedel E., Chessin D.B., Guillem J.G. Association of statin use with a pathologic complete response to neoadjuvant chemoradiation for rectal cancer. Int. J. Radiation Onc. Biol. Phys. 63: 1363-1370; 2005

[17] Elmore R.G., Ioffe Y., Scoles D.R., Karlan B.Y. Li A.J. Impact of statin therapy on survival in epithelial ovarian cancer. Gyn. Onc. 111:102-105; 2008

[18] Tsai H.K., Katz M.S., Coen J.J., Zietman A.L. Kaufman D.S. and Shipley W.U. Association of statin use with local control in patients treated with selective bladder preservation for muscle-invasive bladder cancer. Int. J. Rad. Onc Biol. Phys. 63:2:334; 2005

[19] Cheng M-H, Chiu H-F., Ho S-C and Yang C-Y. Statin use and the risk of female lung cancer: a population-based case-control study. Lung Cancer. doi 10.1016/j.lungcan. 08.014; 2011

[20] Mascitelli L., Pezzetta F., Goldstein M.R. Statin induced angiogenesis and tumour growth. Eur. J. Int. Medicine. 20: 159; 2009

[21] Goldstein M.R., Mascitelli L, Pezzetta F. Might the widespread use of statin drugs explain the increase in prevalence of breast carcinoma in situ? Medical Hypotheses. 74: 613-621; 2010

[22] Garjani A., Rezazadeh H, Maleki-Dizaji N., Barer J, Omidi Y. Mevalonate independent effects of atorvastatin on angiogenesis: relevance to cancer. Bioscience Hypotheses. 1: 67-69; 2008

[23] Koike H, Sekine Y, Furuya Y, Morikawa Y, Matsui H, Shibata Y, Suzuki K. Statin inhibits the proliferation of human prostate cancer cells via down-regulation of the survivin. Eur. Urol. Suppl. 9:273; 2010

[24] Koyuturk M, Ersoz M., Altiok N. Simvastatin induces apoptosis in human breast cancer cells: p53 and estragon receptor independent pathway requiring signalling through JNK. Cancer Lett. 250:220-228; 2007

[25] Ghosh-Choudhury N, Charan Mandal C, Ghosh-Choudhury N, Ghosh-Choudhury G. Simvastatin induces depression of PTEN expression via NFκB to inhibit breast cancer growth. Cellular Signalling. 22:749-758; 2010

[26] Tsubaki M, Yamazoe Y, Yanae M, Satou T, Itoh T, Kaneko J, et al. Blockade of Ras/MEK/ERK and Ras/PI3K/Akt pathways by statins reduces the expression of bFGF, HGF and TGF-β as angiogenic factors in mouse osteosarcoma. Cytokine. 54:100-107; 2011

[27] Jacobs, R., Weil N, Kodach L, Voorneveld P, Wildenberg M, Hommes D, Hardwick J. Statin treatment of colon cancer cells leads to increased cell surface levels of BMP receptors and a shift from non-canonical to canonical BMP signalling Gastroenterology. 140 (1) S; 2011

[28] Mohaupt M, Karas R. Babiychuk E. Sanchez-Freire V. Monastyrskaya K. Lyer L et al. Association between statin-associated myophathy and skeletal muscle damage. CMAJ. 181:E11-E18; 2009

[29] Draeger A, Sanchez-Freire V, Monastyrskaya K, Hoppeler H, Mueller M, Brell F, et al. Statin therapy and the expression of genes that regulate calcium homeostasis and membrane repair in skeletal muscle. Am. J. Path. 177 (1): 291-299; 2010

[30] Liu S-L, Li Yi-H, Shi G-Y, Jiang M-J, Chang J-H and Wu H-L. The effect of statin on the aortic gene expression profiling. Int. J. Cardiol. 114:71-77; 2007

[31] Razuvaev A. Ekstrand J. Folkersen L, Agardh H, Markus D, Swedenborg J, et al. Correlations between clinical variables and gene-expression profiles in carotid plaque instability. Hedin U. Eur. J. Vasc. Endovasc. Surg. 42:722-730; 2011

32 Rodal S. K., Skretting G., Garred O., Vilhart F., van Deurs B. and Sandvig K. Extraction of cholesterol with methyl-β-cyclodextrin perturbs formation of clathrin-coated endocytic vesicles. Mol. Biol. Cell. 10: 961-974; 1999

[33] Thibault A, Samid D, Tompkins A, Figg W, Cooper M, Hohl R et al. Phase I study of lovastatin, an inhibitor of the mevalonate pathway, in patients with cancer. Clin. Cancer Res. 2: 483-491; 1992

[34] Oram JF, Vaughan AM, . ABCA1-mediated transport of cellular cholesterol and phospholipids to HDL apolipoproteins. Curr. Opin. Lipidol. 11 (3): 253–60; 2000

[35] Saigusa K, Imoto I, Tanikawa C, Aoyagi M, Ohno K, Nakamura Y, Inazawa J . RGC32, a novel p53-inducible gene, is located on centrosomes during mitosis and results in G2/M arrest. Oncogene 26 (8): 1110–21; 2007

[36] Huang WY, Li ZG, Rus H, Wang X, Jose PA, Chen SY. RGC-32 mediates transforming growth factor-beta-induced epithelial-mesenchymal transition in human renal proximal tubular cells. J Biol Chem 284 (14): 9426–32; 2009

[37] Kim I, Kim HG, Kim H, Kim HH, Park SK, Uhm CS, Lee ZH, Koh GY. "Hepatic expression, synthesis and secretion of a novel fibrinogen/angiopoietin-related protein that prevents endothelial-cell apoptosis". Biochem J. 346 (3): 603–610; 2000

[38] Burgermeister E, Liscovitch M, Rocken C, Schmid R, Ebert M. Caveats of caveolin-1 in cancer progression. Cancer Lett. 268:187-201; 2008

[39] Chen J-C, Huang K-C, Wingerd B, Wu W-T, Lin W-W. HMG-CoA reductase inhibitors induce COX-2 gene expression in murine macrophages: role of MAPK cascades and promoter elements for CREB and C/EBPβ. Exp. Cell Res. 301:305-319; 2004

[40] Ndaud S, Dupuis M, Brocheriou I, Haloui M, Louedec L, Capron F, Michel J-B, Soubrier F. Counter-regulation by atorvastatin of gene modulations induced by L-NAME hypertension is associated with vascular protection. Vasc. Pharmacol. 51: 253-261; 2009

[41] Thompson P, Clarkson P, Karas R. Statin associated myopathy. JAMA 289: 1681-1690; 2003

[42] While A, Keen L. The effects of statins on mood: a review of the literature. Eur. J. Cardiovasc. Nurs. doi:10.1016/jejcnurse.2010.08.008; 2010

[43] Li J-J, Li Y-S, Chen J, Yang J-Q. Rebound phenomenon of inflammatory response may be a major mechanism responsible for increased cardiovascular events after abrupt cessation of statin therapy. Medical Hypotheses. 66:1199-1204; 2006

APPENDIX 2

Blockade of the mevalonate pathway impacts pluripotency in cancer cells: a key to metastatic quiescence?

David John Garnett and Trevor James Greenhough

Structural Biology Research Group, Institute of Science Technology in Medicine, Keele University, Keele, Staffordshire, ST5 5BG United Kingdom

Running Title: Effects of two cholesterol inhibitors and their differing impacts on gene expression of lung and breast cancer cells, specifically upon stemness and metastatic markers.

Key words: metastasis; pluripotency; gene expression; statins; Pravastatin; Proadifen

Word Count: 5182 (excluding references)

Number of tables: 6

GEO accession number: GSE47463.

Corresponding author email: d.garnett@istm.keele.ac.uk

The authors have no conflicts of interest to disclose.

Abstract

Cancer related morbidity is negatively correlated to the use of statins but the processes underlying this epidemiological observation are poorly understood. Direct anti-neoplastic effects are thought to involve isoprenoid intermediates that permit post-translational modification of the Rho family of GTPases. The role of statins as anti-metastatic agents appears more complex, involving a balance of mesenchymal and epithelial traits.

In breast cancer MB231 and lung adenocarcinoma CaLu-1 treated with either a statin or a Δ-24 oxidoreductase inhibitor we found the statin had the greater effect on mRNA metastatic markers and that lung cancer cells are more vulnerable to this intervention. Overlaps with a hESC marker gene-set revealed that exposure of cells to statins causes changes in gene expression that indicate a partial shift of cellular identity towards mesenchymal status. Wider analysis of the genome revealed that cytoskeleton genes and matrix metalloproteinases, but not growth-related genes, are antagonised by statins. Genes controlling the formation of invadapodia, a characteristic features of motile cancer cells, are down-regulated.

It is hypothesized that chemotaxis local to these protrusions is necessarily diminished. The cellular response to paracrine signals, normally triggering adaptation of the cancer cell to its new environment, is therefore truncated. We conclude that inhibition of the isoprenoid pathway, but not cholesterol *per se*, promotes quiescence of disseminated cancer cells by reducing transduction of extrinsic factors to the nucleus. Thus, farnesyl pyrophosphate (FPP) and geranyl pyrophosphate (GPP) mediate cognition signals that move gene expression in the direction towards pluripotency.

Introduction

The dissemination of solid tumour cell clones often precedes the detection of the primary growth. The metastatic cascade is a multistep process beginning with infiltration through the organ of the primary cancer and into the blood stream[1]. This stage has often occurred prior to treatment (for example, 40% of newly diagnosed patients with non-small lung cancer already have metastases[2]) and it is therefore later steps of the cascade that represent opportunities for useful chemotherapeutic intervention: specifically suppression of existing disseminated cells at a pre-aggressive stage[3]. Typical oncology drugs target replication and promote apoptosis but these are ineffective strategies to kill latent clones and progress has been impeded by a lack of validated predictive biomarkers of metastatic potential[4]. Angiogenesis has been successfully targeted[5] by drugs such as Bevacizumab but newer therapies targeting other phenotypic changes or intrinsic genetic or epigenetic markers are sought to combat metastasis[6]. Statins as incidental inhibitors of isoprenoid pathway have been studied in the context of cell cycle arrest and apoptosis[7] but their putative effects on metastasis per se have not been fully explained.

Paget's 'seed and soil' theory [8] indicates that disseminated cancer cells only fulfil their potential for invasion and proliferation when they are able to adapt to their new environment. It is likely that MET enables the cell to re-acquire the signal processing apparatus that allows cognition of the microenvironment [9] and we hypothesize that MET is restricted by statins. Distal metastases are under stress by their new microenvironment and by any systemic drug regimen - the response being either adaptive[10] or quiescent[11].

Quiescent cells, including micro-metastases, can remain dormant for years yet changes to the microenvironment can then trigger unrestrained proliferation and the re-emergence of disease [12],[13].

EMT (epithelial to mesenchymal transition) can be induced by extrinsic factors such as hepatocyte growth factor, VEGF, platelet derived factor and others [14]. EMT cells are not only motile but also non-senescing and refractory to apoptosis inducing treatments. Van Zijl calls this amoeboid phenotype "the ultimate exit strategy of cancer cells" [15]. A switch into MET is needed for the cell to undergo differentiation into the distal organ identity and lose the plasticity needed for invasion. We propose that only those hESC genes that map to invasion characteristics in MET cells are central to the pathology of metastatic cancer – specifically those genes that mediate response to extrinsic recognition factors. The absence of extracellular matrix (ECM) recognition at this stage can cause the micrometastases to become dormant and that this cognition is inhibited by statins, making their mode of action as antimetastatic agents very useful to study.

Invadapodia and lamellipodia were first observed in MDA-MB-231 cells and these protrusions permit motility and are primary sites of proteolysis[16,17]. They are the structures that allow the cell to sense its environment by chemotaxis[18]. Bravo-Cordero *et al* have described how the micro-environment directs the nature of motility behaviour[19]. This being the case, it is reasonable to suppose that inhibition of the formation of invadapodia will likewise prevent the transduction of extrinsic factors that would normally permit successful MET.

B-catenin, N-cadherin and vimentin are regarded as mesenchymal signature marker proteins contributing to the formation of lamellopodia and increased motility. However, EMT and MET are likely to be characterised by wide scale changes of protein production and require full genomic analysis to measure qualitatively. For this reason, while some cancer markers, cytoskeleton and invadapodia markers and some of the enzymes involved in the mevalonate pathway are extracted for detailed analysis, perhaps more meaningful is the overlap of data of statin-treated groups with a hESC identity and the move of the treated groups towards a quasi-mesenchymal genetic status.

Materials and Methods

Sources: MDA-MB-231 and CaLu-1 cells were obtained from Cell Lines Service, Eppenheim, Germany. Illumina HumanHT12_V4_0_R2_15002873_B human expression microarrays were purchased from Gen-Probe Ltd, UK. RNeasy Maxi Kit was purchased from Qiagen Ltd. All other reagents were sourced from Sigma Aldrich Ltd, UK except where noted.

Treatments: The final concentrations of Pravastatin and Proadifen (N,N-diethylaminoethyl 2, 2-diphenylethanoate hydrochloride) in culture flasks were 8.0µM and 0.00085% (w/v) respectively, dissolved in DMEM plus 10% v/v serum. Pravastatin, a lipophilic statin has previously been shown to have pro-apoptotic properties that are dependent upon inhibition of HM-CoA reductase[20]. The dose of Pravastatin was chosen because low millimolar serum levels are attainable *in vivo* at high doses of other statins (Lovastatin)[21]. Treatment exposure was for 24 hours beginning after cells reached 80% confluence.

Gene Expression Assay

All treatments and controls were conducted in quadruplicate and the microarray was performed using these biological replicates. There were no technical replicates except where noted. Cells were treated in 174ml culture flasks (Nunc) containing the agent dissolved in 40ml of Dulbeco's DMEM with 10% (v/v) FBS per treatment. Negative control flasks contained only the FBS supplemented media. Treatments were 24 hours and treatment start time was 24 hours after sub-culture. Incubation was at 37^{o}C with 5.0% CO_2. Cells from each treatment were harvested with 0.5g/L porcine trypsin w/v and 0.2g/L w/v EDTA in Dulbecco phosphate buffer and immediately spun down to a cell pellet. The cells were then re-suspended in PBS containing 0.1% of Sigma Protease inhibitor cocktail and

then re-centrifuged. The resultant cell pellet was then stored in LN_2 prior to RNA extraction. Array analysis was performed in accordance with the manufacturer's guidance.

Statistical Treatment

Raw array data were assessed for quality, and outliers removed. 47,319 features were transformed using a variance stabilizing transformation (VST) method prior to normalisation across all arrays using the robust spline normalisation (RSN) method. *p* values were adjusted, using Benjamini & Hochberg method for multiple testing, to 0.001 for the comparison of significant array features. Expression measures (summarised intensities) are in log base 2. Assou *et a* [22] published a meta-analysis of stem cells that provided a core set of pluripotency markers. These up and down regulated genes map to 91 and 55 probes on the Illumina HT-12 microarray respectively. This set of 146 markers was contrasted with the drug induced genes in both the treated and control MDA-MB-231 and CaLu-1 experiments. To assess convergence with hESC data the experimental and public datasets were merged (see table 1) and 79 probes that overlapped all groups were retained. An adjusted *p* value threshold was set to <0.05 and then further reduced to the largest 15 up- and down logFC measurements.

Results

Tables 2 and 3 show the 15 most significant values of the convergence sets of hESC gene expression and the two treatments in both cell lines. These have been further re-ordered by log 2 fold change (logFC) data so that the magnitude and the directionality of the changes can be seen. The table shows that the largest effects within these top 15 results have mainly the same directionality as the hESCs and favour EMT. Both treatments caused some markers associated with EMT to be up-regulated with growth factors the most significant group of convergent and up-regulated genes that are affected by the treatments. The top 15 affected genes (by p value) in the statin treatment include 5 genes appearing in both cell lines but Proadifen treatments had no common genes between the two lines.

Table 4 shows that Proadifen (but not Pravastatin) causes a significant up-regulation of the enzymes in the mevalonate pathway in MDA-MB-231. This suggests a feedback loop from the cholesterol pathway to the mevalonate pathway under mRNA control. Both treatments have less impact on mevalonate intermediates in CaLu-1 line in this analysis despite this cell type being more responsive to the treatments overall. Both Proadifen and Pravastatin caused a rise in the level of FDFT1` in CaLu-1.

Table 5 compares the effects of the treatment and cell type on four classic metastasis markers, each of which has an impact on the formation and behaviour of invadapodia. Here, Pravastatin down-regulates the cancer promoters PLAUR/CD87 by a small amount (LogFC -0.089) in MDA-MB-231 but increases the expression of promoter S100A by logFC 0.54. However, this table reveals an asymmetry between the cell types with the statin causing down-regulation of the cancer suppressor NDRG1 in MDA-MB-231 (LogFC -1.4) and (LogFC +0.96) in CaLu-1. Proadifen had a negligible effect

on the expression of both NDRG1 and CDH1. In MDA-MB-231 cells Proadifen effects were all down-regulatory while in CaLu-1 they were all positive.

Table 6 highlights only those genes most active at the membrane of the invadapodia: matrix metalloproteinases (MMPs 1,2, 3,7, 24 and 28) and Rho associated mediators of cytoskeleton rearrangement: Ena VASP[23], ROCK and its regulator PDK1[24], Rac[25] and RhoC[26] .

Only those genes with significant up/down regulation are shown. This analysis shows that on this gene subset, Pravastatin on CaLu-1 cells has the most consistent effects, notably down-regulating CDC42, MMP1, MMP3 and RhoC but surprisingly, up-regulating EGFR. Across both cell lines there are six genes ($p<0.05$) that have opposite directionality following exposure to Proadifen and Pravastatin: of these, ANGPLTL2, a paracrine signal and member of VEGF family is up-regulated by the statin (0.16 in MDA-MB-231 and 0.19 in CaLu-1) and down-regulated by Proadifen (-0.057 and -0.29 respectively). ID1, a transcription factor restricting gene expression is affected in the same way (up-regulated by the statin + 0.98 and +0.67 and down-regulated by Proadifen -0.44 and -2.3 in MDA-MB-231 and CaLu-1 respectively).

Discussion and Conclusions

Much research effort has been focussed on the reduction of cancer related morbidity and mortality in long term statin users and we have previously reported that gene expression of cells treated with statins *in vitro* is profoundly altered[27]. The mevalonate pathway intermediates geranylgeranyl pyrophosphate (GGPP) and farnesylpyrophosphate (FPP) are responsible for the isoprenylation of numerous GTP-ase signal proteins. Here, we present evidence that these post-translational modifications may condition mRNA transcription and reduce phenotypes associated with invadapodia, invasion and motility. Certainly statins appear to reduce these behaviours *in vitro* particularly in combination with farnesyl transferase inhibitors.

Statins competitively inhibit the HMG-CoA reductase enzyme found at the beginning of the mevalonate pathway. They have been implicated in pleiotropic effects such as inflammation, immune modulation and autophagy of cancer cells while epidemiological studies suggest a beneficial role in cancer recurrence. Proadifen is a Δ-24 oxidoreductase inhibitor and truncates the pathway at the desmosterol and lanosterol intermediates. Proadifen prevents conversion of 4,4-Dimethylcholesta-8,[9], 24-dien-3β-ol to 4,4-Dimethylcholesta-8[9},24-en-3β-ol, zymosterol into 7-Dihydroxyzymesterol, 7,24-cholestadien-3β-ol into 7-cholesten-3β-ol and 5,7,24-cholestatrien-3β-ol into 5,7-cholestadi en-3β-ol. It is thus able to prevent the synthesis of cholesterol without an impact on mevalonate or squalene intermediates such as farnesylpyrophosphate or geranylpyrophosphate. It is included in the experiments to identify the involvement, if any, of the distal sterol pathways in EMT-MET transitions.

The results suggest that inhibitors of the mevalonate pathway have considerable impacts on gene expression and that the response varies by cell type: CaLu-1 is much more vulnerable to the effects of statins. The response to Proadifen is significantly less than the response to Pravastatin and this is

unsurprising since its target of Δ-24 reductase features in the cholesterol pathway downstream of the production of farnesyl pyrophosphate and geranylpyrophosphate. Intriguingly however, Proadifen does have notable effects on gene expression and this suggests enzyme inhibition outside of the cholesterol pathway. It may be significant that Proadifen inhibits several of the cytochrome p450 mono-oxygenase reactions in a non-specific manner[28].

A number of nitrogenous bisphosphonates are currently used clinically to reduce bone re-sorption in osteoporosis and bone cancer. They inhibit farnesyl diphosphate synthase[29] probably because bisphosphonic acid is competitively binding in place of pyrophosphonic acid [30,31]: the result is GGPP depletion. Weimer and Hohl[32] have generated bisphosphonate analogues with greater specificity against GGDPS and these are clinically relevant to metastasis. Additional specificity against GGDPS has been added by other researchers using phosphonacetamidooxy- and organoboronfunctional groups[33,34]. The signal transduction of the farnesylated Ras[35] and Rho is blocked by farnesyl transferase inhibitors that have anti-cancer effects[36]. However, Proadifen and Pravastatin caused a small rise in the expression of farnesyl diphosphate farnesyl transferase suggesting a feedback system is employed by the cell.

An inability to process extrinsic factors in the ECM due to inadequate prenylation or phosphorylation appears to truncate the transduction cascade connecting the extrinsic signalling to RNA transcription. Gene expression is thus unchanged and the cells remain quiescent. Likewise, cells forced to maintain a more epithelial identity maybe unable to re-acquire malignant proliferation [37,38].

Inhibitors of the mevalonate pathway weakly blockade farnesylation and geranylation yet this study suggests that statins are able to restrict cytoskeleton rearrangement required for invadapodia function and as a consequence the cell is unable to properly process extrinsic signals that would

normally permit full transition to epithelial identity. Other indicators of pluripotency are affected by the treatments and the response is cell-type specific, with CaLu-1 displaying more sensitivity to the statin compared to MDA-MB-2312. It is proposed that limited decreases in isoprenylation of signal proteins taking place in invadapodia cause an arrest of the MET and could induce cancer cell latency. More targeted inhibition of FFDP and GGDP synthesis using specific and irreversible inhibitors, rather than competitively binding inhibitors, could further impede MET signalling. The indication of such a drug would most usefully be the forced dormancy of disseminated tumour cells and suppression of metastatic disease. Both the statin and Δ-24 reductase inhibitor reduce the formation of invadapodia; in the case of the statin, it is theorized that this attenuates signal transduction from the ECM to the nucleus and could arrest the cells transition towards adaptation. Proadifen treatment does not have the same effect on gene regulation despite the gross changes to the cell morphology. The photomicrographs reveal that both the statin and Proadifen impact the formation of lamellae and invadapodia, yet the statin reduces the metastatic markers and the Δ-24 reductase inhibitor has the only statistically significant effect on the mevalonate pathway enzymes (See table 4).

One explanation for this could be that the statin utilizes a feedback control system for HMG-CoA that involves the sterol element binding proteins (SREBPs) via the isoprenoid pathway while the Proadifen utilises a secondary feedback regulation of reductase mediated by cholesterol and reduces squalene synthase in a manner proposed by Brown *et al*[39].

Suppression of squalene synthase in such a multivalent feedback would leave the isoprenoid pathway and the SREBPs unaffected. This explains why the statins affect isoprenoid mediated

transduction of ECM signals with consequent down-regulation of affected metastatic genes and why Proadifen does not.

For the first time a link between the mevalonate pathway and a metastatic phenotype is established. Inhibition of prenylation of paracrine signals is one possible mechanism for this and provides an explanation of the anti-cancer effects of statins observed in epidemiological studies.

Further work is needed to follow gene expression and protein levels *in vivo* during the metastasis of cancer cells into their ultimate host organ and the cell-type dependant effects of Proadifen deserve additional investigation.

Acknowledgements.

The authors wish to acknowledge assistance with statistical analysis by Andrew Canter of Pathway Intermediates Ltd and Max Bylesjo of Fios Genomics Ltd.

.

TABLE 1 SAMPLE NUMBERS FOR THE TREATMENTS INDICATE BIOLOGICAL REPLICATES. HESC DATA WERE TAKEN FROM THE PUBLIC GEO DATASETS GSE42956, GSE35027 AND GSE37077 (WWW://WWW.NCBI.NLM.NIH.GOV/GEO/)

	MB231	Calu-1	hESCs	Fibroblasts
Pravastatin	**4** GSE47461	**3** GSE47458		
Proadifen	**4** GSE47461	**3** GSE47458		
Control	**4** GSE47461	**3** GSE47458	**3** GSM1053949, GSM1053950 GSM1053951, GSM860961 GSM860962, GSM860963 GSM910308, GSM910309	**6** GSM1053955, GSM1053956, GSM1053957, GSM1053961, GSM1053962, GSM1053963

TABLE 2 HESC MARKER SET FILTERED TO THE 15 LOWEST P VALUE AND ORDERED BY LOGFC

MB-231 Pravastatin P-Factor		Up/Down Regulated in hESCs	Actual direction of FC	Log2 Fold Change	P-Factor
Symbol	Description				
IGFBP3	insulin-like growth factor binding protein 3	▼	▼	-2.70	5.70E-14
IGFBP3	insulin-like growth factor binding protein 3	▼	▼	-2.20	9.70E-14
NDRG1	N-myc downstream regulated 1	▼	▼	-1.40	5.70E-10
PIM2	pim-2 oncogene	▲	▼	-0.38	1.00E-03
NASP	nuclear autoantigenic sperm protein (histone-binding)	▲	▼	-0.17	3.30E-02
UGP2	UDP-glucose pyrophosphorylase 2	▲	▼	-0.06	3.80E-02
DCN	decorin	▼	▼	-0.01	1.90E-02
SNRPN	small nuclear ribonucleoprotein polypeptide N	▲	▲	0.01	4.00E-02
BMP4	bone morphogenetic protein 4	▼	▲	0.03	9.70E-03
HSPA4	heat shock 70kDa protein 4	▲	▲	0.10	2.90E-03
KRT18	keratin 18	▼	▲	0.14	1.00E-02
PHF17	PHD finger protein 17	▲	▲	0.14	2.70E-02
M6PR	mannose-6-phosphate receptor (cation dependent)	▲	▲	0.24	2.60E-02
CDKN1A	cyclin-dependent kinase inhibitor 1A (p21, Cip1)	▼	▲	0.31	5.10E-02
COL5A1	collagen, type V, alpha 1	▼	▲	0.43	2.00E-05

MB-231 Proadifen P-Factor		Up/Down Regulated in hESCs	Actual direction of FC	Log2 Fold Change	P-Factor
Symbol	Description				
IGFBP3	insulin-like growth factor binding protein 3	▼	▼	-0.59	2.10E-04
DLGAP5	discs, large (Drosophila) homolog-associated protein 5	▲	▼	-0.47	2.30E-03
UGP2	UDP-glucose pyrophosphorylase 2	▲	▼	-0.44	1.90E-03
CD47	CD47 molecule	▼	▼	-0.41	8.30E-05
IGFBP3	insulin-like growth factor binding protein 3	▼	▼	-0.36	4.00E-03
SEPHS1	selenophosphate synthetase 1	▲	▼	-0.30	1.60E-03
PSIP1	PC4 and SFRS1 interacting protein 1	▲	▼	-0.28	6.00E-04
HELLS	helicase, lymphoid-specific	▲	▼	-0.18	4.30E-03
CD47	CD47 molecule	▼	▼	-0.11	1.50E-02
DNMT3B	DNA (cytosine-5-)-methyltransferase 3 beta	▲	▼	-0.01	7.30E-03
GABRB3	gamma-aminobutyric acid (GABA) A receptor, beta 3	▲	▲	0.01	1.20E-02
POU5F1	POU class 5 homeobox 1	▲	▲	0.01	8.20E-03
DNMT3B	DNA (cytosine-5-)-methyltransferase 3 beta	▲	▲	0.12	9.60E-03
M6PR	mannose-6-phosphate receptor (cation dependent)	▲	▲	0.39	1.10E-03
PLA2G16	phospholipase A2, group XVI	▲	▲	0.44	6.70E-04

OVERALL MOVEMENT TOWARDS MET AS A PERCENTAGE OF STATISTICALLY SIGNIFICANT (P<0.05) FOLD CHANGES IN ENTIRE DATA SET IN MDA-MB-231 PRAVASTATIN: 50% AND PROADIFEN : 50% BASED ONLY ON DIRECTIONALITY NOT FOLD CHANGE.

TABLE 3

CALU-1 Pravastatin P-Factor		Up/Down Regulated in	Actual direction		
Symbol	Description	hESCs	of FC	**Log2 Fold Change**	**P-Factor**
NASP	nuclear autoantigenic sperm protein (histone-binding)	▲	▼	-1.10	3.70E-10
UNG	uracil-DNA glycosylase	▲	▼	-1.00	1.20E-07
DLGAP5	discs, large (Drosophila) homolog-associated protein 5	▲	▼	-0.93	4.30E-07
COL1A1	collagen, type I, alpha 1	▼	▼	-0.80	7.50E-07
BMP4	bone morphogenetic protein 4	▼	▼	-0.73	7.50E-06
BUB1	budding uninhibited by benzimidazoles 1 homolog (yeast)	▲	▼	-0.67	1.80E-07
MSH2	mutS homolog 2, colon cancer, nonpolyposis type 1 (E. coli)	▲	▼	-0.64	1.50E-07
LUM	lumican	▼	▼	-0.55	8.60E-07
DLGAP5	discs, large (Drosophila) homolog-associated protein 5	▲	▼	-0.52	2.20E-06
AASS	aminoadipate-semialdehyde synthase	▲	▲	0.43	7.30E-06
KRT7	keratin 7	▼	▲	0.66	3.10E-06
PHF17	PHD finger protein 17	▲	▲	0.72	1.20E-06
TERF1	telomeric repeat binding factor (NIMA-interacting) 1	▲	▲	0.72	4.50E-06
SNRPN	small nuclear ribonucleoprotein polypeptide N	▲	▲	0.83	1.50E-08
NDRG1	N-myc downstream regulated 1	▼	▲	0.96	9.20E-08

CALU-1 Proadifen P-Factor		Up/Down Regulated in	Actual direction		
Symbol	Description	hESCs	of FC	**Log2 Fold Change**	**P-Factor**
COL1A1	collagen, type I, alpha 1	▼	▼	-4.20	1.30E-18
BMP4	bone morphogenetic protein 4	▼	▼	-2.60	2.70E-14
COL1A2	collagen, type I, alpha 2	▼	▼	-1.80	1.10E-11
UNG	uracil-DNA glycosylase	▲	▼	-1.80	1.40E-11
ANGEL2	angel homolog 2 (Drosophila)	▲	▼	-1.40	7.70E-13
DLGAP5	discs, large (Drosophila) homolog-associated protein 5	▲	▼	-1.30	1.70E-09
NASP	nuclear autoantigenic sperm protein (histone-binding)	▲	▼	-1.10	2.10E-10
COL5A1	collagen, type V, alpha 1	▼	▼	-1.10	1.20E-09
SEPHS1	selenophosphate synthetase 1	▲	▼	-0.86	8.90E-10
LUM	lumican	▼	▼	-0.80	3.80E-09
SNRPN	small nuclear ribonucleoprotein polypeptide N	▲	▲	1.10	3.30E-10
TERF1	telomeric repeat binding factor (NIMA-interacting) 1	▲	▲	1.10	1.20E-08
PHF17	PHD finger protein 17	▲	▲	1.70	1.70E-12
PHF17	PHD finger protein 17	▲	▲	1.80	1.70E-13
NDRG1	N-myc downstream regulated 1	▼	▲	1.80	4.50E-12

OVERALL MOVEMENT TOWARDS MET AS A PERCENTAGE OF STATISTICALLY SIGNIFICANT (P<0.05) FOLD CHANGES IN ENTIRE DATA SET IN CALU-1 PRAVASTATIN: 60.3% AND PROADIFEN:54% BASED ONLY ON DIRECTIONALITY NOT FOLD CHANGE.

TABLE 4 CHANGES IN GENE EXPRESSION OF ENZYMES INVOLVED IN THE MEVALONATE PATHWAY

			Cell Line			
	ID		MDA-MB-231		Calu-1	
Treatment		**Mevalonate pathway enzymes**	**LOG FC**	**Adj. p**	**LOG FC**	**Adj. p**
Proadifen	DHCR7	Δ-7 reductase	1.5	7.7 E-08	1.5	3.1E-09
	FDFT1	Farnesyl diphosphate farnesyl transferase	1.3	4.10 E-07	1.1	8.4E-12
	LSS	Lanosterolsynthase	1.3	1.70 E-06	-0.012	>0.05
	DHCR24	Δ-24 reductase	1.1	3.2 E-05	0.61	0.0029
	SQLE	Squalene epoxidase	0.87	0.00086	0.89	0.000013
Pravastatin	DHCR7	Δ-7 reductase	-0.25	>0.05	1.6	2.4E-09
	FDFT1	Farnesyl diphosphate farnesyl transferase	0.15	>0.05	1.3	1E-12
	LSS	Lanosterolsynthase	-0.0078	>0.05	-0.099	>0.05
	DHCR24	Δ-24 reductase	0.097	>0.05	0.046	>0.05
	SQLE	Squalene epoxidase	0.15	>0.05	0.033	>0.05

ALL STATISTICALLY SIGNIFICANT CHANGES IN LOGFC ARE POSITIVE SUGGESTING THE CELLS' HOMEOSTASIS RESPONSE TO REDUCED PATHWAY INTERMEDIATE FEEDSTOCK IS UP-REGULATION OF THE RELEVANT ENZYMES. BOTH DRUGS CAUSED Δ7 REDUCTASE AND FDFT1 EXPRESSION TO BE DRASTICALLY INCREASED.

TABLE 5 DIFFERENCES IN RESPONSE BY TREATMENT AND CELL TYPE ON CANCER MARKERS

Cell line			MDA-MB-231						Calu-1					
			Pravastatin v control			**Proadifen v control**			**Pravastatin v control**			**Proadifen v control**		
			logFC	P.Value	adj.P.Val	logFC	P.Value	adj.P.Val	logFC	P.Value	adj.P.Val	logFC	P.Value	adj.P.Val
Cancer Promoters	PLAUR	Plasminogen activator, urokinase receptor	-0.089	p>0.05	n/a	-0.64	0.00068	0.043	-0.87	0.000026	0.00067	0.19	0.24	>0.05
	S100A4	S100 calcium binding protein A4	0.54	1.60E-08	2.00E-05	-0.4	1.00E-06	0.00036	0.88	4.70E-06	1.70E-04	0.43	5.80E-03	0.03
Cancer Suppressors	NDRG1	N-myc downstream regulated 1	-1.4	5.70E-10	1.10E-06	-0.023	0.84	0.98	0.96	9.20E-08	7.50E-06	1.8	4.5E-12	4.8E-10
	CDH1	Cell adhesion molecule	0.00025	p>0.05	n/a	-0.012	0.0015	0.069	0.67	7.6E-09	1.1E-06	0.36	0.00003	0.0003

S100A ACTIVATES SIGNALLING LEADING TO THE RE-MODELLING OF THE CYTOSKELETON AND ACTIVATES SIGNALLING PATHWAYS40(20).PLAUR /CD87 IS OVER-EXPRESSED IN MANY METASTATIC TUMOURS AND IS INVOLVED IN SEVERAL CANCER PHENOTYPES41(21). NDRG1 AND CDH1 ARE METASTASIS SUPPRESSORS42(22).

TABLE 6 DIFFERENCES IN RESPONSE BY TREATMENT AND CELL TYPE ON INVASION MARKERS

		Fold Change				P-Factor			
		MB-231		CALU-1		MB-231		CALU-1	
Symbol	Description	Pravastatin	Proadifen	Pravastatin	Proadifen	Pravastatin	Proadifen	Pravastatin	Proadifen
CDC42	cell division cycle 42 (GTP binding protein, 25kDa)	0.13	0.15	-0.41	0.13	-	-	9.20E-04	-
CDC42EP2	CDC42 effector protein (Rho GTPase binding) 2	-0.014	-0.19	-0.61	-0.014	-	8.30E-03	3.70E-05	-
EGFR	epidermal growth factor receptor	-0.1	0.038	0.77	-0.1	-	-	7.00E-08	-
MMP1	matrix metallopeptidase 1 (interstitial collagenase)	-1.5	0.37	-0.86	-1.5	1.30E-11	1.90E-03	4.40E-06	1.30E-11
MMP3	matrix metallopeptidase 3 (stromelysin 1, progelatinase)	-0.014	0.36	-2.3	-0.014	-	8.70E-07	4.70E-13	-
MMP7	matrix metallopeptidase 7 (matrilysin, uterine)	-0.0037	-0.0044	-0.36	-0.0037	-	-	6.30E-04	-

Regulators of cell motility mediated by actomyosin include ROCK and its regulator PDK1, Rho family GTP-ases especially RhoC and CDC42 control cytoskeleton modifying proteins. The largest changes were observed following treatment with Pravastatin on the lung cell Calu-1 with many large down-regulations that are statistically significant. Calu-1 appears to be very responsive to both of these agents. Notable exceptions are seen in MDA-MB-231 cells where CDC42EP3 was up-regulated on treatment with the statin and MMP3 and PDK3 were both up-regulated on treatment with Proadifen.

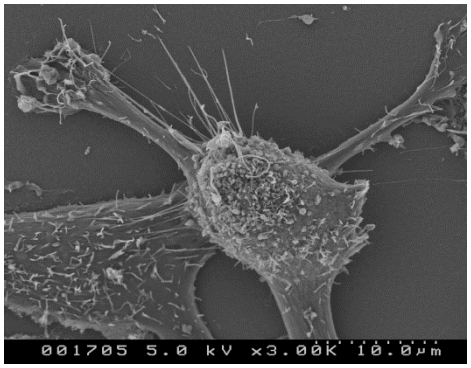

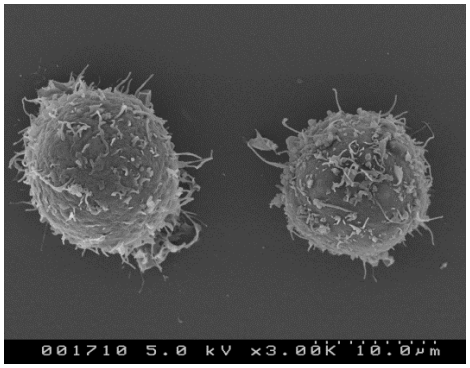

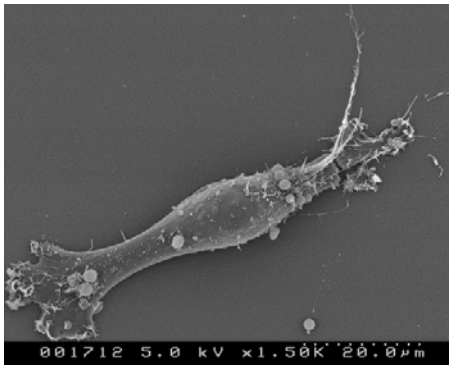

Untreated control cells

Cells treated with Proadifen

Cells treated with Pravastatin

THESE IMAGES SHOW REPRESENTATIVE CELLS FROM STATIN AND 24-DHCR TREATMENTS. THERE IS A SIGNIFICANT ALTERATION TO THE CELL MORPHOLOGY ASSOCIATED WITH FEWER AND SMALLER INVADAPODIA AND CILIA.

References

[1] Talmadge J.E and Fidler I.J. AACR centennial series: the biology of cancer metastasis: historical perspective. Cancer Res. 2010; 70:5649-5669

[2] Goldstraw P, Crowley J, Chansky K, Giroux DJ, Groome PA, Rami-Porta R, et al. The IASLC lung cancer staging project: proposals for the revision of the TNM stage groupings in the forthcoming (seventh) edition of the TNM classification of malignant tumours. Thorac. Oncol. 2007; 2:706–14

[3] Weber G.F. Why does cancer therapy lack effective anti-metastasis drugs? Cancer Letters 2013; 328, (2), 207-211

[4] Vignot S., Besse B., André F., Spano J-P., Soria J-C. Discrepancies between primary tumour and metastasis: A literature review on clinically established biomarkers. Critical Reviews in Oncology/Hematology 2012; 84, (3), 301-313

[5] Shojaei F. Anti-angiogenesis therapy in cancer: Current challenges and future perspectives. Cancer Letters 2012; 320 (2) 28: 130-137

[6] Lehembre F., Regenass U. Metastatic disease: A drug discovery perspective. Seminars in Cancer Biology 2012; 22 (3): 261-271

[7] Mo H., Elson C. Studies of the isoprenoid-mediated inhibition of mevalonate synthesis applied to cancer chemotherapy and chemoprevention. Exp. Biol. Med. 228(7): 567-585; 2004

[8] Paget S. The distribution of secondary growths in cancer of the breast. Lancet 1889; 1: 571-573

[9] Monteiro J and Fodde R. Cancer stemness and metastasis: therapeutic consequences and perspectives. Eur. J. Cancer 2010; 46:1198-1203

[10] Allen M, Louise Jones J. Jeckyll and Hyde: the role of the microenvironment on the progression of cancer. J. Pathol. 2010; 223(2):162-76

[11] Redmond K.M., Wilson T.R, Johnston P.G., Longley D.B. Front. Resistance mechanisms to cancer chemotherapy. Biosci. 2008; 13:5138-5154

[12] Mimeault M., Batra S.K. New promising drug targets in cancer and metastasis-initiating cells. Drug Discovery Today 2010; 15: 354364

[13] Mimeault M., Batra S.K. New advances on the critical implications of tumour and metastasis-initiating cells in cancer progression, treatment resistance and disease recurrence. Histol. Histopathol. 2010; 25(8): 1057-1073

[14] Theiry J.P., Acloque H., Huang R.Y., Nieto M.A. Epithelial-mesenchymal transitions in development and disease. Cell 2009; 139:871-890

[15] Van Zijl F., Krupitza G., Mikulits W. Initial steps of metastasis: cell invasion and epithelial transmigration. Mutation Res. 2011; 728: 23-34

[16] Artym V.V., Zhang Y., Seillier-Moiseiwitsch F., Yamada K.M. Mueller S.C. Dynamic interactions of cortactin and membrane type 1 matrix metalloproteinases at invadapodia: defining stages of invadapodia formation and function. Cancer Res. 2006; 66: 3034-3043

[17] Yilmaz M., Christifori G. EMT, the cytoskeleton, and cancer cell invasion. Cancer Metastasis Rev. 2009; 28:15-33

[18] Desmarais V., Yamaguchi H., Oser M., Soon L., Mouneimne G., Sarmiento C., Eddy R., Condeelis J. N-WASP and cortactin are involved in invadapodium-dependant chemotaxis to EGF in breast tumour cells. Cell. Motil. Cytoskel. 2009; 66: 303-316

[19] Bravo-Cordero J.J., Hodgson L., Condeelis J. Directed cell invasion and migration during metastasis. Curr. Opinion Cell Biol. 2012; 24: 277-283

[20] Kato S., Smalley S., Sadarangani A., Chen-Lin K., Oliva B., Branes J., Carvalal J., Geiman R., Owen G., Cuello M. Lipophilic but not hydrophilic statins selectively induce cell death in gynaecological cancers expressing high levels of HMGCoA reductase. J. Cell Mol. Med. 2010; 14(15): 1180-1193

[21] Wojtkowiak J.W., Sane K.M., Kleinman M, Sloane B.F., Reiners Jr J.J., Mattingly R.R. Aborted autophagy and non apoptotic death induced by farnesyl transferase inhibitor and lovastatin. J. Pharm. Exp. Therapeutics. 2011; 337: 65-74

[22] Assou S., Le Carrour T., Tondeur S., Strom S., Gabelle A., Marty S., et al. A meta-analysis of human embryonic stem cells transcriptome integrated into a web-based expression atlas. Stem Cells 2007; 25(4): 961-973

[23] Bravo-Cordero J.J., Oser M., Chen X., Eddy R., Hodgson L., Condeelis J. A novel spatiotemporal RhoC activation pathway locally regulates cofilin activity at invadapodia. Curr. Biol. 2011; 21:635-644

[24] Pinner S., Sahai E. PDK1 regulates cancer cell motility by antagonising inhibition of ROCK1 by RhoE. Nat. Cell. Biol. 2008; 10: 127-137

[25] Sanz-Moreno V., Gadea G., Ahn J., Paterson H., Marra P., Pinner S., et al. Rac activation and inactivation control plasticity of tumour cell movement. Cell 2008; 135: 510-523

[26] Jing Zhang, Zuozhang Yang, Lin Xie, Lei Xu, Da Xu, Xuefeng Liu. Statins, autophagy and cancer metastasis Review Article : The International Journal of Biochemistry & Cell Biology,. Volume 45, Issue 3, 2013, Pages 745-752

[27] Garnett D.J., Greenhough T.J. Statins cause profound effects on gene expression in human cancer cells in vitro: the role of membrane microdomains. Gene Expression. 2013; 15; 1-10

[28] Anders, M. and Mannering, G. Inhibition of drug metabolism: Induction of drug metabolism by 2-diethylaminoethyl 2,2-diphenylvalerate-HCl (SKF-525-A) and 2,4-dichloro-6-phenylphenoxyethyldiethylamine (Lilly 18947) and the effect of induction on the inhibitory properties of SKF-525-A type compounds. Mol. Pharmacol. 1966; 2 341-346

[29] Fisher J.E., Rogers M.J., Halasy J.M., Luckman S.P., Hughes D.E., Masarachia P.J., et al. Alendronate mechanism of action: geranylgeraniol, an intermediate in the mevalonate pathway, prevents inhibition of osteoclast formation, bone re-sorption, and kinase activation in vitro Proc. Natl. Acad. Sci USA 1999; 96: 133

[30] Goffinet M, Thoulouzan M, Pradines A, Lajoie-Mazenc I., Weinbaum C., Faye J.C., et al Zoledronic acid treatment impairs protein geranyl-geranylation for biological effects in prostatic cells. BMC Cancer 2006; 6:60

[31] Kavanagh K.L., Guo K, Dunford J.E., Wu X., Knapp S, Ebetino F.H., et al. The molecular mechanism of nitrogen-containing bisphosphonates as anti-osteoporosis drugs. Proc. Natl. Acad. Sci. USA 2006; 103: 7829.

[32] Weimer D.F.,Hohl R.J. Geranylgeranyl pyrophosphate synthase inhibitors.. US Patent Application 2006; 20060052347

[33] Minutolo F, Bertini S., Betti L, Danesi R., Gervasi G., Giannaccini G., et al. Stable Analogues of gerenylgeranyl diphosphate possessing improved geranylgeranyl versus farnesyl protein transferase inhibitory selectivity. Bioorg. Med. Chemistry Let. 2003; 13: 4405-4408

[34] Mu Y-Q., Eubanks L.M., Dale Oulter C., Gibbs R.A. Coupling of isoprenoid triflates with organoboron nucleophiles: synthesis and biological evaluation of geranylgeranyl diphosphate analogues. Bioorg. Med. Chem. 2002; 10:1207-1219

[35] Casey P.J., Solski P.A., Der C.J., Buss J.E. p21ras is modified by a farnesyl isoprenoid. Proc. Natl. Acad. Sci. USA 1989; 86:8323

[36] Oliff A. Farnesytransferase inhibitors: targeting the molecular basis of cancer. Biochem. Biophys. Acta. 1999; C19: 1423

[37] Iiizumi M., Liu W., Pai S.K., Furuta E., Watabe K. Drug development against metastasis-related genes and their pathways: a rationale for cancer therapy. Biochim. Biophys Acta. 2008; 1786: 87-104

[38] Aguirre-Ghiso J.A. Models, mechanisms and clinical evidence for cancer dormancy. Nature Reviews Cancer 2007: 7;834-846

[39] Brown M., Goldstein J., Multivalent feedback regulation of HMG CoA reductase, a control mechanism coordinating isoprenoid synthesis and cell growth. J. Lipid Res. 21: 505-517; 1980

[40] G.V.Sherbet. Metastasis promoter S100A is a potentially valuable molecular target for cancer therapy. Cancer Lett. 2009; 280: 13-30

[41] Ploug M., Gardsvoll H., Jorgensen T.J., Lonborg Hansen L., Dano K. Structural analysis of the interaction between urokinase-type plasminogen activator and its receptor: a potential target for anti-invasive cancer therapy. Biochem. Soc. Trans. 2002; 30(2): 177-173

[42] Iizumi M., Liu W., Pai S.K., Furuta E., Watabe K. Drug development against metastasis-related genes and their pathways: a rationale for cancer therapy. Biochim. Biophys Acta. 2008; 1786: 87-104

APPENDIX 3

Detailed results from the gene expression assays.

PROADIFEN RELATIVE TO CONTROL:

361 array features were statistically significant (196 up-regulated, 165 down-regulated). Within the significant features, ABL2, ACACA, ACAT2, ACSS2, ACTR5, AHNAK2, AKR1C3, AP1M2, APBB1IP and ARHGEF18 were up-regulated. Within the significant features, ABCA1, ACOX2, AFAP1L2, AGR2, ALDH1A3, ARSJ, ASF1A, ATP2B1, B3GALNT1 and BCL3 were down-regulated.

The predominant up-regulated pathways include Metabolic pathways (36), Lysosome (13), Steroid biosynthesis (11), terpenoid backbone biosynthesis (7), phagosome (5), Oxidative phosphorylation (4), Pyruvate metabolism (4), Collecting duct acid secretion (4), Vibrio cholerae infection (4), Epithelial cell signalling in Helicobacter pylori infection (4), Amino sugar and nucleotide sugar metabolism (3), propanoate metabolism (3), MAPK signalling pathway (3), Protein processing in endoplasmic reticulum (3), Insulin signalling pathway (3), Synthesis and degradation of ketone bodies (2), Steroid hormone biosynthesis (2), valine, leucine and isoleucine degradation (2), Other glycan degradation (2) and Glycosaminoglycan degradation (2).

The predominant down-regulated pathways include Cytokine-cytokine receptor interaction (12), Metabolic pathways (10), amoebiasis (7), Pathways in cancer (7), Hematopoietic cell

lineage (6), Chemokine signalling pathway (5), NOD-like receptor signalling pathway (5), MAPK signalling pathway (4), Leishmaniasis (4), Graft-versus-host disease (4), ErbB signalling pathway (3), Cell cycle (3), p53 signalling pathway (3), Cell adhesion molecules (CAMs) (3), Tight junction (3), Toll-like receptor signalling pathway (3), Jak-STAT signalling pathway (3), Type I diabetes mellitus (3), Salivary secretion (3) and Prion diseases (3).

In terms of observed fold change (independent of statistical threshold), 33 features exhibited >2-fold up-regulation, while 16 features exhibited >2-fold down-regulation. Fold changes ranged from 20.3-fold up to 4.7-fold down. Within the biggest change loci, MIR1978, MIR1974, HMGCS1, SC4MOL, ACSS2, DHCR7, TMEM97, ACAT2, NSMAF and HMGCR were up-regulated. Within the biggest change loci, IL8, IL1B, CXCL1, IL6, ACTG1, C15orf48, IL11, RASD1, CD24 and THBS1 were down-regulated.

29 KEGG pathways were statistically enriched. Members of Steroid biosynthesis, Terpenoid backbone biosynthesis and Lysosome pathways were amongst those enriched in up-regulated loci. Members of cytokine-cytokine receptor interaction, Amoebiasis and Hematopoietic cell lineage pathways were amongst those enriched in down-regulated loci.

174 GO terms were statistically enriched. Members annotated with sterol biosynthetic process, sterol metabolic process and cholesterol biosynthetic process GO terms were amongst those enriched in up-regulated loci. Members annotated with extracellular space, extracellular region part and cytokine activity GO terms were amongst those enriched in down-regulated loci.

PRAVASTATIN RELATIVE TO CONTROL:

101 array features were statistically significant (27 up-regulated, 74 down-regulated). Within the significant features, ANGPTL2, COL5A1, COPS2, DST, FOS, GAS2L1, GPR56, GPRC5C, ID1 and ID2 were up-regulated. Within the significant features, ABCA1, ADM, ANGPTL4, C10orf10, C13orf15, C15orf48, C7orf68, CCL20, CCL26 and CDCP1 were down-regulated.

The predominant up-regulated pathways include TGF-beta signalling pathway (3), focal adhesion (2) and ECM-receptor interaction (2).

The predominant down-regulated pathways include cytokine-cytokine receptor interaction (9), chemokine signalling pathway (5), NOD-like receptor signalling pathway (5), hematopoietic cell lineage (4), prion diseases (4), amoebiasis (4), pathways in cancer (4), MAPK signalling pathway (3), toll-like receptor signalling pathway (3), Leishmaniasis (3), Chagas disease (3), Malaria (3), Graft-versus-host disease (3), PPAR signalling pathway (2), protein processing in endoplasmic reticulum (2), apoptosis (2), complement and coagulation cascades (2), cytosolic DNA-sensing pathway (2), Jak-STAT signalling pathway (2) and Type I diabetes mellitus (2).

In terms of observed fold change (independent of statistical threshold), 0 features exhibited >2-fold up-regulation, while 24 features exhibited >2-fold down-regulation. Fold changes ranged from 2-fold up to 10.4-fold down. Within the biggest change loci, ID1, NQO1, THBS1, TUBB3, ID3, IGFBP4, PKM2, TRNP1, GPRC5C and VIM were up-regulated. Within the biggest

change loci, PTGS2, IGFBP3, IL8, LOX, IL1B, IL6, MMP1, CXCL1, NDRG1 and CDCP1 were down-regulated.

20 KEGG pathways were statistically enriched. Members of TGF-beta signalling pathway, ECM-receptor interaction and NA pathways were amongst those enriched in up-regulated loci. Members of cytokine-cytokine receptor interaction, NOD-like receptor signalling pathway and Prion diseases pathways were amongst those enriched in down-regulated loci.

170 GO terms were statistically enriched. The R-SMAD binding GO term was enriched in up-regulated loci. Members annotated with extracellular region, extracellular region part and extracellular space GO terms were amongst those enriched in down-regulated loci.

MBCD RELATIVE TO CONTROL:

79 array features were statistically significant (3 up-regulated, 76 down-regulated). Within the significant features, MARCH4, NQO1 and SNX6 were up-regulated. Within the significant features, ABCA1, ADAM8, ADM, AGR2, ANGPTL4, C10orf10, C13orf15, C15orf48, C7orf68 and CCL20 were down-regulated.

The predominant down-regulated pathways include cytokine-cytokine receptor interaction (9), pathways in cancer (6), chemokine signalling pathway (5), NOD-like receptor signalling pathway (5), amoebiasis (5), prion diseases (4), Graft-versus-host disease (4), PPAR signalling pathway (3), MAPK signalling pathway (3), toll-like receptor signalling pathway (3), hematopoietic cell lineage (3), Type I diabetes mellitus (3), Leishmaniasis (3), Chagas disease

(3), malaria (3), bladder cancer (3), metabolic pathways (2), mTOR signalling pathway (2), apoptosis (2) and VEGF signalling pathway (2).

In terms of observed fold change (independent of statistical threshold), 0 features exhibited >2-fold up-regulation, while 13 features exhibited >2-fold down-regulation. Fold changes ranged from 1.6-fold up to 3.2-fold down. Within the biggest change loci, THBS1, AMY1C, FTLP2, NQO1, ID3, FLNC, CAV1, RPL35, SLC7A5 and PSMC1 were up-regulated. Within the biggest change loci, PTGS2, IL8, IGFBP3, IL1B, LOX, NDRG1, CDCP1, IL6, STC1 and C15orf48 were down-regulated.

17 KEGG pathways were statistically enriched. Members of cytokine-cytokine receptor interaction, NOD-like receptor signalling pathway and Prion diseases pathways were amongst those enriched in down-regulated loci.

145 GO terms were statistically enriched. Members annotated with NAD(P)H dehydrogenase (quinone) activity, negative regulation of catalytic activity and NA GO terms were amongst those enriched in up-regulated loci. Members annotated with extracellular pathways and cytokine activity GO terms were amongst those enriched in down-regulated loci.

LPC relative to Control:

5708 array features were statistically significant (2999 up-regulated, 2709 down-regulated). Within the significant features, A1BG, AAMP, AARS2, AARSD1, AATF, ABCB6, ABCB9, ABCC10, ABCC5 and ABCF1 were up-regulated. Within the significant features, AASDHPPT,

ABCA1, ABCB10, ABCC4, ABCF2, ABHD3, EPHX4, ABLIM1, ACAD8 and ACADM were down-regulated.

The predominant up-regulated pathways include metabolic pathways (178), pathways in cancer (41), endocytosis (39), MAPK signalling pathway (38), lysosome (30), focal adhesion (30), Huntington's disease (30), purine metabolism (29), spliceosome (28), protein processing in endoplasmic reticulum (28), oxidative phosphorylation (26), pyrimidine metabolism (26), regulation of actin cytoskeleton (24), cell cycle (23), neurotrophin signalling pathway (23), ubiquitin mediated proteolysis (22), phagosome (21), Insulin signalling pathway (20), Alzheimer's disease (20) and Parkinson's disease (20).

The predominant down-regulated pathways include metabolic pathways (164), pathways in cancer (52), protein processing in endoplasmic reticulum (39), ribosome (37), focal adhesion (37), Huntington's disease (35), cell cycle (33), purine metabolism (32), regulation of actin cytoskeleton (31), endocytosis (30), cytokine-cytokine receptor interaction (29), Alzheimer's disease (28), MAPK signalling pathway (27), spliceosome (26), Wnt signalling pathway (26), ubiquitin mediated proteolysis (25), Parkinson's disease (24), phagosome (23), oxidative phosphorylation (22) and oocyte meiosis (21).

In terms of observed fold change (independent of statistical threshold), 260 features exhibited >2-fold up-regulation, while 569 features exhibited >2-fold down-regulation. Fold changes ranged from 3.3-fold up to 15.9-fold down. Within the biggest change loci, C19orf33, ISG15, NUCKS1, SNRNP70, GPR1, FLNC, ATF5, ACTN4, MRPL2 and PVR were up-

regulated. Within the biggest change loci, IL8, IL1B, ACTG1, RPLP0, ALDOA, SRGN, UBB, PTGS2, ACTB and EIF4A1P4 were down-regulated.

63 KEGG pathways were statistically enriched. Members of metabolic pathways, pyrimidine metabolism and lysosome pathways were amongst those enriched in up-regulated loci. Members of ribosome, Shigellosis and cell cycle pathways were amongst those enriched in down-regulated loci.

393 GO terms were statistically enriched. Members annotated with intracellular, intracellular part and membrane-bounded organelle GO terms were amongst those enriched in up-regulated loci. Members annotated with intracellular pathway and cytoplasm pathway GO terms were amongst those enriched in down-regulated loci.

FLUPHENAZINE RELATIVE TO CONTROL:

6808 array features were statistically significant (3428 up-regulated, 3380 down-regulated). Within the significant features, A4GALT, AAGAB, AAMP, AARS2, AARSD1, AATF, AATK, ABCA7, ABCA8 and ABCB6 were up-regulated. Within the significant features, NCEH1, AASDHPPT, ABCA1, ABCB10, ABCC4, ABCC5, ABCD3, ABCE1, ABCF2 and ABHD12 were down-regulated.

The predominant up-regulated pathways include metabolic pathways (184), pathways in cancer (60), endocytosis (48), focal adhesion (39), Huntington's disease (37), MAPK signalling pathway (36), regulation of actin cytoskeleton (36), protein processing in endoplasmic reticulum (35), lysosome (35), purine metabolism (33), cell cycle (30), phagosome (30), oxidative phosphorylation (29), chemokine signalling pathway (29), pyrimidine metabolism (28), spliceosome (26), Alzheimer's disease (26), ubiquitin mediated proteolysis (24), Parkinson's disease (24) and neurotrophin signalling pathway (23).

The predominant down-regulated pathways include metabolic pathways (202), pathways in cancer (68), protein processing in endoplasmic reticulum (50), ribosome (47), focal adhesion (44), endocytosis (43), regulation of actin cytoskeleton (40), purine metabolism (39), MAPK signalling pathway (39), cell cycle (38), Huntington's disease (37), spliceosome (35), Alzheimer's disease (33), cytokine-cytokine receptor interaction (31), Wnt signalling pathway (31), ubiquitin mediated proteolysis (30), oocyte meiosis (27), neurotrophin signalling pathway (27), chemokine signalling pathway (26) and Parkinson's disease (26).

In terms of observed fold change (independent of statistical threshold), 421 features exhibited >2-fold up-regulation, while 661 features exhibited >2-fold down-regulation. Fold changes ranged from 3.6-fold up to 11.9-fold down. Within the biggest change loci, NUCKS1, NLRP8, C19orf33, C5orf28, GPR1, NUBPL, PNPT1, ALPP, SNRNP70 and ARFGAP1 were up-regulated. Within the biggest change loci, IL8, ACTG1, RPLP0, IL1B, ALDOA, SRGN, ACTB, UBB, PGAM1 and LOX were down-regulated.

67 KEGG pathways were statistically enriched. Members of lysosome, pyrimidine metabolism and endocytosis pathways were amongst those enriched in up-regulated loci. Members of ribosome, protein processing in endoplasmic reticulum and Shigellosis pathways were amongst those enriched in down-regulated loci.

450 GO terms were statistically enriched. Members annotated with intracellular pathways and intracellular organelle GO terms were amongst those enriched in up-regulated loci. Members annotated with intracellular pathways and cytoplasm GO terms were amongst those enriched in down-regulated loci.

PROADIFEN RELATIVE TO PRAVASTATIN:

663 array features were statistically significant (342 up-regulated, 321 down-regulated). Within the significant features, ABL2, ACACA, ACAT2, ACLY, ACO1, ACSS2, ADARB1, ADM, AHNAK2 and ALDOC were up-regulated. Within the significant features, ABCA1, ACOX2, ACTG2, ADAM19, ADNP, AEBP2, AFAP1L2, AIM1, ANGPTL2 and ANXA8L2 were down-regulated.

The predominant up-regulated pathways include metabolic pathways (47), lysosome (20), steroid biosynthesis (11), pathways in cancer (11), phagosome (8), terpenoid backbone biosynthesis (7), oxidative phosphorylation (5), MAPK signalling pathway (5), protein processing in endoplasmic reticulum (5), endocytosis (5), insulin signalling pathway (5), Vibrio cholerae infection (5), epithelial cell signalling in Helicobacter pylori infection (5), PPAR signalling pathway (4), cytokine-cytokine receptor interaction (4), Jak-STAT signalling pathway (4), collecting duct acid secretion (4), amino sugar and nucleotide sugar metabolism (3), glycerophospholipid metabolism (3) and pyruvate metabolism (3).

The predominant down-regulated pathways include metabolic pathways (22), focal adhesion (8), p53 signalling pathway (7), pathways in cancer (7), purine metabolism (5), cell cycle (5), axon guidance (5), pyrimidine metabolism (4), nicotinate and nicotinamide metabolism (4), MAPK signalling pathway (4), endocytosis (4), ECM-receptor interaction (4), Fc gamma R-mediated phagocytosis (4), Type II diabetes mellitus (4), citrate cycle (TCA

cycle) (3), spliceosome (3), protein processing in endoplasmic reticulum (3), phagosome (3), TGF-beta signalling pathway (3) and Jak-STAT signalling pathway (3).

In terms of observed fold change (independent of statistical threshold), 74 features exhibited >2-fold up-regulation, while 26 features exhibited >2-fold down-regulation. Fold changes ranged from 23.7-fold up to 3.6-fold down. Within the biggest change loci, MIR1978, MIR1974, PTGS2, ACSS2, HMGCS1, SC4MOL, IGFBP3, NSMAF, MMP1 and DHCR7 were up-regulated. Within the biggest change loci, THBS1, ACTG1, ID1, RASD1, TUBB, ACTB, IGFBP4, TUBB3, LOC148430 and TUBA1A were down-regulated.

23 KEGG pathways were statistically enriched. Members of steroid biosynthesis, lysosome and terpenoid backbone biosynthesis pathways were amongst those enriched in up-regulated loci. Members of p53 signalling pathway, nicotinate and nicotinamide metabolism and Type II diabetes mellitus pathways were amongst those enriched in down-regulated loci.

143 GO terms were statistically enriched. Members annotated with sterol biosynthetic process, vacuole and sterol metabolic process GO terms were amongst those enriched in up-regulated loci. Members annotated with cytoplasm, non-membrane-bounded organelle and intracellular non-membrane-bounded organelle GO terms were amongst those enriched in down-regulated loci.

PROADIFEN RELATIVE TO MBCD:

564 array features were statistically significant (342 up-regulated, 222 down-regulated). Within the significant features, ABL2, ACACA, ACAT2, ACLY, ACSS2, ADAM8, ADM, AGAP8, AHNAK2 and AKR1C3 were up-regulated. Within the significant features, ABCA1, ACTG2, ADAM19, AFAP1L2, ALDH1A3, ANKRD50, ANP32B, ARSJ, ASF1A and ATL3 were down-regulated.

The predominant up-regulated pathways include metabolic pathways (47), lysosome (17), steroid biosynthesis (11), terpenoid backbone biosynthesis (8), phagosome (8), oxidative phosphorylation (5), endocytosis (5), Vibrio cholerae infection (5), epithelial cell signalling in Helicobacter pylori infection (5), pathways in cancer (5), pyruvate metabolism (4), protein processing in endoplasmic reticulum (4), cell adhesion molecules (CAMs) (4), insulin signalling pathway (4), collecting duct acid secretion (4), glycolysis / gluconeogenesis (3), other glycan degradation (3), amino sugar and nucleotide sugar metabolism (3), glycerophospholipid metabolism (3) and propanoate metabolism (3).

The predominant down-regulated pathways include metabolic pathways (11), oocyte meiosis (9), cell cycle (8), p53 signalling pathway (8), ribosome (5), progesterone-mediated oocyte maturation (5), axon guidance (4), tight junction (4), neurotrophin signalling pathway (4), pyrimidine metabolism (3), MAPK signalling pathway (3), endocytosis (3), Wnt signalling pathway (3), TGF-beta signalling pathway (3), focal adhesion (3), Jak-STAT signalling pathway (3), leukocyte transendothelial migration (3), Insulin signalling pathway (3), GnRH signalling pathway (3) and Huntington's disease (3).

In terms of observed fold change (independent of statistical threshold), 44 features exhibited >2-fold up-regulation, while 16 features exhibited >2-fold down-regulation. Fold changes ranged from 26.6-fold up to 3.2-fold down. Within the biggest change loci, MIR1978, MIR1974, HMGCS1, ACSS2, SC4MOL, DHCR7, NSMAF, HMGCR, IDI1 and INSIG1 were up-regulated. Within the biggest change loci, THBS1, ACTG1, LOC148430, DUSP1, ACTB, CAV1, TUBA1A, EIF4A1P4, TRMT5 and LOC642817 were down-regulated.

19 KEGG pathways were statistically enriched. Members of steroid biosynthesis, terpenoid backbone biosynthesis and lysosome pathways were amongst those enriched in up-regulated loci. Members of p53 signalling pathway, oocyte meiosis and cell cycle pathways were amongst those enriched in down-regulated loci.

240 GO terms were statistically enriched. Members annotated with sterol biosynthetic process, cholesterol biosynthetic process and sterol metabolic process GO terms were amongst those enriched in up-regulated loci. Members annotated with protein binding, cell cycle process and cell division GO terms were amongst those enriched in down-regulated loci.

PROADIFEN RELATIVE TO LPC:

3460 array features were statistically significant (1505 up-regulated, 1955 down-regulated). Within the significant features, A3GALT2, ABCC4, EPHX4, ABL2, ABLIM1, ACAD8, ACADM, ACAT2, ACLY and ACOT1 were up-regulated. Within the significant features, AATF, ABCA1, ABCB6, ABCC10, ABCF1, ABCF2, ABCG1, ABHD10, ABHD14A and ABHD14B were down-regulated.

The predominant up-regulated pathways include metabolic pathways (110), pathways in cancer (30), protein processing in endoplasmic reticulum (25), focal adhesion (21), endocytosis (20), MAPK signalling pathway (18), cytokine-cytokine receptor interaction (18), cell cycle (18), regulation of actin cytoskeleton (18), purine metabolism (17), ribosome (16), lysosome (16), Wnt signalling pathway (16), oocyte meiosis (14), ubiquitin mediated proteolysis (14), phagosome (14), spliceosome (13), glycolysis / gluconeogenesis (12), tight junction (12) and insulin signalling pathway (12).

The predominant down-regulated pathways include metabolic pathways (104), endocytosis (31), pathways in cancer (29), focal adhesion (28), purine metabolism (21), spliceosome (20), MAPK signalling pathway (20), cell cycle (20), regulation of actin cytoskeleton (20), Huntington's disease (20), pyrimidine metabolism (17), ubiquitin mediated proteolysis (16), tight junction (16), Alzheimer's disease (15), oxidative phosphorylation (14), chemokine signalling pathway (14), protein processing in endoplasmic reticulum (14), oocyte meiosis (13), Fc gamma R-mediated phagocytosis (13) and insulin signalling pathway (13).

In terms of observed fold change (independent of statistical threshold), 303 features exhibited >2-fold up-regulation, while 65 features exhibited >2-fold down-regulation. Fold changes ranged from 11.8-fold up to 4.8-fold down. Within the biggest change loci, MIR1978, MIR1974, SRGN, INSIG1, NSMAF, SC4MOL, RPLP0, ACAT2, ALDOA and UBB were up-regulated. Within the biggest change loci, ISG15, ACTN4, NEK2, BCYRN1, C19orf33, GAMT, NUCKS1, MRPL2, KLF2 and C19orf48 were down-regulated.

44 KEGG pathways were statistically enriched. Members of steroid biosynthesis, terpenoid backbone biosynthesis and biosynthesis of unsaturated fatty acids pathways were amongst those enriched in up-regulated loci. Members of base excision repair, endocytosis and aminoacyl-tRNA biosynthesis pathways were amongst those enriched in down-regulated loci.

282 GO terms were statistically enriched. Members annotated with cytoplasm and intracellular pathway GO terms were amongst those enriched in up-regulated loci. Members annotated with intracellular pathway and intracellular organelle GO terms were amongst those enriched in down-regulated loci.

PROADIFEN RELATIVE TO FLUPHENAZINE:

4461 array features were statistically significant (2153 up-regulated, 2308 down-regulated). Within the significant features, ABCC4, ABHD3, ABHD5, EPHX4, ABL2, ABLIM1, ACACA, ACAD8, ACADM and ACAT2 were up-regulated. Within the significant features, A4GALT, AARS2, ABCA1, ABCA7, ABCB6, ABCC10, ABCC3, ABCF2, ABCG1 and ABHD10 were down-regulated.

The predominant up-regulated pathways include metabolic pathways (160), pathways in cancer (40), protein processing in endoplasmic reticulum (32), endocytosis (29), ribosome (26), focal adhesion (26), purine metabolism (25), MAPK signalling pathway (25), lysosome (25), regulation of actin cytoskeleton (24), cell cycle (22), spliceosome (21), ubiquitin mediated proteolysis (21), Huntington's disease (21), Alzheimer's disease (20), cytokine-cytokine receptor interaction (19), oocyte meiosis (18), phagosome (18), Wnt signalling pathway (18) and neurotrophin signalling pathway (18).

The predominant down-regulated pathways include metabolic pathways (127), endocytosis (40), pathways in cancer (37), focal adhesion (30), MAPK signalling pathway (29), regulation of actin cytoskeleton (27), Huntington's disease (26), protein processing in endoplasmic reticulum (24), cell cycle (23), purine metabolism (22), spliceosome (21), tight junction (21), chemokine signalling pathway (20), Alzheimer's disease (20), ubiquitin mediated proteolysis (19), oxidative phosphorylation (18), pyrimidine metabolism (18), oocyte meiosis (18), insulin signalling pathway (18) and Parkinson's disease (18).

In terms of observed fold change (independent of statistical threshold), 381 features exhibited >2-fold up-regulation, while 101 features exhibited >2-fold down-regulation. Fold changes ranged from 14.9-fold up to 4.8-fold down. Within the biggest change loci, MIR1978, MIR1974, SC4MOL, SRGN, NSMAF, ACAT2, INSIG1, CYR61, ALDOA and B2M were up-regulated. Within the biggest change loci, NEK2, NUCKS1, ISG15, BCYRN1, LOC388564, LFNG, KLF2, ACTN4, THOC2 and C19orf33 were down-regulated.

49 KEGG pathways were statistically enriched. Members of steroid biosynthesis, Ribosome and terpenoid backbone biosynthesis pathways were amongst those enriched in up-regulated loci. Members of endocytosis, Aminoacyl-tRNA biosynthesis and NA pathways were amongst those enriched in down-regulated loci.

371 GO terms were statistically enriched. Members annotated with cytoplasm, and intracellular pathway GO terms were amongst those enriched in up-regulated loci. Members annotated with intracellular pathway and intracellular organelle GO terms were amongst those enriched in down-regulated loci.

PRAVASTATIN RELATIVE TO MBCD:

27 array features were statistically significant (16 up-regulated, 11 down-regulated). Within the significant features, ANGPTL2, GAS2L1, GPR56, GPRC5C, ID1, ID2, IGFBP6, ITGB4, MALL and MXD4 were up-regulated. Within the significant features, ABCA1, CRY1, FST, IGFBP3, IL11, LOX, MMP1, PTGER4 and PTGS2 were down-regulated.

The predominant up-regulated pathways include TGF-beta signalling pathway (2). The predominant down-regulated pathways include Pathways in cancer (2).

In terms of observed fold change (independent of statistical threshold), 0 features exhibited >2-fold up-regulation, while 3 features exhibited >2-fold down-regulation. Fold changes ranged from 1.8-fold up to 3.3-fold down. Within the biggest change loci, GPRC5C, S100A4, KRT19, AHNAK2, MXD4, ID1, SLC20A1, SH2B3, LAMA5 and NRP1 were up-regulated. Within

the biggest change loci, PTGS2, IGFBP3, IL8, LOX, IL11, MMP1, HIST1H4C, BCYRN1, DUSP1 and FST were down-regulated.

6 KEGG pathways were statistically enriched. The TGF-beta signalling pathway was enriched in up-regulated loci. 21 GO terms were statistically enriched. Members annotated with regulation of localization, negative regulation of transport and negative regulation of hormone secretion GO terms were amongst those enriched in down-regulated loci.

PRAVASTATIN RELATIVE TO LPC:

6581 array features were statistically significant (3049 up-regulated, 3532 down-regulated). Within the significant features, AASDHPPT, ABCB10, ABCC4, ABCD3, ABCF2, ABHD3, EPHX4, ABLIM1, ACAD8 and ACADM were up-regulated. Within the significant features, A1BG, AAGAB, AAMP, AARS2, AARSD1, AATF, ABCA7, ABCB6, ABCB9 and ABCC10 were down-regulated.

The predominant up-regulated pathways include metabolic pathways (191), pathways in cancer (60), protein processing in endoplasmic reticulum (44), focal adhesion (41), regulation of actin cytoskeleton (39), Alzheimer's disease (38), ribosome (37), cell cycle (37), Huntington's disease (37), purine metabolism (35), Wnt signalling pathway (34), spliceosome (32), oocyte meiosis (31), endocytosis (31), ubiquitin mediated proteolysis (30), MAPK signalling pathway (29), Parkinson's disease (29), oxidative phosphorylation (26), neurotrophin signalling pathway (26) and insulin signalling pathway (25).

The predominant down-regulated pathways include metabolic pathways (197), pathways in cancer (49), endocytosis (45), MAPK signalling pathway (40), lysosome (38), protein processing in endoplasmic reticulum (34), Huntington's disease (33), spliceosome (31), focal adhesion (31), oxidative phosphorylation (30), phagosome (29), regulation of actin cytoskeleton (28), purine metabolism (27), pyrimidine metabolism (25), cell cycle (23), ubiquitin mediated proteolysis (23), neurotrophin signalling pathway (23), Alzheimer's disease (21), Parkinson's disease (21) and insulin signalling pathway (20).

In terms of observed fold change (independent of statistical threshold), 625 features exhibited >2-fold up-regulation, while 359 features exhibited >2-fold down-regulation. Fold changes ranged from 13.6-fold up to 3.8-fold down. Within the biggest change loci, ACTG1, UBB, RPLP0, ALDOA, SRGN, ACTB, EIF4A1P4, ITGB1, B2M and PRDX3 were up-regulated. Within the biggest change loci, NUCKS1, BCYRN1, TDP1, DMC1, PVR, ALPP, SNRNP70, HCG2P7, SEMA3E and GPR1 were down-regulated.

61 KEGG pathways were statistically enriched. Members of ribosome, cell cycle and protein processing in endoplasmic reticulum pathways were amongst those enriched in up-regulated loci. Members of lysosome, metabolic pathways and base excision repair pathways were amongst those enriched in down-regulated loci.

414 GO terms were statistically enriched. Members annotated with intracellular pathway and cytoplasm GO terms were amongst those enriched in up-regulated loci. Members annotated with intracellular pathway and membrane-bounded organelle GO terms were amongst those enriched in down-regulated loci.

PRAVASTATIN RELATIVE TO FLUPHENAZINE:

7510 array features were statistically significant (3643 up-regulated, 3867 down-regulated). Within the significant features, NCEH1, AASDH, AASDHPPT, ABCB10, ABCC4, ABCD3, ABCE1, ABCF2, ABHD11 and ABHD12 were up-regulated. Within the significant features, A4GALT, AAGAB, AAMP, AARS2, AARSD1, AATF, ABCA7, ABCA8, ABCB6 and ABCB9 were down-regulated.

The predominant up-regulated pathways include metabolic pathways (218), pathways in cancer (71), protein processing in endoplasmic reticulum (50), spliceosome (46), focal adhesion (46), ribosome (45), cell cycle (44), endocytosis (43), regulation of actin cytoskeleton (43), Huntington's disease (43), Alzheimer's disease (42), Wnt signalling pathway (38), purine metabolism (37), MAPK signalling pathway (37), ubiquitin mediated proteolysis (32), Parkinson's disease (32), oocyte meiosis (31), oxidative phosphorylation (30), neurotrophin signalling pathway (28) and tight junction (27).

The predominant down-regulated pathways include metabolic pathways (212), pathways in cancer (67), endocytosis (50), MAPK signalling pathway (42), protein processing in endoplasmic reticulum (40), lysosome (40), focal adhesion (38), Huntington's disease (36), oxidative phosphorylation (31), regulation of actin cytoskeleton (31), insulin signalling pathway (31), purine metabolism (30), ubiquitin mediated proteolysis (30), neurotrophin signalling pathway (30), spliceosome (29), Cell cycle (29), pyrimidine metabolism (28), phagosome (28), Alzheimer's disease (28) and chemokine signalling pathway (27).

In terms of observed fold change (independent of statistical threshold), 705 features exhibited >2-fold up-regulation, while 471 features exhibited >2-fold down-regulation. Fold changes ranged from 11.6-fold up to 4.6-fold down. Within the biggest change loci, ACTG1, UBB, ACTB, ALDOA, SRGN, B2M, RPLP0, PGAM1, EIF4A1P4 and PRDX3 were up-regulated. Within the biggest change loci, TDP1, NUCKS1, BCYRN1, ALPP, DMC1, NLRP8, USP49, FCAR, MARCH6 and LOC401098 were down-regulated.

81 KEGG pathways were statistically enriched. Members of ribosome, spliceosome and Cell cycle pathways were amongst those enriched in up-regulated loci. Members of lysosome, base excision repair and metabolic pathways pathways were amongst those enriched in down-regulated loci.

497 GO terms were statistically enriched. Members annotated with intracellular pathway and cytoplasm GO terms were amongst those enriched in up-regulated loci. Members annotated with intracellular pathway and intracellular membrane-bounded organelle GO terms were amongst those enriched in down-regulated loci.

MBCD RELATIVE TO LPC:

6196 array features were statistically significant (2635 up-regulated, 3561 down-regulated). Within the significant features, NCEH1, AASDHPPT, ABCA1, ABCB10, ABCC4, ABCD3, ABCF2, EPHX4, ABLIM1 and ACAD8 were up-regulated. Within the significant features, A1BG,

AAGAB, AAMP, AARSD1, AATF, ABCA7, ABCB6, ABCB9, ABCC10 and ABCC5 were down-regulated.

The predominant up-regulated pathways include metabolic pathways (156), pathways in cancer (48), ribosome (41), focal adhesion (36), cell cycle (35), regulation of actin cytoskeleton (35), protein processing in endoplasmic reticulum (34), spliceosome (31), purine metabolism (30), Huntington's disease (30), ubiquitin mediated proteolysis (29), Alzheimer's disease (27), Wnt signalling pathway (26), oocyte meiosis (25), MAPK signalling pathway (24), endocytosis (24), neurotrophin signalling pathway (23), insulin signalling pathway (23), Parkinson's disease (23) and phagosome (21).

The predominant down-regulated pathways include metabolic pathways (200), endocytosis (50), pathways in cancer (45), MAPK signalling pathway (42), focal adhesion (38), lysosome (35), protein processing in endoplasmic reticulum (33), Huntington's disease (29), regulation of actin cytoskeleton (28), oxidative phosphorylation (26), purine metabolism (25), chemokine signalling pathway (25), neurotrophin signalling pathway (25), ubiquitin mediated proteolysis (24), phagosome (24), insulin signalling pathway (24), Alzheimer's disease (24), spliceosome (23), pyrimidine metabolism (21) and cell cycle (21). In terms of observed fold change (independent of statistical threshold), 557 features exhibited >2-fold up-regulation, while 203 features exhibited >2-fold down-regulation. Fold changes ranged from 11.5-fold up to 3.3-fold down. Within the biggest change loci, ACTG1, SRGN, RPLP0, ALDOA, EIF4A1P4, ACTB, UBB, PRDX3, IL8 and SUMO2 were up-regulated. Within the biggest change loci, C19orf33, NUCKS1, PVR, ISG15, LAMB2, SFN, SNRNP70, CHD8, ALPP and TDP1 were down-regulated.

61 KEGG pathways were statistically enriched. members of ribosome, cell cycle and Shigellosis pathways were amongst those enriched in up-regulated loci. Members of metabolic pathways, lysosome and endocytosis pathways were amongst those enriched in down-regulated loci.

357 GO terms were statistically enriched. Members annotated with intracellular pathway and cytoplasm GO terms were amongst those enriched in up-regulated loci. Members annotated with intracellular pathway and membrane-bounded organelle GO terms were amongst those enriched in down-regulated loci.

MBCD RELATIVE TO FLUPHENAZINE:

7399 array features were statistically significant (3328 up-regulated, 4071 down-regulated). Within the significant features, NCEH1, AASDHPPT, ABCA1, ABCB10, ABCC4, ABCD3, ABCE1, ABCF2, ABCG1 and ABHD11 were up-regulated. Within the significant features, MACC1, A2BP1, A4GALT, AAGAB, AAMP, AARS2, AARSD1, AATF, ABCA3 and ABCA7 were down-regulated.

The predominant up-regulated pathways include metabolic pathways (192), pathways in cancer (64), ribosome (50), protein processing in endoplasmic reticulum (46), endocytosis (45), spliceosome (40), regulation of actin cytoskeleton (40), focal adhesion (39), cell cycle (38), Huntington's disease (37), purine metabolism (36), Alzheimer's disease (34), ubiquitin mediated proteolysis (33), MAPK signalling pathway (32), oocyte meiosis (29), Wnt signalling

pathway (29), Parkinson's disease (27), neurotrophin signalling pathway (25), insulin signalling pathway (25) and oxidative phosphorylation (24).

The predominant down-regulated pathways include metabolic pathways (217), pathways in cancer (61), endocytosis (50), MAPK signalling pathway (43), focal adhesion (42), lysosome (39), protein processing in endoplasmic reticulum (38), regulation of actin cytoskeleton (33), insulin signalling pathway (33), Huntington's disease (33), ubiquitin mediated proteolysis (31), neurotrophin signalling pathway (31), purine metabolism (30), chemokine signalling pathway (30), oxidative phosphorylation (29), phagosome (28), Alzheimer's disease (28), pyrimidine metabolism (24), spliceosome (24) and axon guidance (24).

In terms of observed fold change (independent of statistical threshold), 653 features exhibited >2-fold up-regulation, while 381 features exhibited >2-fold down-regulation. Fold changes ranged from 9.8-fold up to 3.7-fold down. Within the biggest change loci, ACTG1, SRGN, ACTB, RPLP0, ALDOA, EIF4A1P4, UBB, CKS1B, PRDX3 and CYR61 were up-regulated. Within the biggest change loci, NUCKS1, C19orf33, ALPP, TDP1, NLRP8, ARFGAP1, C21orf58, LAMB2, LOC202781 and LRRC37BP1 were down-regulated.

72 KEGG pathways were statistically enriched. Members of ribosome, spliceosome and Protein processing in endoplasmic reticulum pathways were amongst those enriched in up-regulated loci. Members of lysosome, metabolic pathways and base excision repair pathways were amongst those enriched in down-regulated loci.

418 GO terms were statistically enriched. Members annotated with intracellular part, intracellular and cytoplasm GO terms were amongst those enriched in up-regulated loci.

Members annotated with intracellular pathway and intracellular membrane-bounded organelle GO terms were amongst those enriched in down-regulated loci.

LPC RELATIVE TO FLUPHENAZINE:

61 array features were statistically significant (33 up-regulated, 28 down-regulated). Within the significant features, ABL2, FAM26D, CCDC54, CD3EAP, CYP2F1, CCDC93, FST, LOC401093, KIR2DS5 and LDLRAP1 were up-regulated. Within the significant features, ABCC3, ACSS1, ATOH8, PYROXD2, C17orf58, C9orf169, CEBPD, COL8A1, FCGBP and GAA were down-regulated.

The predominant up-regulated pathways include ErbB signalling pathway (2), TGF-beta signalling pathway (2) and natural killer cell mediated cytotoxicity (2).
The predominant down-regulated pathways include metabolic pathways (2) and pathways in cancer (2).

In terms of observed fold change (independent of statistical threshold), 0 features exhibited >2-fold up-regulation, while 4 features exhibited >2-fold down-regulation. Fold changes ranged from 1.6-fold up to 2.4-fold down. Within the biggest change loci, DKK1, ODC1, FLNC, CTGF, EXOSC8, FTL, SC4MOL, CYR61, RND3 and GNPDA1 were up-regulated. Within the biggest change loci, TFPI, RN18S1, PTGS2, COL8A1, FCGBP, WBP5, PTGES, IL1B, VEZT and TDG were down-regulated.

6 KEGG pathways were statistically enriched. 7 GO terms were statistically enriched. Members annotated with phosphotyrosine binding, protein phosphorylated amino acid

binding and phosphoprotein binding GO terms were amongst those enriched in up-regulated loci.

In the figure below, the enrichment analyses are shown graphically, with comparisons along the X axis, and KEGG pathways along the Y axis. Note that only comparisons with enriched pathways are shown; up- and down- regulated enrichments are shown separately, as different components of a given pathway could be up- and down- regulated within a single comparison. Colour (red for up-regulated pathways, blue for down-regulated pathways) is assigned on a 20 point scale based on the -log10 (enrichment p value), with white being least statistically robust.

CALU-1 CELLS GENE EXPRESSION

A total of 24 Illumina HumanHT12_V4_0_R2_15002873_B arrays were QC analysed using the array Quality Metrics Bioconductor package to identify sub-standard and/or outlier arrays. No arrays were identified as outliers. None of the arrays failed QC.

At the QC stage, it is clear that there is good correlation between replicates particularly for the Controls (13-15), LPE (10-12), Pravastatin (16-18), Proadifen (19-21) and MβCD (22-24) (Q.1.7 Sample Relations). Raw data were transformed using a variance stabilizing transformation (VST) method prior to normalisation across all arrays using the robust spline normalisation (RSN) method. Expression measures (summarised intensities) are in log base 2.

LPC RELATIVE TO CONTROL

181 array features were statistically significant (44 up-regulated, 137 down-regulated). Within the significant features, ALCAM, ANGPTL4, APITD1, C11orf41, CAMK2N1, CRIP1, DUSP6, E2F5, EGR1 and ESAM were up-regulated. Within the significant features, ABCA1, ADAMTS9, ALDH1A1, ALOX5AP, ALPK2, ANKRD33, ANXA8L2, APOE, ART1 and BACE2 were down-regulated. The predominant up-regulated pathways include MAPK signalling pathway (2), cell cycle (2), apoptosis (2) and cell adhesion molecules (CAMs) (2). The predominant down-regulated pathways include cytokine-cytokine receptor interaction (9), metabolic pathways (8), phagosome (6), chemokine signalling pathway (5), amoebiasis (5), pathways in cancer (5), systemic lupus erythematosus (5), lysosome (4), complement and coagulation cascades (4), toll-like receptor signalling pathway (4), NOD-like receptor signalling pathway

(4), hematopoietic cell lineage (4), Leishmaniasis (4), Chagas disease (4), malaria (4), graft-versus-host disease (4), Other glycan degradation (3), MAPK signalling pathway (3), apoptosis (3) and TGF-beta signalling pathway (3).

In terms of observed fold change (independent of statistical threshold), 5 features exhibited >2-fold up-regulation, while 17 features exhibited >2-fold down-regulation. Fold changes ranged from 3.3-fold up to 4.7-fold down. Within the biggest change loci, FOS, EGR1, RN28S1, ANGPTL4, RN18S1, SFN, KHDRBS3, TAOK1, MGLL and GPR126 were up-regulated. Within the biggest change loci, CHI3L1, SAA1, CXCL1, PDZK1IP1, CXCL6, CFB, IL8, APOE, SAA2 and GPNMB were down-regulated.

23 KEGG pathways were statistically enriched. Members of other glycan degradation, cytokine-cytokine receptor interaction and Graft-versus-host disease pathways were amongst those enriched in down-regulated loci. 135 GO terms were statistically enriched. The activation of NF-kappaB-inducing kinase activity GO term was enriched in up-regulated loci. Members annotated with defense response, inflammatory response and response to wounding GO terms were amongst those enriched in down-regulated loci.

MβCD RELATIVE TO CONTROL

6868 array features were statistically significant (3417 up-regulated, 3451 down-regulated). Within the significant features, A4GALT, AARS, AASS, ABCA1, ABCB6, ABCB9, ABCG1, ABHD3, ABHD4 and ABHD8 were up-regulated. Within the significant features, NCEH1, ABCB10, ABCC4, ABCC5, ABCD3, ABCE1, ABCF2, ABHD12, ABHD5 and ABI3 were down-regulated. The predominant up-regulated pathways include metabolic pathways (173), pathways in cancer

(50), endocytosis (39), MAPK signalling pathway (37), insulin signalling pathway (34), lysosome (30), cytokine-cytokine receptor interaction (29), Jak-STAT signalling pathway (26), phagosome (23), regulation of actin cytoskeleton (23), protein processing in endoplasmic reticulum (22), neurotrophin signalling pathway (22), ribosome (21), ubiquitin mediated proteolysis (21), purine metabolism (20), Cell cycle (20), Wnt signalling pathway (19), Huntington's disease (19), ErbB signalling pathway (18) and axon guidance (18). The predominant down-regulated pathways include metabolic pathways (174), pathways in cancer (73), spliceosome (61), cell cycle (53), purine metabolism (49), ubiquitin mediated proteolysis (40), protein processing in endoplasmic reticulum (40), MAPK signalling pathway (38), Huntington's disease (37), pyrimidine metabolism (36), oocyte meiosis (36), focal adhesion (36), Wnt signalling pathway (34), Alzheimer's disease (32), endocytosis (30), regulation of actin cytoskeleton (29), neurotrophin signalling pathway (28), cytokine-cytokine receptor interaction (26), oxidative phosphorylation (25) and Parkinson's disease (25).

In terms of observed fold change (independent of statistical threshold), 393 features exhibited >2-fold up-regulation, while 349 features exhibited >2-fold down-regulation. Fold changes ranged from 16.4-fold up to 8.1-fold down. Within the biggest change loci, GDF15, NUPR1, TRIB3, DDIT3, RNF165, ASNS, PDE5A, CTH, DDIT4 and FBXO32 were up-regulated. Within the biggest change loci, CTGF, STC1, NPPB, BMPER, CYP24A1, GLIPR1, TXNIP, MMP3, EDN1 and MARCH4 were down-regulated. 66 KEGG pathways were statistically enriched. Members of steroid biosynthesis, valine, leucine and isoleucine degradation and insulin signalling pathways were amongst those enriched in up-regulated loci. Members of

spliceosome, cell cycle and DNA replication pathways were amongst those enriched in down-regulated loci.

500 GO terms were statistically enriched. Members annotated with intracellular pathway and membrane-bounded organelle GO terms were amongst those enriched in up-regulated loci. Members annotated with intracellular organelle pathway GO terms were amongst those enriched in down-regulated loci.

5107 array features were statistically significant (2535 up-regulated, 2572 down-regulated). Within the significant features, A4GALT, AARS, AASS, ABCA1, ABCB6, ABCB9, ABCC3, ABCC6, ABHD4 and ABHD8 were up-regulated. Within the significant features, NCEH1, ABCB10, ABCC5, ABCD3, ABCE1, ABCF2, ABHD11, ABHD12, ABHD5 and ABR were down-regulated. The predominant up-regulated pathways include metabolic pathways (154), pathways in cancer (37), endocytosis (35), insulin signalling pathway (29), MAPK signalling pathway (28), lysosome (26), cytokine-cytokine receptor interaction (22), Jak-STAT signalling pathway (21), neurotrophin signalling pathway (19), regulation of actin cytoskeleton (19), focal adhesion (18), cell adhesion molecules (CAMs) (18), cell cycle (17), axon guidance (17), purine metabolism (16), ErbB signalling pathway (16), calcium signalling pathway (16), protein processing in endoplasmic reticulum (16), phagosome (16) and peroxisome (16). The predominant down-regulated pathways include metabolic pathways (126), pathways in cancer (57), spliceosome (49), cell cycle (44), protein processing in endoplasmic reticulum (37), purine metabolism (35), oocyte meiosis (31), ubiquitin mediated proteolysis (30), Huntington's disease (27), pyrimidine metabolism (26), Wnt signalling pathway (26), focal adhesion (26), Alzheimer's disease (25), MAPK signalling pathway (24), cytokine-cytokine receptor interaction (23), regulation of actin cytoskeleton (22), DNA replication (21), endocytosis (21), Jak-STAT signalling pathway (19) and Parkinson's disease (19).

In terms of observed fold change (independent of statistical threshold), 219 features exhibited >2-fold up-regulation, while 174 features exhibited >2-fold down-regulation. Fold changes ranged from 11.1-fold up to 5.1-fold down. Within the biggest change loci, NUPR1, GDF15, TRIB3, RNF165, DDIT3, ASNS, DDIT4, PDE5A, CTH and PCK2 were up-regulated.

Within the biggest change loci, TXNIP, MMP3, STC1, CTGF, GLIPR1, NPPB, BMPER, EDN1, MAP2K3 and CYP24A1 were down-regulated.

59 KEGG pathways were statistically enriched. Members of steroid biosynthesis, valine, leucine and isoleucine degradation and terpenoid backbone biosynthesis pathways were amongst those enriched in up-regulated loci. Members of spliceosome, Cell cycle and DNA replication pathways were amongst those enriched in down-regulated loci.

408 GO terms were statistically enriched. Members annotated with intracellular pathway and cytoplasm GO terms were amongst those enriched in up-regulated loci. Members annotated with nuclear pathway, organelle pathway and intracellular pathway GO terms were amongst those enriched in down-regulated loci.

PROADIFEN RELATIVE TO CONTROL

9839 array features were statistically significant (4938 up-regulated, 4901 down-regulated). Within the significant features, A4GALT, AARS, AARSD1, AASS, AATF, AATK, ABCB7, ABCB9, ABCF3 and ABHD14B were up-regulated. Within the significant features, NCEH1, AAK1, AARS2, AASDHPPT, ABCA6, ABCB10, ABCC4, ABCC5, ABCC9 and ABCD3 were down-regulated. The predominant up-regulated pathways include metabolic pathways (225), pathways in cancer (66), MAPK signalling pathway (60), endocytosis (55), protein processing in endoplasmic reticulum (48), cytokine-cytokine receptor interaction (42), lysosome (37), Jak-STAT signalling pathway (36), purine metabolism (34), phagosome (33), regulation of actin cytoskeleton (33), insulin signalling pathway (33), Huntington's disease (33), chemokine signalling pathway (31), cell cycle (30), axon guidance (29), neurotrophin

signalling pathway (29), natural killer cell mediated cytotoxicity (28), focal adhesion (27) and cell adhesion molecules (CAMs) (26). The predominant down-regulated pathways include metabolic pathways (249), pathways in cancer (87), focal adhesion (61), spliceosome (59), Huntington's disease (59), cell cycle (55), regulation of actin cytoskeleton (54), purine metabolism (53), Alzheimer's disease (51), ubiquitin mediated proteolysis (47), protein processing in endoplasmic reticulum (43), MAPK signalling pathway (40), endocytosis (40), oocyte meiosis (39), Parkinson's disease (39), oxidative phosphorylation (38), pyrimidine metabolism (37), Wnt signalling pathway (36), phagosome (35) and calcium signalling pathway (31).

In terms of observed fold change (independent of statistical threshold), 830 features exhibited >2-fold up-regulation, while 971 features exhibited >2-fold down-regulation. Fold changes ranged from 29.9-fold up to 31.7-fold down. Within the biggest change loci, GDF15, NUPR1, ATF3, RNU1-3, RN18S1, RNU1-9, RNU1-5, RN5S9, TRIB3 and RNU1-1 were up-regulated. Within the biggest change loci, CTGF, COL1A1, THBS1, MAT2A, NPPB, RGS4, F3, SRSF1, CYR61 and BMPER were down-regulated.

81 KEGG pathways were statistically enriched. Members of Protein processing in endoplasmic reticulum, Lysosome and Amino sugar and nucleotide sugar metabolism pathways were amongst those enriched in up-regulated loci. Members of spliceosome, DNA replication and Cell cycle pathways were amongst those enriched in down-regulated loci.

522 GO terms were statistically enriched. Members annotated with intracellular, intracellular part and intracellular membrane-bounded organelle GO terms were amongst

those enriched in up-regulated loci. Members annotated with intracellular part, intracellular organelle part and organelle part GO terms were amongst those enriched in down-regulated loci.

LPC RELATIVE TO MBCD

7302 array features were statistically significant (3669 up-regulated, 3633 down-regulated). Within the significant features, NCEH1, AAGAB, ABCB10, ABCC4, ABCC5, ABCD3, ABCE1, ABCF1, ABCF2 and ABCG2 were up-regulated. Within the significant features, A4GALT, AARS, AASS, ABCA1, ABCB9, ABCC3, ABCG1, ABHD14B, ABHD4 and ABHD8 were down-regulated. The predominant up-regulated pathways include metabolic pathways (178), pathways in cancer (73), spliceosome (60), cell cycle (54), purine metabolism (49), protein processing in endoplasmic reticulum (46), ubiquitin mediated proteolysis (42), MAPK signalling pathway (41), focal adhesion (41), oocyte meiosis (38), endocytosis (38), Huntington's disease (38), pyrimidine metabolism (37), regulation of actin cytoskeleton (34), Wnt signalling pathway (31), neurotrophin signalling pathway (31), Alzheimer's disease (29), DNA replication (26), Parkinson's disease (26) and small cell lung cancer (25). The predominant down-regulated pathways include metabolic pathways (169), pathways in cancer (52), lysosome (43), endocytosis (41), MAPK signalling pathway (37), phagosome (36), cytokine-cytokine receptor interaction (31), Jak-STAT signalling pathway (30), protein processing in endoplasmic reticulum (26), cell adhesion molecules (CAMs) (26), insulin signalling pathway (26), Huntington's disease (25), antigen processing and presentation (24), regulation of actin cytoskeleton (24), ribosome (23), calcium signalling pathway (22), ubiquitin mediated

proteolysis (22), focal adhesion (22), Leishmaniasis (22) and neurotrophin signalling pathway (21).

In terms of observed fold change (independent of statistical threshold), 421 features exhibited >2-fold up-regulation, while 473 features exhibited >2-fold down-regulation. Fold changes ranged from 8.9-fold up to 34.9-fold down. Within the biggest change loci, CTGF, EGR1, STC1, HBEGF, BMPER, TXNIP, CYP24A1, ANGPTL4, MARCH4 and UHRF1 were up-regulated. Within the biggest change loci, GDF15, NUPR1, TRIB3, DDIT3, FBXO32, DDIT4, PDE5A, ASNS, ATF3 and CCNG2 were down-regulated.

62 KEGG pathways were statistically enriched. Members of spliceosome, DNA replication and Cell cycle pathways were amongst those enriched in up-regulated loci. Members of lysosome, other glycan degradation and glycosaminoglycan degradation pathways were amongst those enriched in down-regulated loci.

521 GO terms were statistically enriched. Members annotated with organelle part, intracellular organelle part and intracellular part GO terms were amongst those enriched in up-regulated loci. Members annotated with intracellular, intracellular part and cytoplasm GO terms were amongst those enriched in down-regulated loci.

LPC RELATIVE TO PRAVASTATIN

5757 array features were statistically significant (2912 up-regulated, 2845 down-regulated). Within the significant features, NCEH1, ABCB10, ABCC4, ABCC5, ABCD3, ABCE1, ABCF2,

ABCG2, ABHD12 and ABHD15 were up-regulated. Within the significant features, A4GALT, AARS, AASS, ABCA1, ABCB6, ABCB9, ABCC3, ABHD14B, ABHD4 and ABHD8 were down-regulated. The predominant up-regulated pathways include metabolic pathways (138), pathways in cancer (63), spliceosome (52), cell cycle (50), Protein processing in endoplasmic reticulum (41), MAPK signalling pathway (36), purine metabolism (35), oocyte meiosis (34), focal adhesion (34), pyrimidine metabolism (32), Huntington's disease (32), ubiquitin mediated proteolysis (31), regulation of actin cytoskeleton (30), Wnt signalling pathway (28), Alzheimer's disease (27), endocytosis (26), p53 signalling pathway (22), neurotrophin signalling pathway (21), small cell lung cancer (21) and DNA replication (20).

The predominant down-regulated pathways include metabolic pathways (173), pathways in cancer (46), lysosome (40), phagosome (36), MAPK signalling pathway (35), endocytosis (34), cell adhesion molecules (CAMs) (25), insulin signalling pathway (25), cytokine-cytokine receptor interaction (24), focal adhesion (22), antigen processing and presentation (22), neurotrophin signalling pathway (22), regulation of actin cytoskeleton (22), calcium signalling pathway (21), Leishmaniasis (21), Jak-STAT signalling pathway (20), cell cycle (19), valine, leucine and isoleucine degradation (18), ubiquitin mediated proteolysis (18) and protein processing in endoplasmic reticulum (18).

In terms of observed fold change (independent of statistical threshold), 199 features exhibited >2-fold up-regulation, while 283 features exhibited >2-fold down-regulation. Fold changes ranged from 6.4-fold up to 23.1-fold down. Within the biggest change loci, EGR1, CTGF, TXNIP, ANGPTL4, STC1, HBEGF, BMPER, GLIPR1, FOS and CYP24A1 were up-regulated.

Within the biggest change loci, GDF15, NUPR1, TRIB3, DDIT3, DDIT4, PDE5A, ASNS, RNF165, SCD and FBXO32 were down-regulated.

70 KEGG pathways were statistically enriched. Members of spliceosome, cell cycle and DNA replication pathways were amongst those enriched in up-regulated loci. Members of lysosome, valine, leucine and isoleucine degradation and Steroid biosynthesis pathways were amongst those enriched in down-regulated loci.

489 GO terms were statistically enriched. Members annotated with nuclear part, intracellular organelle part and organelle part GO terms were amongst those enriched in up-regulated loci. Members annotated with cytoplasm and intracellular pathway GO terms were amongst those enriched in down-regulated loci.

LPC RELATIVE TO PROADIFEN

10096 array features were statistically significant (5010 up-regulated, 5086 down-regulated). Within the significant features, NCEH1, AAK1, AARS2, AASDH, AASDHPPT, ABCB10, ABCB6, ABCC4, ABCC5 and ABCD1 were up-regulated. Within the significant features, A4GALT, AARS, AARSD1, AATF, AATK, ABCA1, ABCB9, ABCC3, ABCF3 and ABHD12 were down-regulated.

The predominant up-regulated pathways include metabolic pathways (249), pathways in cancer (82), spliceosome (62), cell cycle (60), focal adhesion (60), purine metabolism (58), Huntington's disease (56), regulation of actin cytoskeleton (52), ubiquitin mediated proteolysis (48), oocyte meiosis (47), protein processing in endoplasmic reticulum (47), Alzheimer's disease (47), MAPK signalling pathway (45), endocytosis (45), pyrimidine metabolism (42), Wnt signalling pathway (40), Parkinson's disease (39), oxidative phosphorylation (36), tight junction (32) and calcium signalling pathway (31).

The predominant down-regulated pathways include metabolic pathways (252), pathways in cancer (71), MAPK signalling pathway (59), endocytosis (57), protein processing in endoplasmic reticulum (52), lysosome (51), phagosome (47), cytokine-cytokine receptor interaction (44), Huntington's disease (41), purine metabolism (35), Jak-STAT signalling pathway (35), Alzheimer's disease (33), chemokine signalling pathway (32), cell adhesion molecules (CAMs) (32), oxidative phosphorylation (31), antigen processing and presentation (30), neurotrophin signalling pathway (30), ubiquitin mediated proteolysis (29), regulation of actin cytoskeleton (29) and insulin signalling pathway (29). In terms of observed fold change (independent of statistical threshold), 1068 features exhibited >2-fold up-regulation, while 930 features exhibited >2-fold down-regulation. Fold changes ranged from 30.6-fold up to 63.7-fold down. Within the biggest change loci, CTGF, THBS1, COL1A1, MAT2A, RGS4, F3, SRSF1, CYR61, BMPER and CSTF3 were up-regulated. Within the biggest change loci, GDF15, NUPR1, RNU1-9, ATF3, RNU1-3, RNU1-5, TRIB3, DDIT3, MIR1974 and RN5S9 were down-regulated.

81 KEGG pathways were statistically enriched. Members of spliceosome, cell cycle and DNA replication pathways were amongst those enriched in up-regulated loci. Members of lysosome, antigen processing and presentation and protein processing in endoplasmic reticulum pathways were amongst those enriched in down-regulated loci.

534 GO terms were statistically enriched. Members annotated with intracellular organelle pathway GO terms were amongst those enriched in up-regulated loci. Members annotated with intracellular pathway and membrane-bounded organelle GO terms were amongst those enriched in down-regulated loci.

MβCD RELATIVE TO PRAVASTATIN

382 array features were statistically significant (210 up-regulated, 172 down-regulated). Within the significant features, AARS, ABCA1, ADM, ARHGAP24, ARRDC3, ASNS, ATF3, ATP6V1C1, ATXN3 and BEND7 were up-regulated. Within the significant features, ACAA2, ACOX2, ADAMTS5, ADCY9, AGL, AKR1B10, ALPK2, ANGEL2, ANKRD1 and ANXA8L2 were down-regulated. The predominant up-regulated pathways include metabolic pathways (8), cytokine-cytokine receptor interaction (7), protein processing in endoplasmic reticulum (6), MAPK signalling pathway (4), apoptosis (4), prion diseases (4), pathways in cancer (4), p53 signalling pathway (3), NOD-like receptor signalling pathway (3), hematopoietic cell lineage (3), neurotrophin signalling pathway (3), renal cell carcinoma (3), graft-versus-host disease (3), purine metabolism (2), pyrimidine metabolism (2), lysine degradation (2), inositol phosphate metabolism (2), ErbB signalling pathway (2), calcium signalling pathway (2) and phosphatidylinositol signalling system (2).

The predominant down-regulated pathways include metabolic pathways (17), cell cycle (8), pathways in cancer (7), DNA replication (6), Wnt signalling pathway (5), TGF-beta signalling pathway (5), pancreatic cancer (5), purine metabolism (4), pyrimidine metabolism (4), p53 signalling pathway (4), focal adhesion (4), Jak-STAT signalling pathway (4), prostate cancer (4), chronic myeloid Leukaemia (4), small cell lung cancer (4), MAPK signalling pathway (3), cytokine-cytokine receptor interaction (3), chemokine signalling pathway (3), oocyte meiosis (3) and endocytosis (3).

In terms of observed fold change (independent of statistical threshold), 4 features exhibited >2-fold up-regulation, while 0 features exhibited >2-fold down-regulation. Fold changes ranged from 2.8-fold up to 1.9-fold down. Within the biggest change loci, RNU1-9, RNU1-5, RNU1-3, LOC730167, IL24, IGFBP3, HRK, IL6, RNU1-1 and LOC400750 were up-regulated. Within the biggest change loci, CTGF, MCM3, DUSP6, RGS4, DHCR24, TPI1, FOSL1, NUCKS1, NEDD4L and FAM20C were down-regulated.

23 KEGG pathways were statistically enriched. Members of prion diseases, protein processing in endoplasmic reticulum and NA pathways were amongst those enriched in up-regulated loci. Members of DNA replication, cell cycle and pancreatic cancer pathways were amongst those enriched in down-regulated loci.

113 GO terms were statistically enriched. Members annotated with cellular response to stress and response to stimulus GO terms were amongst those enriched in up-regulated loci.

Members annotated with cell division, DNA replication and organelle fission GO terms were amongst those enriched in down-regulated loci.

MβCD RELATIVE TO PROADIFEN

4955 array features were statistically significant (2575 up-regulated, 2380 down-regulated). Within the significant features, NCEH1, AAK1, AARS2, AASDH, AASDHPPT, ABCA1, ABCA5, ABCB10, ABCB6 and ABCC4 were up-regulated. Within the significant features, A4GALT, AAGAB, AARSD1, AATF, ABCB9, ABCF1, ABHD12, ABHD14A, ABHD14B and ABHD2 were down-regulated. The predominant up-regulated pathways include metabolic pathways (158), pathways in cancer (56), focal adhesion (42), insulin signalling pathway (29), cell cycle (28), endocytosis (28), regulation of actin cytoskeleton (28), MAPK signalling pathway (27), TGF-beta signalling pathway (27), phagosome (25), Wnt signalling pathway (25), purine metabolism (23), Alzheimer's disease (22), pathogenic Escherichia coli infection (22), calcium signalling pathway (21), ubiquitin mediated proteolysis (21), axon guidance (21), neurotrophin signalling pathway (21), small cell lung cancer (21) and oocyte meiosis (20). The predominant down-regulated pathways include metabolic pathways (106), pathways in cancer (44), MAPK signalling pathway (35), protein processing in endoplasmic reticulum (35), cytokine-cytokine receptor interaction (30), endocytosis (27), chemokine signalling pathway (24), spliceosome (23), purine metabolism (22), Cell cycle (21), Huntington's disease (20), Jak-STAT signalling pathway (19), Chagas disease (19), neurotrophin signalling pathway (18), lysosome (17), pyrimidine metabolism (16), phagosome (16), axon guidance (16), RIG-I-like receptor signalling pathway (16) and natural killer cell mediated cytotoxicity (16).

In terms of observed fold change (independent of statistical threshold), 179 features exhibited >2-fold up-regulation, while 152 features exhibited >2-fold down-regulation. Fold changes ranged from 6.8-fold up to 16.6-fold down. Within the biggest change loci, COL1A1, ID1, THBS1, HEG1, F3, MAT2A, CYR61, CTGF, CDH11 and COL1A2 were up-regulated. Within the biggest change loci, HSPA1A, RN5S9, MIR1974, HSPA6, CSF2, HSPA1B, RNU1-9, RN18S1, IL8 and RNU1-5 were down-regulated.

59 KEGG pathways were statistically enriched. Members of pathogenic Escherichia coli infection, TGF-beta signalling pathway and valine, leucine and isoleucine degradation pathways were amongst those enriched in up-regulated loci. Members of protein processing in endoplasmic reticulum, Amino sugar and nucleotide sugar metabolism and bladder cancer pathways were amongst those enriched in down-regulated loci.

353 GO terms were statistically enriched. Members annotated with intracellular pathway and intracellular organelle GO terms were amongst those enriched in up-regulated loci. Members annotated with intracellular pathway and membrane-bounded organelle GO terms were amongst those enriched in down-regulated loci.

PRAVASTATIN RELATIVE TO PROADIFEN

6172 array features were statistically significant (3166 up-regulated, 3006 down-regulated). Within the significant features, NCEH1, AAK1, AARS2, AASDH, AASDHPPT, ABCA1, ABCA2, ABCB10, ABCB6 and ABCC4 were up-regulated. Within the significant features, A4GALT, AAGAB, AARS, AARSD1, AATF, AATK, ABCB9, ABCF1, ABCF3 and ABHD12 were down-

regulated. The predominant up-regulated pathways include metabolic pathways (207), pathways in cancer (62), focal adhesion (55), cell cycle (39), regulation of actin cytoskeleton (38), MAPK signalling pathway (37), insulin signalling pathway (37), ubiquitin mediated proteolysis (36), Wnt signalling pathway (34), purine metabolism (31), endocytosis (31), axon guidance (31), oocyte meiosis (29), TGF-beta signalling pathway (29), Alzheimer's disease (29), Huntington's disease (29), calcium signalling pathway (28), phagosome (28), bacterial invasion of epithelial cells (25) and spliceosome (24). The predominant down-regulated pathways include metabolic pathways (118), pathways in cancer (46), protein processing in endoplasmic reticulum (44), MAPK signalling pathway (41), endocytosis (35), cytokine-cytokine receptor interaction (32), chemokine signalling pathway (28), spliceosome (27), purine metabolism (25), lysosome (24), Huntington's disease (23), phagosome (22), neurotrophin signalling pathway (21), Jak-STAT signalling pathway (20), cell cycle (19), axon guidance (19), pyrimidine metabolism (18), natural killer cell mediated cytotoxicity (18), ubiquitin mediated proteolysis (17) and Alzheimer's disease (17).

In terms of observed fold change (independent of statistical threshold), 334 features exhibited >2-fold up-regulation, while 263 features exhibited >2-fold down-regulation. Fold changes ranged from 10.7-fold up to 20.7-fold down. Within the biggest change loci, COL1A1, ID1, THBS1, CTGF, HEG1, F3, CYR61, MAT2A, CDH11 and RGS4 were up-regulated. Within the biggest change loci, RNU1-9, RN5S9, HSPA1A, RNU1-5, RNU1-3, MIR1974, HSPA6, RNU1-1, RNU1-8 and CSF2 were down-regulated. 69 KEGG pathways were statistically enriched. Members of valine, leucine and isoleucine degradation, focal adhesion and cell cycle pathways were amongst those enriched in up-regulated loci. Members of protein

processing in endoplasmic reticulum, protein export and Vibrio cholerae infection pathways were amongst those enriched in down-regulated loci.

384 GO terms were statistically enriched. Members annotated with intracellular pathway and organelle pathway GO terms were amongst those enriched in up-regulated loci. Members annotated with intracellular pathway and membrane-bounded organelle GO terms were amongst those enriched in down-regulated loci.

APPENDIX 4

Heatmaps

Heatmaps were used in this study as a quick way of checking the quality of the data. In the gene expression experiments the treatments and controls were either in triplicate or quadruplicate. For this reason the data appears in bands that have clusters of significance. These indicate that the replicates are all similar. No technical replicates were used in this study.

Significant genes (adjusted $p<0.01$) from each contrast were analysed for enrichment of KEGG pathway membership using a hypergeometric test. Enrichment ($p < 0.05$) was assessed for up-regulated and down-regulated genes separately. In the figures below, the enrichment analyses are shown graphically, with comparisons along the X axis, and KEGG pathways along the Y axis. Note that only comparisons with enriched pathways are shown; up- and down- regulated enrichments are shown separately, as different components of a given pathway could be up- and down- regulated within a single comparison. Colour (red for up-regulated pathways, blue for down-regulated pathways) is assigned on a 20 point scale based on the -log10(enrichment p value), with white being least statistically robust.

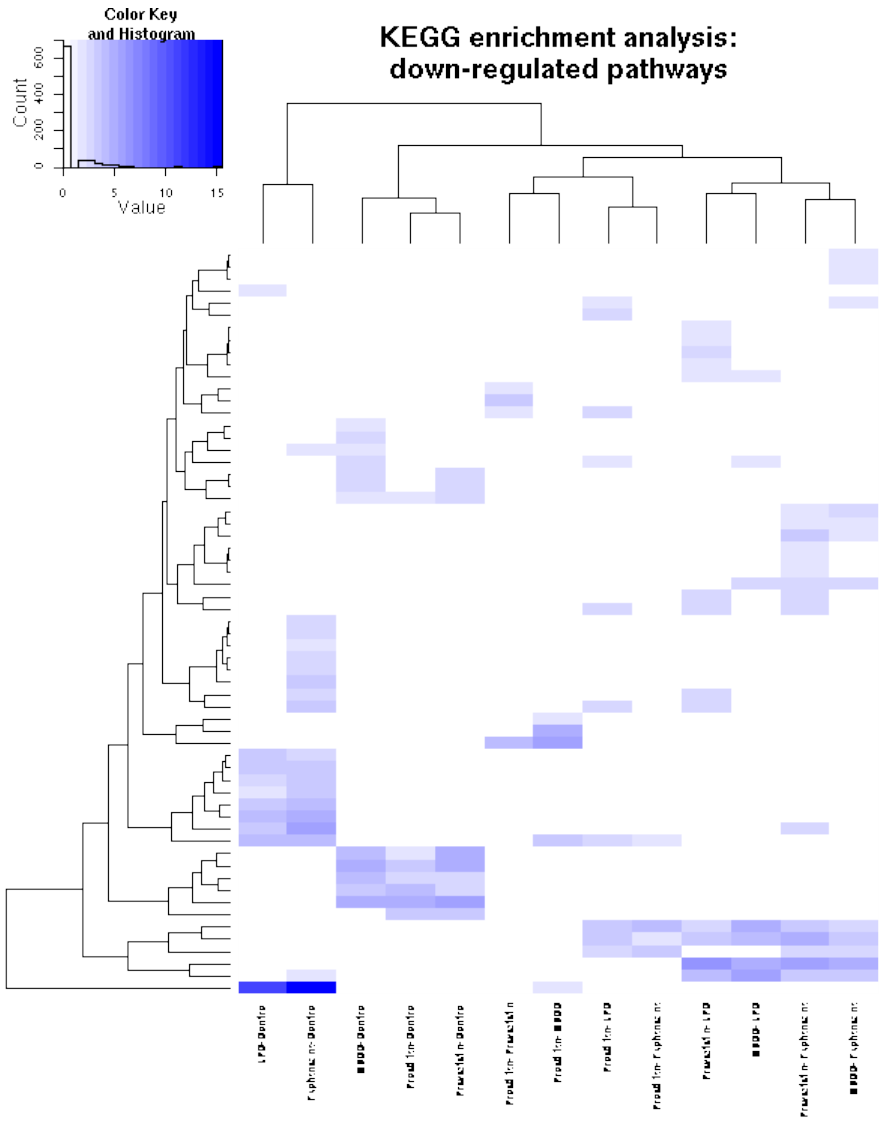

HEATMAP OF DOWN REGULATED KEGG PATHWAYS (MDA-MB-231)

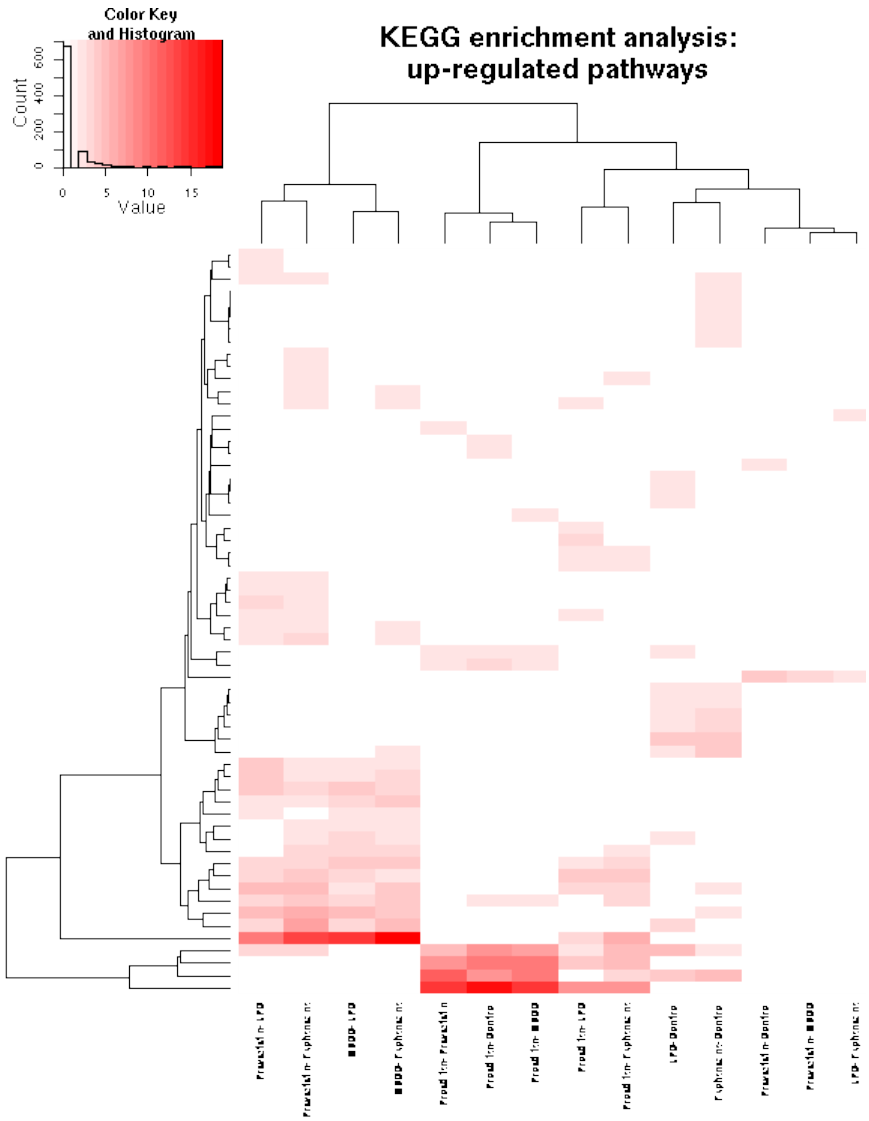

HEATMAP OF UPREGULATED KEGG PATHWAYS (MDA-MB-231)

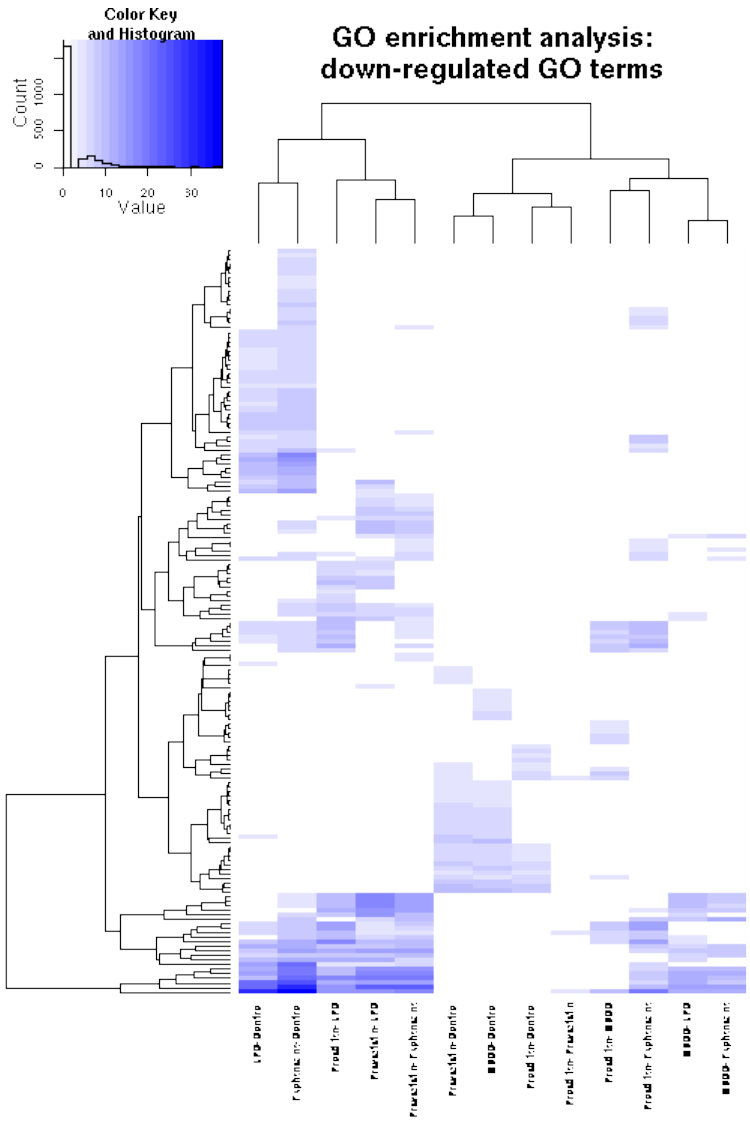

HEATMAP OF DOWN REGULATED GO TERMS (MDA-MB-231)

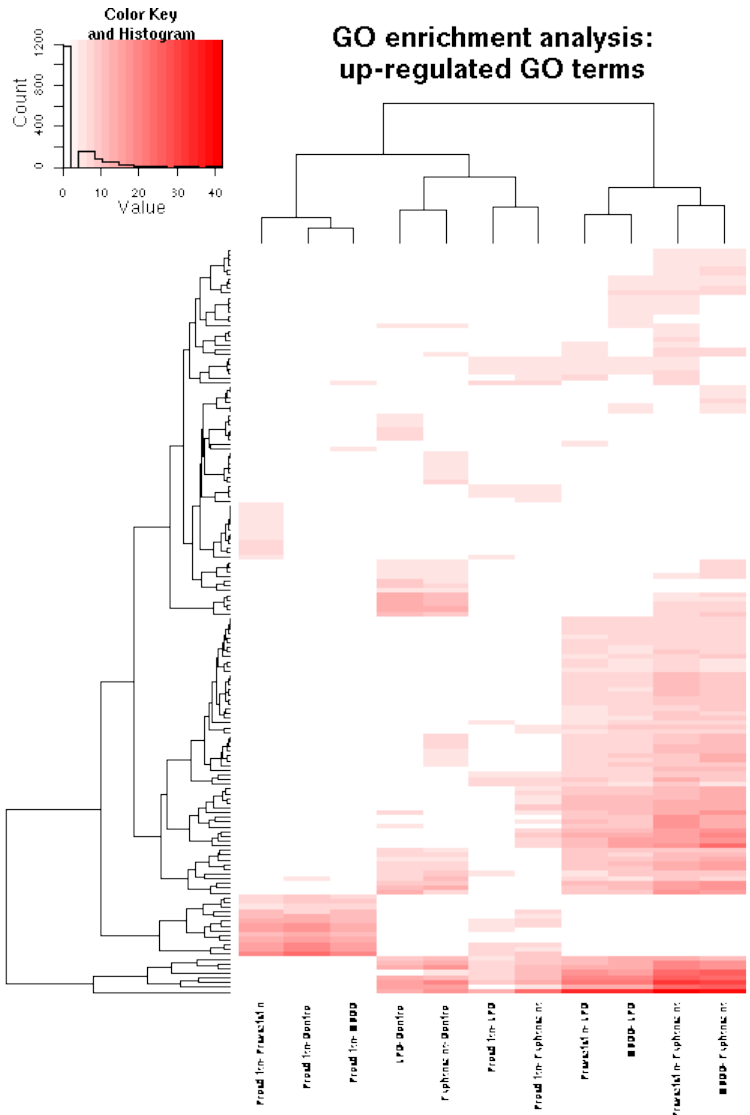

HEATMAP OF UP REGULATED GO TERMS (MDA-MB-231)

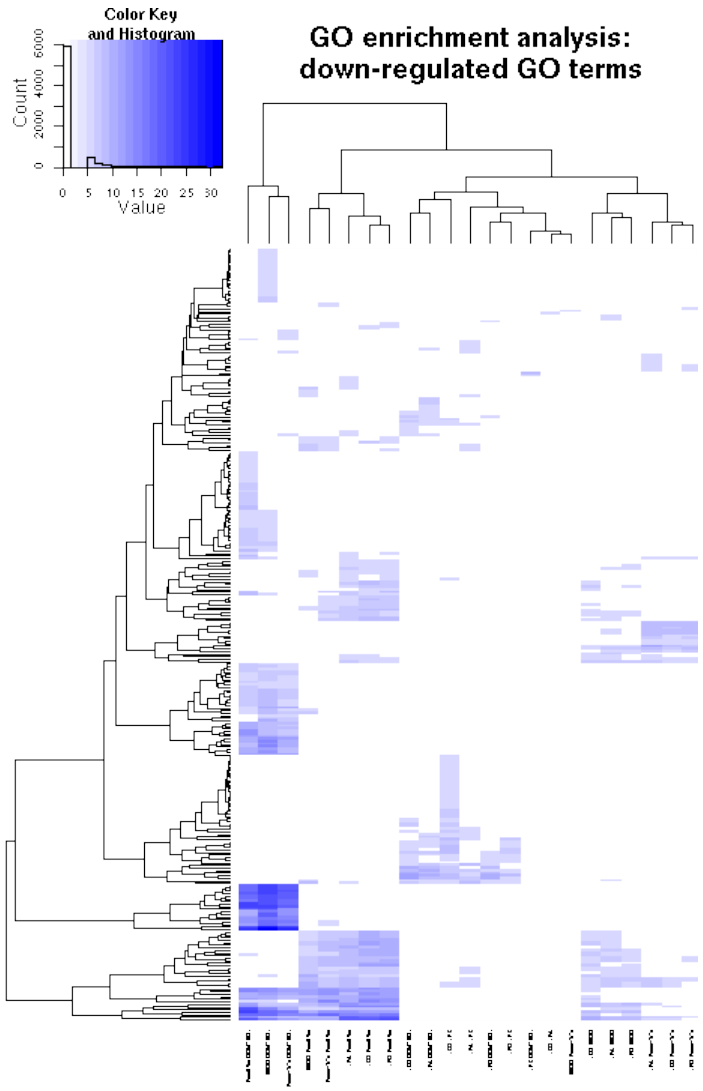

COMBINED HEATMAP DOWN REGULATED GO TERMS (CALU-1)

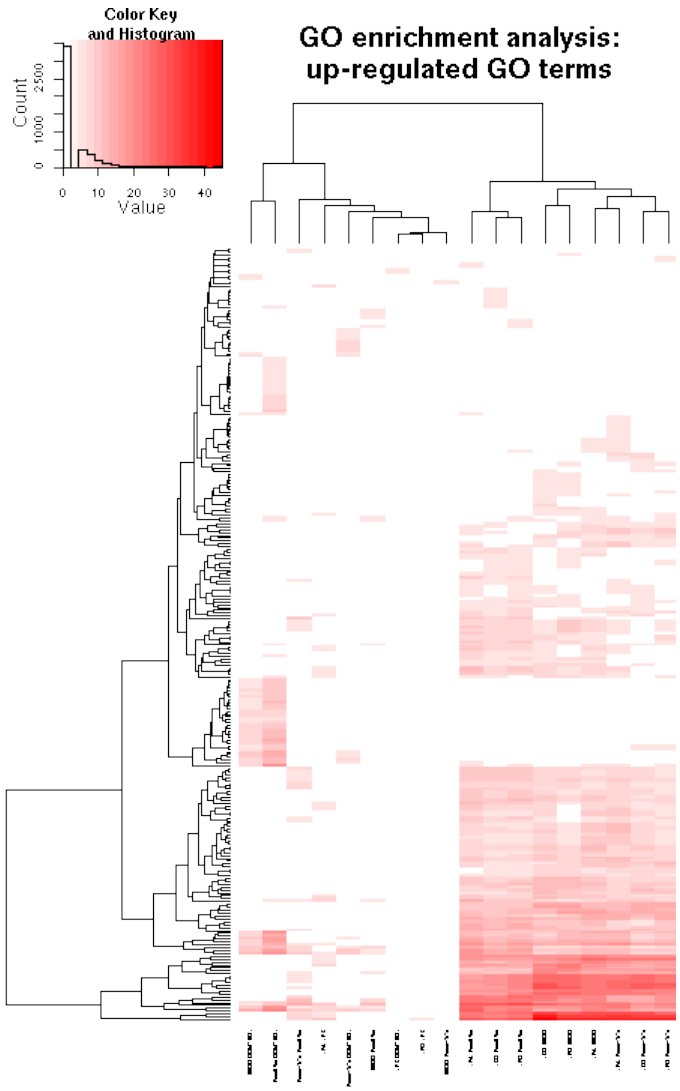

COMBINED HEATMAP UP REGULATED GO TERMS (CALU-1)

In the figures below, the enrichment analyses are shown graphically, with comparisons along the X axis, and GO terms along the Y axis. Note that only comparisons with enriched GO terms are shown; up- and down- regulated enrichments are shown separately, as different markers with the same GO term could be up- and down- regulated within a single comparison. Colour (red for up-regulated pathways, blue for down-regulated pathways) is assigned on a 20 point scale based on the -log10(enrichment p value), with white being least statistically robust.

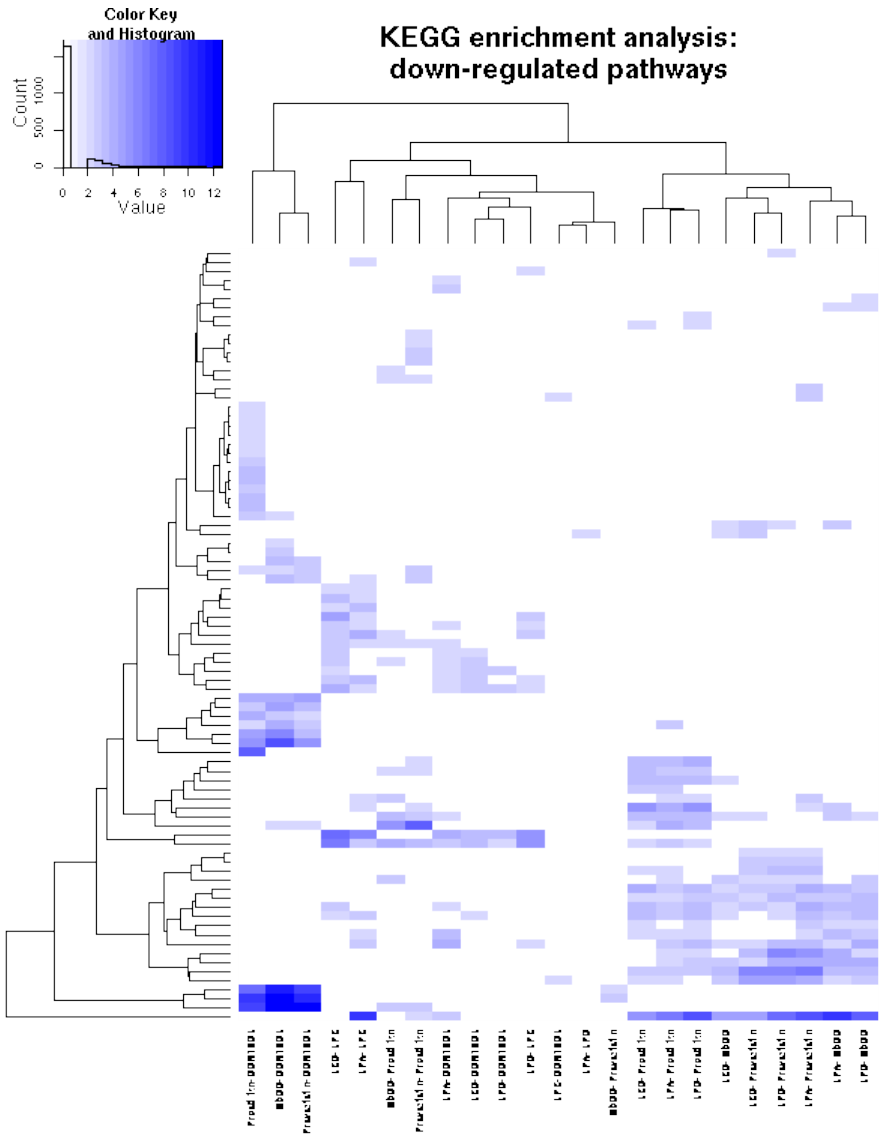

COMBINED HEATMAP DOWN REGULATED KEGG PATHWAYS (CALU-1)

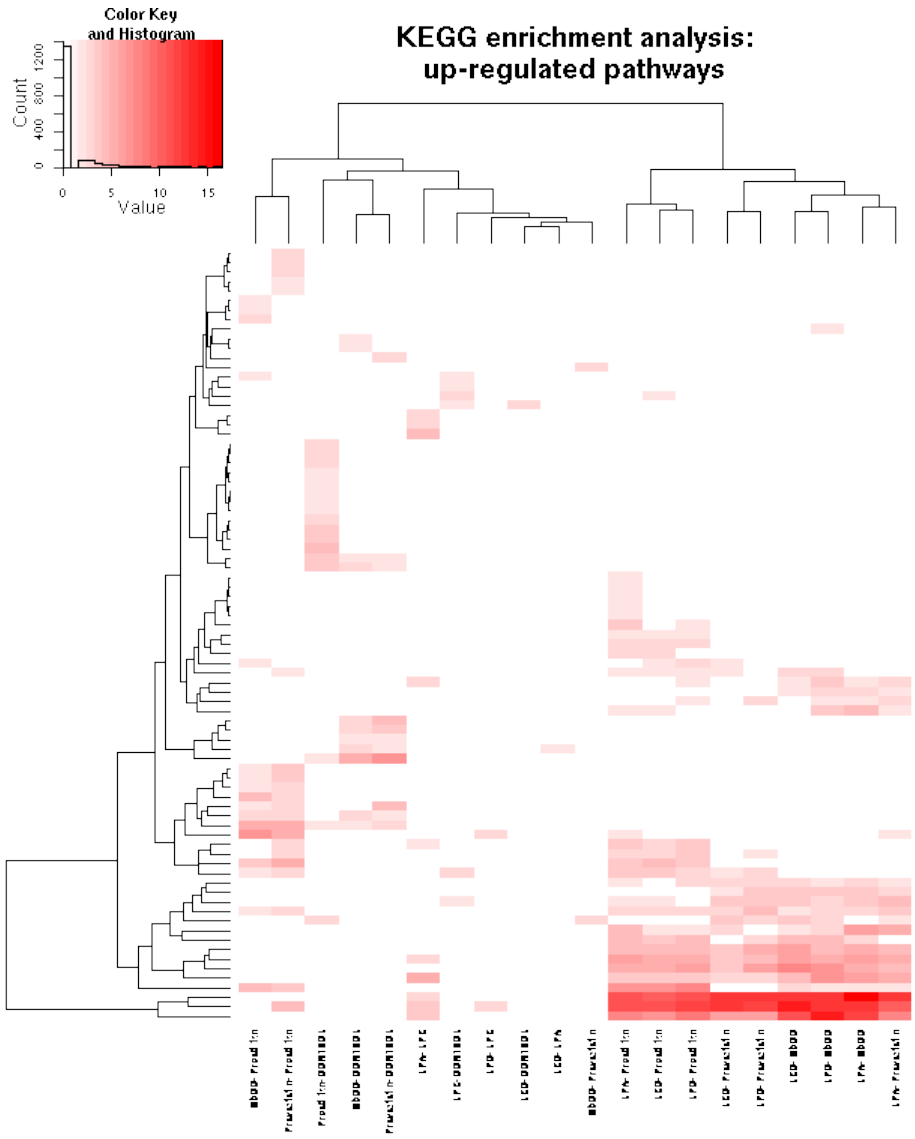

COMBINED HEATMAP UP REGULATED KEGG PATHWAYS (CALU-1)

APPENDIX 5

Proton nuclear magnetic resonance spectra of the key analogues of Proadifen synthesized for the study.

2,2-Diphenylheptanoic acid amide

17/05/2011 07:58:55
David Garnett

Acquisition Time (sec)	2.6542	***Comment***	2,2-DIPHENYL HEPTANOIC ACID AMIDE			***Date***	27 Apr 2011 12:18:24
Date Stamp	27 Apr 2011 12:18:24			***File Name***	C:\Users\David\Desktop\NMRs April 27 2011\PI Tube 2 27-04-2011\10\pdata\1\1r		
Frequency (MHz)	300.13	***Nucleus***	1H	***Number of Transients***	50	***Origin***	dpx300
Original Points Count	16384	***Owner***	CAR	***Points Count***	16384	***Pulse Sequence***	zg30
Receiver Gain	1625.50	***SW(cyclical) (Hz)***	6172.84	***Solvent***	CHLOROFORM-d		
Spectrum Offset (Hz)	1853.4263	***Spectrum Type***	STANDARD	***Sweep Width (Hz)***	6172.46	***Temperature (degree C)***	19.160

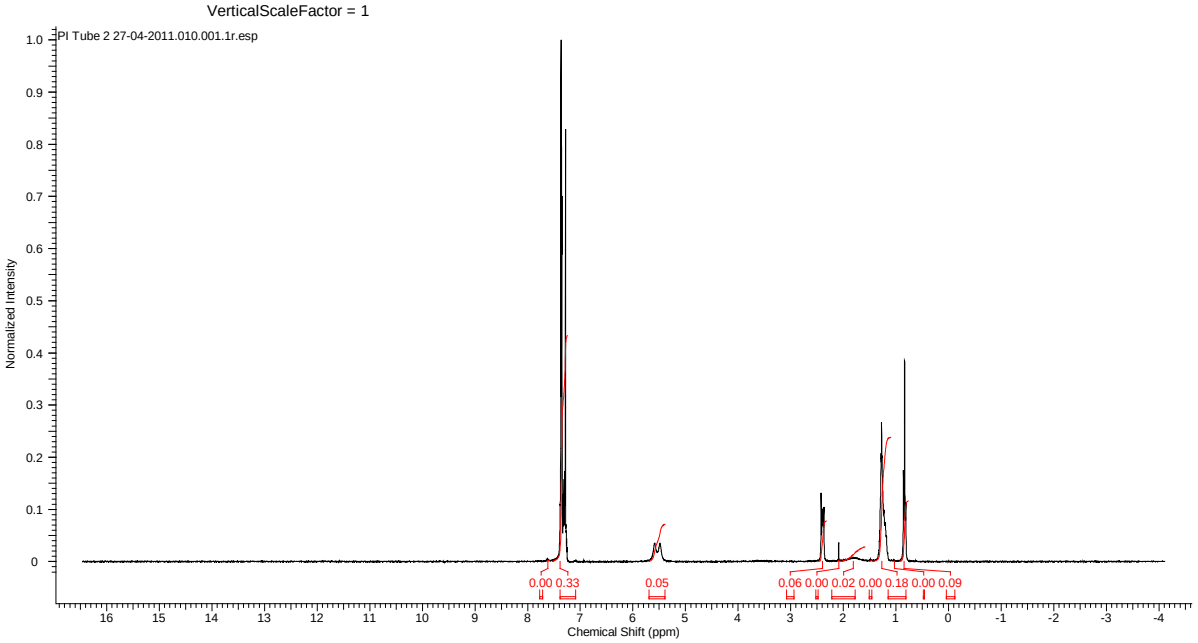

2,2-Diphenyloctanoic acid amide

16/05/2011 09:48:32
David Garnett

Acquisition Time (sec)	2.6542	***Comment***	2,2-DIPHENYLOCTANOICACID AMIDE			***Date***	27 Apr 2011 12:07:44
Date Stamp	27 Apr 2011 12:07:44			***File Name***	C:\Users\David\Desktop\NMRs April 27 2011\PI- Tube 1 27--04-2011\10\pdata\1\1r		
Frequency (MHz)	300.13	***Nucleus***	1H	***Number of Transients***	50	***Origin***	dpx300
Original Points Count	16384	***Owner***	CAR	***Points Count***	16384	***Pulse Sequence***	zg30
Receiver Gain	1149.40	***SW(cyclical) (Hz)***	6172.84	***Solvent***	CHLOROFORM-d		
Spectrum Offset (Hz)	1853.4263	***Spectrum Type***	STANDARD	***Sweep Width (Hz)***	6172.46	***Temperature (degree C)***	19.160

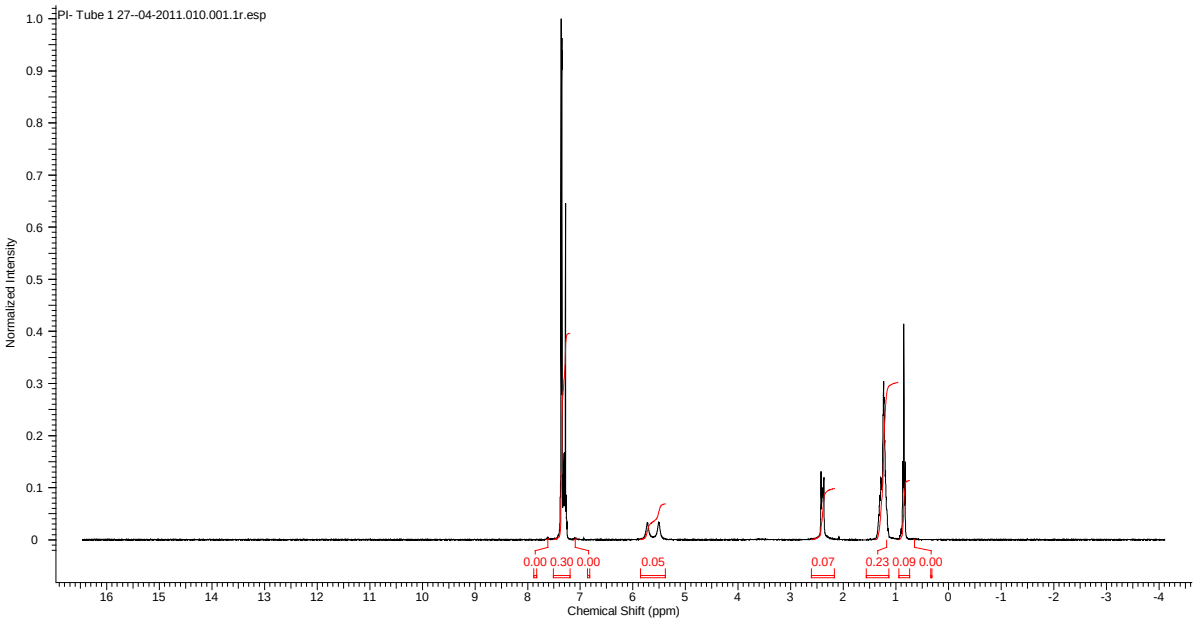

2,2-Diphenylhexanoic acid amide

17/05/2011 08:01:25
David Garnett

Acquisition Time (sec)	2.6542	***Comment***	2,2-DIPHENYL HEXANOIC ACID AMIDE			***Date***	27 Apr 2011 12:29:04
Date Stamp	27 Apr 2011 12:29:04			***File Name***	C:\Users\David\Desktop\NMRs April 27 2011\PI Tube 3 27-0402011\10\pdata\1\1r		
Frequency (MHz)	300.13	***Nucleus***	1H	***Number of Transients***	50	***Origin***	dpx300
Original Points Count	16384	***Owner***	CAR	***Points Count***	16384	***Pulse Sequence***	zg30
Receiver Gain	1024.00	***SW(cyclical) (Hz)***	6172.84	***Solvent***	CHLOROFORM-d		
Spectrum Offset (Hz)	1853.4263	***Spectrum Type***	STANDARD	***Sweep Width (Hz)***	6172.46	***Temperature (degree C)***	27.000

VerticalScaleFactor = 1

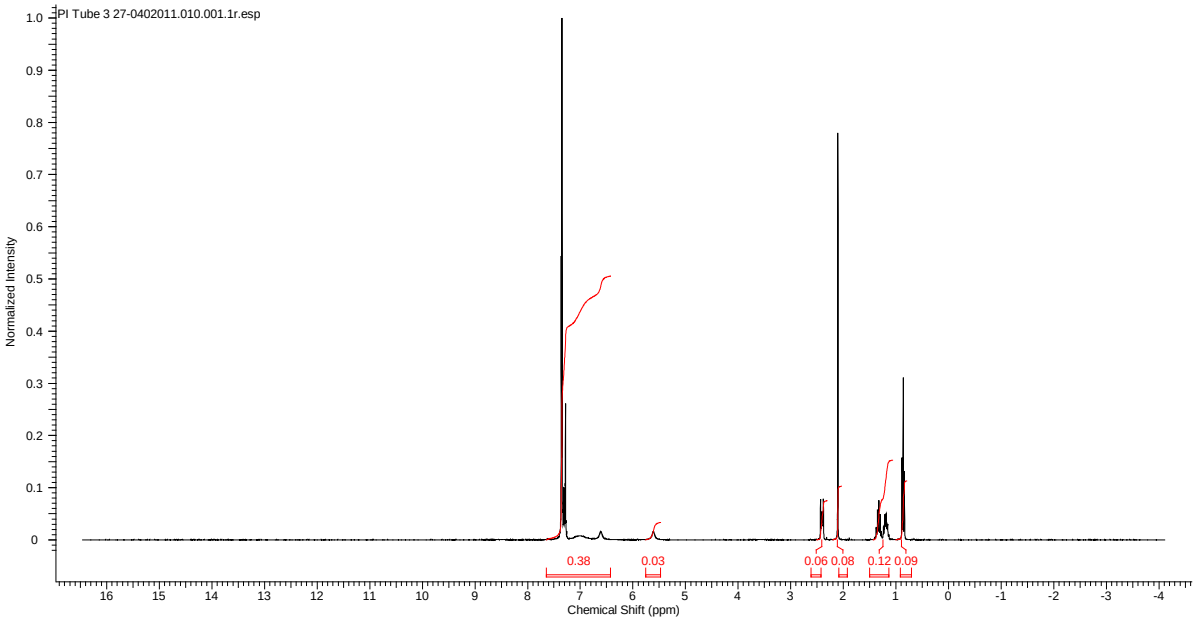

2,2-Diphenylpentanamide

17/05/2011 08:06:53
David Garnett

Acquisition Time (sec)	2.6542	***Comment***	PWI Tube 1	***Date***	29 Mar 2011 14:45:36			***Date Stamp***	29 Mar 2011 14:45:36
File Name	E:\NMRs March 29 2011\PITube1\10\pdata\1\1r			***Frequency (MHz)***	300.13	***Nucleus***	1H	***Number of Transients***	100
Origin	dpx300	***Original Points Count***	16384	***Owner***	CAR	***Points Count***	16384	***Pulse Sequence***	zg30
Receiver Gain	1149.40	***SW(cyclical) (Hz)***	6172.84	***Solvent***	DMSO-d6	***Spectrum Offset (Hz)***	1832.6725	***Spectrum Type***	STANDARD
Sweep Width (Hz)	6172.46	***Temperature (degree C)***	19.160						

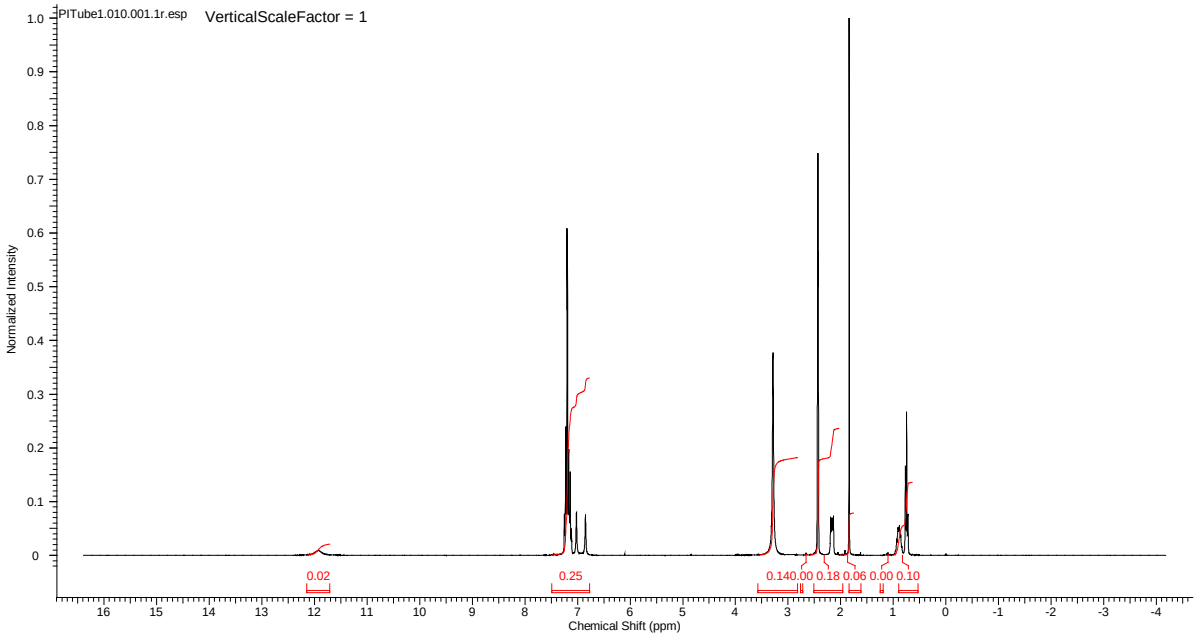

2,2-Diphenylpentanoic acid morpholino ethyl ester

17/05/2011 08:08:54
David Garnett

Acquisition Time (sec)	2.6542	***Comment***	PWI Tube 2	***Date***	29 Mar 2011 15:00:32				
Date Stamp	29 Mar 2011 15:00:32			***File Name***	E:\NMRs March 29 2011\PItube2\10\pdata\1\1r			***Frequency (MHz)***	300.13
Nucleus	1H	***Number of Transients***	100	***Origin***	dpx300	***Original Points Count***	16384	***Owner***	CAR
Points Count	16384	***Pulse Sequence***	zg30	***Receiver Gain***	2298.80	***SW(cyclical) (Hz)***	6172.84	***Solvent***	DEUTERIUM OXIDE
Spectrum Offset (Hz)	1853.4263	***Spectrum Type***	STANDARD	***Sweep Width (Hz)***	6172.46	***Temperature (degree C)***	19.160		

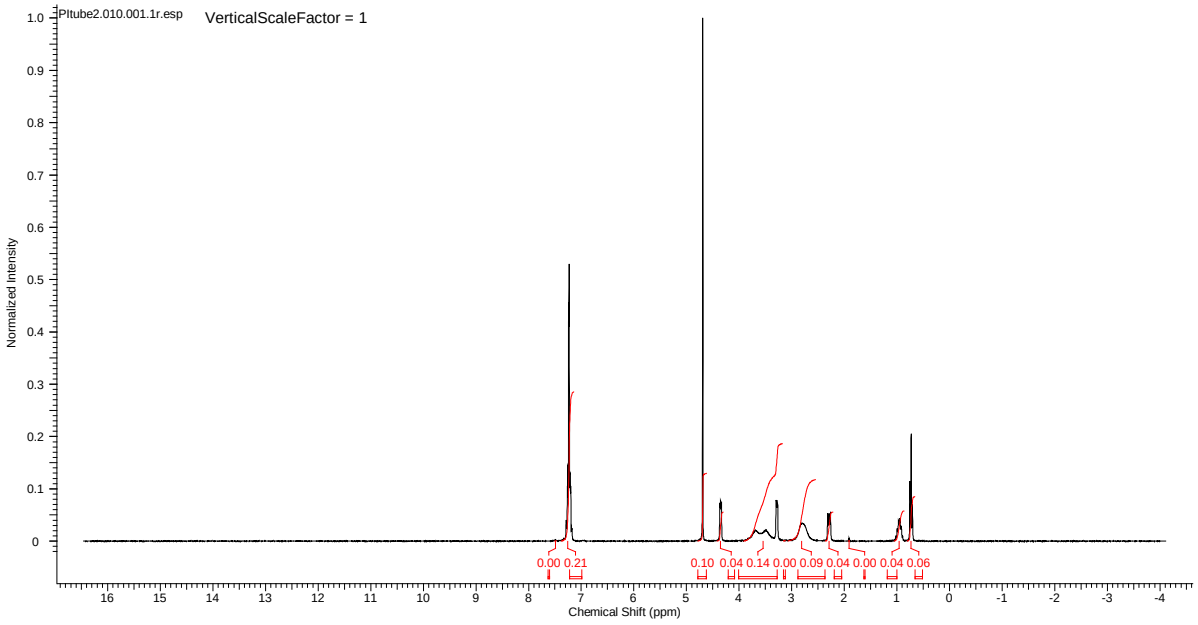

2,2-Diphenylpentanoic acid

17/05/2011 08:10:20
David Garnett

Acquisition Time (sec)	2.6542	***Comment***	PWI Tube3	***Date***	29 Mar 2011 15:13:20			***Date Stamp***	29 Mar 2011 15:13:20
File Name	E:\NMRs March 29 2011\PITube3\10\pdata\1\1r			***Frequency (MHz)***	300.13	***Nucleus***	1H	***Number of Transients***	100
Origin	dpx300	***Original Points Count***	16384	***Owner***	CAR	***Points Count***	16384	***Pulse Sequence***	zg30
Receiver Gain	1824.60	***SW(cyclical) (Hz)***	6172.84	***Solvent***	METHANOL-d4			***Spectrum Offset (Hz)***	1853.4263
Spectrum Type	STANDARD	***Sweep Width (Hz)***	6172.46	***Temperature (degree C)***	19.160				

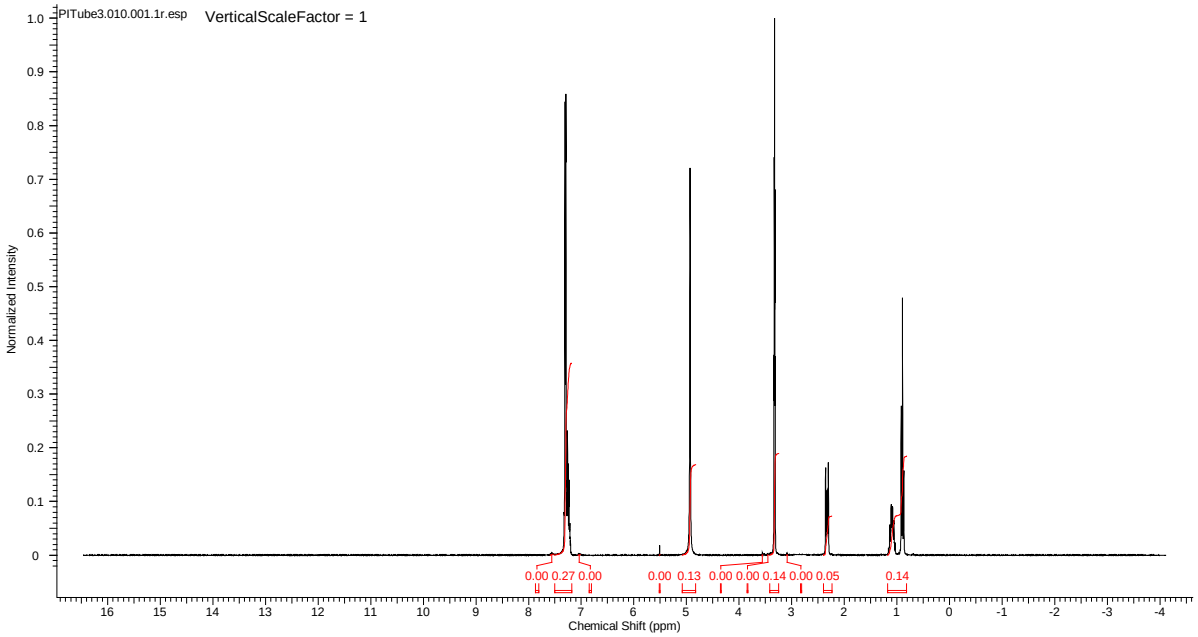

2-(N,N-diethylamino)ethyl 2,2-diphenylethanoate

17/05/2011 08:59:11
David Garnett

Acquisition Time (sec)	2.6542	***Comment***	Pathway NMR			***Date***	04 Jan 2011 13:37:04		
Date Stamp	04 Jan 2011 13:37:04			***File Name***	E:\Pathway NMR 04-01-11\10\pdata\1\1r			***Frequency (MHz)***	300.13
Nucleus	1H	***Number of Transients***	16	***Origin***	dpx300	***Original Points Count***	16384	***Owner***	CAR
Points Count	16384	***Pulse Sequence***	zg30	***Receiver Gain***	228.10	***SW(cyclical) (Hz)***	6172.84	***Solvent***	CHLOROFORM-d
Spectrum Offset (Hz)	1853.4263	***Spectrum Type***	STANDARD	***Sweep Width (Hz)***	6172.46	***Temperature (degree C)***	19.160